Specialization:	Transport Engineering and Logistics
Report number:	2013.TEL.7784
Title:	**Defining parameters for buckling checks of plated structures in finite element software packages**
Author:	B. Aberkrom

Title (in Dutch)	Definiëren van parameters voor het uitvoeren van knikanalyses in eindige elementen software pakketten.

Assignment:	Master thesis
Confidential:	yes
Initiator (university):	prof. ir. J.C. Rijsenbrij
Initiator (company):	ir. T.E. Santegoeds (Femto Engineering bv, Delft)
Supervisor:	ir. W. van den Bos
Date:	January 13, 2014

Student:	B. Aberkrom	Assignment type:	Master thesis
Supervisor (TUD):	ir. W. van den Bos	Creditpoints (EC):	35
Supervisor (Company)	ir. A.T. Naatje	Specialization:	TEL
		Report number:	2013.TEL.7784
		Confidential:	Yes

Subject: **Defining parameters for buckling checks of plated structures in finite element software packages.**

Plated structures are widely used in many engineering structures. Most designs are poor in resisting compressive forces. Usually, the buckling phenomena observed in compressed conditions take place rather suddenly and may lead to catastrophic structural failure. Therefore it is important to know the buckling capacities of the plates in order to avoid premature failure.

The linear buckling analyses of specific parts of a structure cost a lot of engineering time, let alone the non-linear analyses. The results from finite element packages cannot directly be compared to the standards like the ABS or DNV-RP-C201 either. However with the more extensive possibilities of FEM packages nowadays, the recognition of individual plates and stiffened plated structures is within reach. A new method has to be designed. One that analyses the complete plated structures with the potential to:

- Substantially reduce calculation time by the FEM program
- Omit the need to analyze each plate individually with the associated stresses and imperfections
- Automate the process to reduce the amount of work of the engineer

This master thesis is a follow up on the work of Ottar Hillers. The assignment contains an in-depth research into what problems arise with different buckling modes and the parameters that define these problems. The relations and models should lead to the extraction of correct design factors out of the FEM analyses. In such a way that a realistic comparing between the model and the standards can be made. The factors include specific in-plane compression stresses in the plates, stiffeners and girders, and shear stresses on the structure. The study mainly aims on the conversion of the FEM results into design factors needed to check buckling of plated structures.

The intended result should be a complete method to define the correct parameters of the buckling check, in such a way that it could be certified or be approved by a classification bureau and ready to be implemented into SDC Verifier.

The professor,

Prof. ir. J.C. Rijsenbrij

Panels are valuable structural designs in many structures nowadays [1].

Although not always designed as carefully as should have been done [2].

Preface

This report is my thesis for the conclusion of my Master program Transport Engineering at the Technical University of Delft. It is the result of 7 and half months of research at the engineering company Femto Engineering located in the center of Delft. All of the work presented henceforth was conducted in the office of Femto.

In my own perception, some sort of curse results in an urge to carry out new analyses, in order to look at the problems at still another way, over and over again. Buckling seems to be an engineering problem which is under defined; there are many solutions, good, bad and indifferent. The amount of available studies and literature with different approaches on the subject emphasizes this. While going through a far too large report I came across the following quote:

"Engineering is the art of modeling materials we do not wholly understand, into shapes we cannot precisely analyse so as to withstand forces we cannot properly assess, in such a way that the public has no reason to suspect the extent of our ignorance.", A.R. Dykes.

This is especially true for the buckling phenomena. Subsequently I would have liked to make a small report with an understandable impression of what buckling really is. I think I can safely say that the report gives an extensive overview of all problems, parameters and relationships which influence panel buckling. This may have become a result at the expense of the size of the report. I realized this especially when the report became so large it was too big to add as an attachment in ordinary email. Luckily there are many pictures within.

I am grateful to all those people from Femto that were involved in this study, for the everyday joy at the office, the hope for good results and even the sadness with failing software. In particular, I would like to thank ir. Tom Santegoeds for giving me the opportunity to take part in this project. Moreover, two people are really appreciated for their assistance on my analyses: my supervisors ir. Alexander T. Naatje and ir. Wouter van den Bos. I thank them for always being willing to help me when confronted with problems during the analyses. Furthermore I would like to thank Bohdan Melnyk and his colleagues at SDC Verifier for all help with obtaining results in a well-arranged, easy-viewed and accessible manner. I am grateful to prof. ir. Joan C. Rijsenbrij for spending several extensive meetings including his perspective on reality. I thank prof.dr.ir. Mirek L. Kaminski for his perspective on the subject as well. And last but not least I would like to thank in particular my parents and grandpa for their moral support.

Today I finished my report and I will continue to challenge myself in the future with what I learned. This is not the end but only the beginning. At the end, thanks to you, reader. If you are reading this line after the others, you at least read one page of my thesis. Thank You.

Summary

Big models for planes, cranes, ships or other kind of offshore structures can consist of a large amount of plated structures. Buckling is a more prominent phenomenon in such slender constructions. Buckling is a loss of stability in the structure due to a compressive load. Usually a sudden deformation takes place when reaching a critical combination of stresses. Nowadays the calculations are mostly done with finite element models. However not every model and/or analysis is suitable for an accurate buckling assessment by a FEM analysis. Most details such as imperfections, material properties or residual stresses are not included within the models. Different ways of modeling and mesh sizes increase the difficulties and parameters as well. A FEM buckling analysis most likely provides a result for a specific part of the structure. Instead you would like an individual check of each section. Therefore a new approach is needed to do a buckling check on finite element models.

Part of the plated structure can be distinguished as a panel: A rectangular plate in between girders and with stiffeners on top. Buckling is a complicated phenomenon. Hence the behaviour of a panel is simplified by subdividing into several individual buckling modes of which the most important are:

1. Unstiffened plate buckling
2. Stiffeners local buckling
3. Stiffeners flexural buckling
4. Stiffeners torsional buckling

Many properties and parameters influence these modes. The plate width and thickness have the most impact on the maximum allowable plate buckling stress. Conversely the length and stiffener dimensions have more impact on the critical beam-column buckling stress. Furthermore you have different load cases, imperfections, material properties, residual stresses and coupled effects between all of these parameters.

The lack of a satisfying analysis is tried to resolve with a combination of FEM results and standards since the standards already take these details into account. They also work with the simplified subdivided sections; plate fields and beam-columns. Each with simplified input design stresses (fig 0.1). The actual problem lies within how to accurately transforming the real stress results from your linear static FEM analysis into these design stresses. Only the ABS and DNV standards are considered for now. However the lack of an actual implementation method for these standards is what motivates this study and sets the research questions.

- Is linearization/simplification of stress distributions on individual plate fields allowable and if yes then what should the implementation method be like?
- Is it allowable to base the column buckling checks on stress results from beam elements only and if yes then what should the implementation method be like?
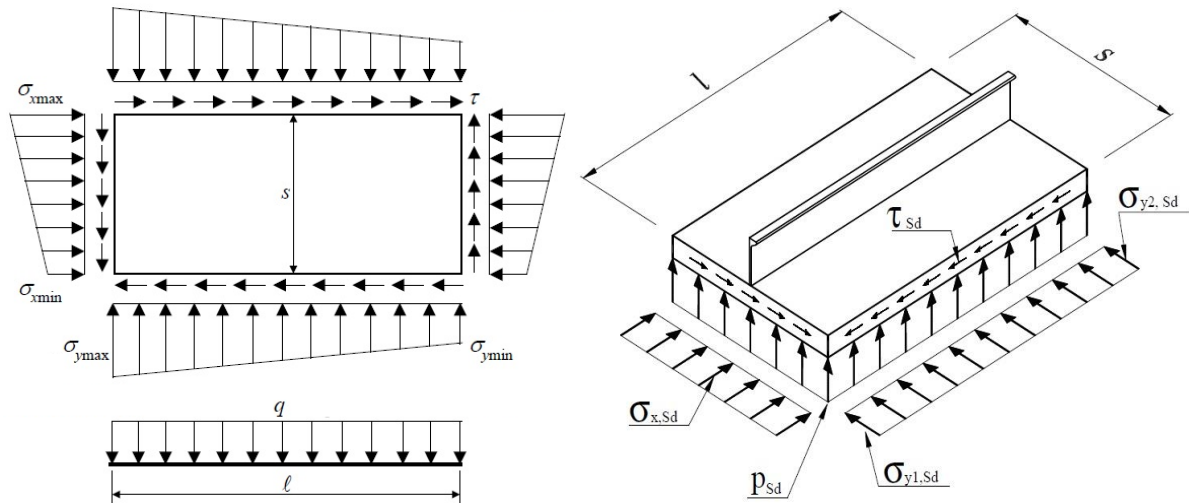
Fig 0.1 Overview of the input design stresses for (a) plate buckling and (b) column buckling.

The real stress distributions of a plate field are formed by the corner stress result from FEM plate elements along each edge. Linearizations of these stresses are used to form the distribution such as in the standards. Together with a simple average or maximum of the shear stress results, the transformed design stress is compared to the real stresses and hence can be concluded that the deviations are actually really small. To always get conservative results several adjustments on the linearization are attempted. Mostly they produce far more conservative results than desired. However several situations still lead to non-conservative transformations. The stress gradient effect is to blame: a difference between the real stress distributions on the opposite edges as where the standards require equal values for both edges. As a result of subdividing the real stresses into longitudinal, transverse and shear portions it can also be concluded that simply using the average of maximum shear stress is incorrect. The new proposal is to form the design stress after the subdivided portions have been formulated. Overall the implementation method is considered as allowable.

The considered way of modeling is with plate elements for the plate fields and beam elements for the stiffeners. Hence the results from beam element stress recovery points may be sufficient to base the local stiffener web and flange stresses and the axial beam-column stress on. With a proper combination of stress recovery points of the beam elements an implementation method for the web and flange is formed. However the method is not sufficiently checked and hence no solid conclusions can be made.

The approach for the beam-column also includes the associated plate fields. An extrapolation of stress recovery points is proposed and tested with varying results. Again the stress gradient effect produces problems with testing. A comparison of axial stresses reveals that the stiffeners have considerable different results than the associated plate fields at the point of attachment. This difference influences the results to such an extent that the present implementation method is insufficient.

Summary (in Dutch)

Grote modellen voor vliegtuigen, hijskranen, schepen of andere offshore bouwwerken kunnen bestaan uit een grote hoeveelheid plaatconstructies. Knik komt veel voor bij dunne en slanke plaatconstructies. Het knikverschijnsel is een onstabiel gedrag in de constructie bij een drukbelasting. Normaal treedt er een plotselinge vervorming op wanneer er zich een kritische combinatie van drukspanningen voor doet. Tegenwoordig worden de berekeningen voornamelijk gedaan met eindige elementen modellen. Maar niet elk model is ook geschikt om te gebruiken voor een knikanalyse in de zelfde software. Dit komt bijvoorbeeld doordat te weinig details zoals de onvolmaaktheden, materiaaleigenschappen of restspanningen in de praktijk onbekend zijn of te veel werk om te modeleren. De manier van modeleren en de fijnheid van de eindige elementen mesh maken de mogelijke problemen alleen maar groter. Daarom is een nieuwe aanpak van berekenen benodigd.

Een onderdeel van een plaatconstructie is het paneel: een rechthoekige plaat tussen girders en met langs en dwars verstijvers ter versteviging. Knik is een ingewikkeld fenomeen en daarom wordt het paneel meestal bekeken in simpele individuele secties met elk zijn eigen knikvormen en de bijbehorende kritische belastingen. De belangrijkste knikvormen die daaronder vallen zijn:

1. De onverstijfde plaatknik
2. De lokale plaatknik van verstijvers
3. De kolomknik van de verstijver-plaat combinatie
4. De torsieknik van de verstijver

Veel eigenschappen van de constructie hebben invloed op het knikgedrag. Zo zijn de dikte en breedte van de plaat vooral van belang voor de maximale belasting op individuele platen en zijn de lengte en de vorm van de verstijvers vooral van belang voor de kolomknik en torsieknik. Verder zijn de specifieke belastingcombinaties, onvolmaaktheden in de constructie, de materiaaleigenschappen, de restspanningen en de combinatie van al deze parameters allemaal van belang om te bepalen wat de maximale belasting op het ontwerp kan zijn.

Een combinatie van lineair statische analyses en de normen is overwogen als een prima oplossing omdat dergelijke details daar al in zijn verwerkt. Ook de normen werken met de simpele individuele secties; plaatvelden en kolommen. Iedere sectie heeft zijn invoer van ontwerpspanningen (fig 0.1). Het probleem is echter het bepalen van deze werkelijke spanningsverdelingen en de transformatie hiervan naar de basis input ontwerpspanningen. De implementatie om de resultaten van een FEM analyse als input voor de normen te gebruiken ontbreekt. Op zoek naar de mogelijke implementatie kunnen twee onderzoeksvragen worden opgesteld.

- Is linearisatie van spanningen op plaatvelden toelaatbaar en zo ja hoe zou de implementatie er dan uit zien?
- Is het toelaatbaar de uniform axiale druk in een verstijver-plaat combinatie te baseren op balk element resultaten alleen en zo ja hoe zou de implementatie er dan uit zien?

De werkelijke spanningsverdeling langs de randen van een plaatveld wordt gevormd door de hoekspanningen van de plaatelementen. Vervolgens wordt van deze spanningsresultaten een linearisatie gemaakt zodat je een lineaire verdeling krijgt zoals in de norm. Van alle schuifspannings-resultaten wordt het gemiddelde of maximum genomen. Deze implementatie kan worden vergeleken met de werkelijke spanningsverdeling door middel van lineaire eigenvalue analyses. Verschillen tussen de twee blijken erg klein maar niet conservatief. Daarom zijn enkele aanpassingen op de linearisaties onderzocht. Ze produceren voornamelijk veel te conservatieve resultaten maar er zitten nog steeds enkele uitzonderingen tussen. De spanningsgradiënt lijkt daarvan de boosdoener: ongelijke spanningsverdelingen op de tegenovergestelde randen van een plaat. Het onderverdelen van de werkelijke spanningen in aparte porties voor de spanningsgradiënt en de overblijvende schuifspanning maakt duidelijk dat de implementatie juist op deze onderverdeling gebaseerd zou moeten worden. Voornamelijk de gemiddelde of maximale schuifspanning van de originele spanningsresultaten is onjuist. In het algemeen lijkt de implementatie uitstekend bruikbaar.

Modellen worden gemaakt met plaatelementen voor de plaatvelden en balkelementen voor de verstijvers. De werkelijke spanningen in de lijfplaat en flensen van de verstijver zijn daarom lastig te bepalen. Een implementatie methode is opgesteld met combinaties van de hoekresultaten in de balk elementen. De methode is te weinig getest om daadwerkelijk conclusies uit te trekken.

Om de hoeveelheid data te beperken zou je kunnen proberen om alleen de resultaten van de balk elementen te gebruiken om de uniforme drukspanning in de kolom te bepalen. Omdat de bijbehorende plaatvelden wel degelijk belangrijk zijn is een nieuwe implementatie onderzocht die resultaten van de balk elementen extrapoleert. Opnieuw zorgt de spanningsgradiënt voor lastig the analyseren situaties. Gebaseerd op alleen de spanningswaarden kan worden geconcludeerd dat de implementatie onvoldoende is. Dit is vanwege een te groot verschil tussen de spanningen in de verstijver en de plaatvelden rond het gebied van bevestiging.

List of symbols

Geometric properties

L	Plate length / beam-column buckling length
s	Plate width
t	Plate thickness
h_w	Web height
t_w	Web thickness
b_f	Flange width
t_f	Flange thickness
A_p	Cross section area of only the associated plate in the beam-column
A_s	Cross section area of only the stiffener in the beam-column
A	Total cross section area of the beam-column
s_e	Effective width of the associated plate in the beam-column
A_e	Effective cross section area of the beam-column
I	Moment of inertia of beam-column about the y axis
I_e	Effective moment of inertia of the beam-column
I_z	Moment of inertia of stiffener about axis through centroid of stiffener and parallel to web
I_p	Polar moment of inertia of only the stiffener about center of rotation ($I_y + I_z$)
I_t	Torsional moment of inertia of only the stiffener (St. Venant torsion)
r_e	Radii of gyration
Γ	Warping constant
c	Eccentricity of the load
h_s	Distance between the attachment point of the stiffener and the shear center of the stiffener
z_p	Distance between the beam-column center and the outer plate fiber
z_t	Distance between the beam-column center and the outer stiffener fiber
z_{max}	Maximum from z_p and z_t
W	Section modulus
W_{min}	Minimum effective section modulus
α	Aspect ratio
β	Plate slenderness
λ	Column slenderness
γ	Adjusted column slenderness
m	Number of half waves in the longitudinal direction
n	Number of half waves in the transverse direction

Material properties and strength parameters

E	modulus of elasticity
ν	Poison ratio
G	Shear modulus
σ_0	Yield strength of material
σ_E	Euler buckling strength
σ_{ET}	Torsional buckling strength against an axial compression
σ_T	Adjusted torsional buckling strength
$\sigma_{critical}$	Critical stress for buckling
$\sigma_{cr\,(column)}$	Critical stress for buckling for the beam-column
$\sigma_{cr\,(plate)}$	Critical stress for buckling for the plate field
$\sigma_{cr\,(tripping)}$	Critical stress for the tripping phenomenon
σ_{ult}	Ultimate stress at which failure occurs in post buckling stage
$\sigma_{Cx}, \sigma_{Cy}, \tau_C, \sigma_{Ux}, \sigma_{Uy},$ $\tau_U, \sigma_{x,Rd}, \sigma_{y,Rd}$ and τ_{Rd}	Critical stresses defined by the standards
k	Buckling factor
σ_x, σ_{axial}	The longitudinal stress in the beam-column
$\sigma_{bending}$	The longitudinal stress in the beam-column due to bending
σ_{max}	The combined maximum stress in the structure
$\sigma_{Xmax}, \sigma_{Xmin}, \sigma_{Ymax},$ σ_{Ymin} and τ	Input design stresses for the standards
σ_{av}	Average stress result from the stress gradient effect
r	Value determining the stress gradient
q, q_{Sd}	Input design lateral pressure for the standards
P_{Sd}	Adjusted lateral pressure
τ_A, τ_B, τ_C and τ_D	Shear stress results in a plate field
M_x	torsional moment
M, M_y	vertical bending moment
M_z	Horizontal bending moment
M_w	Warping bending moment
F_x	Uniform longitudinal force
F_y	Horizontal shear force
F_z	Vertical shear force
σ_a	Uniform stress in longitudinal direction
σ_b	The maximum stress only resulting from the bending moment
τ_c	Shear stress over the associated plating in the beam-column
η	Safety factor defined in the standards

Contents

1.   Introduction

The future aim for finite element modeling software packages would be to automatically design the structure, or at least as far as possible. You would make the plates and apply load groups and the program would place stiffeners and girders in an optimal way (fig 1.1). One press on a button would finish the model such that it is stiff enough, easy to produce and optimal in material usage. But before all of that it is first necessary to know when exactly the structure is indeed stiff enough.
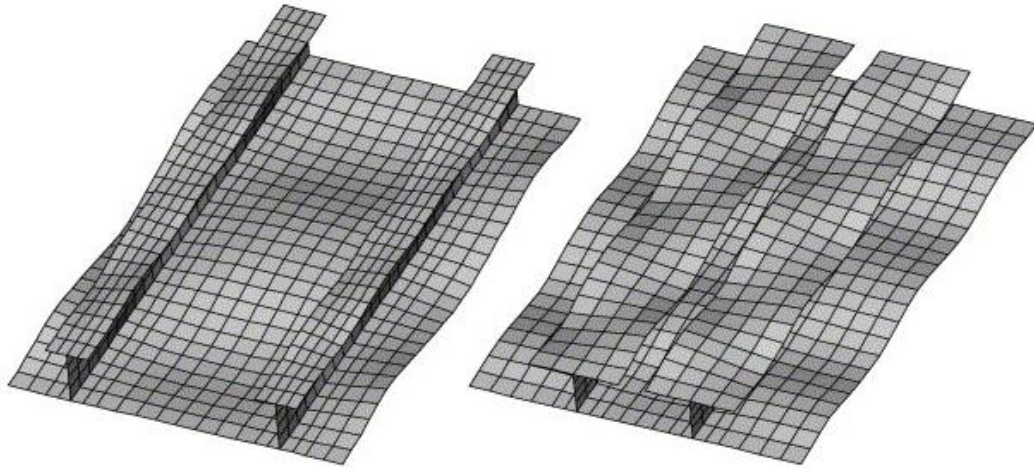

Fig 1.1 Example of different stiffener placements in search of the optimal design.

Big models for planes, cranes, ships or other kind of offshore structures can consist of a large amount of panels. The linear buckling analyses in finite element packages of specific parts of a structure cost a lot of engineering time, let alone the non-linear analyses. Even worse, such an analysis over the whole model is almost always useless since it provides only insight in the lower bound buckling factor and of course in the area that you are not interested in. Therefore an individual check of each plate field is required which is not only a lot of engineering work but also brings more uncertainties in the calculation. What are the stress results that should be applied? How fine does the mesh size have to be? What are the boundary conditions? What kind of imperfection should be applied? An engineer will need considerable knowledge of the subject in order to evaluate the design.
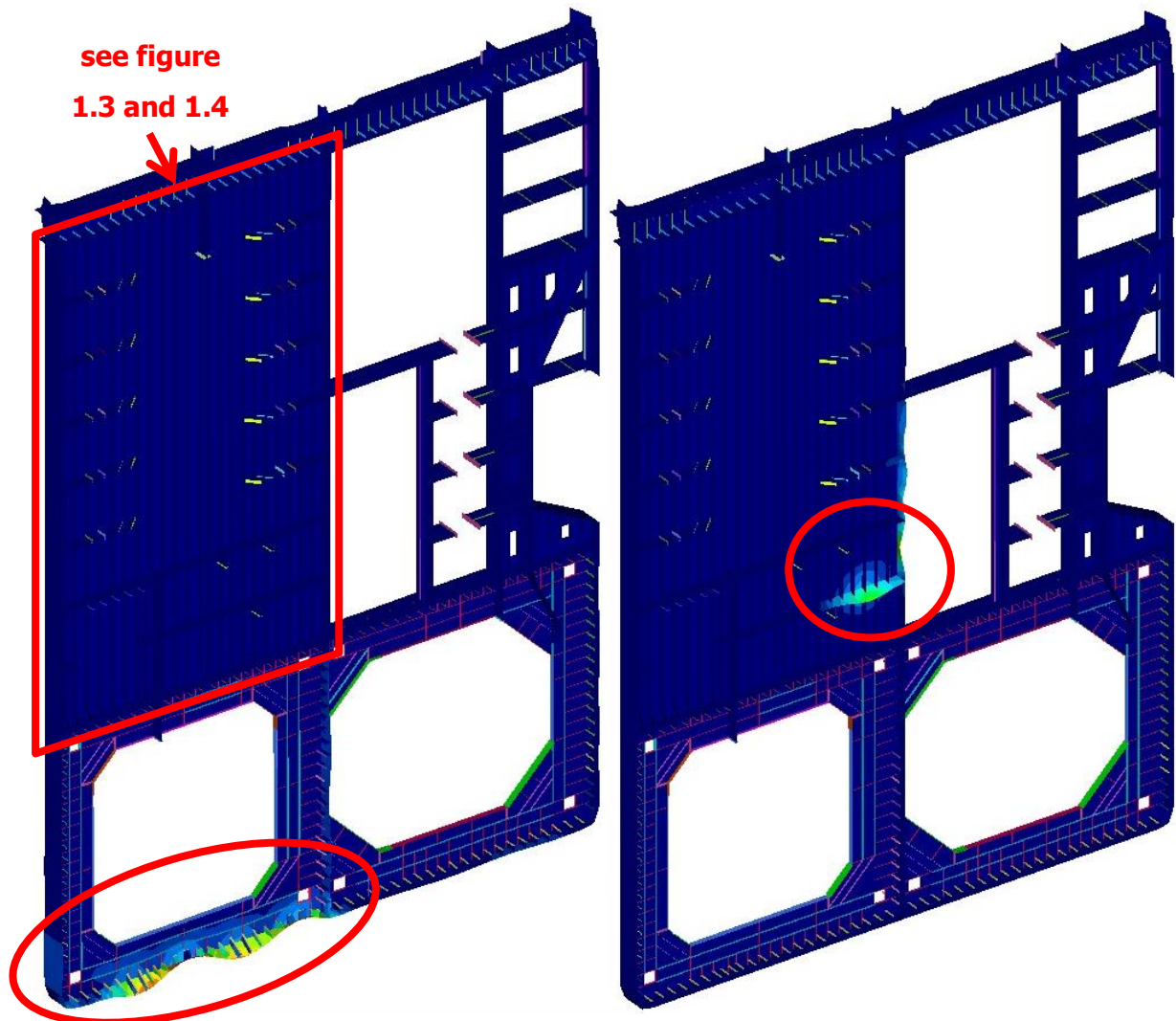
see figure
1.3 and 1.4

Fig 1.2 This analysis is to calculate buckling stiffness of the heavily stiffened panel section top left but the example does not give interesting results. A serious amount of precautionary measures as extra constraints will be needed.

You can do both linear and nonlinear buckling analysis in a finite element software package but the present study considers doing a buckling check in a FEM software program specifically according to a standard. Customers generally ask the engineer to use a standard to evaluate a design. Validating if the design meets the requirements of a standard is a simple check. However the method to extract results from the finite element analysis and using them for the check in the standard seems to be rather non-existent for general FEM programs such as Femap. Two specific standards [3] [4] are chosen for an in-depth evaluation.

- American Bureau of Shipping (ABS) Guide for buckling and ultimate strength assessment for offshore structures provides formulation to assess buckling criteria of plates and stiffened panels.
- Det Norske Veritas (DNV) Recommended practise DNV-RP-C201: Buckling strength of plated structures is a buckling code for stiffened and unstiffened panels of steel.
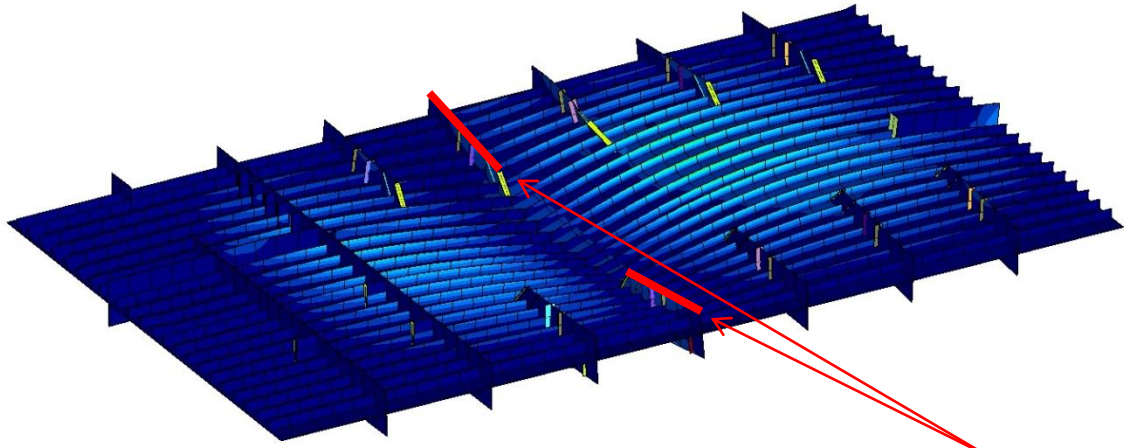
Fig 1.3 A possible buckling mode as a follow-up on figure 1.2. Whether the boundary conditions are correctly included is unreliable and unlikely.
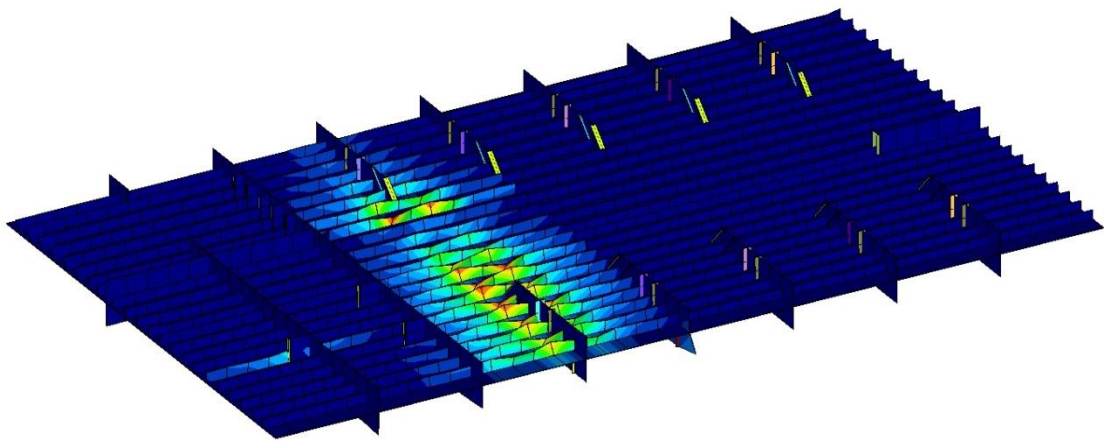

Fig 1.4 Same as figure 1.3 only with a different buckling mode.

Hence, the goal of the present study is not so much to redefine the buckling problems and phenomena but to set up a good implementation method to apply these standards to a finite element model. That includes fine meshed models with the use of beam elements for the stiffeners. In order to come to an implementation, an understanding of the influencing parameters is needed, hence the modes and problem areas are studied first. A more extensive description of the research questions is given in chapter 4.

Next to making the buckling check according to the standards accessible this study ultimately aims to provide a tool to make constructions less overdimensioned. When executing a check becomes rather simple, a quick and clarifying insight in your design will give the opportunity to see which parts in the model can actually do with less material.

This project consists of mainly the problem analysis, the formulation of new or improved methods and, as far as possible within the time limit, the validation of those methods. All for stiffened panels (fig 1.5) including plate fields, stiffeners and girders as defined below in chapter 2. That includes an in-depth analysis of all buckling modes and parameters involved described in chapter 3 and 5. And the aim of the project, to provide an implementation method, is described in chapters 8, 9 and 10.
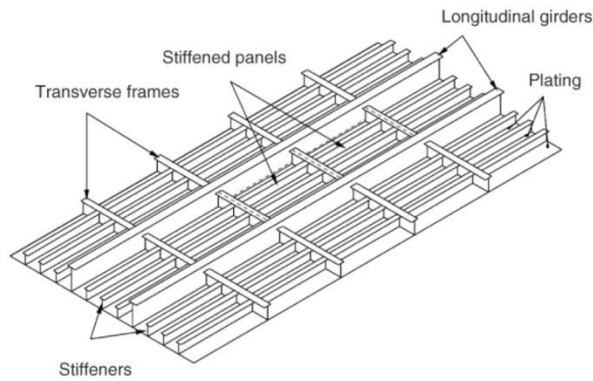
Fig 1.5 Definition of the Panel [5].

The design and validation of the method are the goal of the project such that implementation will result in a buckling check of the panel. The method itself describes the process in theory and includes an implementation up to the point necessary for validation checks. SDC Verifier will provide help. Only buckling analyses in the finite element software program Femap are performed for comparison.

The project is assigned by Femto Engineering and in cooperation with SDC Verifier and the TU Delft.

Student: B. Aberkrom
Supervisor (TUD):   ir. W. van den Bos
Supervisor (TUD):   prof. ir. J.C. Rijsenbrij
Supervisor (Company): ir. A.T. Naatje
Supervisor (Company): ir. T.E. Santegoeds

2.   The buckling phenomena

Within mechanical engineering you have structures designed using limit states. Ultimate, damage, fatigue or service limit states to name a few. Accurate tools are required to predict the strength of the structure and to assess the forces at which its limits are reached. Buckling is one of these limits. The word buckling literally means loss of the stability of an equilibrium configuration, without fracture or separation of the material or at least prior to it. Usually, the buckling phenomena observed in compressed conditions take place rather suddenly and may lead to catastrophic structural failure. Therefore it is important to know the buckling capacities of the design in order to avoid premature failure. Failure could occur due to excessive loads, poor design or construction errors. In most cases at the point of instability some sort of plastic hinge arises somewhere in the construction which results in excessive deformation. Figures 2.1 and 2.2 give to examples of failures where you can clearly see or imagine the plastic hinges.

Fig 2.1 The hull of the Prestige has buckled after first damage which caused severe flooding and thus made the construction overstressed by the flooded load condition.
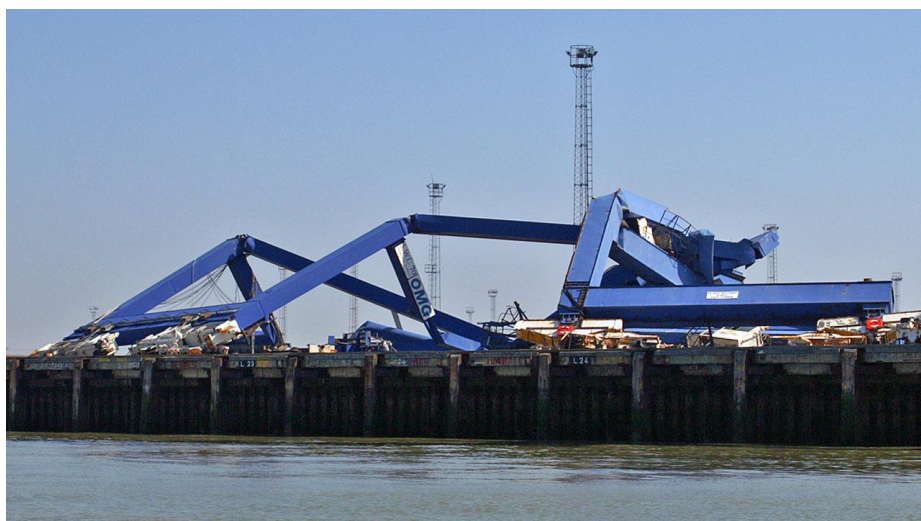

Fig 2.2 Two ship-to-shore gantry cranes at Felixstowe's Landguard Terminal after a ship crashed into them.

The buckling problem becomes increasingly important since structures are more and more designed on their critical limits in order to reduce the use of material and/or reduce the weight. New and better materials make new designs possible and lead to a shifting towards the buckling limits. And problem areas from the static analysis do not necessarily indicate where the buckling problem areas are.

In general the buckling strength analysis is based on the characteristic buckling strength for the most unfavorable buckling mode. Normally the critical buckling stress is calculated and the load combination is defined. The critical stress is then compared to the stress results from the load case applied. The difference defines the buckling factor.

$$\frac{\sigma_{applied}}{\sigma_{critical}} = k \leq 1 \qquad \{1\}$$

Stresses due to applied loads contain in-plane results, bending moments and shear stresses. The definition of correct load cases is already a study on itself but for now we are interested in the critical stress just so we can say something about buckling. The offshore field can provide numerous studies on for example the ultimate moment in sagging or hogging that a hull may sustain. Figure 2.3 illustrates a random load case on a ship which results in stress results that could maybe lead to buckling problems.
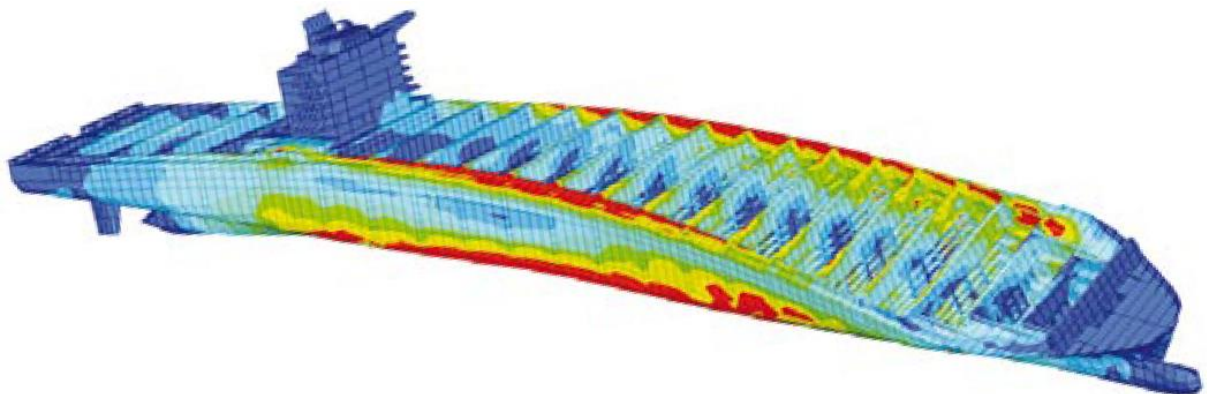

Fig 2.3 Load case with high torsional loads [6].

2.1   Column buckling

There are many types of compression members, the column being the best known. Columns are usually thought of as straight vertical members whose lengths are considerably greater than their cross-sectional dimensions. An initially straight column, compressed by gradually increasing equal and opposite axial forces at the ends is considered first. If the column is "short", the applied forces will cause a compressive strain, which results in the shortening in the direction of the applied forces. Under incremental loading, this shortening continues until the column "squashes". However, if the column is "long", similar axial shortening is observed only at the initial stages of incremental loading (fig 2.4). Thereafter, as the applied forces are increased in magnitude, the column becomes "*unstable*" and develops a deformation in a direction normal to the loading axis.
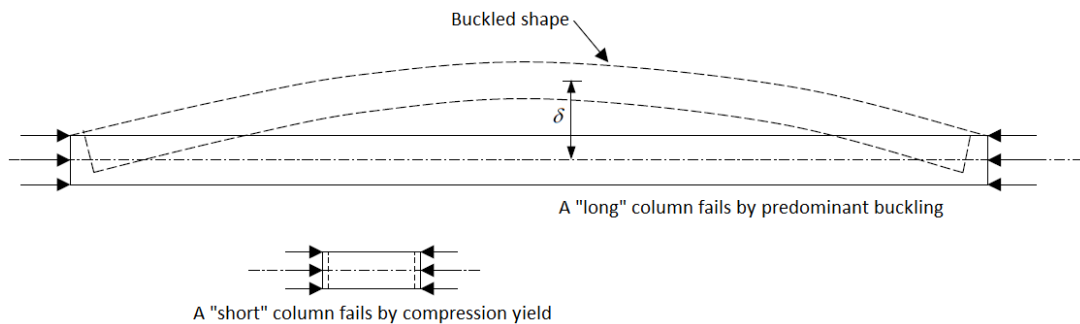

Fig 2.4 "short" vs "long" columns [7].

Buckling behaviour is thus characterized by deformations developed in a direction (or plane) normal to that of the loading that produces it. When the applied loading is increased, the buckling deformation also increases. Buckling occurs mainly in members subjected to compressive forces. If the member has high bending stiffness, its buckling resistance is high. Also, when the member length is increased, the buckling resistance is decreased. This is schematically illustrated in figure 2.5. This analytical solved critical load $P_{cr} = \frac{k \cdot L}{4}$ is hence easily seen to be influenced by the length and the bending stiffness. Thus the buckling resistance is high when the member is "stocky" (i.e. the member has a high bending stiffness and is short) conversely, the buckling resistance is low when the member is "slender".
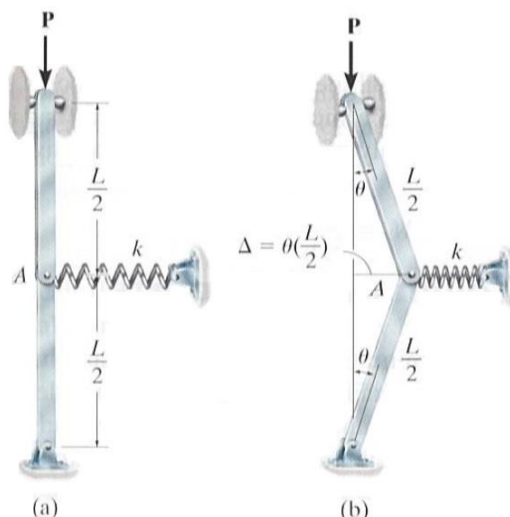

Fig 2.5 schematic illustration of the buckling problem. [8]

Structural steel has high yield strength and ultimate strength compared with other construction materials. Hence compression members made of steel tend to be slender. Structures fabricated from steel plating and subjected to compressive stresses also experience local buckling of the plate elements as discussed further in the subsequent chapter.

Stiff structures carry their design loads primarily by axial or membrane action, rather than by bending action. Their response usually involves very little deformation prior to buckling. The formula derived by Euler for ideal straight columns which gives a very stiff response to a compressive axial load. When a critical load is reached it will bend suddenly and exhibits a much lower stiffness. The Euler's buckling stress σ_E is:

$$\sigma_E = \frac{\pi^2 EI}{Al^2} \tag{2}$$

The critical buckling load becomes

$$P_{cr} = k\sigma_E A \tag{3}$$

This formula is subsequently used to define the maximum compressive stress at the extreme fiber which reaches the yield strength of material. The same critical stress is therefore considered to initiate buckling. Theoretically the maximum stress in the column can be determined by realizing that it is caused by both the axial load and the bending moment. A beam-column may thus fail by reaching either the buckling strength as governed by weak axis bending or by reaching the yield material strength if the column is stocky. The simplified axial stress and bending stress in a beam-column can be formulated as:

$$\sigma_{max} = \sigma_{axial} + \sigma_{bending} = \frac{F}{A} + \frac{M \cdot c}{I} \tag{4}$$

Failure is assumed to occur when a plastic hinge is formed. Since the most compressed portion of the structure are the flanges or the plate and the rest cannot take that much more bending load, the failure is assumed to happen when the cross section reaches the yield (fig 2.6b) or the entire section in the structure loses its flexural stiffness (Fig. 3.30).
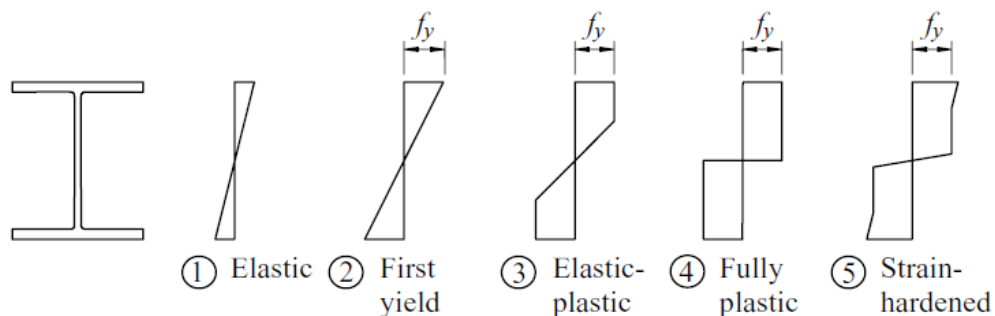

Fig 2.6 Stress distributions with pure bending.

A fairly good amount of parameters influences this behaviour of columns. Eccentric or in-plane loads, initial deformation in the geometry or torsional effects are just some of the possibilities (fig 2.7 and 2.8).
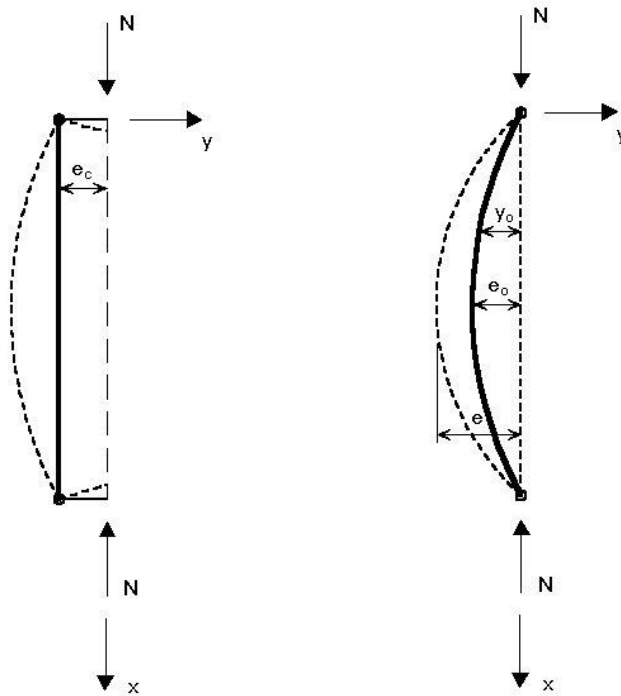
Fig 2.7 Difference between (a) eccentric axial loads and (b) imperfection due to initial deformation.
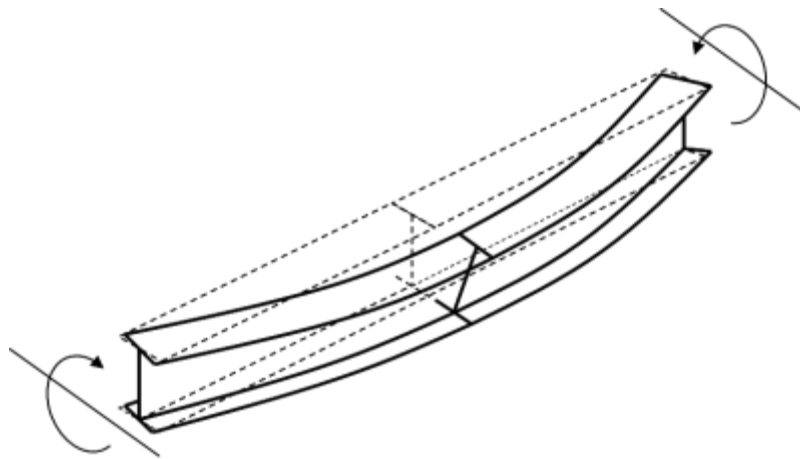

Fig 2.8 Overview of lateral torsional buckling.

You can make the buckling phenomenon as complicated as you want. Combined and coupled distortions form a substantial amount of relations; two examples are given in figures 2.9 and 2.10.
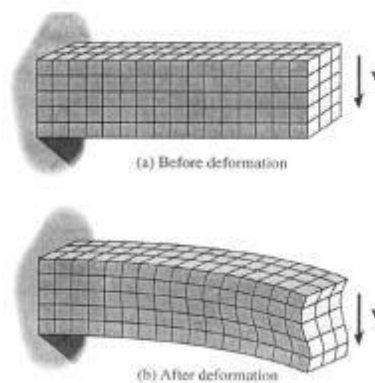

Fig 2.9 Distortion in a bend beam due to shear forces.

2.2   Plate buckling

If you change the column from stocky towards thin and wide that would give plate buckling instead of column buckling. The mechanism of plate collapse is complex and does not usually occur at the theoretical Euler elastic buckling stress as mentioned above. Collapse of a relatively stocky plate occurs before the critical elastic buckling stress is reached. Conversely, a relatively slender plate does not collapse at the critical buckling stress and has additional strength in the post buckled region as can be seen in figure 2.13b.

This is due to the boundary conditions at the unloaded edges which prevent the portions of the plate close to the boundaries from deflecting. Only the center region of the plate deflects and therefore partially escapes the compressive load. Local yielding in the middle of the plate causes a new non-uniform stress redistribution meaning no more additional load can be supported in this region. The outer portions of the plate provide additional strength in the post buckling region. As the load increases, the maximum stress (average equivalent stress given by the von Mises failure criterion) in the plate sides eventually reach the material yield and failure occurs.

The theoretical elastic buckling stress of more stocky plates is relatively close to the yield stress. The mechanism of collapse is therefore somewhat different, as the name stocky implies more like column buckling. It is significantly more influenced by initial imperfections in the plate. Initial deflections are magnified as the applied load increases, causing a loss of stiffness. Since the ultimate strength of the slender plate lies beyond the buckling, the local initial imperfection has still effect on its particular buckling mode but less effect in general.

The elastic buckling stress, σ_{cr}, is defined according to the solution of the Euler differential equations governing the buckled shape of a plate. The buckling limit stress for long flat rectangular plates with simply supported edges can be approximated with some adjustments to equation seen above.

$$\left. \begin{array}{r} \sigma_{cr\,(column)} = k\,\dfrac{\pi^2 EI}{Al^2} \\[2mm] I = \dfrac{st^3}{12} \\[2mm] A = st \end{array} \right\} \sigma_{cr\,(column)} = k\,\frac{\pi^2 Est^3}{12stl^2} = k\,\frac{\pi^2 E}{12}\left(\frac{t}{l}\right)^2 \qquad \{5\}$$

Due to the wide plate dimension compared to a regular column the behaviour is firstly changed for the distortions in the transverse direction. A column will bend along the transverse axis as a reaction at the bending along the axial axis and vice versa (fig 2.10). A combination of the moment-displacement relationships and Hooke's law bring forth the influences of the poison ratio. And since the (unloaded) edges are generally constraint, the plate will be less dependent on the length but instead more dependent on the width.
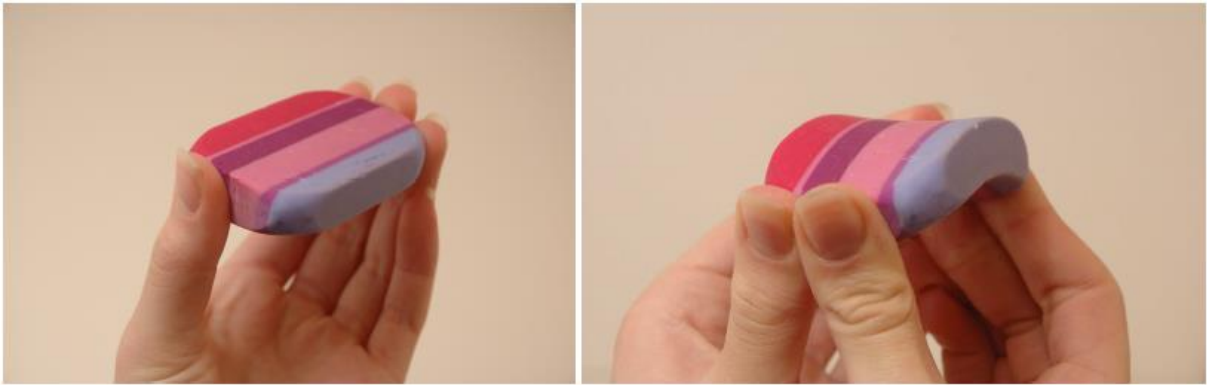
Fig 2.10 The material does not only bend in one direction but there is a curvature in the other direction as well. The cross section is not rectangular anymore either. This behavior is the effect of the poison ratio.

Applying the two transformations will result in:

$$\sigma_{cr\,(plate)} = \left(\frac{mL}{s} + \frac{n^2 s}{mL}\right)^2 \frac{\pi^2 E}{12(1 - v^2)}\left(\frac{t}{s}\right)^2 = k\frac{\pi^2 E}{12(1 - v^2)}\left(\frac{t}{s}\right)^2 \qquad \{6\}$$

The variables m and n are the number of half waves in the longitudinal and transverse directions. The flexural rigidity of the plate is defined as:

$$D = k\frac{Et^3}{12(1 - v^2)} \qquad \{7\}$$

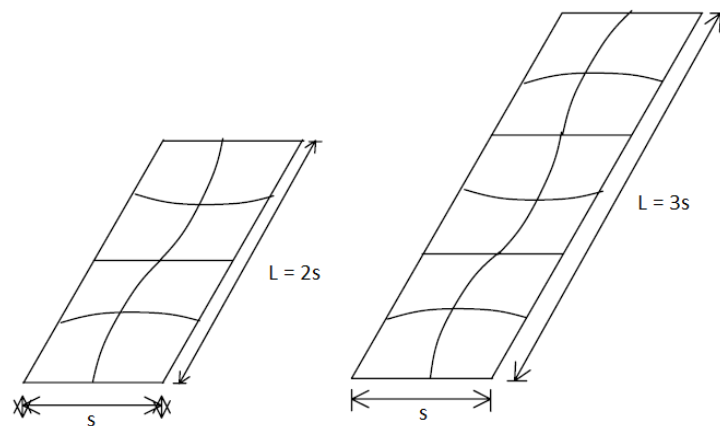The coefficient k is a function of the boundary support, aspect ratio and the buckling shape of the plate.

Fig 2.11 Typical behaviour of plate buckling.

$$EI = \frac{Ebt^3}{12}$$

$$EI\frac{d^4 v}{dx^4} = -N\frac{d^2 v}{dx^2}$$

(a) Column buckling

$$bD = \frac{Ebt^3}{12(1-v^2)}$$

$$bD\left(\frac{\partial^4 v}{\partial x^4} + 2\frac{\partial^4 v}{\partial x^2 \partial z^2} + \frac{\partial^4 v}{\partial z^4}\right) = -N\frac{\partial^2 v}{\partial x^2}$$
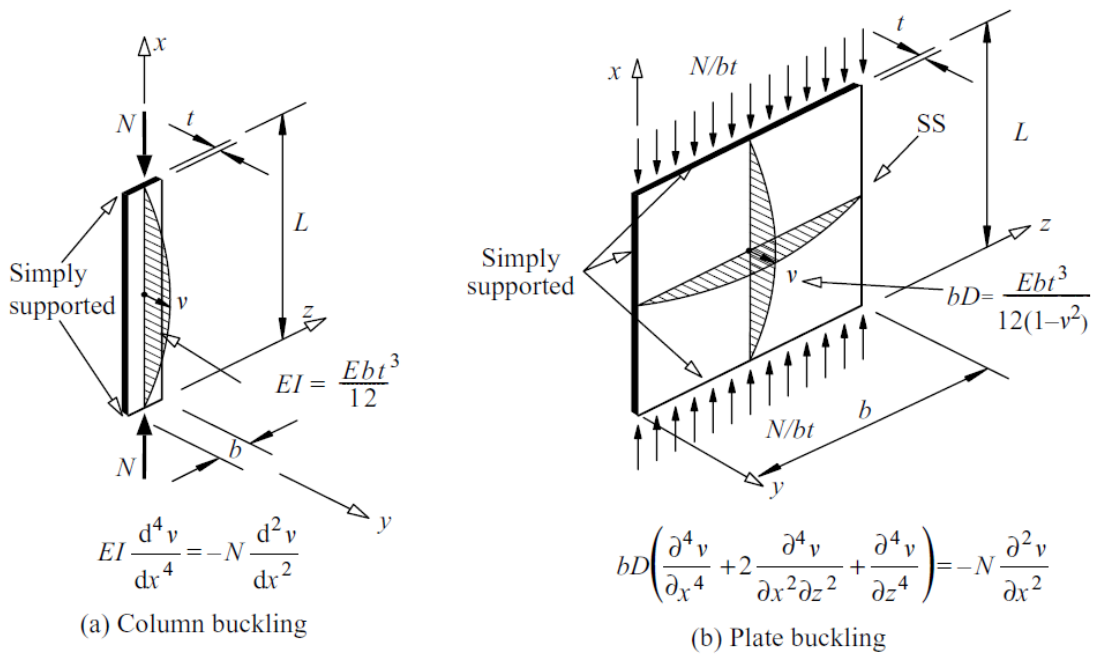
(b) Plate buckling

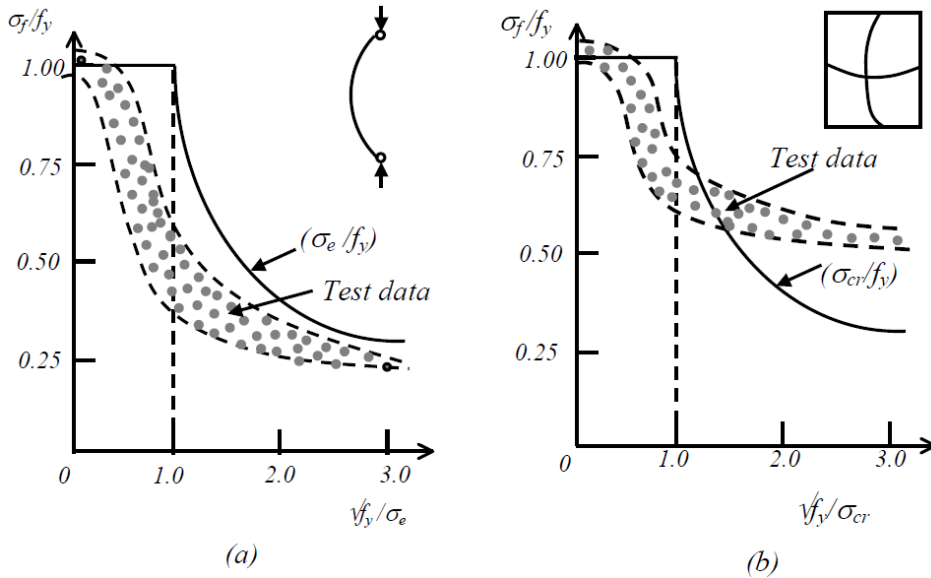Fig 2.12 Difference between column and plate buckling.

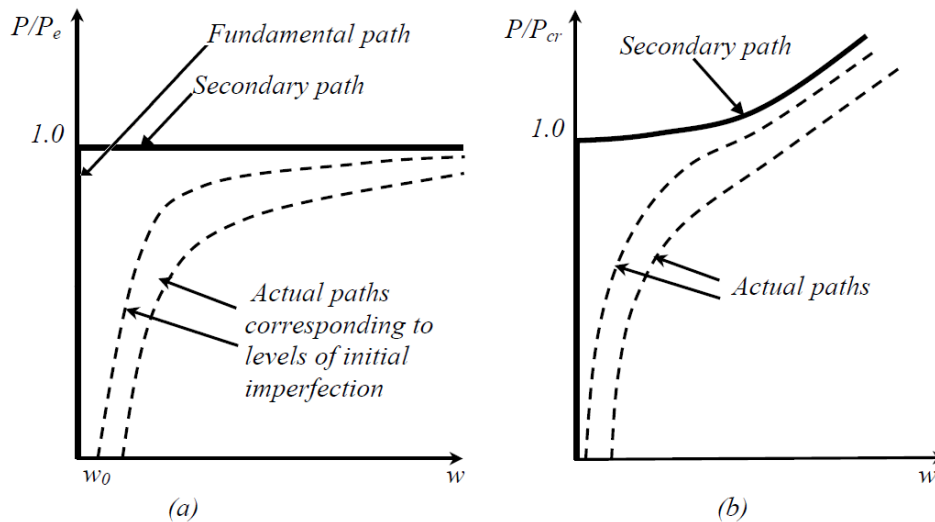Fig 2.13 (a) Column and (b) plate strength curves.

Fig 2.14 Load versus out-of-plane displacement curves for the (a) column and the (b) plate.

2.3   Panel: the part of interest

Plated structures are widely used in many engineering structures. Most of these designs are poor in resisting compressive forces with their slender dimensions. A construction generally consists out of plates, stiffeners and girders. The latter two consist of the flange (on top) and the web (between the plates and the flanges). The plate field is the part in between the stiffeners. Within structures you can also define individual panels. A panel is the field in between major supports known as the very stiff longitudinal and transverse girders. The girders are assumed to be much stronger than stiffeners. Generally, a panel is part of the structure which contains a big plate with on top of that all the stiffeners. The panel may for example be part of beams, box girders, bulkheads, pontoons, hulls or integrated plated decks.
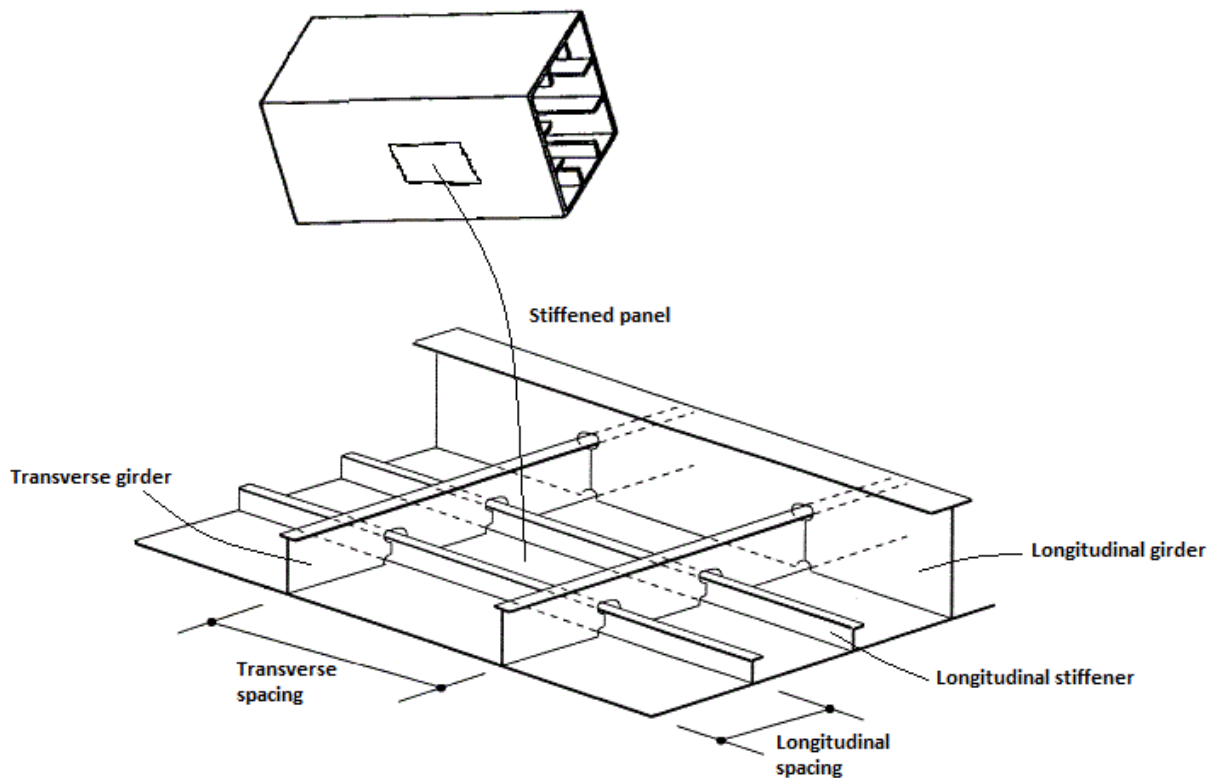

Fig 2.15 Definition of a panel (part of a plated structure).

Stiffeners fulfill local and global strength functions. At the local level they are effective in maintaining the stiffness and hence the integrity of the structure under lateral and in-plane loads. They prevent excessive deflection. Adding regularly spaced stiffeners is an effective way of improving the panel strength economically using a minimum of additional structural weight.

This report will not go too much in-depth into diverse models other than plates, stiffeners and plate-stiffener combinations although besides the defined panel there are of course a lot more different structures made out of plates like corrugated panels, brackets, web stiffeners or other perpendicular adjacent (stiffened) panels. Combinations of these with stiffened panels are frequent in real structures but the buckling phenomena is complicated to such an extent that for now these things are out of the scope of this report.
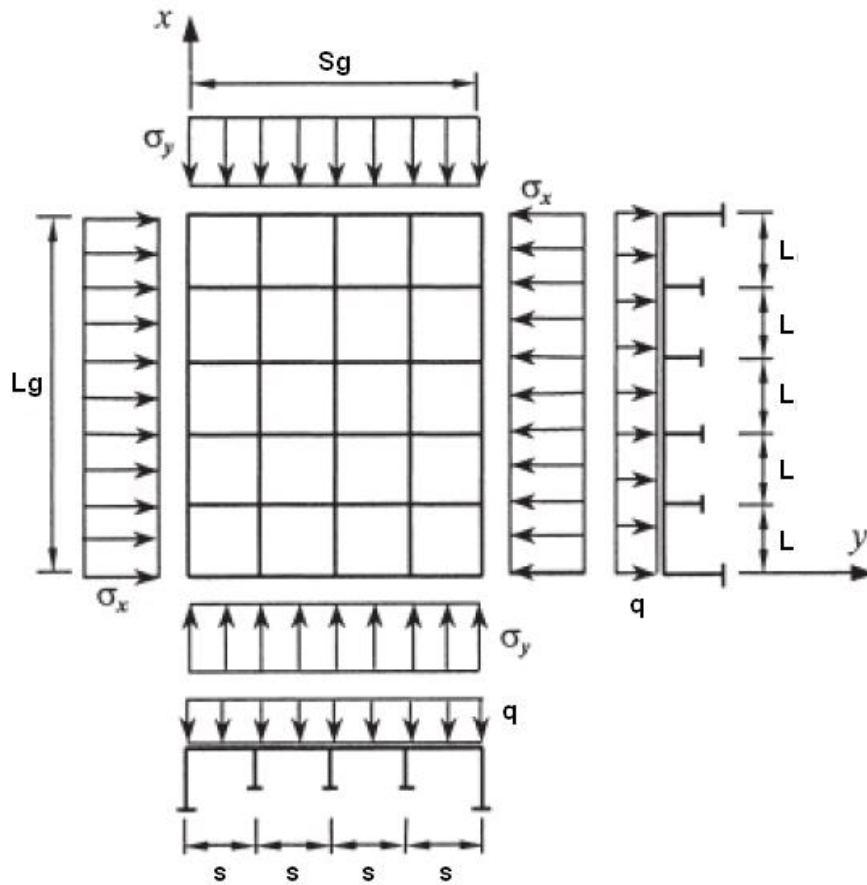
Fig 2.16 Orthotropic panel geometry and coordinate system.

The same counts for plate fields with variations in thickness, holes, cut outs, non-rectangular plates, cracks or other irregularities and anisotropic behaviors including composite materials. Besides the fact that it is out of the scope of the project, the standards do not or hardly specify any methods about it and therefore it becomes difficult to compare results.
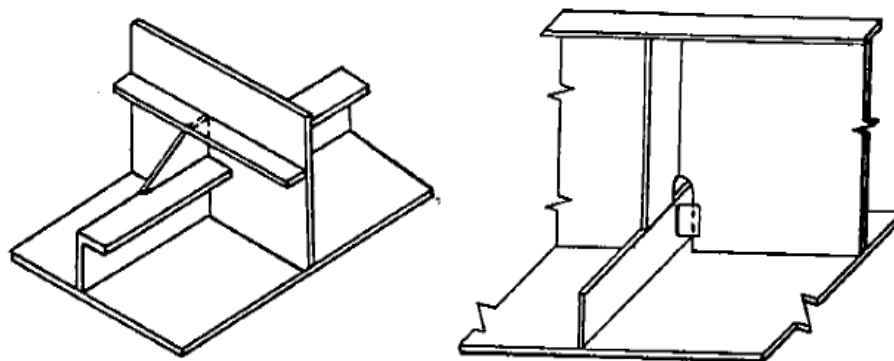

Fig 2.17 Example of a structures that are more difficult to check in detail on buckling [9].

3. Different buckling checks

The plates, stiffeners and girders can buckle in diverse ways. Firstly each plate field in between its support/stiffeners can buckle on its own. Secondly every of these plate sections has different buckling modes. And thirdly combinations of plates and supports have their separate buckling modes and parameters. Different buckling modes can be seen in fig 3.1 and include:

1. Unstiffened plate buckling limit
2. Unstiffened plate ultimate strength
3. Stiffeners local buckling limit
4. Stiffeners flexural buckling limit
5. Stiffeners torsional buckling limit
6. Lateral load limit
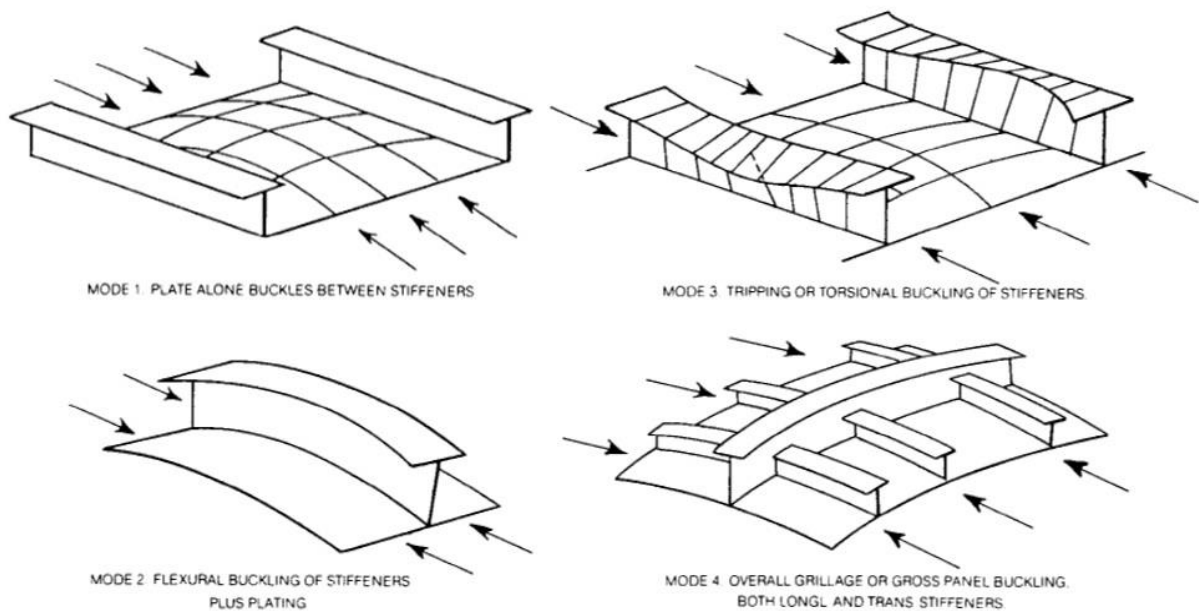7. Stiffened panel grillage buckling limit

Fig 3.1 Buckling modes within a panel. [10]

In short you could categorize the modes in three groups. The individual plate fields, the stiffener-plate combinations which you could call beam-columns and the girder-panel combination. In figure 3.2 the most significant cross sections are outlined in blue. Generally the minimum result of all these buckling factors will define the critical load for the complete panel.

When you try to search for a specific mode it becomes increasingly complicated. The different modes influence each other and are coupled in more than one way. Hence, a random buckling mode can show more types of buckling. Two different combinations from random analyses are illustrated in figures 3.3 and 3.4.
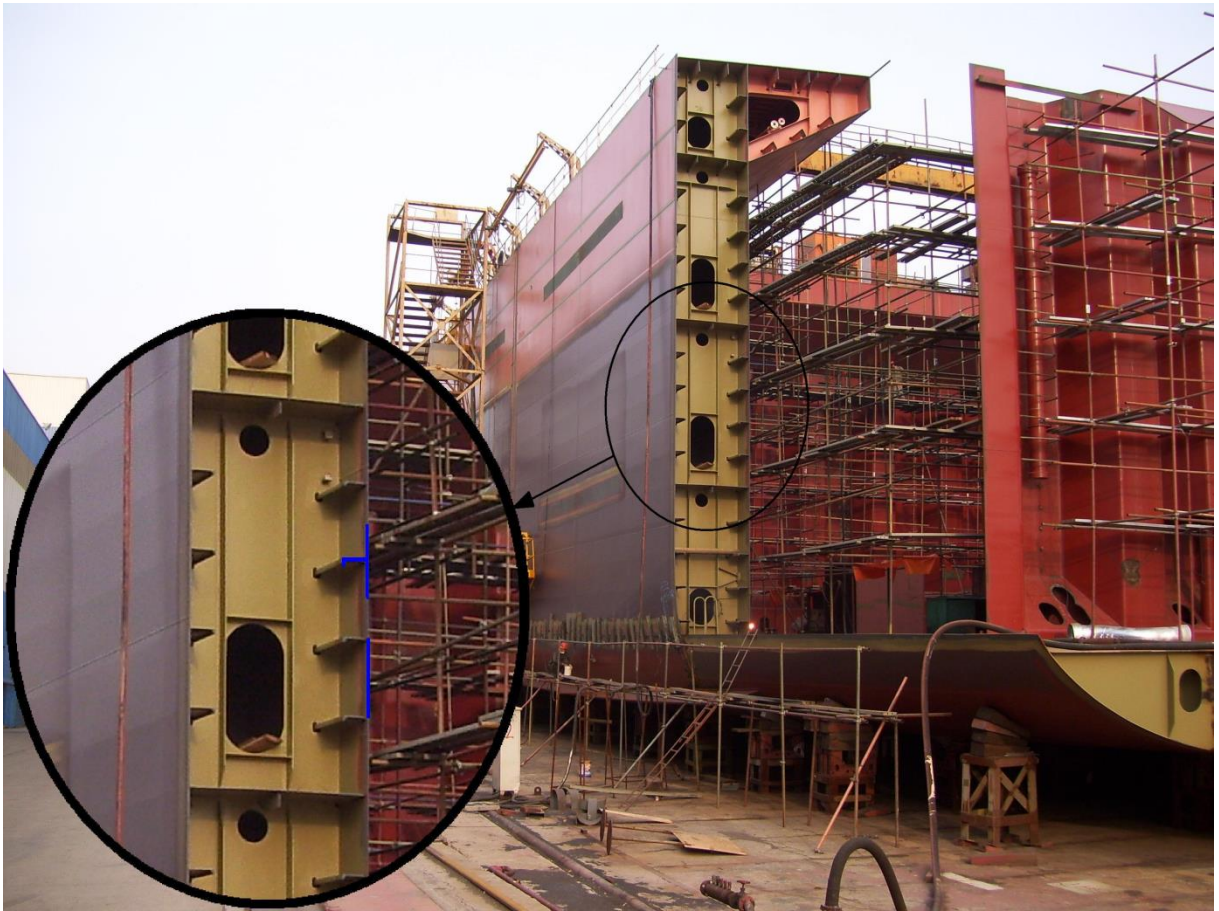
Fig 3.2 Illustration of the plate and column concept in a real plated structure.
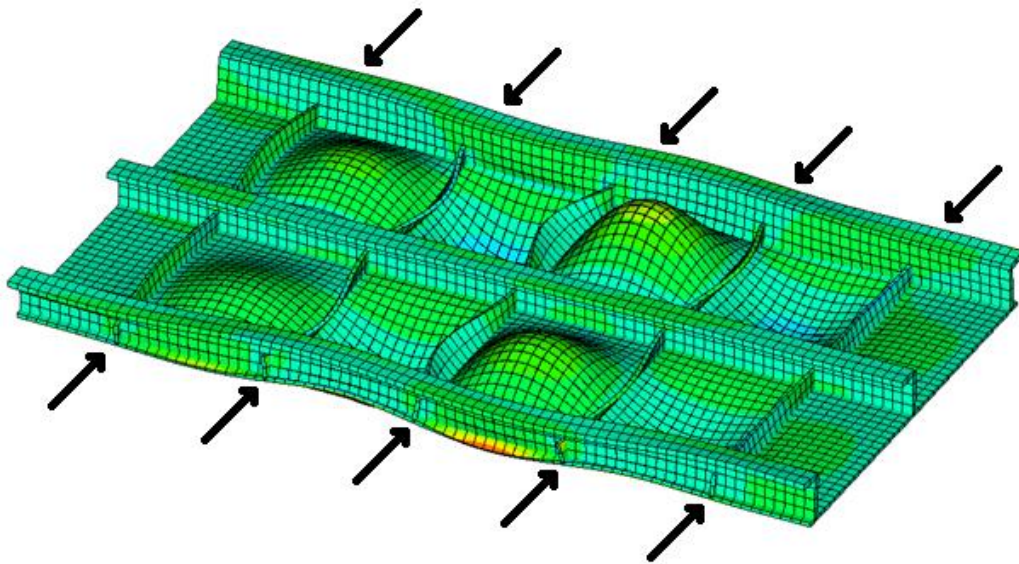
Fig 3.3 A combination of plate buckling and torsional stiffener buckling.
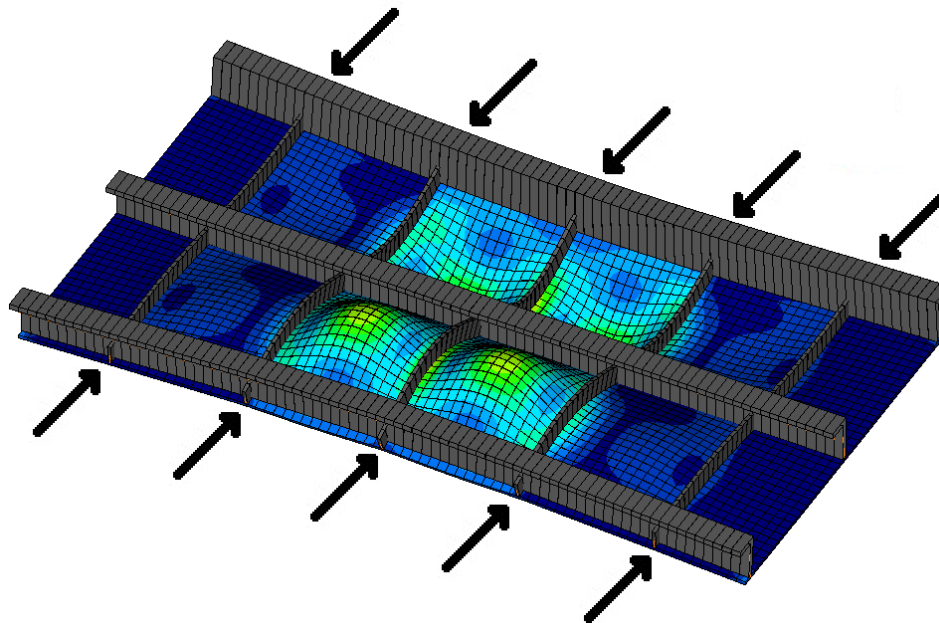
Fig 3.4 A combination of plate buckling, flexural stiffener buckling and grillage buckling.
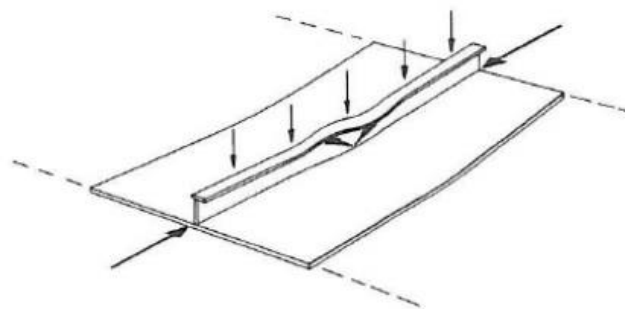
Figure 1.9 Mode III-2 – Local S-shaped mechanism
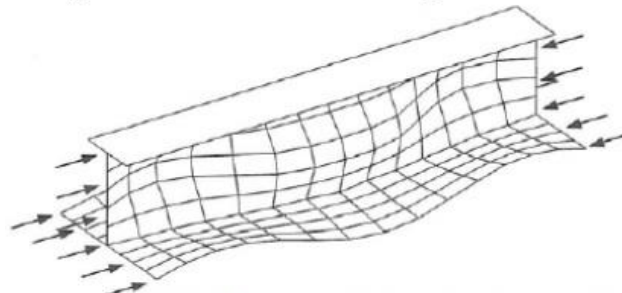
Figure 1.10 Mode IV – Local buckling of stiffener web

Figure 1.11 Mode V – Collapse due to stiffener tripping

Fig 3.5 A more detailed illustration of difference between stiffener buckling modes:

(a) local flange buckling, (b) local web buckling and (c) stiffener torsional buckling. [11]

3.1   Unstiffened plate buckling limit

The plate field in between stiffeners or other adjacent supporting structures is generally checked as an individual section. Web and flanges are plate fields as well but they are considered as local buckling of stiffeners discussed below. Theoretically in a perfect straight plate the in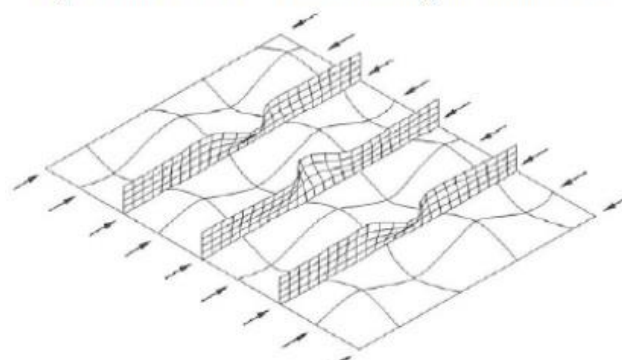-plane normal stresses and shear stresses will rise with increasing loads until bifurcation takes place and a sudden deflection occurs. In practice imperfections and (eccentric) applied loads will lead to plate bending up to a critical point when plate behaves non-linear. This critical point is the plate buckling limit.
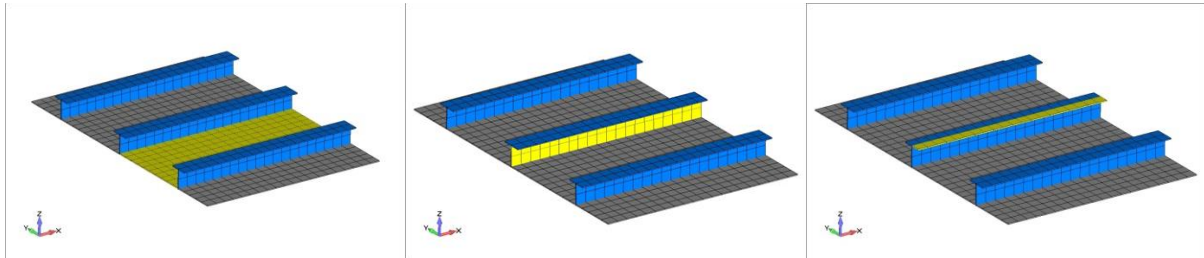
Fig 3.6 Overview of plate fields within the stiffened structure, each with its own design stresses to define: (a) plate field in between stiffeners, (b) web of stiffeners and (c) the flange of stiffeners.

There are two distinct parameters for plate fields, the aspect ratio α and the plate slenderness β. The aspect ratio is defined by the length L and width s of the plate, namely L/s. Plates in stiffened structures are usually bounded by relatively closely spaced longitudinal and widely spaced frames. The plate slenderness is calculated by dividing the width by the plate thickness t, s/t, and other parameters discussed in chapter 5.

It is well known that the elastic buckling of a simply supported plate under uniform compression forms a pattern of approximately square sinusoidal half waves along the plate length. The first eigenmode therefore normally forms a shape whereby the length of a longitudinal half wave is approximately equal to the width of the plate. Theoretically the number of half waves n equal the aspect ratio α. That means α=n or α=n+1 with non-integer aspect ratios. If the in-plane stresses do not form a uniform compression but also in-plane bending moments and/or shear stress, the buckling modes change shape accordingly (fig 3.9 and 3.10). In general a combination of the individual eigenmodes will occur.
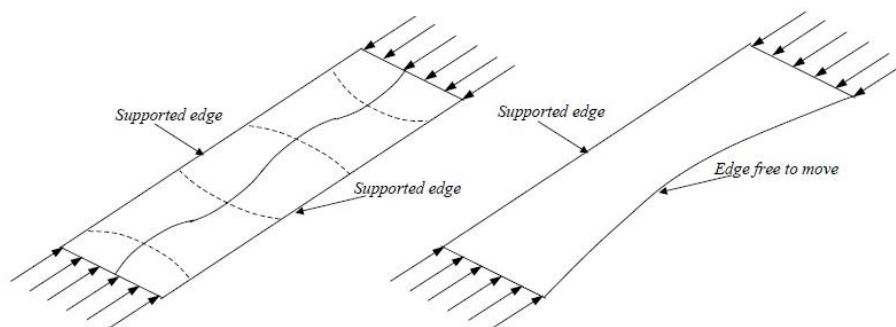
Fig 3.7 The simply supported and free edge boundary conditions with distinct buckling modes. [12]
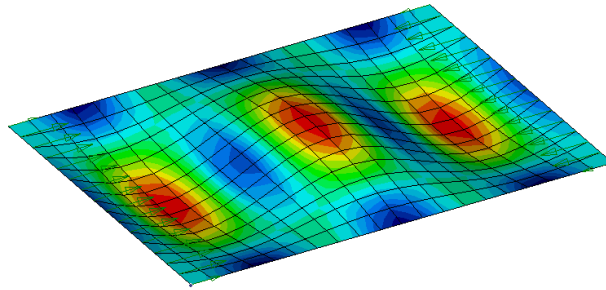
Fig 3.8 Third eigenmode for a longitudinal uniform compression.
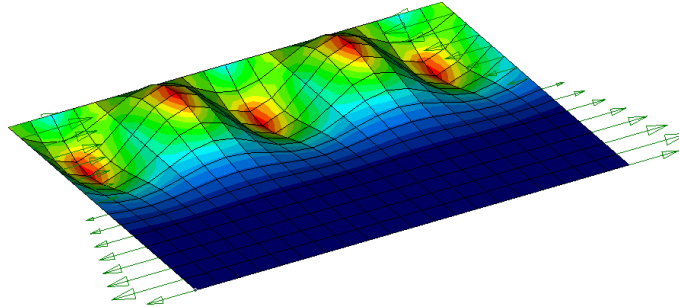
Fig 3.9 Fifth eigenmode for longitudinal in-plane bending moments.
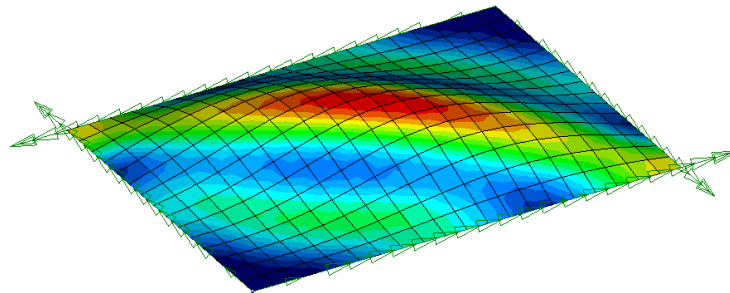
Fig 3.10 First eigenmode for uniform in-plane shear forces.

Several other parameters such as the boundary conditions (fig 3.7) also influence the behaviour. Lateral pressure will most definitely influence the buckling mode and the in-plane axial stresses. Plate fields are actually allowed to exceed their buckling limit as long as the ultimate strength is met. However, whether the plate will fail the buckling limit or not does also influence the other buckling checks for neighboring structures like stiffeners or the next side of a box girder.

3.2   Unstiffened plate ultimate strength

Permanent buckles are not accepted, but a thin elastic plate does not fail soon after it buckles, meaning that the plate exhibits stable post buckling behavior. By ensuring the maximum membrane stresses within a panel to stay below the yield stress condition (von Mises), permanent sets and buckles are prevented. This check has no meaning if the specific plate field already fails the buckling limit check discussed above and can be skipped in this case. But otherwise they can support loads significantly greater than its elastic buckling load without deflecting excessively. This is in contrast to the behavior of a compressed column section. Figure 3.11 below shows the transition from the buckling limit to the ultimate strength for a column. The plate fields act as sub sections of the model and fold in a pattern until at some point no additional strength can be retained and the yield strength is reach somewhere along the edge of one of the fields.
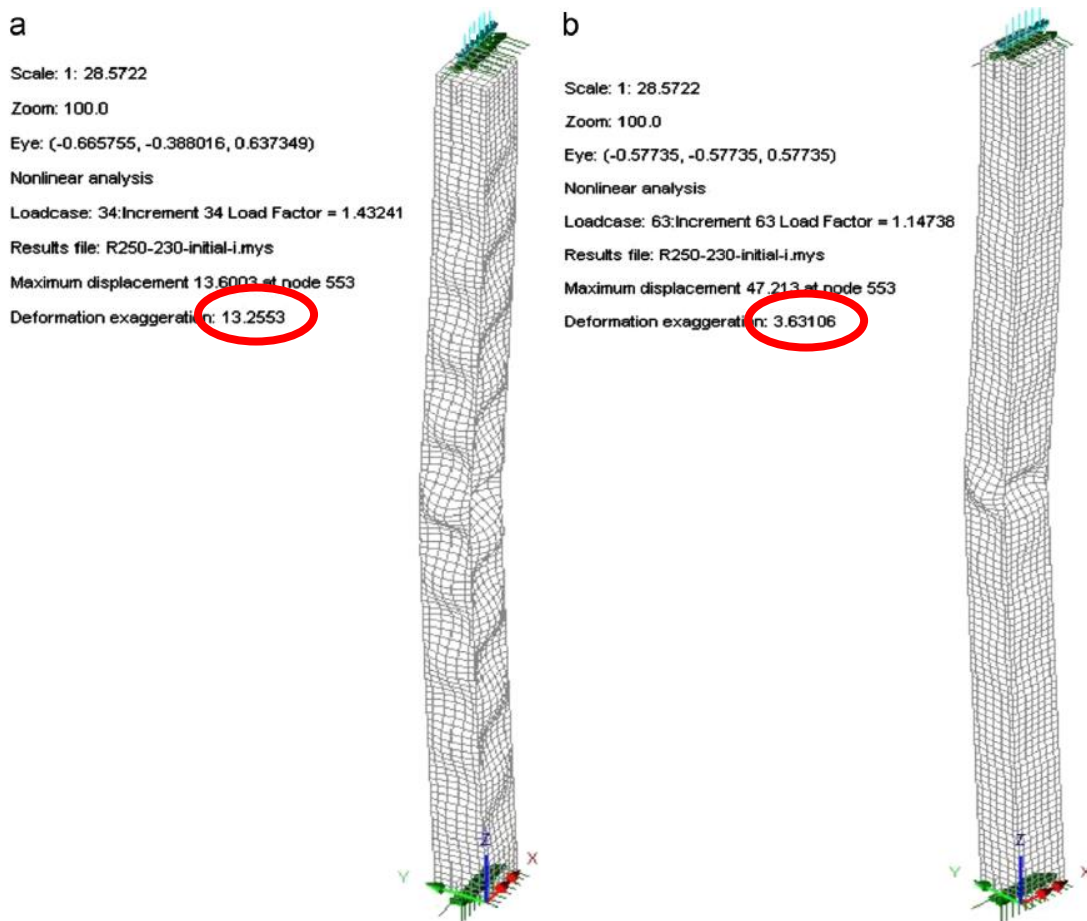
Fig 3.11 (a) Buckled shape (b) Collapsed shape. [13]

This post-buckling behaviour of a thin plate is due to the fact that the deflected shape cannot be developed from the pre-buckled configuration without a redistribution of the in-plane stresses within the plate. The plate will cease to behave linearly. Slender plate structures under compressive loading will tend to redistribute the present stresses to the edges, as indicated in Figure 3.12. This redistribution, usually favors the less stiff portions of the plate, and causes an increase in the efficiency of the plate.

The post-buckling effect is greater in plates supported along both longitudinal edges than it is in plates which are free along one longitudinal edge. This is because the deflected shapes of the latter have much less curvature than the former and the redistributions of the in-plane stresses are not as pronounced. In addition it is not possible to develop any lateral in-plane stresses along free edges. Therefore it is common to ignore any post-buckling reserves of slender flange outstands.

The redistribution of the in-plane stresses after buckling continues with increasing load until the yield stress σ_0 is reached at the supported edges. Yielding then spreads rapidly and the plate fails soon after.
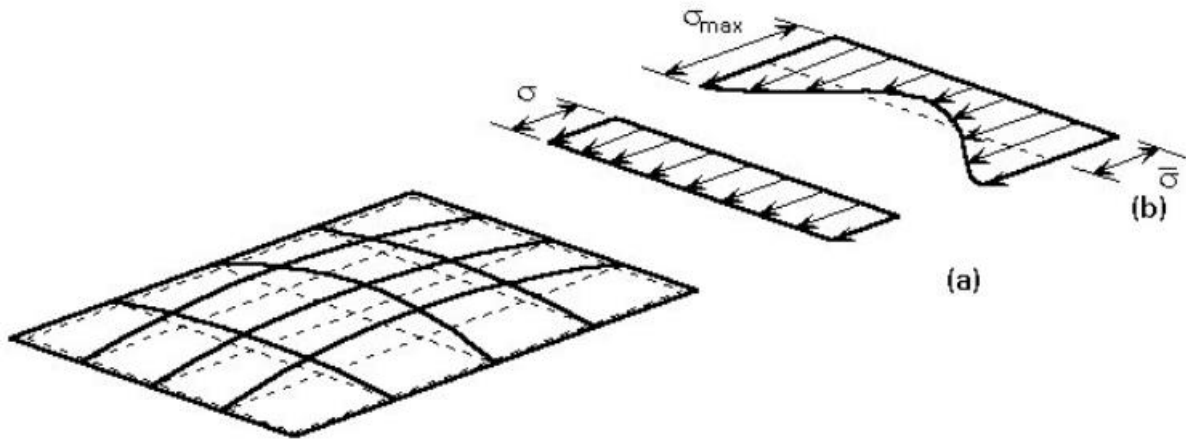
Fig 3.12 Stress distribution: in the pre-buckling range (a) and in the post-buckling range (b).

Since the determination of the ultimate strength of a thin flat plate is difficult, another method has been found. This method is called the effective width concept and can lead to satisfactory approximations. According to this concept, the actual ultimate stress distribution in a simply supported plate is replaced by a simplified distribution for which the central portion of the plate is ignored and the remaining effective width s_e carries the yield stress σ_0. It was proposed that this effective width should be approximated by

$$\frac{s_e}{s} = \sqrt{\frac{\sigma_{cr}}{\sigma_0}} = \frac{\sigma_{ult}}{\sigma_0} \qquad \{8\}$$

which is equivalent to supposing that the ultimate load carrying capacity of the plate $\sigma_0 * s_e * t$ is equal to the elastic buckling load of a plate of width s_e. Alternatively, this proposal can be regarded as determining an effective average ultimate stress σ_{ult} which acts on the full width s of the plate. Experiments on real plates with initial curvatures and residual stresses have confirmed the qualitative validity of this effective width approach, but suggest that the quantitative values of the effective width should be obtained with a correction.

$$\frac{s_e}{s} = \alpha \sqrt{\frac{\sigma_{cr}}{\sigma_0}} \qquad \{9\}$$
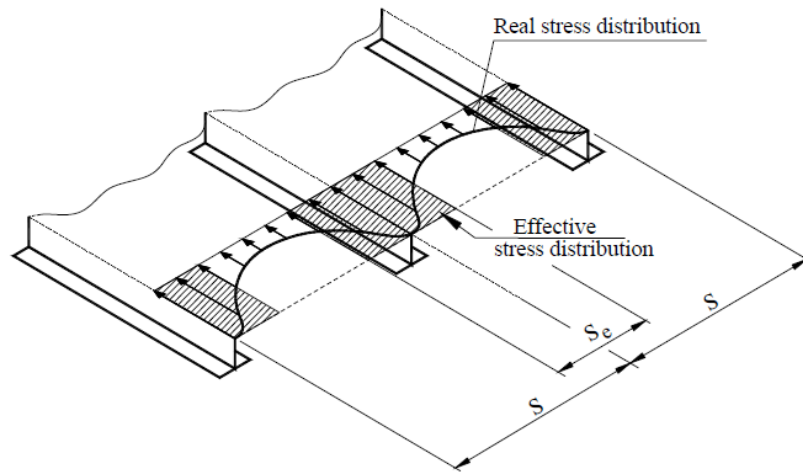
Fig 3.13 The redistributed post-buckling stress variation from an initial uniform stress distribution.

3.3   Stiffeners local buckling limit

Webs and flanges of stiffeners or girders are plate fields just like discussed above for the unstiffened plate buckling limit. They can be checked with the same methods. In general the standards make the assumption that stiffeners are designed correctly and stiff enough to resist local buckling. Simplified stiffness checks and stiffener proportions checks are therefore incorporated. This mode specifically implies a deformation as in figure 3.15b and no yielding or crippling problems. Note that local buckling and stiffener tripping as discussed below are two fundamentally different checks. Figure 3.14b clearly shows flange buckling however 3.14a does not clearly show web buckling as stated by the reference. Instead it has more resemblance with flexural and torsional stiffener buckling modes.
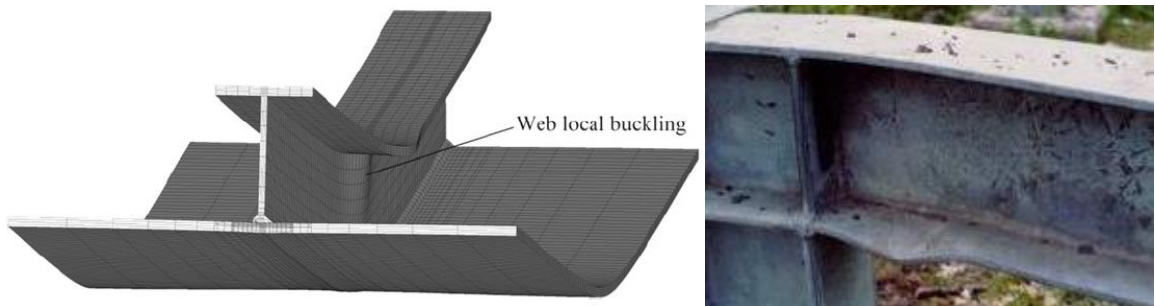
Fig 3.14 (left) Local web buckling and (right) local flange buckling. [14]
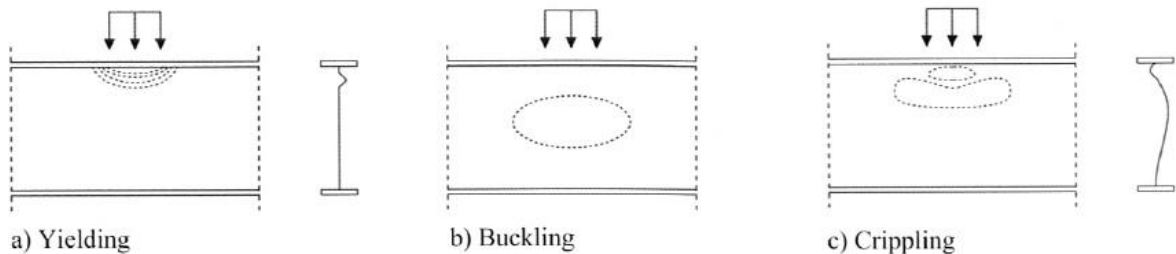
Fig 3.15 Failure modes at patch loading. [3]

Whether the plate will pass the buckling check or produce substantial redistributed stresses has an impact on the stiffeners and vice versa: the local buckling of webs may have an influence on the plates, see fig 3.16. Their influence can be either positive or negative depending on the buckling mode and direction of buckling. Depending on the type of stiffener, the web or flange has a free edge. Remember from the previous section that these plate fields will not need an ultimate strength check.
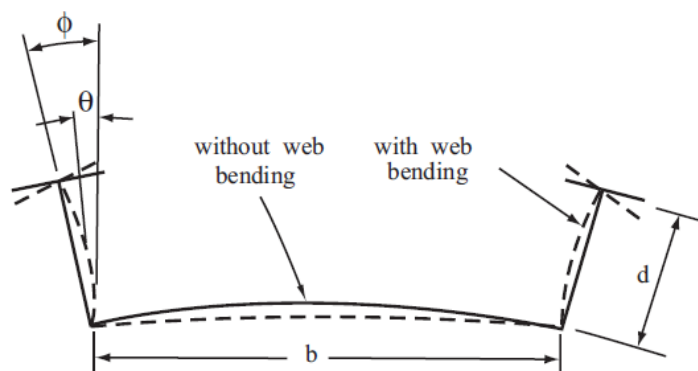
Fig 3.16 Effect of web buckling.

3.4 Stiffeners flexural buckling limit

The beam-column buckling is executed with the stiffener and part of the associated plate. Half the width of the adjoining plates is joined together with the stiffener itself to form a beam (fig 3.17). The standards and most theory consider such a part of the model so that it can be seen as an individual section. This section includes the stiffener and associated plating within an unsupported span. Accordingly, these methods check the beam-column on stresses due to axial compression and bending moments.

Fig 3.17 Illustration of the stiffener together with part of the associated plates.

The buckling modes depend on the bending resistances, the buckling length and the boundary conditions. The initial buckling is generally in the direction for which there is a weak bending stiffness, normal to the plate as shown in figure 3.18a. The stiffeners are placed on a plate with a reason. Stiffeners and girders work in much the same way but only with different buckling lengths.
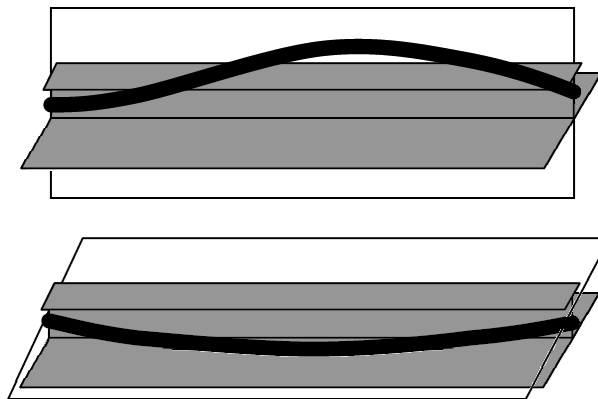
Fig 3.18 An arbitrary buckling mode in the (a) 'weak' bending direction
and (b) 'strong' bending direction. [15]

The two distinct parameters for beam-columns are the length L and the column slenderness λ. The longer and/or more slender columns are more prone to buckling. The length need to be carefully defined as the standards have corrections for when the end supports include brackets etc. Generally those details are not included in the model. This also means that you miss this extra stiffness in the stress results. Therefore, as long as the model is not that detailed, the buckling length should be manually decreased following the formulations in the standards. The column slenderness will follow from the dimensions.

O.F. Hughes and J.K. Paik give a clear explanation of effects due to lateral forces in chapter 3.8 of Ship Structural Analysis and Design [16]. Simple beam theory assumes that in any type of box girder, the stress should be constant across the flanges. However, in most cases the bending is not caused by the application of a pure couple to the ends of the beam. Rather, it is caused by lateral loads, and these loads are absorbed by the webs of the beam and not by the flanges. That is even for the case in which the lateral loads may initially act on the flanges such as pressure on the top or bottom. They are immediately transferred to the webs in the structure. The plating of the flanges can only take longitudinal in-plane loads if small local loads are not taken into account. Therefore the vertical loads act on the webs and cause them to deflect to some radius of curvature, thus inducing maximum strain in the flanges (fig 3.20). Since they carry maximum strain, and hence maximum stress, the flanges make the largest contribution to the bending stiffness. But, it is important to note that this maximum strain comes initially from the webs and only reaches the flanges by shear. This is illustrated in figure 3.19.
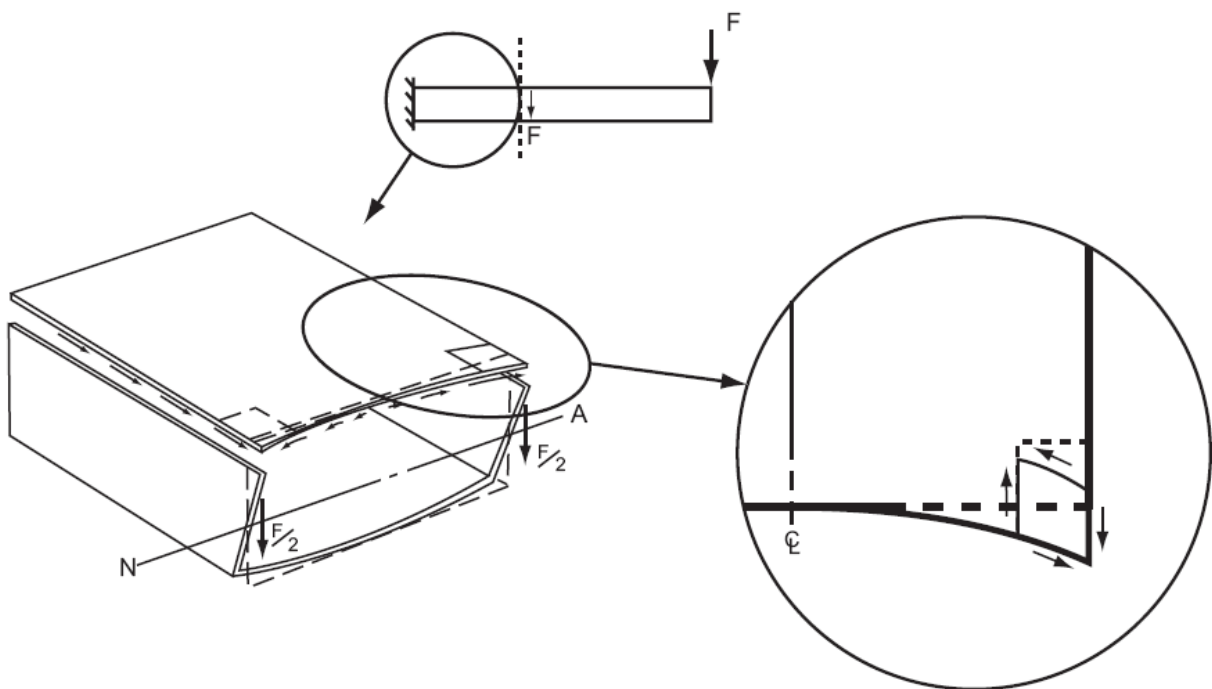
Fig 3.19 Shear lag in box girders.

At the upper edge the elongated web pulls the flange plating with it and this sets up shear stresses in the flange. The bending and shear stresses cause stretching and in-plane distortion of the flange. This phenomenon is termed the shear lag. Shear forces may also originate from torsional effects (fig 3.21). Shear lag occurs in any wide-flanged section. Conversely, there is no shear lag effect in pure bending. The exact distribution of stress in a wide-flanged section can be found using the mathematical theory of elasticity but this analysis is too complex for design calculations.
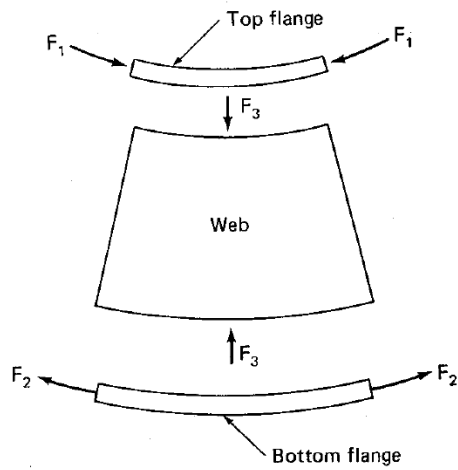
Fig 3.20 Squeezing of the web due to bending of the girder. [17]
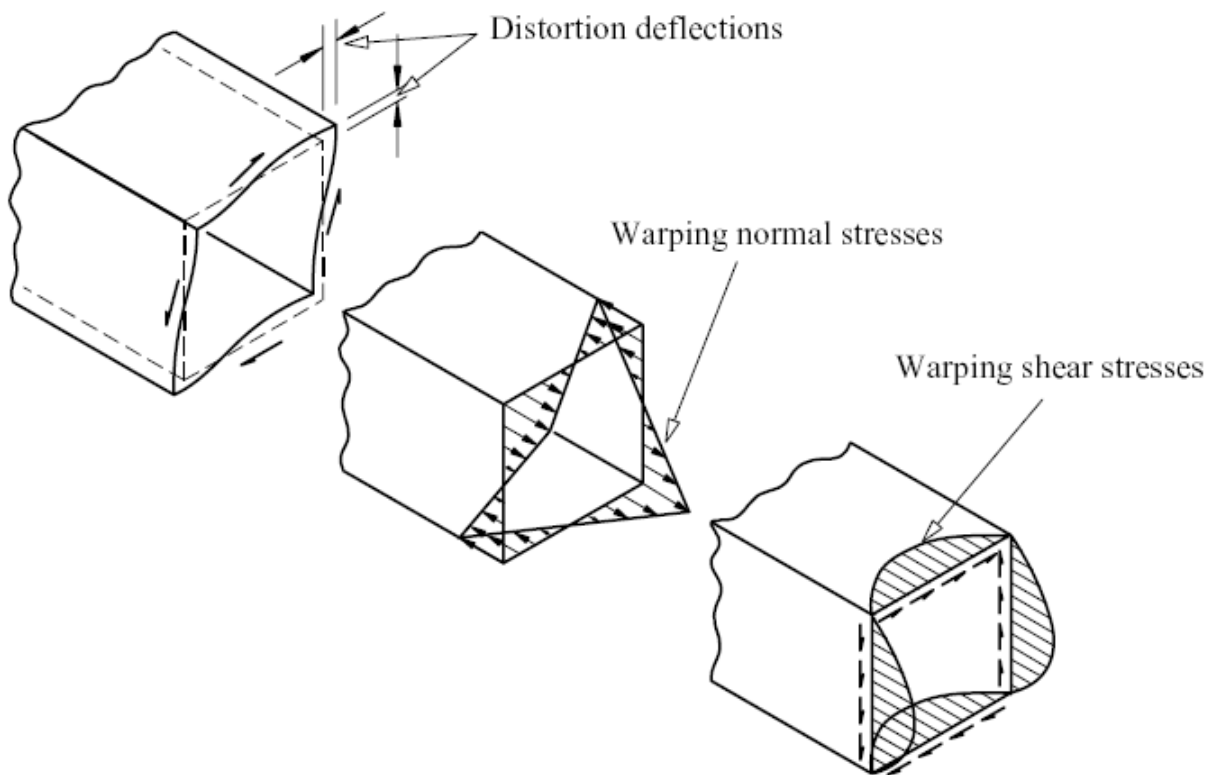
Fig 3.21 Warping stresses due to non-uniform distortions.

The shear lag effect in general varies from point to point along the length. Shear lag is of importance in beams having very wide flanges and shallow webs, such as aircraft wings. In steel box girders the effect is smaller. Even in box girder bridges which have large concentrated loads due to the point supports the effect is small. The magnitude of the shear lag effect dependent on the aspect ratio, the distribution of lateral loads, the relative proportions of web and flanges and the type of stiffener. The simple beam theory:

$$\sigma_{max} = \frac{M_y \cdot z_{max}}{I} \qquad \{10\}$$

is difficult to apply due to the shear lag. Rather than using a mean value of the stress distribution as a way of allowing for shear lag, it is preferable to retain the value of the maximum stress σ_{max}. Therefore, generally an effective width method is used which is illustrated in Fig 3.22 and is defined as:

"The width of plating which, when used in calculating the moment of inertia of the beam-column section, will give the correct maximum stress σ_{max} using simple beam theory. Also, the effective width must be such that the total longitudinal force in the flange is equal in the actual and simplified cases."
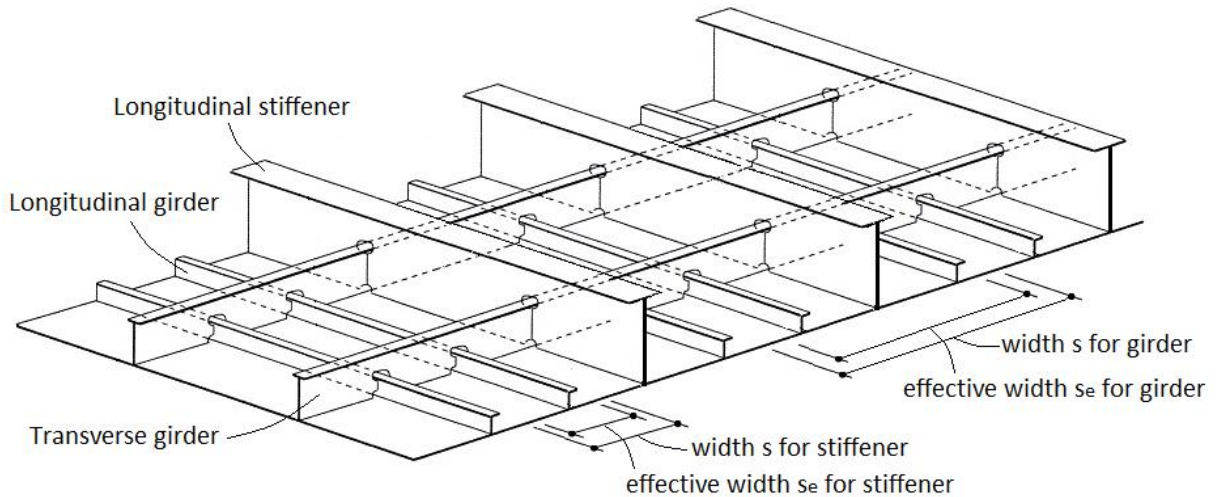
Fig 3.22 Overview of a plated structure with an illustration of the effective width method.

The effective width of the adjoining plates can be seen as the part that collaborates in the strength of the stiffener. These widths should then be used in calculating the effective moment of inertia I_e of the section, and hence the maximum bending stress in the beam. The method redefines the formula to:

$$\sigma_{max} = \frac{M_y \cdot z_{max}}{I_e} \qquad \{11\}$$

The most important parameter that determines effective width of plating is the ratio of flange width s to the span length L. A low L/s ratio results in a small ratio of s_e/s. But other parameters are available as well for calculation of s_e within different standards. The ABS, for example, reduces the effective width of the plate when the associated plates themselves do not satisfy the unstiffened plate buckling limit.

Note that the Euler's buckling stress σ_E is also influence by the same phenomenon. The formula (eq 2) seen in the previous chapter therefore changes to:

$$\sigma_E = \frac{\pi^2 E I_e}{A_e l^2} \qquad \{12\}$$

with use of both the effective moment of inertia and the effective area of the beam-column.

3.5   Stiffeners torsional buckling limit

Stiffeners are generally open thin-walled cross-sections and therefore have relatively small torsional stiffness. A stiffener may buckle by twisting (or rotating) about its line of attachment to the plating. This is referred to as the torsional buckling or tripping (fig 3.23). Tripping is usually plastic and catastrophic. The phenomenon is not the same as the column or beam-column type of buckling we have discussed above. It originates from torsional bending moments or from warping.

Torsional bending moments may be due to eccentric lateral forces on the stiffener in horizontal or vertical direction. Or due to the associated plates that do not satisfy the unstiffened plate buckling limit. When the adjoining plates buckle they may produce a torsional moment on the stiffener around the welding line as illustrated in fig 3.24. This is extra complicated since the second cause also depends on the particular buckling mode which the adjacent plates have. While if warping is the cause, then the adjacent plates may also rotate to some extent to accommodate the stiffener rotation. Notice in fig. 3.27a that the rotation of the plate fields in between stiffeners can be arbitrary. Basically, the torsional buckling says something about the rotation and translation of the cross section.
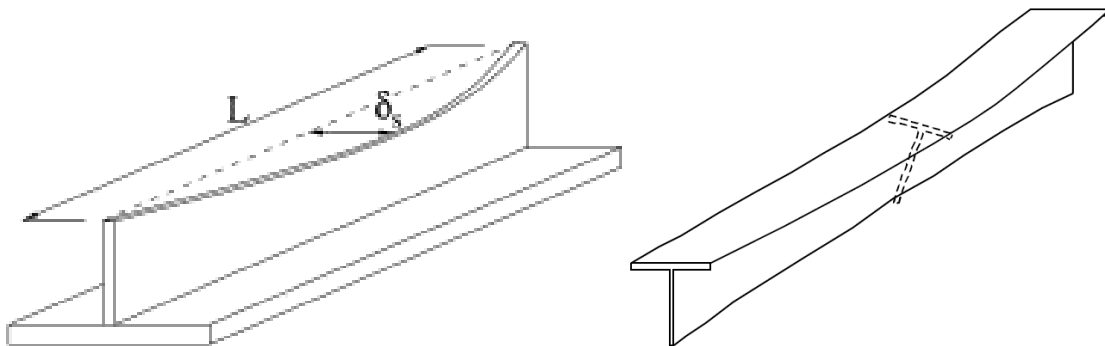
Fig 3.23 Illustration of torsional buckling (tripping).

Torsional buckling should not be confused with local web buckling. The disadvantages of the torsional buckling limit is that when a structure surpasses it, there is no additional ultimate strength left and immediate collapse of the stiffener is inevitable if the remaining structure also fails.
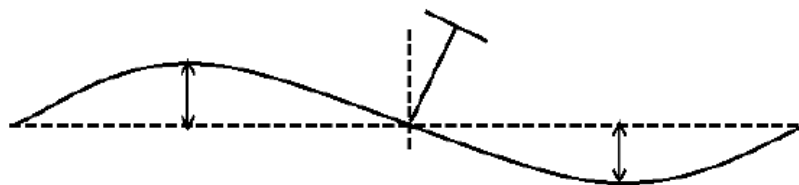
Fig 3.24 Buckled plates and a corresponding rotation of the stiffener. [18]

Shear stresses are generated when a thin-walled beam is subjected to an applied torque or as overall result from shear lag as discussed in the previous section. In turn, these shear stresses cause deformations of the cross-section. Flanges undergo in-plane longitudinal distortion and therefore cross sections do not remain plane. This distortion is commonly referred to as warping of the cross section

(fig 3.25). The stresses developed are illustrated in figure 3.26. When these deformations are not allowed to develop then the result can be a significant alteration of the torsional behavior. An example can be an axial movement restriction of end conditions. It occurs especially in the case of open sections such as stiffeners.
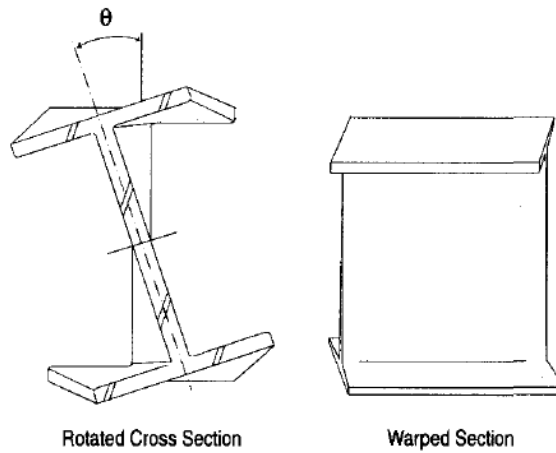
Fig 3.25 Illustration of the warping phenomenon.
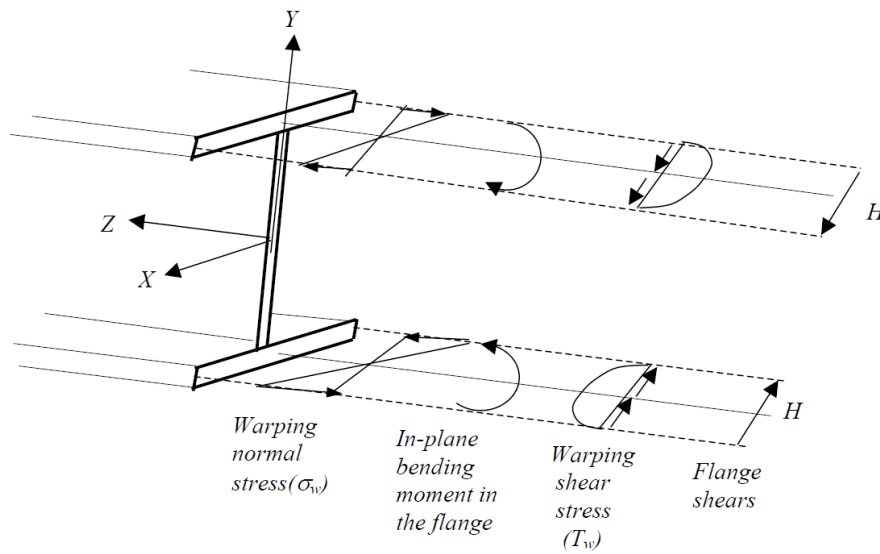
Fig 3.26 Visualization of torque and warping stress results [19]
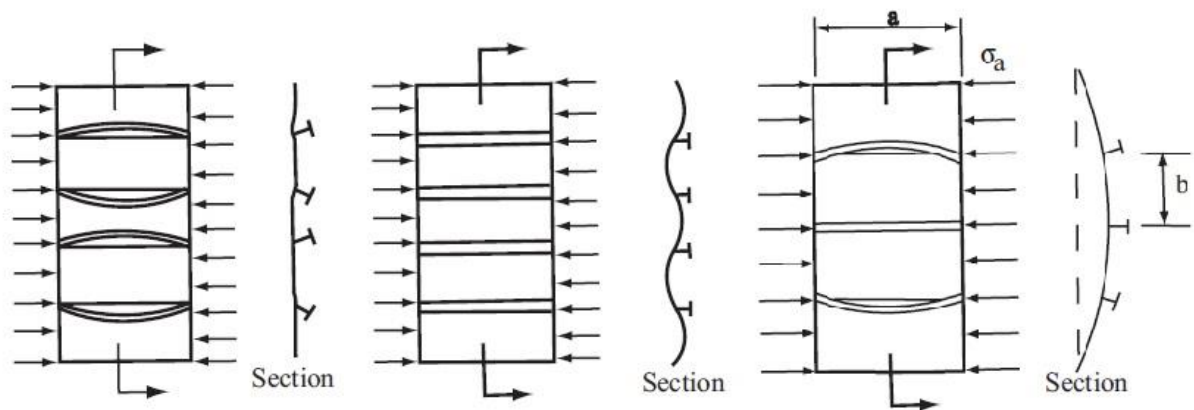
Fig 3.27 (a) Torsional buckling, (b) plate buckling and (c) grillage buckling.

A slightly simplified solution for stiffener tripping is presented in Hughes and used in the DNV. The result is one for stiffener tripping due to a uni-axial compression:

$$\sigma_{cr,tripping} = torsion + warping = \left(\beta \frac{GI_t}{I_p}\right) + \left(h_s{}^2 \frac{\pi^2 EI_z}{I_p l^2}\right) \qquad \{13\}$$

The key to minimizing the possibility of this torsional buckling mode is to maximize the torsional stiffness GI_t/I_p of the stiffener. Note that the shear modulus or modulus of rigidity G is already high for steel. Therefore, the best way to minimize tripping is by maximizing the polar moment of inertia I_t/I_p of the stiffener.

Taking a look at the second half of the formula, you should be able to see that the design goal to prevent tripping is to desire a stiffener to be short (small I_p) and wide (large I_z). Figure 3.28 illustrates the idea however notice that this is the opposite from the desire to maximize vertical bending stiffness which is the main purpose of the stiffener. Therefore, designing a stiffener to resist tripping is partially a compromise with the resistance to vertical bending. Additionally the webs and flanges should not get too wide for that may lead to local buckling.
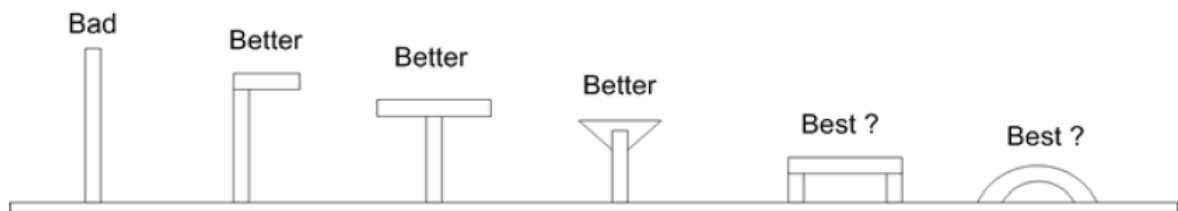
Fig 3.28 Stiffener design options for torsional stiffener buckling. [20]

Another solution is to install tripping brackets at several spots along the length of the stiffener to reduce the buckling length and increase the warping resistance and thus increase the tripping resistance.

3.6   Lateral load limit

In real practice the lateral pressure is a load that has its influence on a structure such that it should be a key parameter on all the previous buckling modes. Still, the unstiffened plate buckling limit and the unstiffened plate ultimate strength do not depend on the lateral pressure according to the ABS while the DNV only has some kind of reduction factor. For compensation there is a lateral load limit check in the ABS, but it is strange that standards are so different from each other. One should think that the lateral load at least should be an important influence. It is after all one of the key parameters that give rise to in-plane normal stress results as shown in figure 3.29.
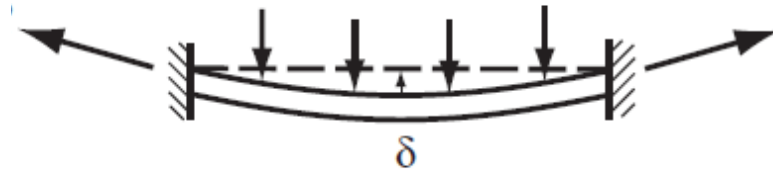
Fig 3.29 Influence of in-plane stresses and the relationship with the lateral pressure.

An explanation of influences at the shear stresses has been made above already but there are also influences at the local buckling. Besides the in-plane stresses there are out of plane bending moments as well. The local buckling of the plate influences the behaviour of the supporting structure. Figure 3.30 illustrates that the load may induce a change in the constraints from simply supported to a more clamped situation. This can have a positive result on the buckling resistance although it may also have an effect on the shear lag which would be more of a disadvantage.
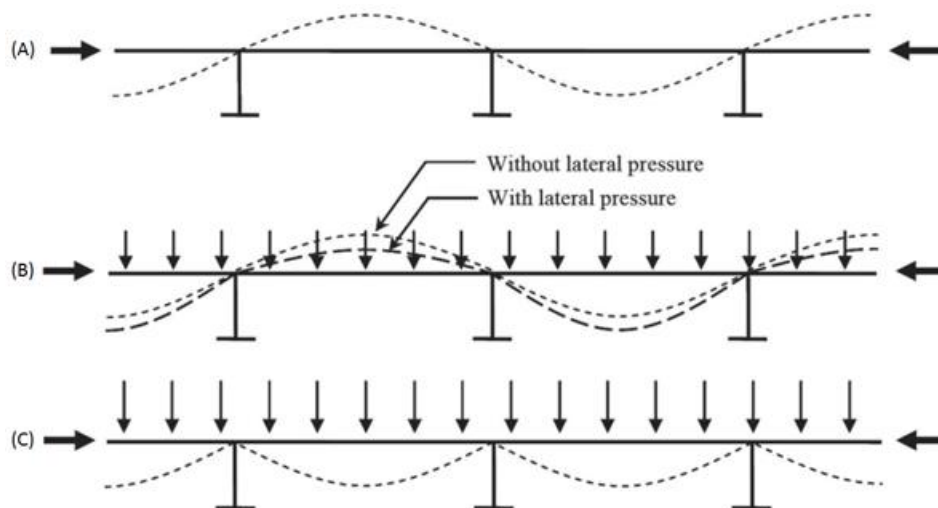
Fig 3.30 Schematic of the axial compressive buckling patterns of a plate (a) Without lateral pressure, (b) with a relatively small amount of lateral pressure and (c) with a relatively large amount of lateral pressure.

For more details about the lateral load limit, see the standards or more specific literature. The present study will be restricted to the previous five buckling modes, a considered choice to limit the amount of parameters while keeping the most common real live situations.

3.7　　Stiffened panel grillage buckling limit

The global buckling factor of a panel seems to count as the minimum from all previous checks. However, besides individual buckling modes the structure could also buckle in a combined overall direction as seen in figure 3.32. Coupled structures would highly probable be very influencing as well (fig 3.31).
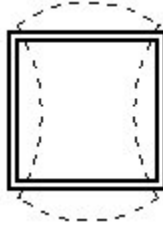
Fig 3.31 Example of coupling between stiffened panels.

Each separate section, plate fields and beam-columns, may reach a relatively small, non-catastrophic deflection while the combined deflections of all sections see to an excessive amount of deflection in the entire panel. Thus elastic or inelastic buckling of an entire panel made up of several frame bays. This is also known as "global buckling", "gross panel buckling", or "overall grillage buckling". The general solution is formed by analyzing if the major supports of the panel are sufficient by checking whether girders pass their column buckling and tripping buckling analyses. And considering the panel as an equivalent stiff plate field with average in-plane compressions delivers a second available check.

The first approach is doable since girders can be checked in the same manner as stiffeners. However, the definition of a girder, and what sets it apart from stiffeners, is not clear. Figure 3.22 illustrates an effective width for girders but not only the plate but also stiffeners are within this area, hence these should be an influencing parameter in the calculations. Neither do the dimensions clearly state when a supporting structure should be considered a stiffener of a girder. The buckling length is part of this choice as well. A small literature study did not provide suitable answers so further research should be carried out.
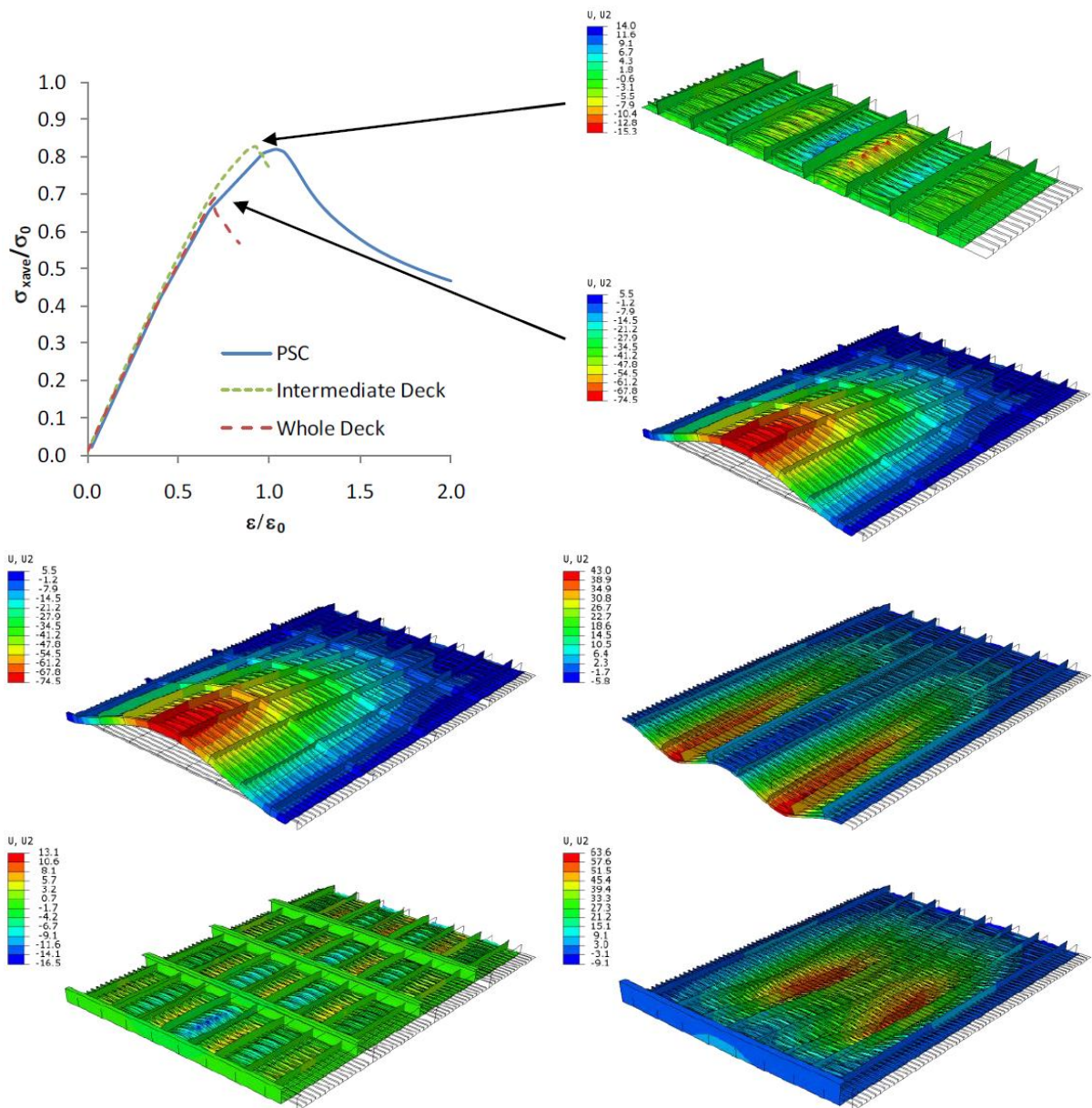
Fig 3.32 Several gross panel buckling modes. Notice the analysis done by S. Benson in which buckling of the whole deck may substantially reduce the total critical load.

4.   Problem definition

The studies on the ultimate strength of plated structures have continued over several decades and significant progress has been achieved. However, there are some aspects of this subject unresolved. Research efforts in the ultimate strength of plated structures are mainly devoted to: development of analytical formulas, development of simplified methods, assessment of effects of initial imperfections and assessment of effects of fatigue cracks. However little to none research is known in which the development of simplified methods is used for implementation of the standards. Which is weird since those are generally accepted assesment methods.

4.1   How to check buckling

Analyzing whether a plated structure is vulnerable to buckling is a complicated task. Instability of structures under a wide variety of loading conditions has been extensively studied using numerous approaches. Analytical approaches to predict the strength include design charts, empirical approaches, the beam column method, deflection theory, minimum potential energy formulations and standards. Not surprisingly, the last approach is a combination of many of the other approaches.

Empirical approaches need test setups which are widely used to check different kind of structures, designs or materials. Nowadays the checks with real subjects are very limited, understandable because of the high costs but also the difficulties in applying the correct boundary condition and loads (see appendix P for some examples).

The ability of a plated structure to sustain an applied load may be understood as the summation of individual contributions of each stiffened plate element in the entire cross section between two frames. The main difficulty of this beam column approach is to know the relation between the stress and the strain over a large range of strains including pre-collapse, collapse and post-collapse.

Classical theory, founded on the large deflection plate theory of von Karman and Maguerre, can be implemented to calculate the local buckling of a stiffened panel assuming an orthotropic plate model. The use of large deflection equations means that the stress distribution over the panel is non-uniform. The governing nonlinear equations (fig 4.1) of large deflection orthotropic plate theory deliver complicated coupled partial differential equations. When assuming several deflection functions one can approximate the buckling limit.

Energy methods include Galerkin and Rayleigh-Ritz. These techniques assume the structure is elastic and will buckle conservatively. Thus they are limited to calculate the elastic buckling load of beam-columns. Numerical methods are more appropriate for inelastic beam-columns. This is because the beam is divided into segments, with displacements calculated at each point in between, rather than the assumption of the energy method that displacement is a continuous function.
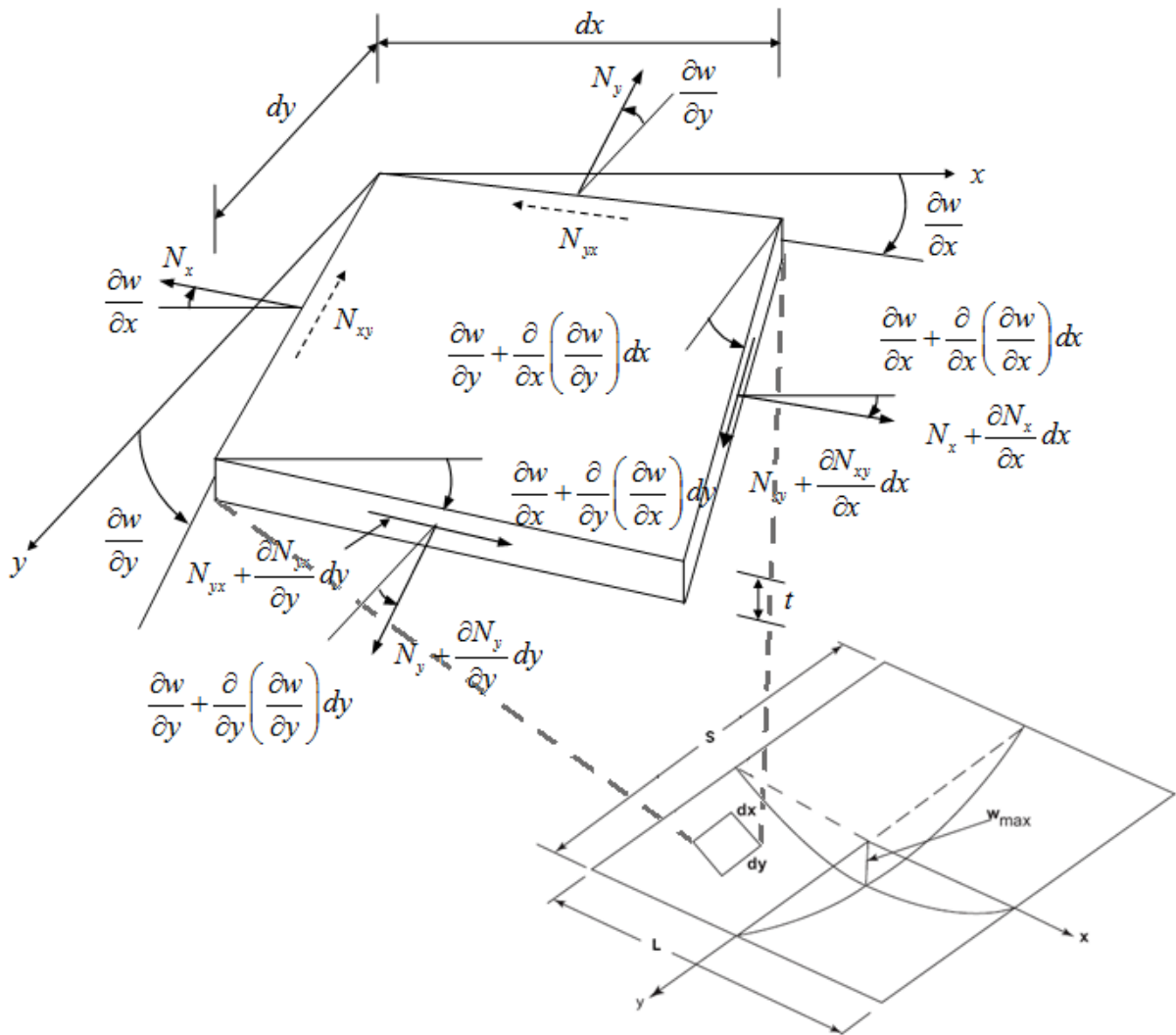
Fig 4.1 Large displacement theory with the in-plane forces on a plate field.

The numerical analyses can be linear and non-linear calculations in FEM software packages. Some extra explanations about these are given in appendix J. None of the methods is perfect but the standards are generally accepted as sufficient. However the idea is to combine the numerical linear FEM analysis and the standards and their strengths to get a consistent design procedure.

4.2   Problems with current way of checking

Without taking other methods than standards and FEM analyses into account there are still some serious difficulties at hand. The standards provide several checks but they are some sort of blank form with large and complicated formulas which should be filled in to check if your design is ok. Whether average engineers also understand how the checks work is questionable. Nowadays everyone can model something in a finite element package but doing a correct analysis is something completely different. Even more, it is already surprisingly difficult to define what parameters/values you should fill in the formulas of the standards.

Big models for planes, cranes, ships or other kind of offshore structures can consist of a large amount of panels. Methods in FEM packages become therefore necessary purely due to the amount of checks needed but the size of the complete models make correct use a lot more difficult. You most likely get an upper bound value which only says something over a specific part of the structure and gives no information about the rest of the model. Therefore an individual check of each plate field is required which is not only a lot of engineering work but also brings more uncertainties in the calculation. What parameters do you take into account? Or even, what kind of analysis do you carry out?

Eigenvalue buckling analysis predicts the theoretical buckling strength of an ideal elastic structure. It computes the structural eigenvalues for the given system loading and constraints. This is known as classical Euler buckling analysis. However, in real-life, structural imperfections and nonlinearities prevent most real structures from reaching their eigenvalue predicted buckling strength; it over-predicts the expected buckling loads. This method is therefore generally not recommended for accurate, real-world buckling prediction analysis. In-depth explanation of the method can be found in appendix J.

Nonlinear buckling analysis is more accurate than eigenvalue analysis and gives good conclusions if correctly executed. Its method is very simple: it gradually increases the applied load until a level is found whereby the structure becomes unstable. The true non-linear nature of this analysis thus requires the modeling of geometric imperfections, material nonlinearities and loads such as residual stresses. These requirements initiate a good amount of uncertainty in the analysis since all parameters have to be known fairly detailed and applying them correct requires a good understanding from the engineer. Therefore, whilst nonlinear FEM is feasible for a stiffened panel model, simplified methods are also highly relevant to provide an efficient prediction of buckling strength behavior of a structure.

Whether it is a linear or non-linear analysis, your model might not be suitable for these types of analyses. Figures 4.2 and 4.3 show eigenmodes for the same model with different mesh sizes. While the linear static stress results are rather consistent, the eigenmodes and eigenvalues are not. A coarse meshed model may actually say that it can take up more than twice the amount of load compared to a fine meshed model as illustrated in figure 4.2. Neither can the coarse meshed model show individual plate buckling or flexural stiffener buckling etc. The question whether the buckling analyses from finite

element modeling software programs are correct or not, hence indicates the need for a different check. The standards are already specifically the method which the engineer would like to compare his or her model with, even though the analysis is being done in a FEM package. However even the linear static stress results cannot be compared directly to standards like the ABS or DNV.

Whatever FEM analysis you do, stress results will be the outcome you get. But the input for the ABS and DNV standards are no stress results but simplified applied loads, described in figure 4.4a for the plate field and figure 4.4b for the beam-column. Considerable research has been done on theoretical buckling modes, deflection functions and reduction factors. However the method on how to convert FEM results into parameters for standards remains unknown. The interaction formulae given in standards are conservative and simple, considering the complicated nature of buckling, which is not that obvious from a FEM perspective.

Fig 4.2 Plate model - Load case 1: (left) Results of the linear static analysis for the coarse, middle and fine meshed models, (right) results of the first buckling mode for the coarse, middle and fine meshed models. The model itself is discussed in chapter 6.
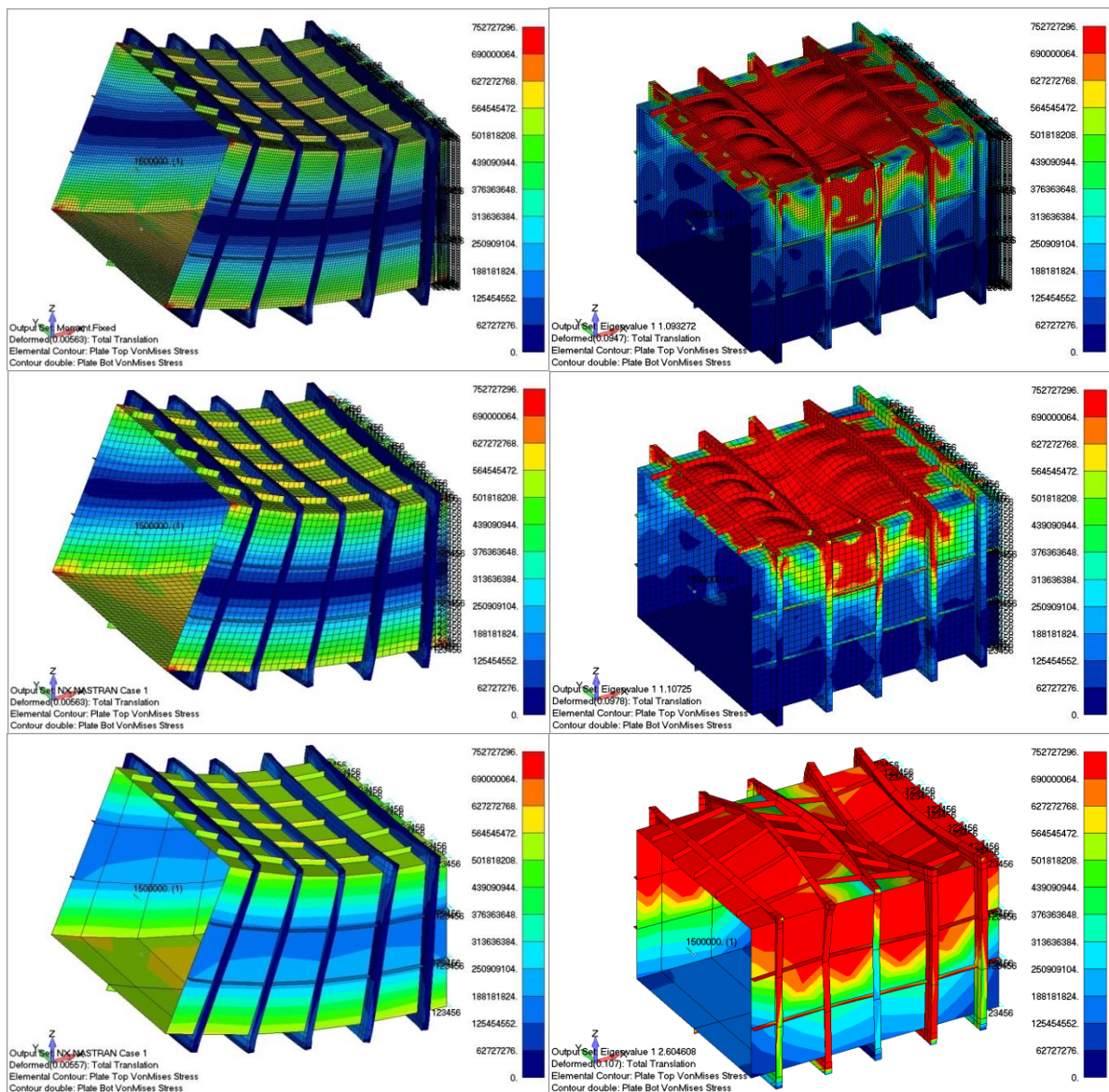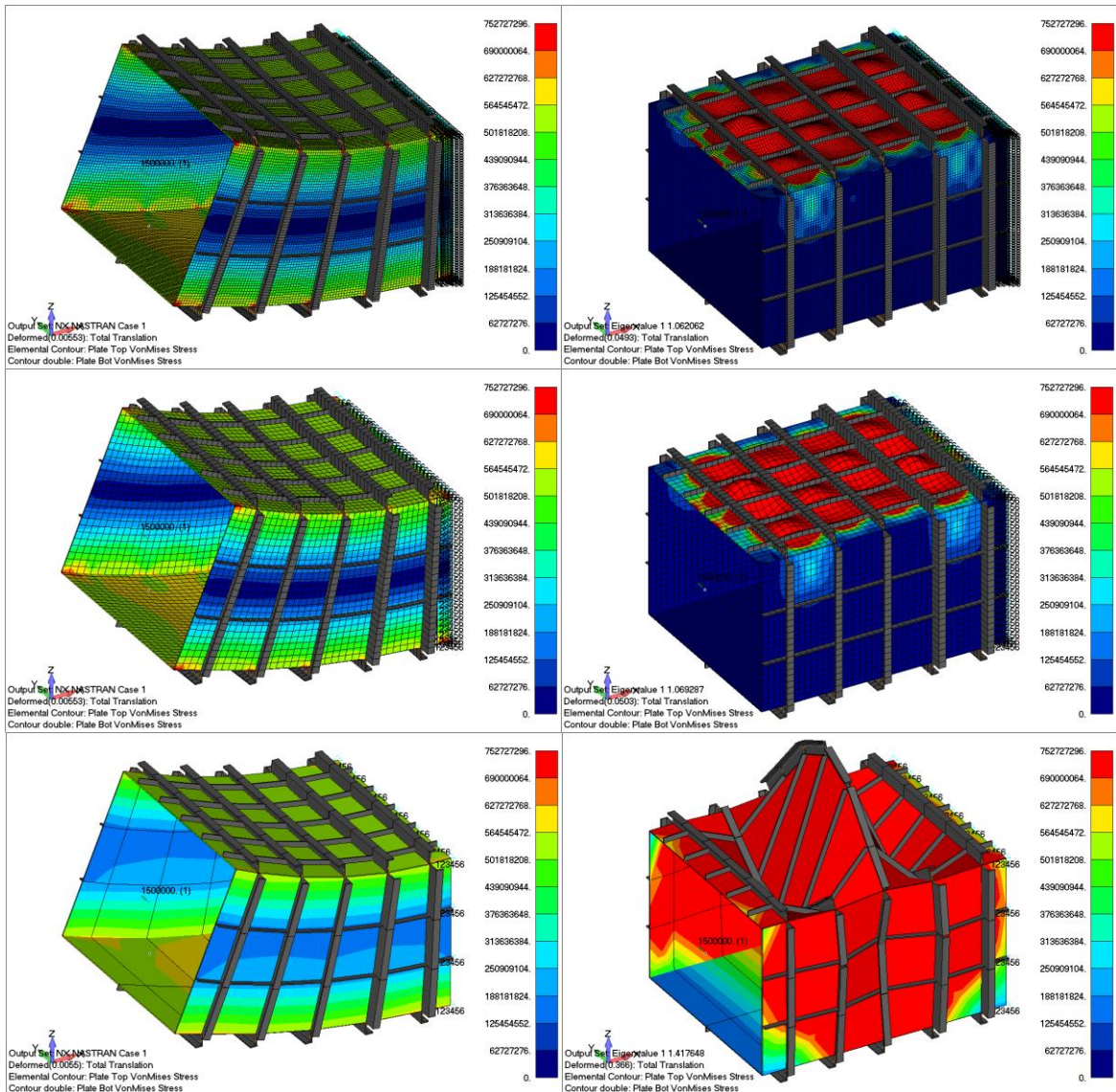
Fig 4.3 Beam model - Load case 1: (left) Results of the linear static analysis for the coarse, middle and fine meshed models, (right) results of the first buckling mode for the coarse, middle and fine meshed models. The model itself is discussed in chapter 6.
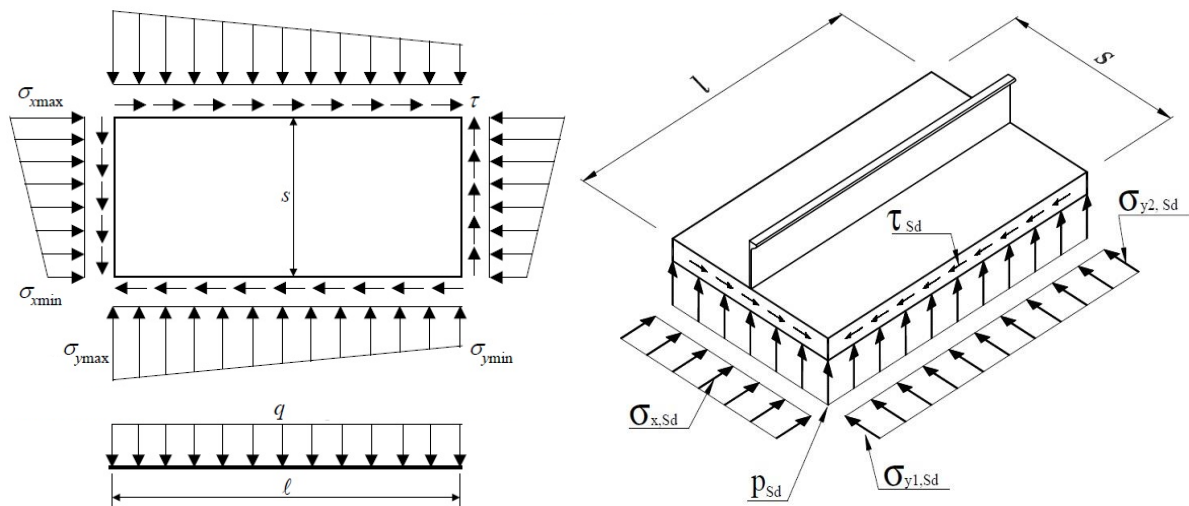

Fig 4.4 Overview of the input design stresses for (a) plate buckling and (b) column buckling.

4.3   Solving the panel

Hence, the aim is to form a method on how to convert FEM results into parameters for standards. The study mainly aims on how to convert linear FEM results into design stresses needed for the buckling checks of unstiffened plates and beam-columns. A new implementation method will be set up to provide these factors. The combination of FEM static stress results, the new methods and standards will provide buckling factors. These can subsequently be compared with the linear or non-linear FEM buckling checks. The new method should have the potential to:

- Reduce the uncertainties in current buckling checks due to the processing by the engineer.
- Substantially reduce calculation time and automate the process to reduce the amount of work for the engineer.

This thesis is a follow up on the work of Ottar Hillers [21]. He already made a good start on the extraction of design parameters for the unstiffened plate buckling limit and unstiffened plate ultimate strength. His conclusions provide some initial research start points. The buckling of the beam-columns will be the extension from that.

Input design stresses:

Plate buckling	Column buckling
σ_{Xmax} = maximum stress in longitudinal direction	σ_x = uniform stress in x direction
σ_{Xmin} = minimum stress in longitudinal direction	σ_{Ymax} = maximum stress in transverse direction
σ_{Ymax} = maximum stress in transverse direction	σ_{Ymin} = minimum stress in transverse direction
σ_{Ymin} = minimum stress in transverse direction	τ = uniform shear stress
τ = uniform shear stress	q = lateral pressure
q = uniform lateral pressure	

Apart from all parameters you have to consider to get to realistic input design stresses, there are two subjects specifically of interest for the buckling check, namely the mesh size in the model and the use of beam elements in the model.

In practice models are made with different mesh sizes. A fine mesh (fig 4.5a) requires more engineering time but provides more detailed results which should be better in approximating the reality. Furthermore you can provide more details in the model such as holes, gabs, non-continuous stiffeners etc. which are impossible with only one element per plate field. However known buckling analyses are based on very coarse meshed models with only one element per plate field/web/stiffener (fig 4.5b). This is because a plate element in FEM software gives per definition the exact input loads as described in figure 4.4a. These can immediately be used in the standards. While in contrast a finer mesh gives some sort of stress distribution which does not need to be linear at all.
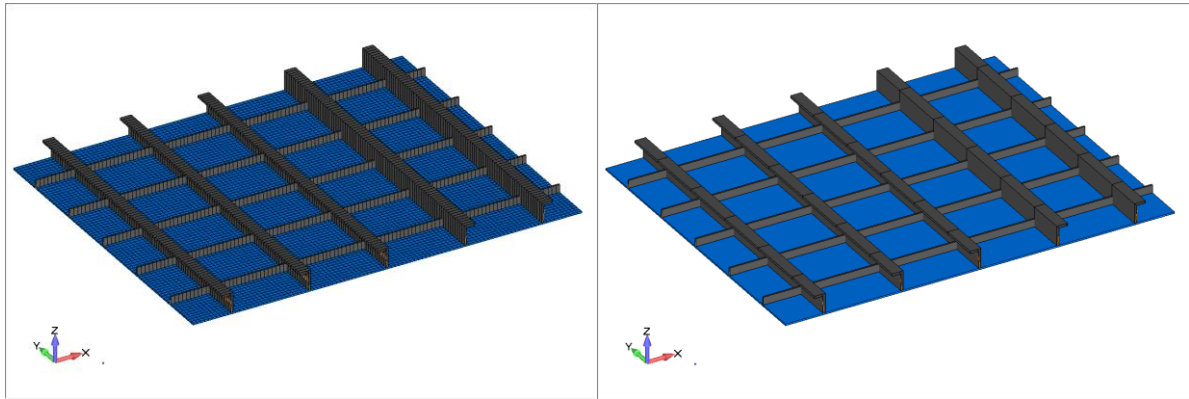
Fig 4.5 Difference between a fine (a) and a coarse (b) meshed panel.

The use of beam elements in the model applies to stiffeners and girders. Instead of detailed modelling one can provide a line element with specific cross section area properties. These input parameters such as the shape of the stiffeners, web height, web thickness, flange width and flange thickness can easily be changed or updated. It provides a rather good improvement in options for engineers so no wonder it is therefore used a lot in practice. A secondary advantage is that for the buckling check recognition of the webs, flanges and the shape of stiffeners is necessary and the properties of a beam element provides them instantly. Otherwise one should first recognize which plate elements form a web or flange and how these plate fields then together form a stiffener or girder.
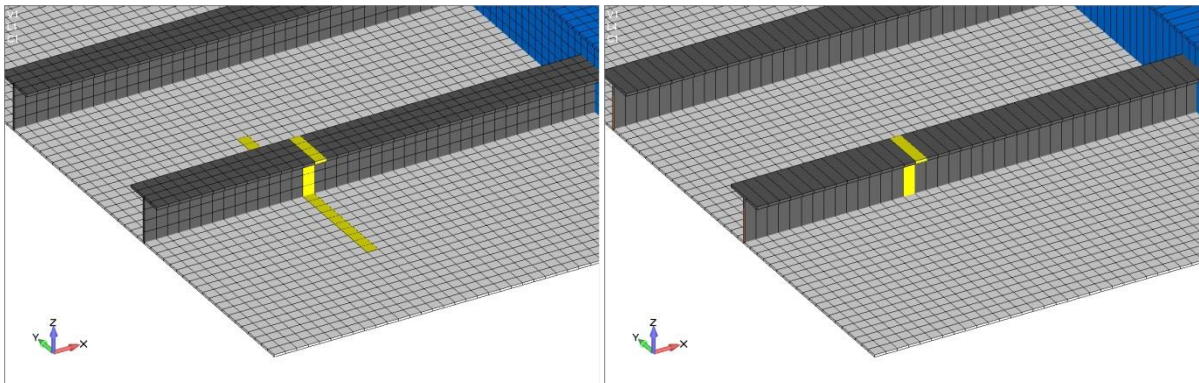
Fig 4.6 Difference between stiffeners modeled with plate elements (left) or beam elements (right).

The type of elements used in models logically influence results from the FEM calculations. Plate elements behave differently than beam elements. The latter cannot give any local web or flange buckling (fig 9.1). Neither will it provide torsional column buckling in the analysis due to the 6 degrees of freedom rather than 12 within plate elements. The mesh size also has influence on these elements since second order effects are rather difficult to get with one element per stiffener. Somehow the results from different kind of models should all be able to provide the correct parameters for the buckling check. That includes the use of different mesh sizes.

A second choice for the implementation method is to find a suitable approach with only the beam element results (fig 4.9c). This would make the method immediately usable for the present implementation in SDC Verifier and also reduce calculation time even further.

A stiffener can also be modeled with a combination of plate and beam elements. For now, plate elements only or beam elements only are compared without taking other modeling techniques or other elements such as solids into account. The specific modeling techniques exclude effective width methods as well. The current check will only be based on a correct offset of the beam elements as illustrated in figure 4.7b and more extensive described in appendix M.
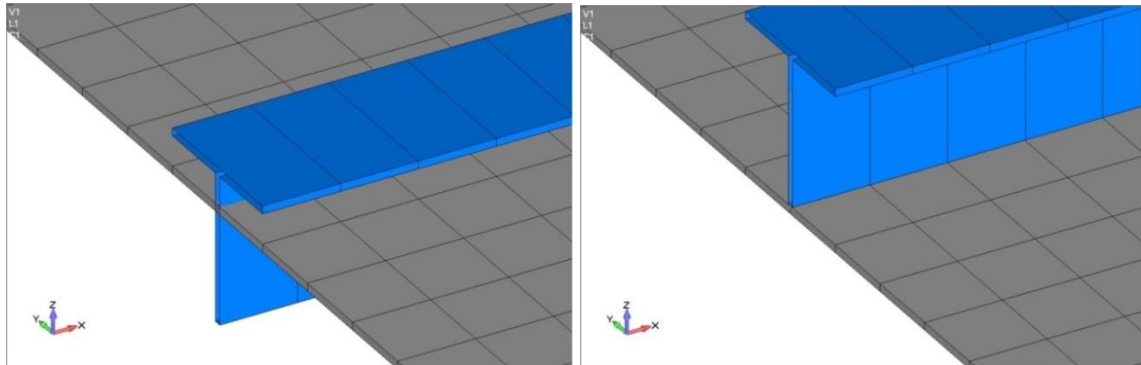
Fig 4.7 Examples of beam offsets when modeling: (a) no offset and (b) offset to the top of the plate.

The project contains an in-depth research into what exactly defines buckling for stiffened panels. All different buckling modes are already described above in chapter 3. The problems that arise with each mode and the influencing parameters within these problems are defined first. The relations and models should lead to the extraction of correct design factors out of the FEM analyses in such a way that a realistic comparing between the model and the standards can be made.

Local buckling of plate fields, webs and flanges will be checked and flexural and torsional column buckling limits of stiffeners will be checked. The other subjects as grillage buckling and lateral loads will be out of the scope. And as mentioned before the present study does only see to rectangular plates and panels. These choices are made based on the fact that non-rectangular structures and lateral pressure on them are far less used in practice when considering compressed plated structures. The cross section view of a cruise ship as in figure 4.8 gives a good impression to illustrate this point.
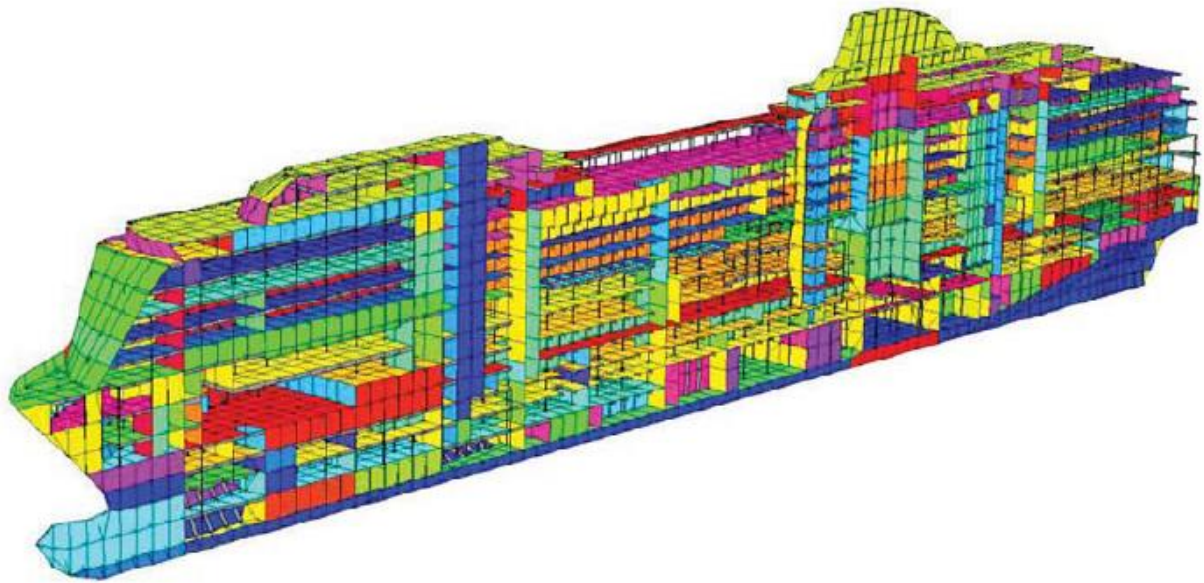
Fig 4.8 Model of a cruise ship.

(Picture courtesy of Kvaemer Masa Marine, Vancouver, BC, Canada, V6J 1T5)

To conclude everything the following main research question and sub-questions can be established: What should be the implementation method for the ABS and DNV standards buckling check for the complete stiffened panel, based on linear static FEM results?

- What defines buckling? Which problems does buckling of stiffened panels include? And what are the influencing parameters?
- Is linearization/simplification of stress distributions on individual plate fields allowable and if yes then what should the implementation method be like?
- Is it allowable to base the column buckling checks on stress results from beam elements only and if yes then what should the implementation method be like?

Immediate and preferred aim from the project, besides the actual method and checks, would be a more accurate and a less conservative analysis. While a fine meshed model would provide detailed and accurate results, do the standards give fairly conservative results. So the search is towards a smart package of input parameters. And still an implementation method that will be reliable although such that the construction will be less over-dimensioned.

The intended result should be a complete implementation method to define the correct parameters of the buckling check in the ABS and DNV standards, in such a way that it could be certified or be approved by a classification bureau and ready to be implemented into SDC Verifier.

Fig 4.9 Overview of considered cross sections to define the necessary design stresses: (a) plate elements including associated plate width, (b) beam elements including associated plate width and (c) only the beam elements.

5. Parameters

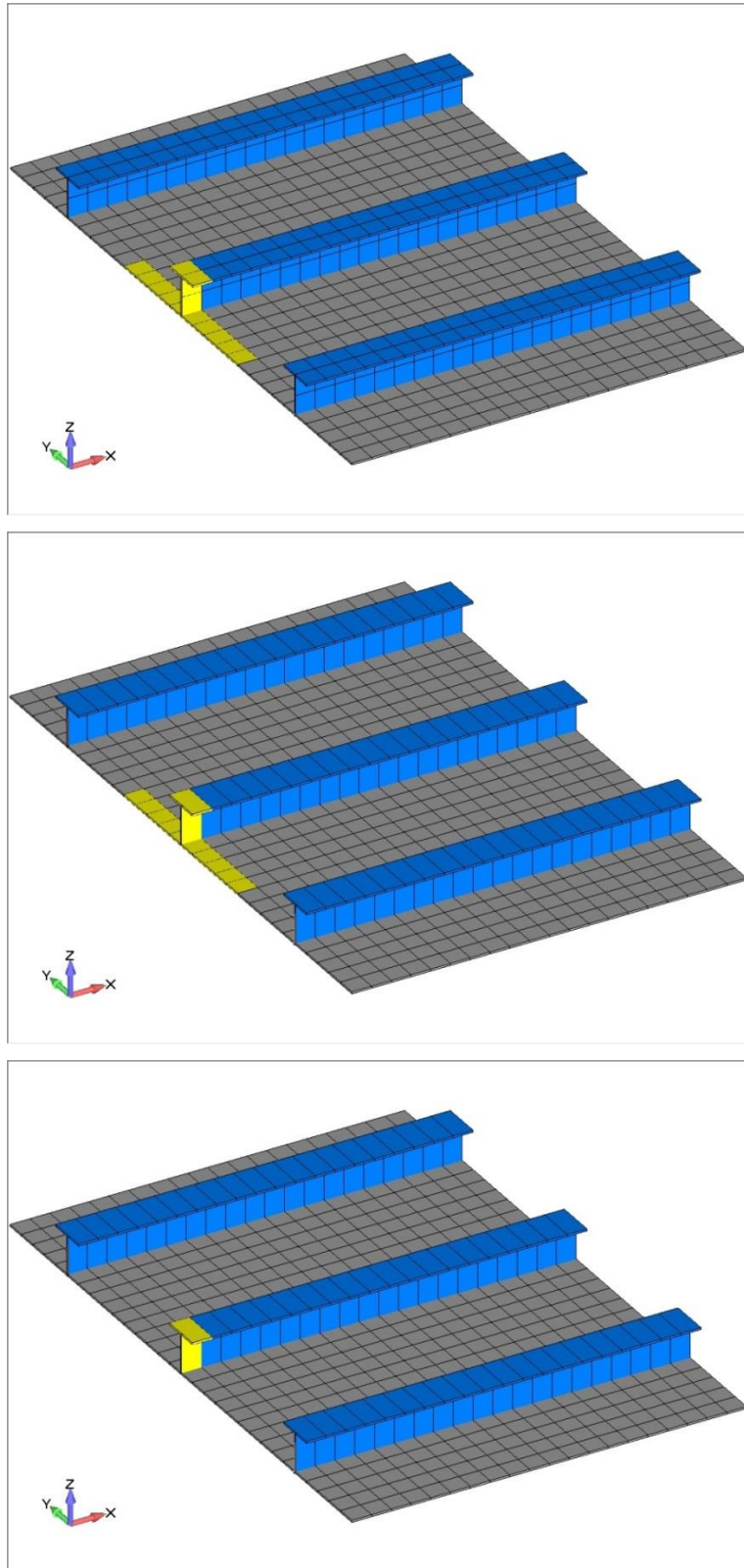Material and geometric parameters like edge boundary conditions, initial imperfections, material properties and production induced residual stresses influence the buckling limits. Some have relatively minimal effect on the panel behavior while others can influence strength significantly. Relations between them should produce conclusions for the new methods. A key objective is to reduce the uncertainties inherent in appropriately modeling these factors.

5.1 Load cases

We have seen above that the panel is subdivided into simplified plate fields and beam-columns. The real stresses in both types of sections are compared to the Euler's buckling critical stress as discussed. The formulas are transformed with correction factors due to the interaction between the sections. But the real stresses do not change. All the applied loads such as pressures, concentrated forces, prescribed displacements, and/or thermal loadings will produce stresses. A more complete function of all stresses in normal direction of the stiffener-plate combination is given in an extensive form by Equation 7.79 in Analysis and design of elastic beams by W.D.Pilkey [22].

$$\sigma_x = \frac{\widehat{N}}{A} - \frac{I_{\bar{y}\bar{z}}\widehat{M}_y + I_{\bar{y}}\widehat{M}_z}{I_{\bar{y}}I_{\bar{z}} - I_{yz}^2}\bar{y} + \frac{I_{\bar{z}}\widehat{M}_y + I_{\bar{y}\bar{z}}\widehat{M}_z}{I_{\bar{y}}I_{\bar{z}} - I_{y\bar{z}}^2}\bar{z} + \frac{\widehat{M}_\omega\omega^*}{\Gamma} - E\alpha\,\Delta T$$

Uniform pressure ⏜ | Bending moments ⏜ | Warping moment | Temperature dependency

The temperature dependency is of course far too much detail and therefore out of the scope. When you know the real stresses, they should be transformed in a combination of the stresses in figure 5.2 in order to use the simplified formulas. But the main parameters are the uniform pressure σ_x and bending moment M_y described below in figure 5.2a and 5.2b. Due to second order effects along the axis of the beam-column the stresses also vary over the length.

The same principal is in order for the plate fields. Any kind of applied loads such as local loads, patch loads, in-plane compressions, shear forces and lateral pressures produce the in- and out of plane stresses which have to be simplified for the standards. In the FEM program, each plate element can provide a number of stress results. These include top and bottom in-plane normal element stresses and a uniform shear stress, for eight corners both σ_x and σ_y and a lateral pressure on the complete element (fig 5.1). Plate fields consisting out of a mesh with more plate elements thus produces a number of stress distributions.
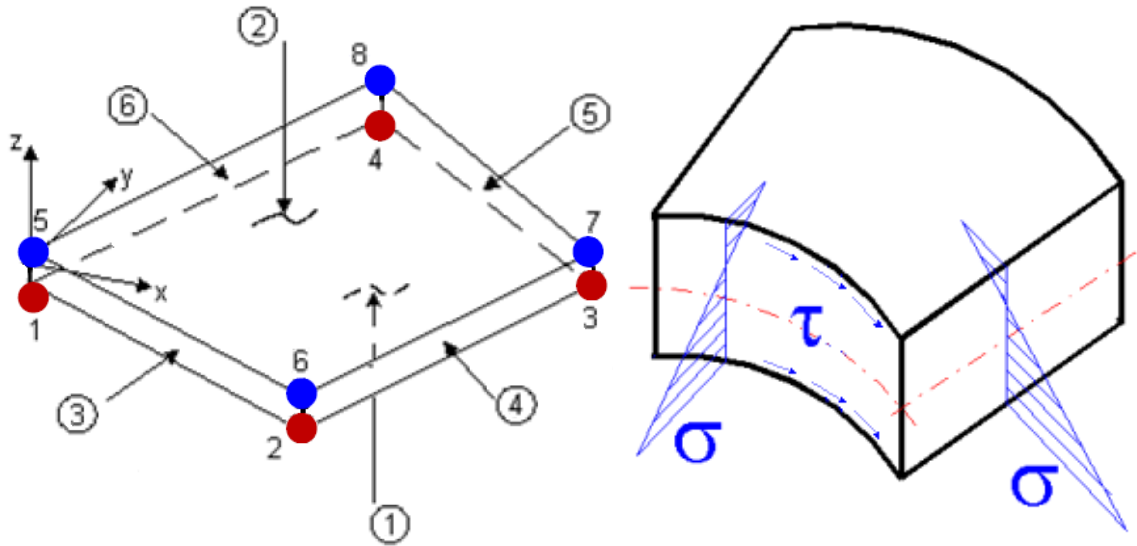
Fig 5.1 Stress results in plate elements.

The research will not go too much into detail of local peak loads, in-plane (fig 5.4) and out-of-plane. Again, mainly because the standards do not specify methods about local loads and therefore there is not really anything to compare to. Possibly since local peak loads will already cause problems for allowable stresses in the static analysis and the construction should be designed in such a way that it diverge the loads more evenly. With brackets or extra stiffeners for example. Furthermore dynamics, impact forces, yielding or crippling problems (fig 3.14), temperature and time parameters are completely out of the scope of the project.
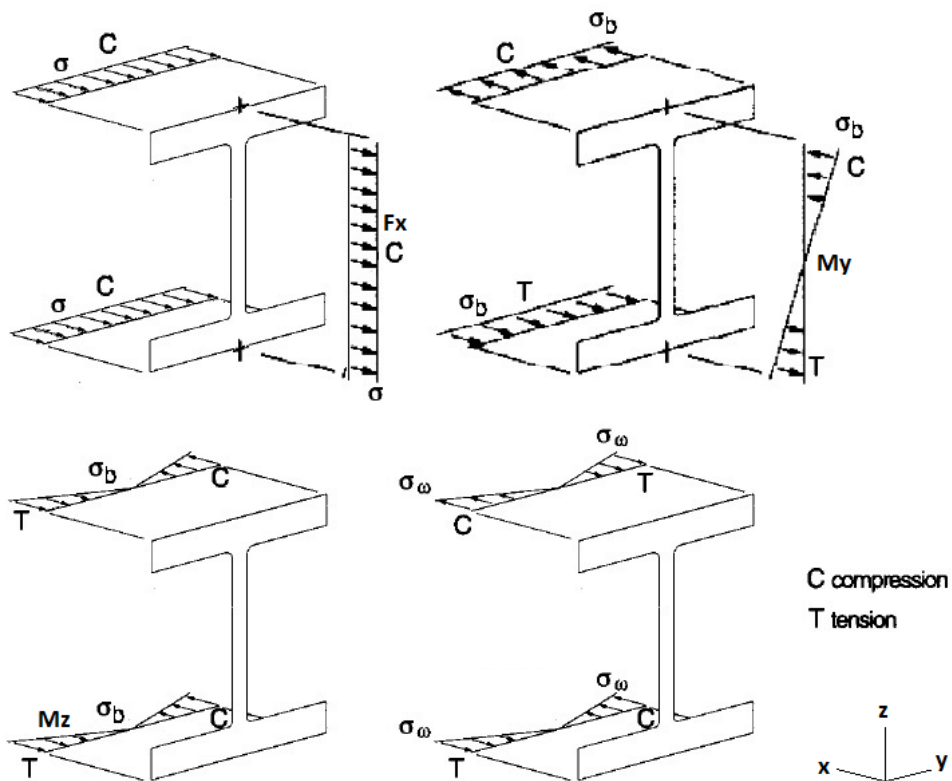
Fig 5.2 Stress results in plane direction due to (a) uniform pressure σ_x, (b) bending moment M_y, (c) bending moment M_z and (d) warping bending moment M_w [23].
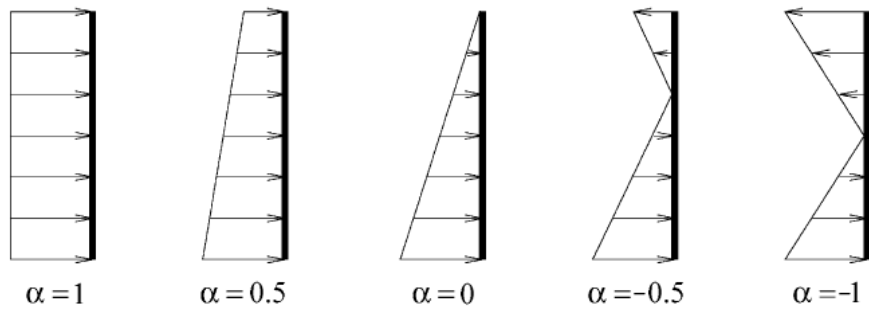
Fig 5.3 Examples of simplified in-plane loading along the edge. [24]
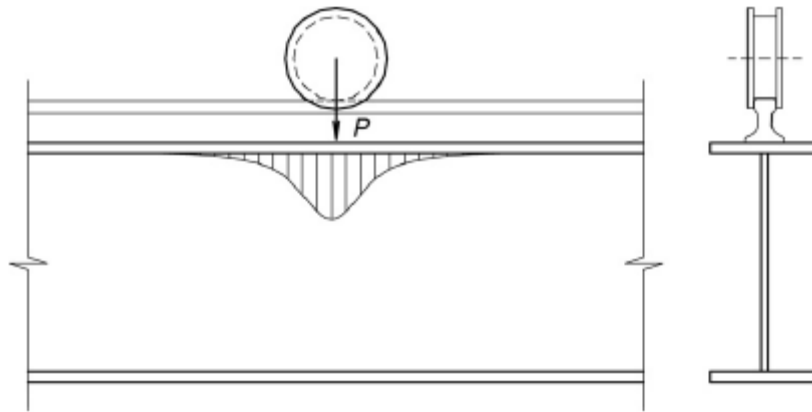
Fig 5.4 A model of an I-girder with peak loading. [25]

5.2   Geometry

The geometry of your model provides the main parameters for the checks. These include dimensions of the complete panel, of individual plate fields, of stiffener or girders shapes and thicknesses. The geometric characteristics of interest are the span (L) and the width (s) of the structural elements, as well as their thickness (t) and the radii of gyration (r) of the cross section of the stiffener with an appropriate associated plate. Other geometric characteristics may affect the behaviour of the stiffener in special cases. This may occur when the stiffener is very weak or it has low torsional rigidity, promoting a different mode of collapse such as tripping. Parameters such as the sections modulus, moment of inertia, torsional moment of inertia and polar moment of inertia generally are calculated from the geometry.

To provide a good explanation of geometry influence an overview of important and commonly used parameters is in order. Considered are the aspect ratio, the plate slenderness and the column slenderness.

$$Aspect\ ratio\ \alpha = \frac{l}{s} \qquad\qquad \{14\}$$

$$\sigma_{cr} = \sigma_0 = k\frac{\pi^2 E}{12(1-v^2)}\left(\frac{t}{s}\right)^2 \quad \rightarrow \quad plate\ slenderness\ \beta = \sqrt{\frac{k\pi^2}{12(1-v^2)}} = \frac{s}{t}\sqrt{\frac{\sigma_0}{E}} \qquad \{15\}$$

$$\sigma_{cr} = \sigma_0 = k\frac{\pi^2 E I_e}{A_e l^2} = k\frac{\pi^2 r_e^2 E}{L^2} \quad \rightarrow \quad column\ slenderness\ \lambda = \sqrt{k} = \frac{L}{\pi r_e}\sqrt{\frac{\sigma_0}{E}} \qquad \{16\}$$

The higher the slenderness the more susceptible to buckling. Variations of L, s, t (fig 5.5) and the stiffener shapes may lead to an optimal design. Lowering the thickness has a magnified effect on increasing the plate slenderness which leads to a reduction of the plate buckling limit as seen in figure 2.13b. And an increase of the plate slenderness has in turn an inverse influence on the effective plate width reducing it very much. For longitudinal uniform compression the following formulations are given.

$$(ABS) \rightarrow \frac{s_e}{s} = \frac{2\beta - 1}{\beta^2} \qquad\qquad \{17\}$$

$$(DNV) \rightarrow \frac{s_e}{s} = \frac{1.905\beta - 0.419}{\beta^2} \qquad\qquad \{18\}$$

For not only the effective width for the individual plate fields but also for the column one may have a further reduction due to the change on the effective radii of gyration $\sqrt{I_e/A_e}$ that results from the decrease of the effective area of the column and the shift in the neutral axis of the plate-stiffener combination. Thus this can have significant influence on both the plate buckling limit and the column buckling limit.

Increasing the plate width therefore has the same results as briefly noted above for the change in plate thickness. For slender plates (β>2.5) the elastic buckling stress lies significantly below the material yield stress. Thus the longitudinal stiffeners are spaced such that the slenderness ratio of the adjacent plating is not excessive, giving the plate field an adequate strength to resist compressive in-plane forces. Furthermore a reduction in the aspect ratio reduces the shear buckling resistance.
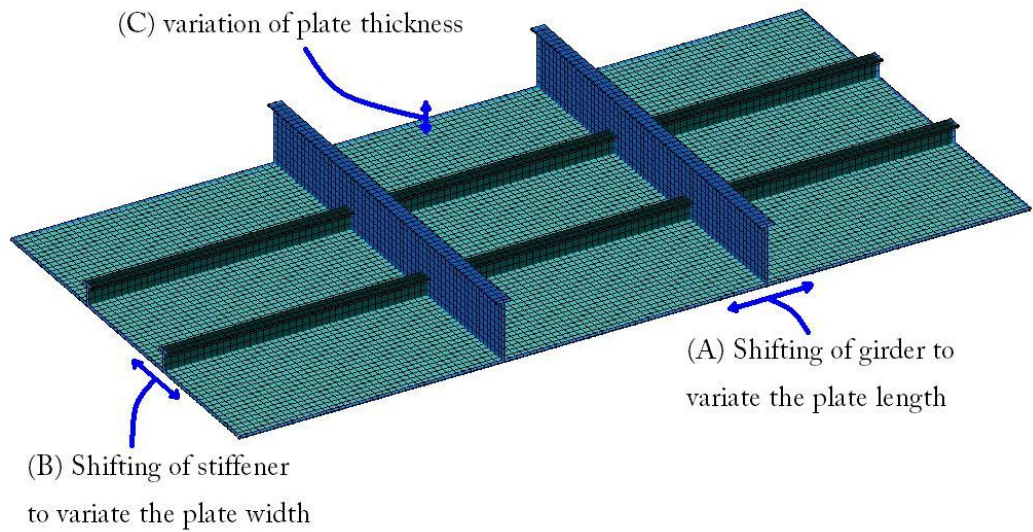
Fig 5.5 Dimension variations for plate fields.
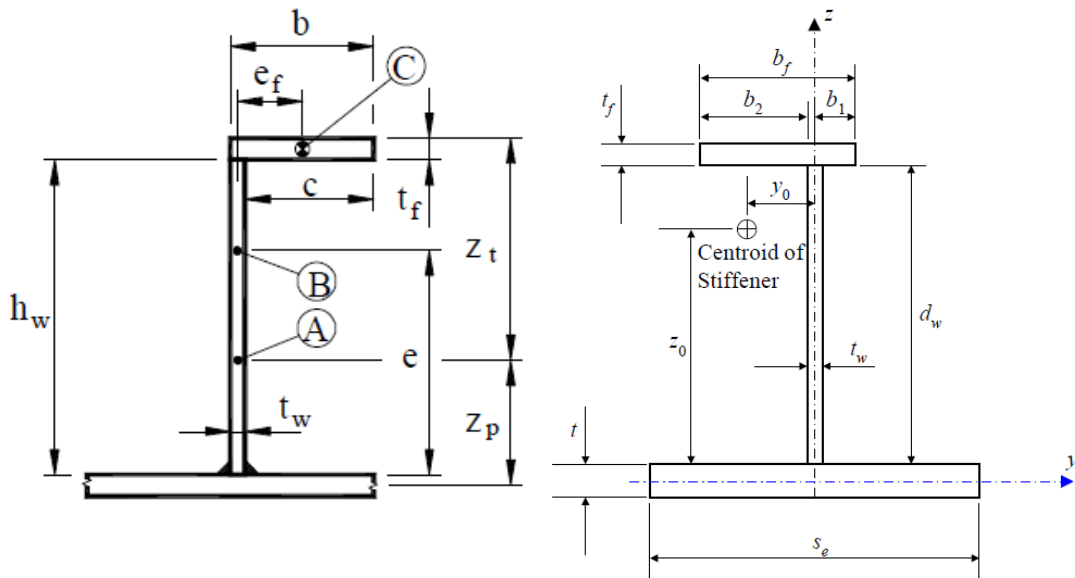
Fig 5.6 schematic illustration of (a) DNV and (b) ABS stiffener dimensions.

The length has more impact on the transverse compression and on the beam-column buckling resistance. Transverse frames are typically spaced between 2 and 5 times the distance between the longitudinal parts. Load shortening curves are normally given in terms of the plate slenderness ratio only, thus assuming that the strength of long plates is independent of the aspect ratio. The reason is

already seen in chapter 3.1. Since the buckling mode will seek a pattern with square half waves the mode will get more half waves when lengthening the plate but the strength will not reduce.

The buckling lengths seem rather undefined which asks for some further elaboration on the problems like connections and proportions of stiffness and dimensions between the stiffeners and girders. The buckling length is particularly important parameters as seen in equation 2. Do you take the stiffener length or the girder length for a transverse stiffener? And does the type of connection influence this? The standards distinguish stiffeners and girders but no values are specified, nor difference in welding connections. For now, due to the extensive amount of possibilities, the engineer should choose what a girder is and what a stiffener.
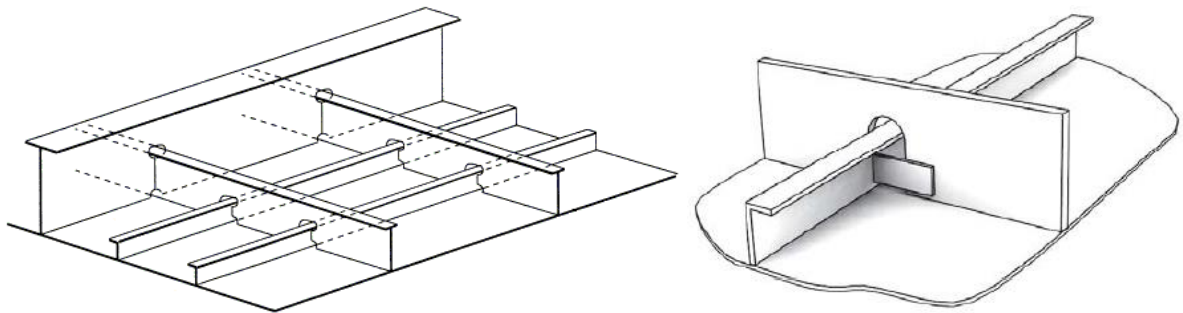
Fig 5.7 Example of a stiffened panel and effective longitudinal material. [16]

Standards speak of the unsupported span which can be the distance between transverse girders. But for the torsional buckling mode for example, an unsupported span is defined in a different way and is generally considered the length in between sideways supports of stiffeners or tripping brackets. However details like that are generally left out of the model. Certainly design considerations as in figure 5.7b which makes it hard to define the correct span.

Klöppel and Scheer together formed theoretical relations of panel buckling. In their work [26] they give an extensive collection of graphs which show buckling factor value for many dimensions. Each distinct graph is formed by two parameters, the cross section area ratio A_s/A_p and the stiffness ratio (moment of inertia) I_s/I_p.

The column slenderness is in practice also adjusted to compare designs with different shaped stiffeners. Column slenderness with influence of stiffener geometry (t or L stiffener) becomes:

$$\gamma = \frac{h_w/t_f}{b_f/t_w} * \lambda \qquad \{19\}$$

Column slenderness with influence of stiffener geometry (flat bar stiffener) becomes:

$$\gamma = \frac{h_w}{t_w} * \lambda \qquad \{20\}$$

While the plate resistance benefits from smaller and longer plates, the column buckling would like the opposite, stocky and short. Plate fields may be made smaller but then the stiffeners themselves should be designed bigger and thicker. An optimum between these factors should be pursued.

The longitudinal and transverse girders dimensions are important as well to provide sufficient resistance to the loads. They contribute to the stiffness by providing intermediate support to the longitudinal and transverse stiffeners, effectively acting as nodal supports to shorten the column length and increase the buckling strength.

5.3 Boundaries

Forces can be both in-plane and normal to the surface of the plate due to common load scenarios including in-plane compression, shear, torsion and lateral pressure. To represent a plate or column as a part of a bigger structure the boundary conditions of the model needs to adequately reflect the local support and load scenarios.

Whether the critical buckling stress is calculated through theory, FEM calculation or standards, for all of the methods the engineer need to decide which boundaries conditions are appropriate for the model. Plate bending, web bending and flange bending behave differently due to the other boundaries and so you get different buckling modes as well. This is mainly due to a change in the buckling length of the specific part in the structure. The so called unsupported span.

	(a)	(b)	(c)	(d)	(e)	(f)
BUCKLED SHAPE OF COLUMN IS SHOWN BY DASHED LINE						
THEORETICAL K VALUE	0.5	0.7	1.0	1.0	2.0	2.0
RECOMMENDED DESIGN VALUE WHEN IDEAL CONDITIONS ARE APPROXIMATED	0.65	0.80	1.2	1.0	2.10	2.0
END CONDITION CODE	ROTATION FIXED AND TRANSLATION FIXED					
	ROTATION FREE AND TRANSLATION FIXED					
	ROTATION FIXED AND TRANSLATION FREE					
	ROTATION FREE AND TRANSLATION FREE					

Fig 5.8 Illustration of different boundary conditions that provide different buckling lengths.

Beam-column methods typically only consider a single span with pinned or clamped supports corresponding to figure 5.8a and 5.8d. And plate fields are generally chosen to be simply supported unless there is a free edge. These corresponds to conditions (d) and (e) in figure 5.8. There could be far more optimistic results for various situations with for example the clamped boundaries but one should logically doubt that fixing the edges will provide a good representation of reality. The reality will be something in between simply supported and fixed edges. The more conservative simply supported boundary condition is applied to be on the safe side. The difference in fixed or supported edges is difficult to recognize and dependent on many parameters. A free edge however does have a huge impact on the strength of the plate but is easily recognizable in the design and other formula can be taken accordingly.

For modeling you can split the boundaries into out of plane, in-plane and rotational restraints:
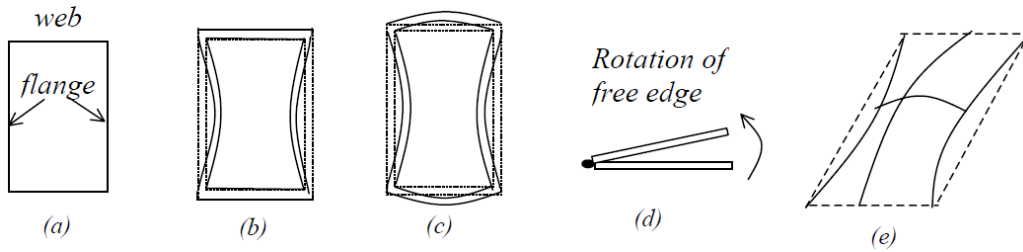
Fig 5.9 Plate elements with different edge conditions. [7]

The out of plane restraints are as simple as set out above. The stiffeners and girders are assumed to be stiff and should not buckle. They prevent out of plane displacements and keep the plate boundary straight at the ends of a column and at all edges of a plate (except for a free edge).

The in-plane restraints are less simple to define. In-plane longitudinal load will produce a displacement of the short edges. Correspondingly a combination of the poison ratio and the buckling mode influences the displacement on the long edges illustrated in fig 5.11a. Chapter 3.2 mentioned redistribution of stresses in the post buckling stage. One of the most common causes of this behaviour is associated with the in-plane boundary conditions at the edges of the plate. A common assumption for the unloaded edges is to constrain the edge to remain straight but free to move in-plane, the so called multi point constraint. Adjacent plates and stiffeners or girders will probably want to produce the same sort of displacement in which case they will cancel the irregular deformed edge, fig 5.11b. However, if considered as part of a panel, the edge could also remain constrained from all in-plane movement as they would be under similar load conditions as well. This would lead to a zero displacement edge constraint and have a further redistribution of the in-plane stresses, fig 5.11c. Whether the support consists of very stiff elements or a more slender construction will define a suitable constraint. S. Benson mentions that the difference between fig 5.11b and 5.11c is not a significant one since they seem to result in more or less the same stress strain relationship for the plate.
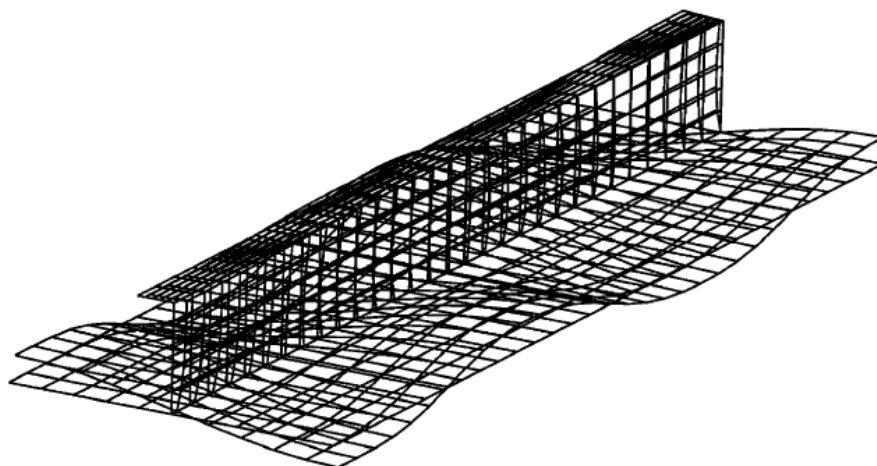

Fig 5.10 Part of a plated structure (to analyze column buckling) on which the engineer now has to decide what boundaries need to be applied and where.

The rotational restraints depend on the supporting structure but can also depend on the specific stress results like big lateral pressure stresses in relation to the other stresses or imperfection

patterns, see fig 5.12. A clamped support provides additional strength to the plate as would be expected. The conservative approach is to assume that the rotational restraint at the boundary is minimal and thus the plate is simply supported along its edges. An explanation of why the conservative simply supported approach is generally accepted can be found in the theoretical approach described in appendix K.
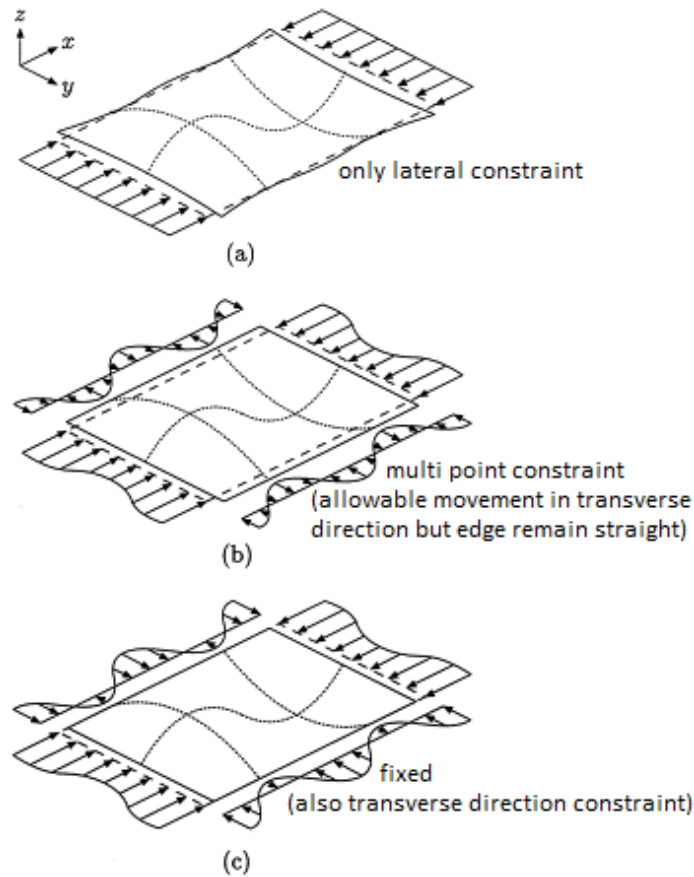
Fig 5.11 Possible edge displacements and corresponding stress distributions for different constraints.
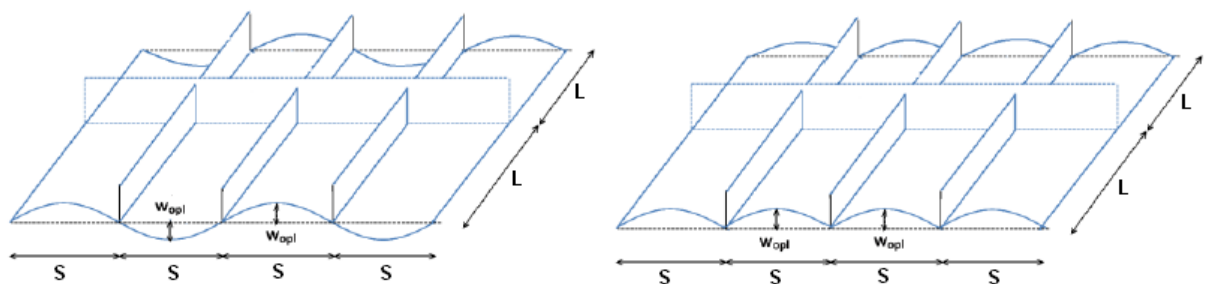
Fig 5.12 buckling patterns due to initial imperfection or lateral pressure with (a) the alternating pattern/simply supported and (b) the hungry horse pattern/fixed boundaries.

Boundary conditions of the beam-columns are even worse. As you can see in fig 5.10 one cannot simply use similar constraints as with plate fields. In reality all edges would be allowed to move or rotate. However, besides the fact that an analysis will need constraints to accommodate specifically the correct buckling mode, the beam-column is considered as a separate section which may be checked individual. Concluding you get: out of plane constraints at the ends and out of plane bending constraints on the unloaded edges, described in chapter 10.

5.4   Imperfections

With imperfections in a structure is meant that it is not completely straight. It therefore implies an initial deformation in the geometry. Imperfections arise when producing the material or when making the product. There are imperfections in each individual plate field, web and flange, twisting of the stiffeners and girders and also imperfections over entire panels or combinations of panels.
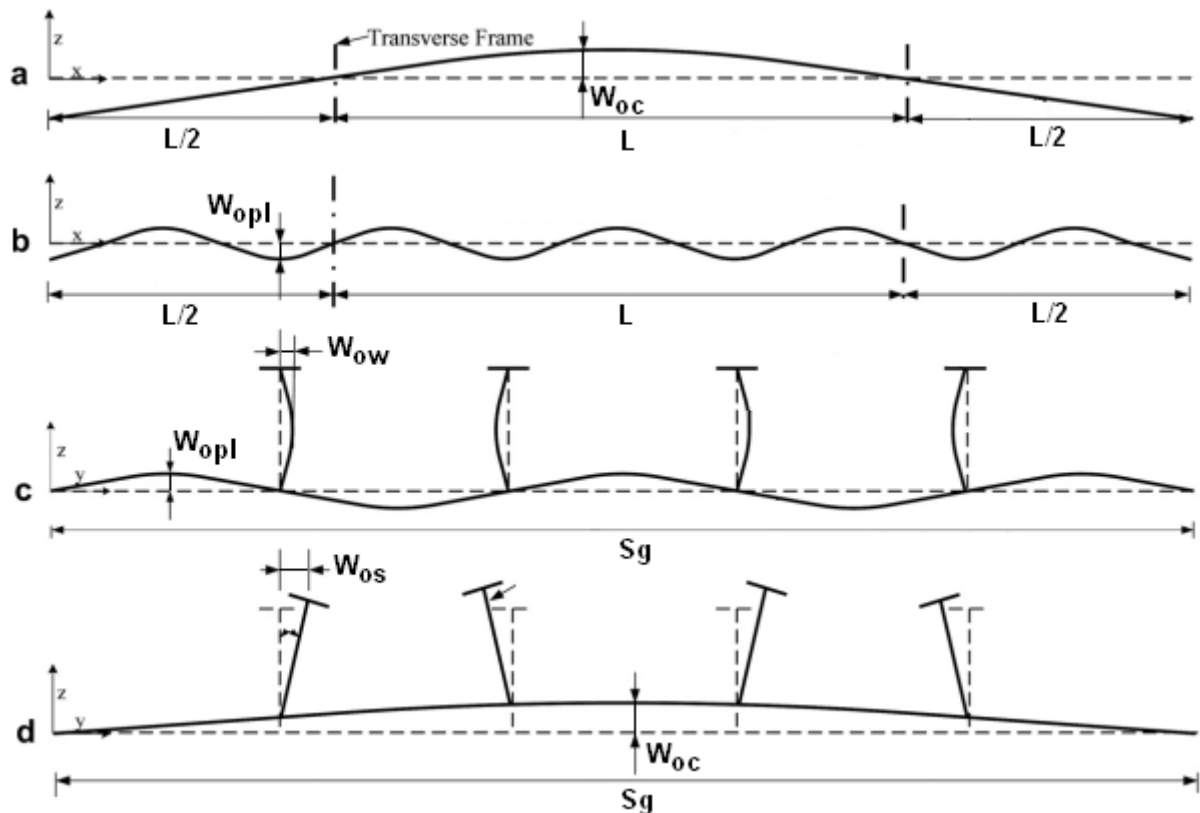
Fig 5.13 Initial imperfections of a stiffened panel. (a) and (b) Panel section at y=s/2, (c) and (d) Panel section at x=L/2.

Initial buckling and the buckling strength may be greatly influenced by the imperfections. Standards state several values to what is permitted. However the resistance of stiffened plate structures is dependent on imperfections in several elements. Both the imperfection size and pattern for both the plate and stiffener are important and generally the resistance is also dependent on more than one panel. It is less probable that all individual sections have their most detrimental imperfection pattern and size at the same time. Furthermore the importance of the imperfection is largest for stocky sections while the likelihood of deviations are largest for slender sections.

Therefore a nonlinear FEM analysis of the panel including the worst combination of allowable imperfections may yield less resistance than obtained from the formulas in standards. What is more, there are several supportive effects in a real plated structure that are disregarded in the resistance formulations. In many cases that will mean a capacity reserve which is larger than the effect from imperfections. Thus the formulas in standards are stated as being relevant for normal good practice even if results do not match with nonlinear FEM analyses. It again emphasizes the complexity of the buckling phenomena.

The exact imperfections in plate fields or beam-columns can only be as in reality when you measure the real product. Thus the buckling strength analysis in general is based on the characteristic buckling strength for the most unfavorable buckling mode. This mode can be any shape depending on the specific part in which you are interested.

The imperfection may in practice be approximated by the first eigenmode. However it has been shown that the preferred mode can change as the plate undergoes post buckling, switching from a linear type shape before buckling to a shorter wave pattern in the post buckling range. The plate field may thus snap into a different mode due to the redistribution of stresses. Other parameters as the material properties and residual stresses may influence the preferred buckling mode shape as well. S. Benson [27] checked a plate with a nonlinear analysis over and over with different imperfections applied by imposing different eigenmodes. Results showed that the first eigenmode does not give a lower bound solution. This suggests that a more conservative mode shape is induced with an imperfection with a shorter half wave length than the plate width. The choice should therefore not be based on solely a linear analysis. Furthermore the use of a single eigenmode to approximate the imperfection is an overly conservative routine since it is very unlikely for a plate to be distorted in an exact sinusoidal pattern.

Benson therefore proposes an introduction of initial imperfections by applying an out of plane Fourier series translation to each node in the mesh. An external script is used to directly edit the node coordinate input file. He uses slight, average and severe characteristic levels of imperfection typical for steel plates. More details can be found in the work of Benson. He proposes a combination of three eigenmodes for individual plate fields, one global half wave mode, a second theoretical most unfavorable eigenmode and a third mode to make the imperfection unsymmetrical so the structure will always fail at one place and not at 2 places at the same time.

$$w = w_{0pl}\left(B_1 \sin\left(\frac{\pi x}{L}\right) + B_m \sin\left(\frac{m\pi x}{L}\right) + B_{m+1} \sin\left(\frac{(m+1)\pi x}{L}\right)\right)\sin\left(\frac{\pi y}{s}\right) \qquad \{21\}$$

Note that beside the imperfection one may have from heat induced effects or other internal material stresses, you can have simple misalignments when constructing as well. This is the reason that most of the time stiffeners are continuous and go through specially made spaces in the girders.
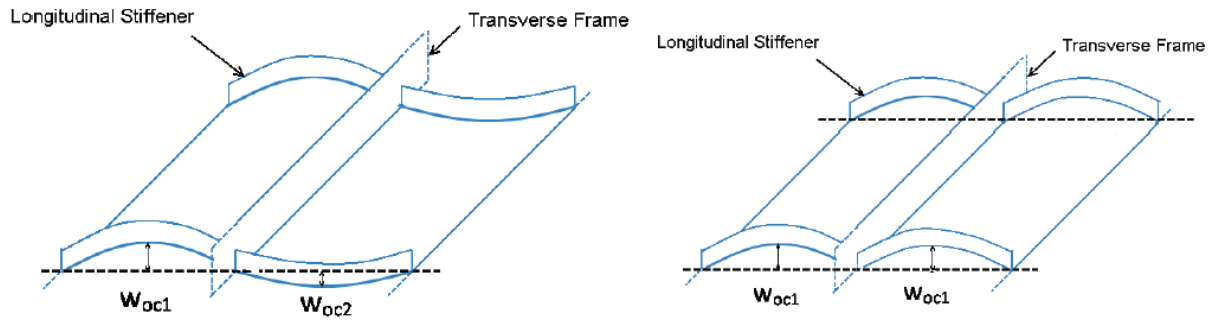
Fig 5.14 The panel imperfection, difference between symmetrical and unsymmetrical patterns.

ID	Name	m	n	w_{opl}	Plate	w_{oc}	$w_{oc1}/$ w_{oc2}	w_{os}	w_{ow}
S	Slight	$a/b+1$	a/h_w+1	$0.05\beta^2 t$	$B_1=0.8$ $B_m=0.2$ $B_{m+1}=0.01$	$0.0002a$	-0.25	$0.0004a$	$0.0002a$
A	Average	$a/b+1$	a/h_w+1	$0.1\beta^2 t$	$B_1=0.8$ $B_m=0.2$ $B_{m+1}=0.01$	$\lambda<0.2: 0.0008a$ $\lambda<0.6: 0.0012a$ $\lambda>0.6: 0.0015a$	-0.25	$0.002a$	$0.001a$
L	Severe	$a/b+1$	a/h_w+1	$0.3\beta^2 t$	$B_1=0.8$ $B_m=0.2$ $B_{m+1}=0.01$	$0.006a$	-1	$0.005a$	$0.0025a$
ISSC		$a/b+1$		$b/200$	$B_m=1$	$0.001a$	-1	$0.001a$	$h_w/200$

Fig 5.15 Imperfection parameters as proposed by Benson. [28]

5.5   Material properties

In general all thoughts and explanations remain applicable for only steel metal or similar material behaviour. Provided that the model is based on an isotropic material and the same material is used for plates, stiffeners and girders. Or equivalent average material properties should be known. Designs made with composite materials are out of the scope for now. The material properties of interest are the yield stress σ_0 the modulus of elasticity E, the poison ratio v and the shear modulus of elasticity G.
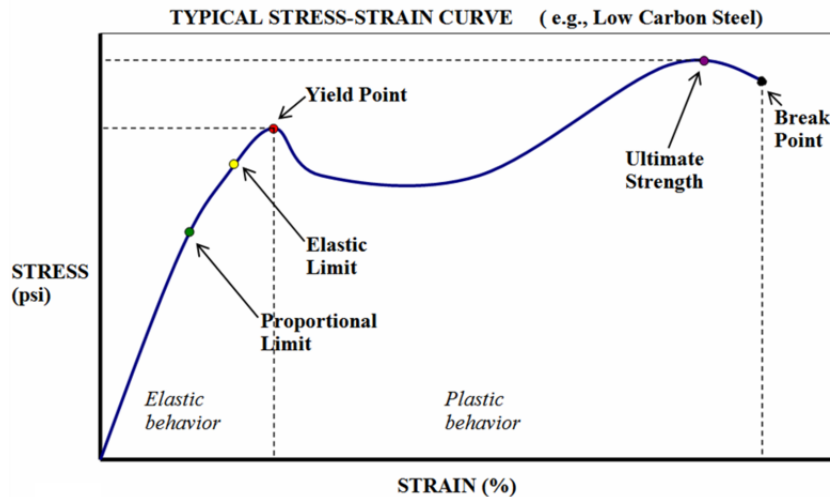

Fig 5.16 A typical stress-strain curve.

A typical stress-strain curve illustrates steel material behaviour. The yield stress is the main critical stress to compare your design stress with. This is already defined before in the Euler's critical stress. But after the yield point and until the ultimate strength in practice there exists reserve strength in the panel due to strain-hardening. This implies that calculated critical stress also have some safety factor within already. In standards there might be use a strain-hardening modulus where a correction factor $\sqrt{\sigma_0/235}$ is employed.

The use of high tensile steel instead of other normal steels for the fabrication of the construction has several different main effects on the ultimate strength. Firstly you can count on an increase of the global strength corresponding to the other types of steel, proportional to the ratio between the yield strength. That is for the same geometry of course. However a construction of for example HTS 690 has a reduction on the effectiveness of the structural elements compared to one of normal mild steel, as there are differences in the yield strength but the modulus of elasticity is the same (remember the square root in equations 15 and 16). But secondly while having an increase of the global strength does give the opportunity to reduce the geometry. You normally use a better quality material in order to reduce the amount of material and/or weight. However, lowering the thickness has a magnified effect on the plate slenderness, effective width and column slenderness and thus influences both the plate buckling and the column buckling in negative ways. Thus the structure made of high tensile steel is therefore more prone to collapse by buckling than one mild steel structure. One can have a reduction of weight but may need several design corrections to satisfy the buckling criteria.

The modulus of elasticity E does not remain linear when approaching the post buckling stage. Approximations to account for material plasticity could be applied, by replacing the elastic modulus with the so called tangent modulus. This is however not simply implemented. Different materials behave differently as well. For Aluminum both the ultimate elongation and the ultimate strength to yield strength ratio is lower than that of steel for example. In general calculations are done with a linear E modulus.

Another feature is the significant effect that welding can have on the strength of the material in the heat affected zone. Caused by the heat that softens the material adjacent to the weld. The welding process causes therefore a strength reduction in this zone. Since these zones at the edges of plate fields are already disadvantage in the post-buckling range, this phenomenon may actually have a fair amount of influence for some materials such as aluminum. The softening of steel reduces the ultimate strength to a value near the yield stress which is used for the simplified calculations and therefore relatively will not have much impact.

The influence of the poison ratio v has been discussed above. The shear modulus of elasticity has some influence as well, mainly on the tripping stress of the stiffener. Luckily steel has already a high shear modulus.

5.6 Residual stresses

Residual stresses due to welding are very likely to cause imperfections as well. Or at least many available theory and publications make the assumption that initial deformation and residual stresses can be taken as the same problem. The reality is of course a bit different. Residual stresses in the material cannot be seen from the outside. When cooled down after welding, the weld bead at the joint is resisted from contracting by the bulk of the parent material. This causes tensile residual stresses to form within and near the weld and compressive stress fields in the unheated plate regions to form equilibrium. These compressions may reach levels such that they initiate local buckling and hence imperfections before applying the load cases. In a straight compression member, the residual compressive stresses cause premature yielding under reduced axial loads and the member buckles inelastically at a load which is less than the elastic buckling load.

Recent studies suggest that the quantity of heat introduced during welding is the primary contributor to residual stress rather than the specific levels of plastic deformation caused by the weld method. Therefore there is an advantage in using new developed, less heat intense weld methods. Remember that not only welding but producing steel plates and beams on itself influence the present residual stresses as well. Computer numerical control (CNC) methods like fluid jet cutting have advantage of leaving no heat affected zone close to the cut edge. And moreover these types of methods are usually the most accurate and efficient methods to employ for their weld ready edges and possible shapes and cutouts.
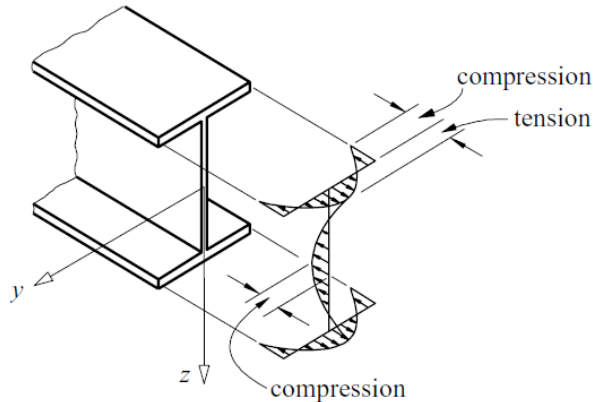

Fig 5.17 A pattern of residual stresses in the area of the plate stiffener combination. [29] [30]

For a steel plate the tensile residual stress zone should usually be considered to be equal to or just less than the material yield stress. Take note that for other materials the softening produced in the heat affected zone will also affect the yield and thus the amount of residual stress.

The residual stress are complicated to describe accurately thus for implementation a simplified pattern is taken. However Yusuke states that the actual residual stresses represent the simplified pattern (fig 5.18 and 5.19) fairly well when the boundary constraint is done with a multipoint constraint along the edges as described above (fig 5.11b).
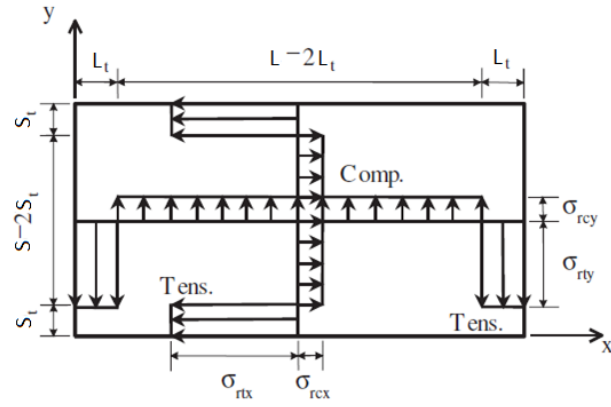
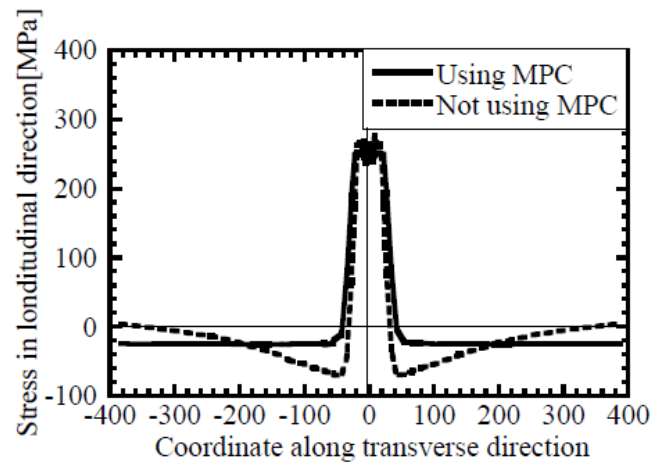Fig 5.18 Idealized distribution of the welding residual stresses in a plate

Fig 5.19 Comparison of stress distributions with different boundary constraints. [31]

6.   Research approach

So now the main problems and parameters have been reviewed it is time to do new tests to form and check new implementation methods. Validation, to see if model is fit to provide answers regarding the real world, will be done with an already existing real size model.

6.1   The experiment

Within a European project a concept of a new ship hull was studied in which very high strength steel was used to allow a lighter structure to be developed. Such departure from normal practice motivated studies on fatigue strength and on ultimate strength. The authors of the paper aimed to validate a buckling check method against data from several small scale experiments where the loading conditions could be well established. They used models representing simplified typical sections of ships, box girders subjected to pure bending moments. Details of the test setup at LISNAVE shipyard are presented in figure 6.3. The experimental study which was conducted is also described and worked out in the work of S. Benson [28].

The material used in the experiments is HTS 690 with a yield stress of 690 MPa and a Young modulus of 200 GPa as the principal material properties for structural analysis respectively. There are three different models tested. One four span model with 200mm length space framing, one three bays span model of 300mm length space framing and one with three bays span of 400mm length. The longitudinal stiffeners are bar stiffeners of 20x4mm made of HTS 690 as well. The transverse frames are 'L' stiffeners L50x28x6mm made of mild steel. The longitudinal stiffeners are made continuous through the model in order to avoid misalignments. All three models are made of 4 mm thick plate. The rest of the dimensions are shown in figure 6.1.
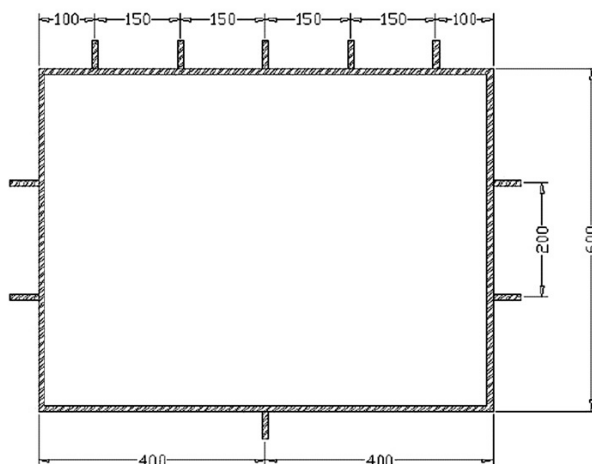

Fig 6.1 the cross section of the box girders.

The experimental results cover an appropriate range of the governing parameters of the plated structure such that the limits of plate, column and grillage buckling are in the same range. At the same time the parameters for the evaluation of the stiffener tripping stress were controlled in order to

avoid large reduction on the global efficiency. The range of the column slenderness is very high due to the high ratio between the plate and the total area of the representative stiffened plate. This means that for actual design practice one may obtain a global efficiency of the HTS 690 on the order of 2.5 taking as basis the normal mild steel (MS) structure.

Model	Length (mm)	b (mm)	t (mm)	h (mm)	t_h (mm)	Area (mm^2)	No. of frames
H200	1000	150	4	20	4	680	5
H300	1100	150	4	20	4	680	4
H400	1400	150	4	20	4	680	4

Table 6.1 Geometry of the test specimens.

Model	b/t	β	λ_{nom}	λ_{ef}	ϕ_p	ϕ_s	A_p/A_t
H200	37.5	2.20	0.97	0.85	0.702	0.604	0.88
H300	37.5	2.20	1.45	1.28	0.702	0.437	0.88
H400	37.5	2.20	1.93	1.70	0.702	0.255	0.88

Table 6.2 Geometrical parameters and predicted collapse strength of the specimens. Plate slenderness β, column slenderness λ_{nom}, effective column slenderness λ_{ef}, effectiveness ϕ_p according to Faulkner's formula, and variation of the average ultimate strength ϕ_s.

The tests consist of a four point bending of a beam like box girder. The box girder is subjected to pure bending moment, inducing tension on the bottom and compression on the top of the box. Benson mentions a deviation between the four point bending and a pure moment due to shear forces in the load though still justifying the use of a rigid body tie (fig 6.4) for applying the load (fig 6.2).
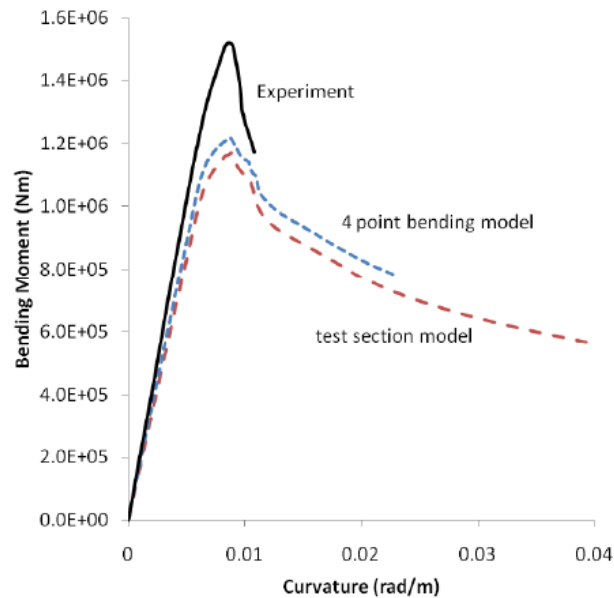
Fig 6.2 The Box girder experiment comparison with FEM models. Applying the load with use of the rigid body tie matches the complete set up fairly well.

Fig 6.3 Test setup of the box girder H200 including part
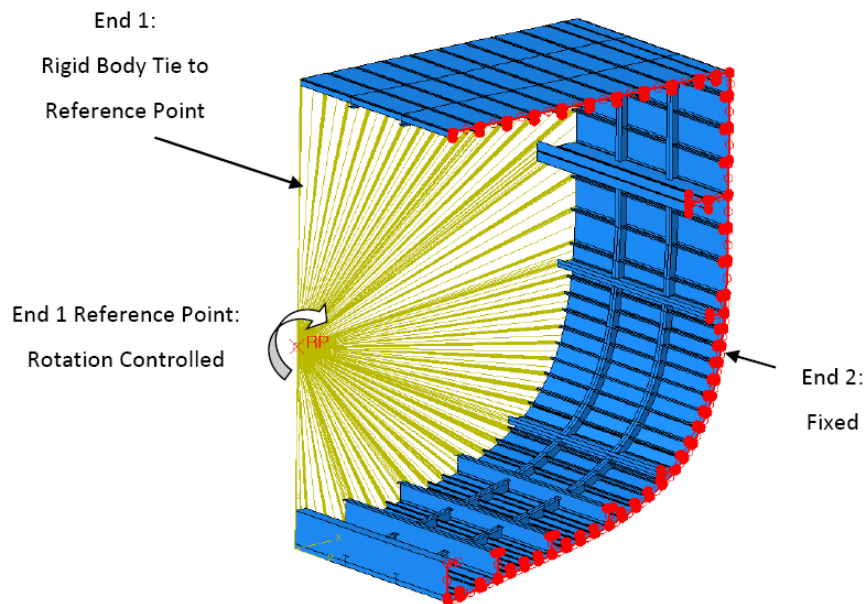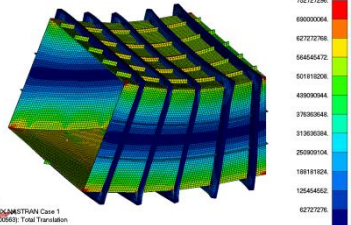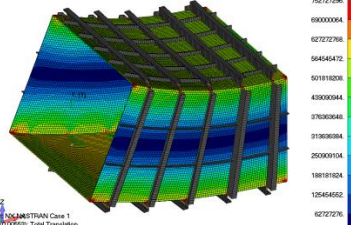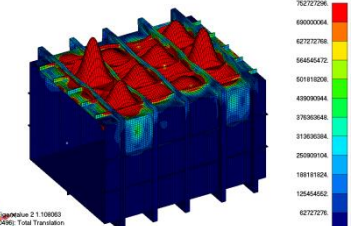of the supporting structure and the loading device. [32]

End 1:
Rigid Body Tie to
Reference Point

End 1 Reference Point:
Rotation Controlled

End 2:
Fixed
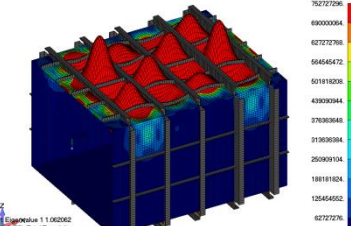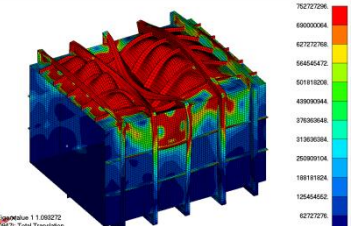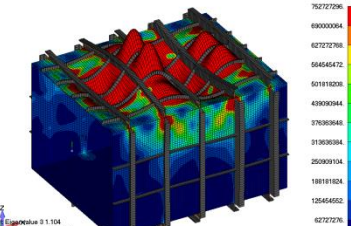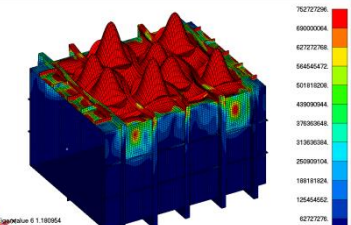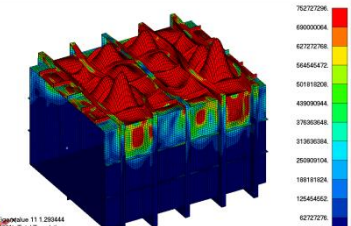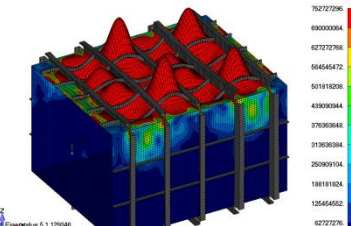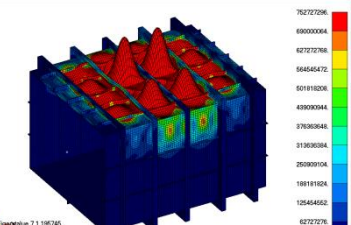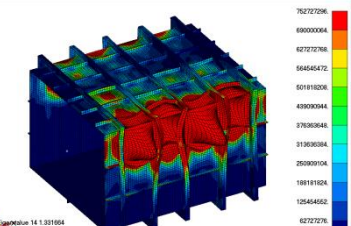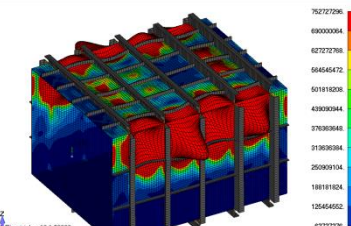
Fig 6.4 Principal of the rigid body tie in order to apply a load on the structure. [27]

6.2   The finite element model

The benefits of the real model from above make it as an excellent basis for the FEM model. The boundary constraint is easily applied. The same for the load due to the rigid body tie which also make it easily varied too in order to perform different checks. It is a very common structure in practice and therefore represents realistic results. Generally the stiffeners are placed on the inside of the structure but now the model can, apart from providing a clear sight on the sections, show beam-column buckling as where otherwise the stiffeners would be loaded with tension due to the bending moment. And lastly the fact that the different buckling modes are within the same range may have some advantages in checking the results when advancing towards grillage buckling as well.

The model is made with only plate elements and a second equal model is made with the stiffeners modeled with beam elements. From now on they will be mentioned as the "plate model" and the "beam model". Since there will be made several comparisons between the plate model and the beam model, first a small check is in order to see if both models are equal. Figure 6.5 shows eigenmodes and eigenvalue results for the applied bending moment on the structure as described above in the previous section. The results match fairly well. They have similar buckling limits and both show plate and grillage eigenmodes in close range of each other. The beam model seems to be slightly stiffer. Still the comparisons should be justified.

Eigenmodes Plate model	Eigenmode nr-Eigenvalue	Eigenmodes Beam model	Eigenmode nr-Eigenvalue
	Linear static solution Deformation =0.00563		Linear static solution Deformation =0.00553
	Plate 02-1.108063 03-1.112179 05-1.16301 09-1.214865		Plate 01-1.062062 02-1.070521 04-1.116732 07-1.155375 10-1.229593 12-1.284767
	Grillage 01-1.093272 04-1.11501 12-1.298755		Grillage 03-1.104 06-1.153851 09-1.173976 18-1.368425
	Deformation of girders 06-1.180954 08-1.202592 10-1.270054 18-1.392817		
	Column 11-1.293444 13-1.323736		Column 05-1.129346 08-1.162891 11-1.262995 17-1.358603
	Tripping 07-1.195745		
	Side panels 14-1.331664 15-1.332331 16-1.377801 17-1.378379		Side panels 13-1.29008 14-1.290584 15-1.3407 16-1.342865 21-1.408078 22-1.418745 27-1.474202

	Second mode Plate fields 19-1.425301		Second mode Plate fields 19-1.372495 20-1.401301
	Second mode + Column 20-1.441569 21-1.449362 22-1.449532 23-1.461671 25-1.494094 26-1.494663 27-1.504493		Second mode + Column 23-1.424876 24-1.428618 25-1.452072 26-1.455079 28-1.487452 29-1.488516 30-1.50475
	Second mode + Deformation of girders 24-1.469557 29-1.515876 30-1.519878		
	Second mode + Grillage 28-1.513573		

Fig 6.5 Linear eigenmodes and eigenvalues compared for the plate model and the beam model.

Note that this is only for Load case 1 and only for the fine meshed models.

6.3 Comparing between reality and standards and FEM

With a random load case you can simply get stress results from the linear elastic analysis in the FEM program. FEM analysis will not need extra formulations developed to estimate specific stress result requested by the standards such as unknown bending moments at intermediate supports or mid-span of beam-columns. The standards allow to make use of the linear elastic stress results. Therefore there will be made an attempt to form a robust combination of the linear FEM approach and the approach of the standards. Safety factors are supposed to be already in the standards and thus the implementation method will only simplify stress results but will not try to find new correction factors.

Potential for plate buckling, local web buckling, stiffener flexural buckling and stiffener tripping must be checked using separate procedures. Recognition of the individual sections is done with SDC Verifier. Figures 6.6 and 6.7 illustrate random sections within the upper panel of the FEM model. The plate model provides webs and flanges as individual plate fields which simplifies the possibilities while the beam model will need transformations of stress results.
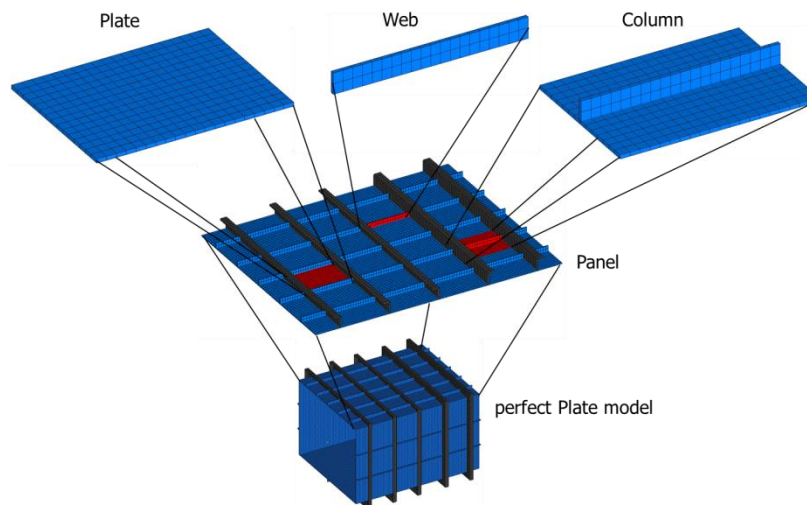
Fig 6.6 Analysis of individual sections in the plate model.
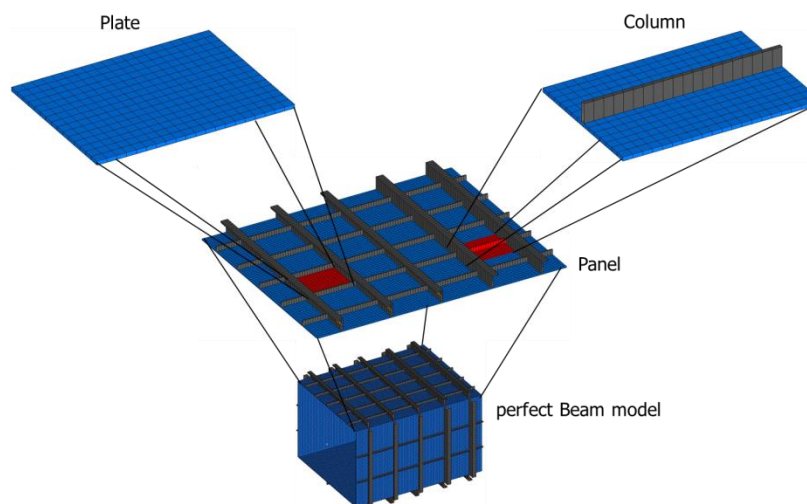
Fig 6.7 Analysis of individual sections in the beam model.

To reduce the amount of checks for validation of the implementation methods, only one specific plate field, beam-column and web are analyzed as shown in figure 6.8. The middle sections are chosen for easy identification of load conditions. However for a thorough validation it is recommended to check some other sections as well.
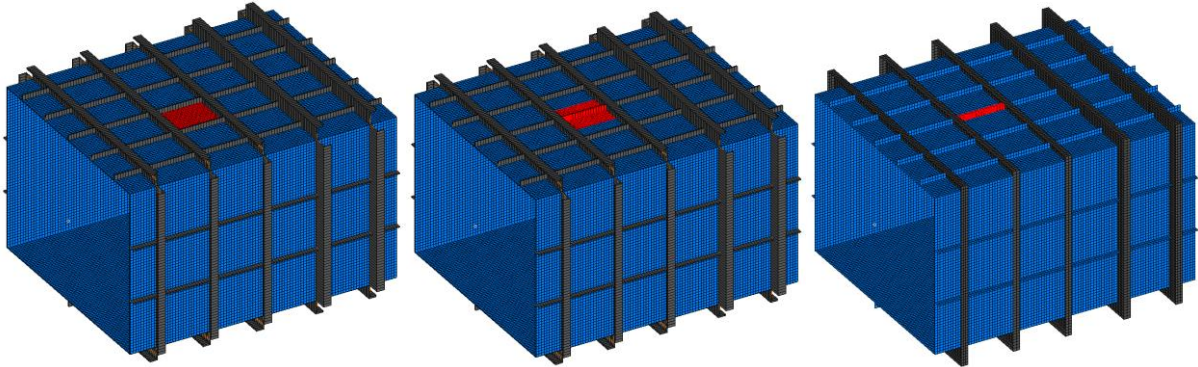
Fig 6.8 Individual sections which are checked on buckling: (a) the plate field, (b) the beam-column and (c) the web/flange.

6.4   Variation of parameters

Variations of parameters will consist of load combinations and dimensions. Seven different load combinations are compared see figure 6.9. The first five loads mainly consider longitudinal stresses while the sixth case exerts a transverse stress on the structure. The last load case is a combination of the first and the sixth. Several variations in the model are produced by scaling the model in longitudinal and transverse direction, by varying the plate thickness and changing the shape of the stiffeners.

Load case	Load case name				
1	(0.15.0)	$Mx = 0Nm$	$My = 1.5e6Nm$	$Mz = 0Nm$	$Fy = 0N$
2	(2.13.2)	$Mx = 2.0e5Nm$	$My = 1.3e6Nm$	$Mz = 2.0e5Nm$	$Fy = 0N$
3	(6.10.1)	$Mx = 6.0e5Nm$	$My = 1.0e6Nm$	$Mz = 1.0e5Nm$	$Fy = 0N$
4	(6.1.10)	$Mx = 6.0e5Nm$	$My = 1.0e5Nm$	$Mz = 1.0e6Nm$	$Fy = 0N$
5	(0.0.10)	$Mx = 0Nm$	$My = 0Nm$	$Mz = 1.0e6Nm$	$Fy = 0N$
6	(Fy)	$Mx = 0Nm$	$My = 0Nm$	$Mz = 0Nm$	$Fy = 2.4e6N$
7	(0.15.0 + Fy)	$Mx = 0Nm$	$My = 1.2e6Nm$	$Mz = 0Nm$	$Fy = 2.4e6N$

Table 6.3 Load cases

Model variations	Dimensions plate fields (mm)	Dimensions stiffeners hw, tw, bf, tf (mm)
1	200x150x3	Bar 20x4
2	200x150x4	Bar 20x4
3	200x150x5	Bar 20x4
4	200x150x4	Bar 40x4
5	200x150x4	T profile 20x4x20x4
6	200x150x4	T profile 40x4x20x4
7	600x150x4	Bar 20x4
8	200x400x4	Bar 20x4

Table 6.4 Model dimensions

As explained above only plate elements and beam elements are used within the finite element models. As small parametric study will also provide a check on results between different mesh sizes. It is based on three different models with plate fields modeled with 20x15, 8x6 and 1x1 elements. Therefore, frequent comparison will be made between several different load cases and between several different mesh sizes.

To give an idea of the initial plate field, the theoretical critical stress is:

$$\sigma_{cr} = 4\frac{\pi^2 2e11}{12(1-0.3^2)}\left(\frac{0.004}{0.15}\right)^2 = 5.142e8 N/m^2 = 514.2 MPa$$

While the yield material stress is 690MPa. This illustrates again that the critical stress is less than the yield stress as suspected.
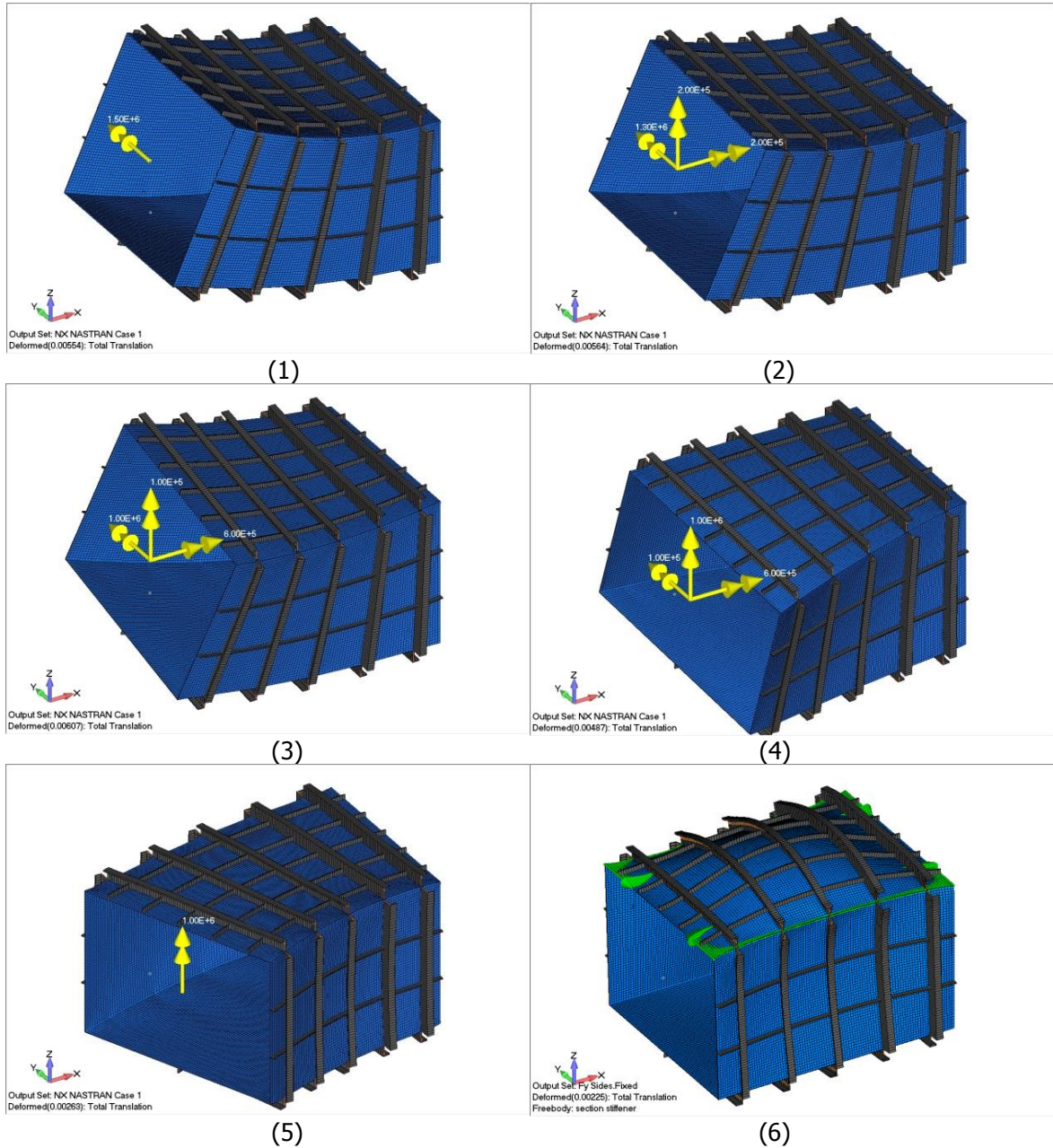
Fig 6.9 Loadcases 1 to 6 for the analysis of the plates and columns within the model under different circumstances.

(1 & 2 & 3)

(4)

(5)

(6)

Output Set: 2.13.2.Fixed
Deformed(0.0049): Total Translation

(7)

(8)
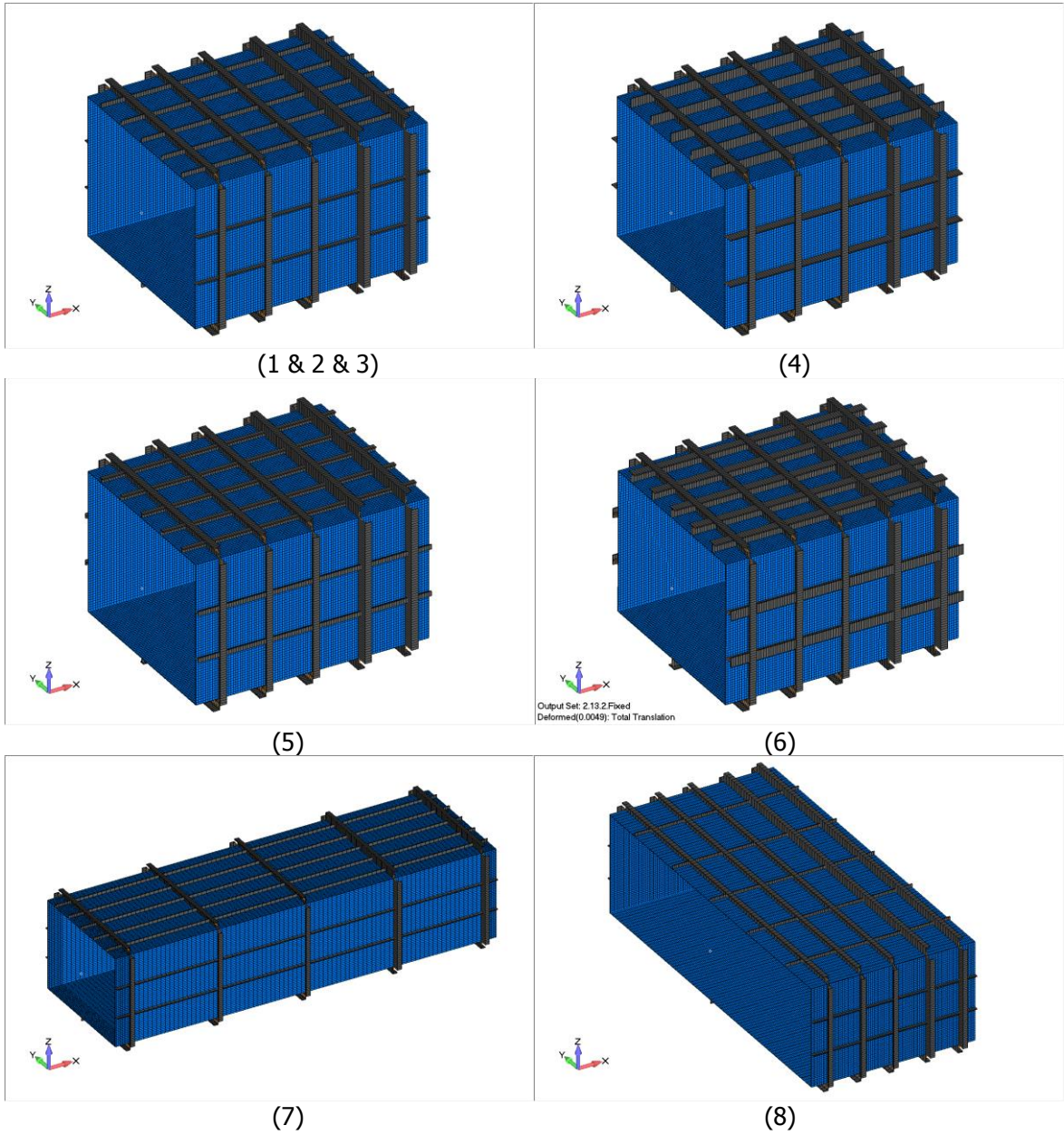
Fig 6.10 Variation in dimensions.

7.   Implementation with help of SDC Verifier

With the model described above there is now a search for all result stresses of the individual plate fields, stiffeners, girders, webs, flanges and columns. More extensive possibilities are available for FEM packages nowadays though. FEMAP is recognized as the world's leading CAD-independent Windows-native pre- and post- processor for advanced engineering finite element analysis. FEMAP delivers high performance FEA modeling for the engineering desktop. SDC Verifier enhances FEMAP with a new functionality and can be seen as an extension. Together they provide an accepted and sound solution for the verification of constructions according to Structural Design Standards.

SDC Verifier uses FEMAP as the pre-processor for the generation of model and its graphical interface to visualize the results. While modeling complex products, systems and processes SDC Verifier enhances the possibilities even further. It provides fast calculation for load combinations and Load Groups. It allows to find minimum and maximum values for displacement, stresses and their locations. It provides extra calculations to check structures according to any standards. And the extension can generate all those results into user defined calculation reports presenting results in a variety of tables with the possibility to add them to a word report or export to an excel document.

SDC is able to provide recognition of individual plates, stiffeners and girders. It renders easy access to stress results for each of these sections. The aim is to supplement this functionality with the implementation method described in this report. A full scale buckling check of a panel in your FEM model should become a simple task. The recognition looks like figures 7.1 and 7.2. Stress results are sorted and filled into tables as shown in figure 7.3.
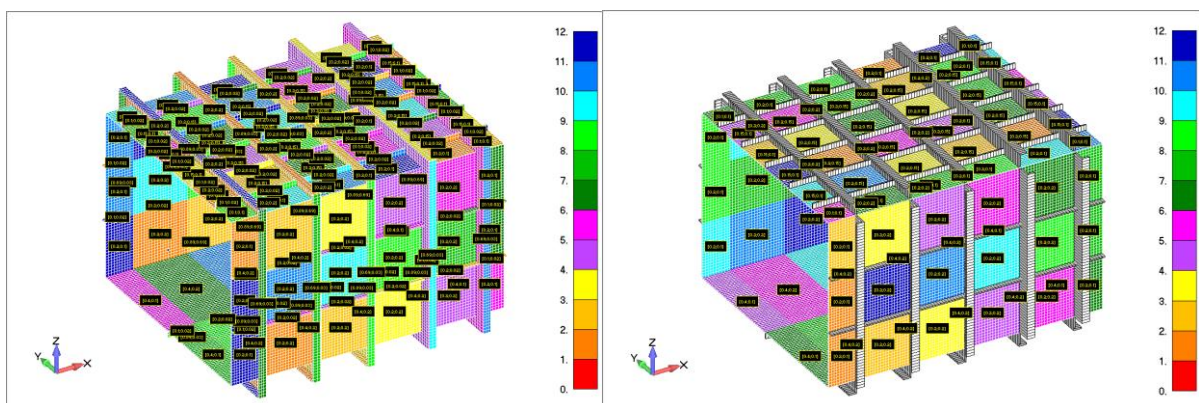
Fig 7.1 The FEM plate model and the FEM beam model with individual plate fields indicated in different colors with each their dimensions given.
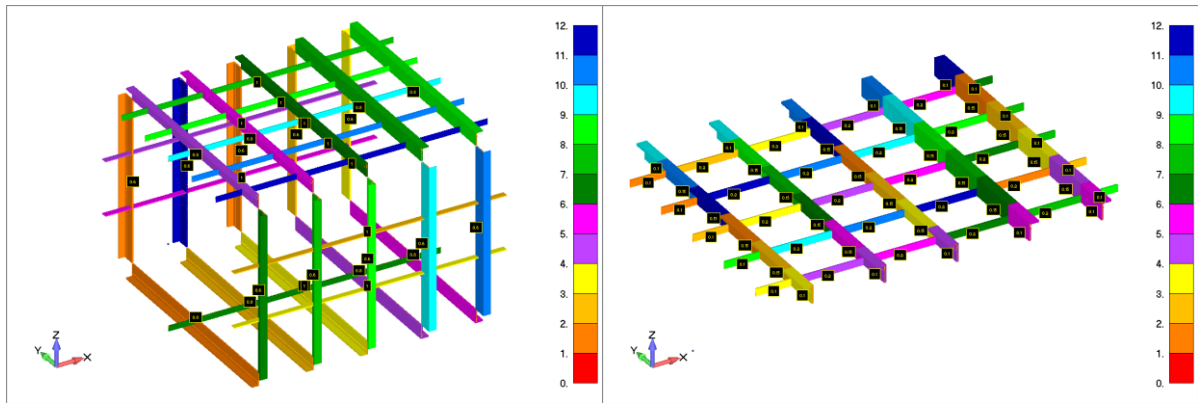
Fig 7.2 The FEM beam model with individual girders indicated and the top panel from the beam model wherein each girder is subdivided into stiffeners in between other girders, all in different colors with each their dimensions given.
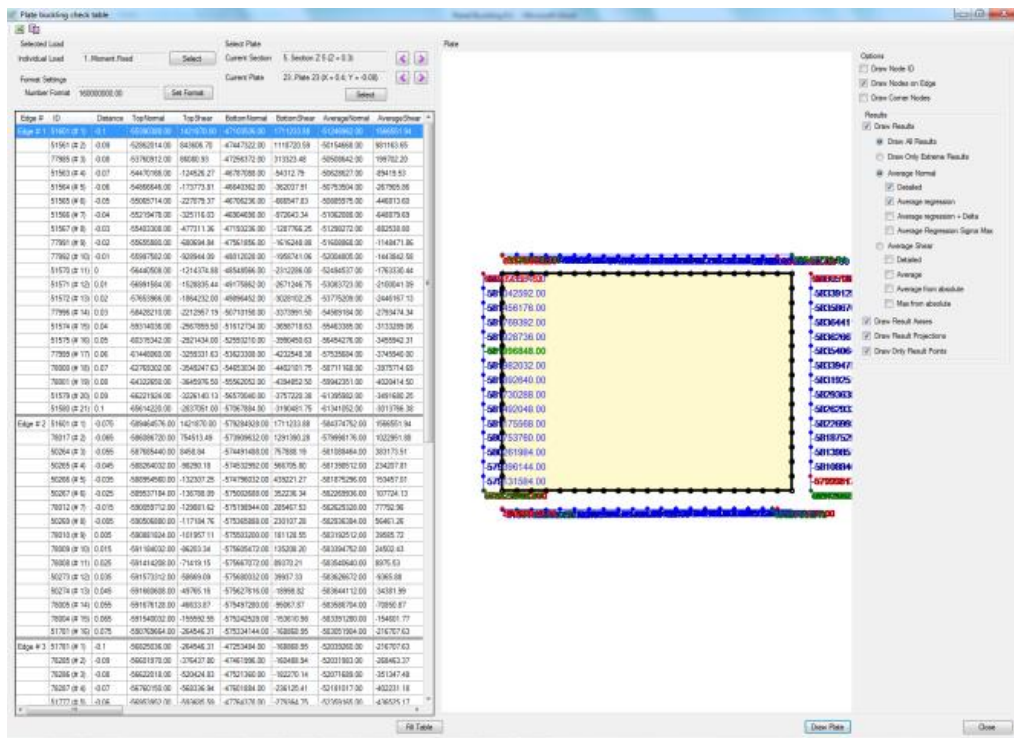
Fig 7.3 In-plane stress results for a single plate field extracted by SDC Verifier from FEMAP.

8. Analysis of unstiffened plate buckling limit

In present methods the checks are based on individual FEM plate elements. The benefit for analyzing individual elements would be the possibility to analyze varying cross-sectional areas in the plates. You could imagine that optimization possibilities arise, still having the automatic placement of stiffeners in mind. However if you look at a fine meshed plate field, then it is wrong to take the result of a single element as representative for the complete plate field. Thus the whole plate field, independent of the mesh size, is checked instead.

O. Hillers had some research questions left on the definitions of design stresses. The in-plane stresses are discussed in chapter 8.2 and the stress gradient effect is discussed in chapter 8.3. Note that the lateral loads on plate fields are disregarded for now.

8.1 Approach of the standards

The aim is to work to the unstiffened plate buckling limits in the ABS and DNV. Various formulas are presented in literature to predict the interaction of biaxial compression loads. The formulas generally take a similar form to the von Mises yield criterion. An illustration of the concept is shown in figure 8.3. Since the constants coefficients in the power terms are not entirely true for all situations, standards weave some additional parameters into the formula.

Unstiffened plate buckling limit:

$$(ABS) \rightarrow \left(\frac{\sigma_{xmax}}{\eta\sigma_{Cx}}\right)^2 + \left(\frac{\sigma_{ymax}}{\eta\sigma_{Cy}}\right)^2 + \left(\frac{\tau}{\eta\tau_C}\right)^2 \leq 1 \qquad \{22\}$$

The DNV has several individual checks for σ_x, σ_y and τ but no combined formula for the plate buckling limit. However, the more important ultimate strength is available for both standards in the same form. The extra parts, which use the coefficients φ and c_i to reflect interaction between longitudinal and transverse stresses, are not the only changes to separate the formula from the plate buckling limit. Most of the other coefficients change as well for the ultimate strength is something fundamental different from the plate buckling limit as described. For details can be looked into the standards themselves.

Unstiffened Plate Ultimate strength:

$$(ABS) \rightarrow \left(\frac{\sigma_{xmax}}{\eta\sigma_{Ux}}\right)^2 + \left(\frac{\sigma_{ymax}}{\eta\sigma_{Uy}}\right)^2 - \varphi\left(\frac{\sigma_{xmax}}{\eta\sigma_{Ux}}\right)\left(\frac{\sigma_{ymax}}{\eta\sigma_{Uy}}\right) + \left(\frac{\tau}{\eta\tau_U}\right)^2 \leq 1 \qquad \{23\}$$

$$(DNV) \rightarrow \left(\frac{\sigma_{x,Sd}}{\sigma_{x,Rd}}\right)^2 + \left(\frac{\sigma_{y,Sd}}{\sigma_{y,Rd}}\right)^2 - c_i\left(\frac{\sigma_{x,Sd}}{\sigma_{x,Rd}}\right)\left(\frac{\sigma_{y,Sd}}{\sigma_{y,Rd}}\right) + \left(\frac{\tau_{Sd}}{\tau_{Rd}}\right)^2 \leq 1 \qquad \{24\}$$

Multiple load combinations complicate the implementation. Remember the simple input design stresses from figure 8.1. The figure is deliberately repeated from chapter 4 to accentuate the importance of this principal. The linear distributions for in-plane normal stresses are prominent. Within the standards the calculated resistances make use of the Euler definition described before as

$$\sigma = k_s \frac{\pi^2 E}{12(1 - v^2)} \left(\frac{t}{s}\right)^2 \qquad \{25\}$$

in which k_s is dependent on the in-plane bending moment and thus the ratio of edge stresses κ,

$$\kappa = \frac{\sigma_{imin}}{\sigma_{imax}} \qquad \{26\}$$
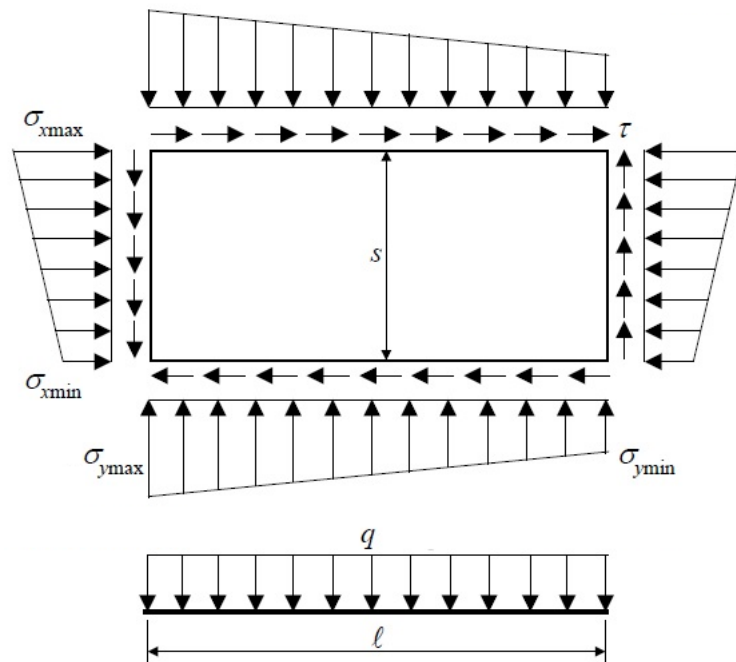
Fig 8.1 Plate field input design stresses.

On a side note, these simplified combinations tend to raise new questions regarding the input design stresses. Equations 22 to 24 simply combine relations of the individual σ_x, σ_y and τ. The IACS Common Structural Rules for bulk carriers gives a description to adjust the stresses from the finite element model results σ_x^* and σ_y^* to account for the poison ratio. But a finite element program is understand to produce stress results in which the poison ratio is already calculated hence this adjustment should probably only be applicable with theoretical approaches.

$$\sigma_x = \frac{\sigma_x^* - 0.3\sigma_y^*}{1 - v^2} \quad and \quad \sigma_y = \frac{\sigma_y^* - 0.3\sigma_x^*}{1 - v^2} \qquad \{27\}$$
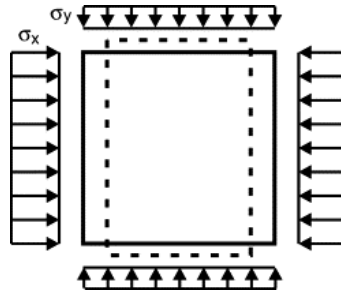
Fig 8.2 Due to contraction in the y direction and thus expansion in the x direction will the axial resulting force increase in the column and vice versa.
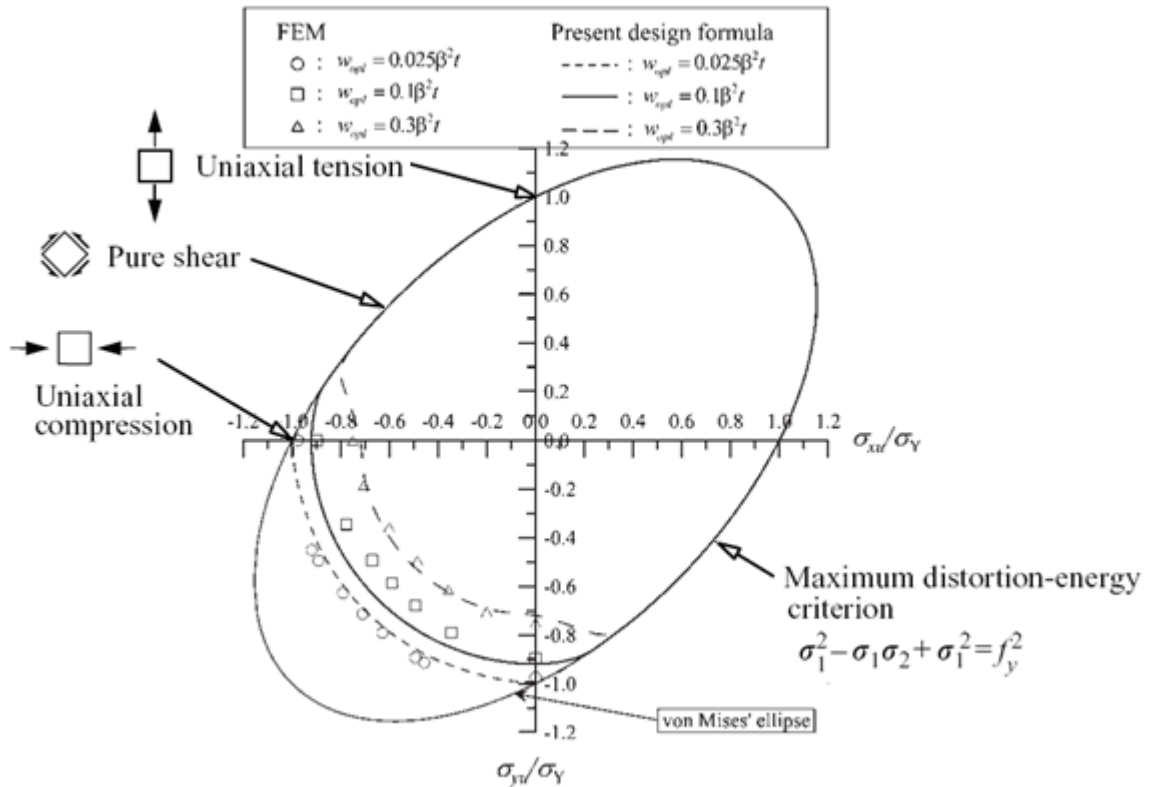
Fig 8.3 Ultimate strength interaction relationship between biaxial compression and tension for a thick plate, when L/s = 1 and t = 25 mm.

8.2   In-plane stresses

Remember the six input stresses for plate buckling as defined in figure 8.1:

σ_{Xmax} =   maximum stress in longitudinal direction

σ_{Xmin} =   minimum stress in longitudinal direction

σ_{Ymax} =   maximum stress in transverse direction

σ_{Ymin} =   minimum stress in transverse direction

τ =   uniform shear stress

q =   uniform lateral pressure

The principal works with corner stress results from individual plate elements. This choice is made due to the simple implementation, you will not need to separate forces which work on several elements and secondly you will not need to convert forces to stresses for use in the standards. A, further non-studied question rises whether linearized forces would produce other results than linearized stresses. The first thought is that these two approaches theoretically should be equal.

The difference between the maximum and minimum normal in-plane stresses on a single edge at the same time defines an in-plane bending moment. But except for the uniform lateral pressure all other out of plane local stress results are disregarded. In the first place this assumption is adequate since the out of plane bending moments are generally very small. But secondly this is due to the chosen conservative simply supported boundary condition which theoretically cannot absorb any bending moments. Since the standards cannot work with the results the only solution is to go with in-plane normal stresses anyway (fig 8.4b). Therefore the average stress from the top and bottom stress results is taken.
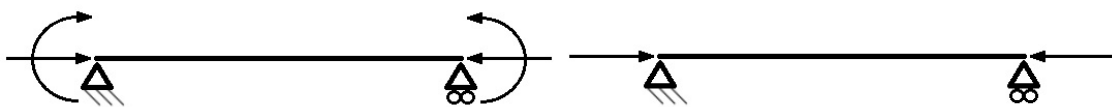
Fig 8.4 Stresses on the edges of a plate field with (left) also the out of plane bending stresses and (right) only the in-plane normal stresses.

Furthermore, for each node on the edge, the average from the two adjoining plate elements is taken. This leaves a straightforward distribution of stress results along each edge.

That means that in figure 8.5 you get 9 values averaged for the two long edges and 5 values averaged for the two short edges. For all test done in this study all elements have the same dimensions in the plate field, so numbering along the edge would be enough. While keeping track of stress results there is made certain that number 1 is on the opposite of the other number 1 and number 2 is on the opposite of the other number 2 and so on (fig 8.6a). However in the random situation the elements do not have the same dimension. So numbering of the nodes need to include

interval distance or better jet distance with reference to a point. The reference is taken from the middle of the plate edge. This can only be done with distances because of the situations where there are an even amount of nodes along the edge. The short edges are done in the same manner.
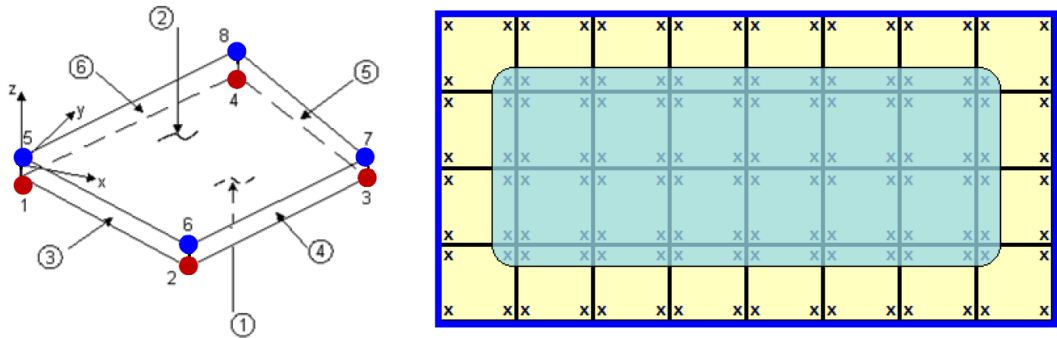
Fig 8.5 Corner stress results in a plate field.
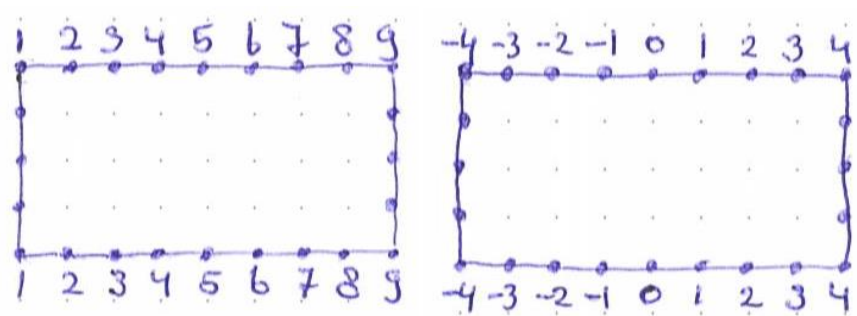
Fig 8.6 Approach for keeping track of stress results along the long edges of a plate field.

Accordingly Hillers proposed to use linear regression to go from a complicated distribution to a simple linear variation. A short description from literature on linear regression gives the following formulas:

$$y = ax + b$$

$$a = slope = \frac{(n \sum x_i y_i) - (\sum x_i)(\sum y_i)}{(n \sum x_i^2) - (\sum x_i)^2}$$

$$b = intercept = \frac{(\sum x_i^2)(\sum y_i) - (\sum x_i)(\sum x_i y_i)}{(n \sum x_i^2) - (\sum x_i)^2}$$

{28}

More details are described in the work Hillers work. Any least squares curve- or line-fitting algorithm optimizes the constants of a fitting equation by minimizing the sum of the squares of the deviations of the actual (data) values from the values predicted by the equation. Since the standards ask for a linear distribution, linear least squares fitting is an excellent choice to provide each edge with a σ_{max} and a σ_{min}. However, just a linear regression does not always give a conservative approximation of the real situation. Therefore the linear line may have to be moved with an appropriate value. Four methods are proposed.

1. **Linear Regression Stress Average**: The linear regression from all corner stress points on the edges along a plate field. The principle is given and explained in earlier work from Ottar Hillers.

2. **Linear Regression Stress Average + Including all stress results**: The proposed adaption from the normal linear regression by Ottar Hillers. It shifts the line to the point in which all stress points fall under the area such that an overestimate and very conservative load is taken for each edge.

3. **Linear Regression Stress Average + Updated to σmax**: A new proposal to adapt the linear regression such that σ_{max} of the linear regression matches the σ_{max} of all stress points along the edge. The standards specifically use the maximum compressive stress in the longitudinal or transvers direction which raises the question whether taking a higher value than the highest stress points is not an overestimate already.

4. **Linear Regression by the Eurocode clause**: Clause 4.6(3) in Eurocode 3, part 1.5 delivers an adaption to compensate the stress gradient phenomenon described in the next section.

The first three methods produce linear lines on all 4 edges and afterwards take the average of opposite edges because the in-plane stresses on opposite edges need to be symmetrical. Thus the idea is to first make two conservative linear distributions and then take a non-conservative average. The last method is the same as the first except for the last step, it does not take the average but the value is then determined at a distance 0,4L or 0,5s from the greater stress distribution. This may actually alter the slope of the linear line though. Note that the first method is equal to combining all stress results from both opposite edges into one graph and then calculating a linear regression.
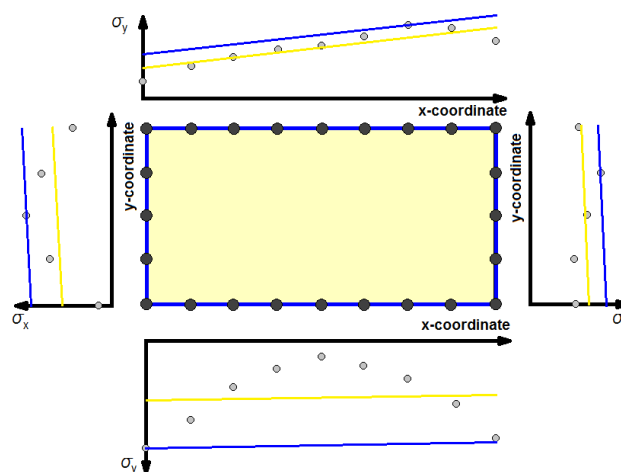
Fig 8.7 Proposed method by O. Hillers.
The yellow lines indicate method 1 and the blue lines indicate method 2.

Method 3 originates from interpretation of equations 22 to 24. The specific input design stresses are σ_{Xmax} and σ_{Ymax}. The linearizations may regularly produce input design stresses where σ_{max} is greater than the maximum real stress result. But why should one take a greater stress than actual exists in the model? The DNV literally states: "The linearized buckling stress should be carefully selected to be maximum compressive stress in the analysis". The differences between the three types of linearizations are illustrated in figures 8.7 and 8.8.

Figure 8.9 give the stress results of a plate field with load case 1 as an example of the actual implementation method. The right graph shows results for the short edge and the lower graph shows results for the long edge. Blue and red results represent the opposite edge while the green are the average from those two and the black are the combination defined by the Eurocode clause. The linearizations are drawn in the graphs as well.
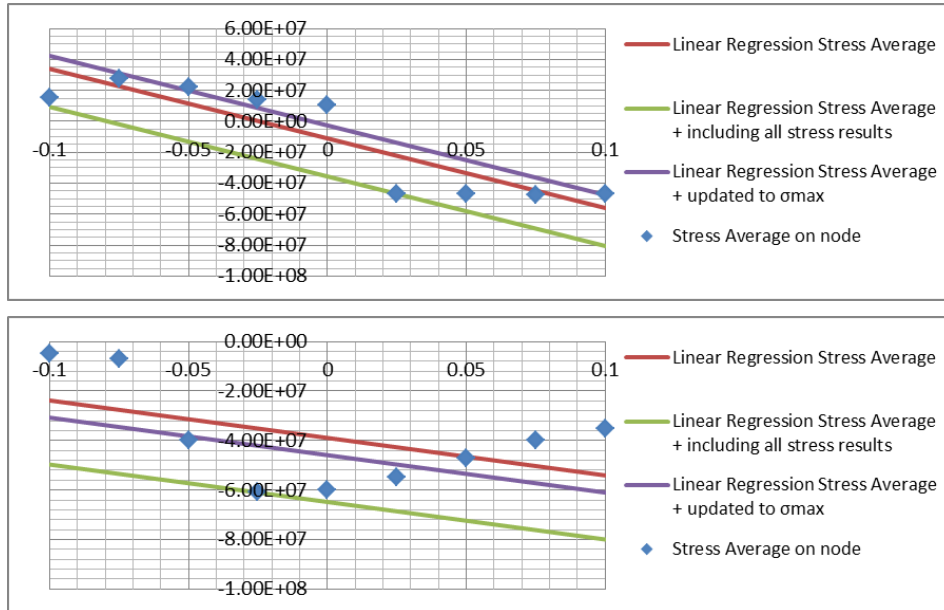
Fig 8.8 Illustration of the three methods with random stress points. The method stays the same when some or all stress results along an edge are positive (tension instead of pressure). Notice that method 3 (purple line) may be less conservative than the average linear regression.

Notice that all four of the linear regression methods produce equal results for the single element mesh size models. These models provide a linearized stress distribution by definition as mentioned before.

On a side note, the linear stress results may provide a distribution which is the opposite from what you expect to get at the bifurcation point when the edges will take a greater part of the load than the middle of the plate. The parabolic shape of the distribution can thus be positive or negative (fig. 8.10). According to the standards the use of linear stress results is allowed. The DNV literally states: "The linear elastic buckling stress found by FEM eigenvalue analyses may be used as basis for determination of buckling resistance". In order to account for material non-linearity, residual stresses and imperfection, a suitable buckling curve may be used as long as the effective width parameters are employed.
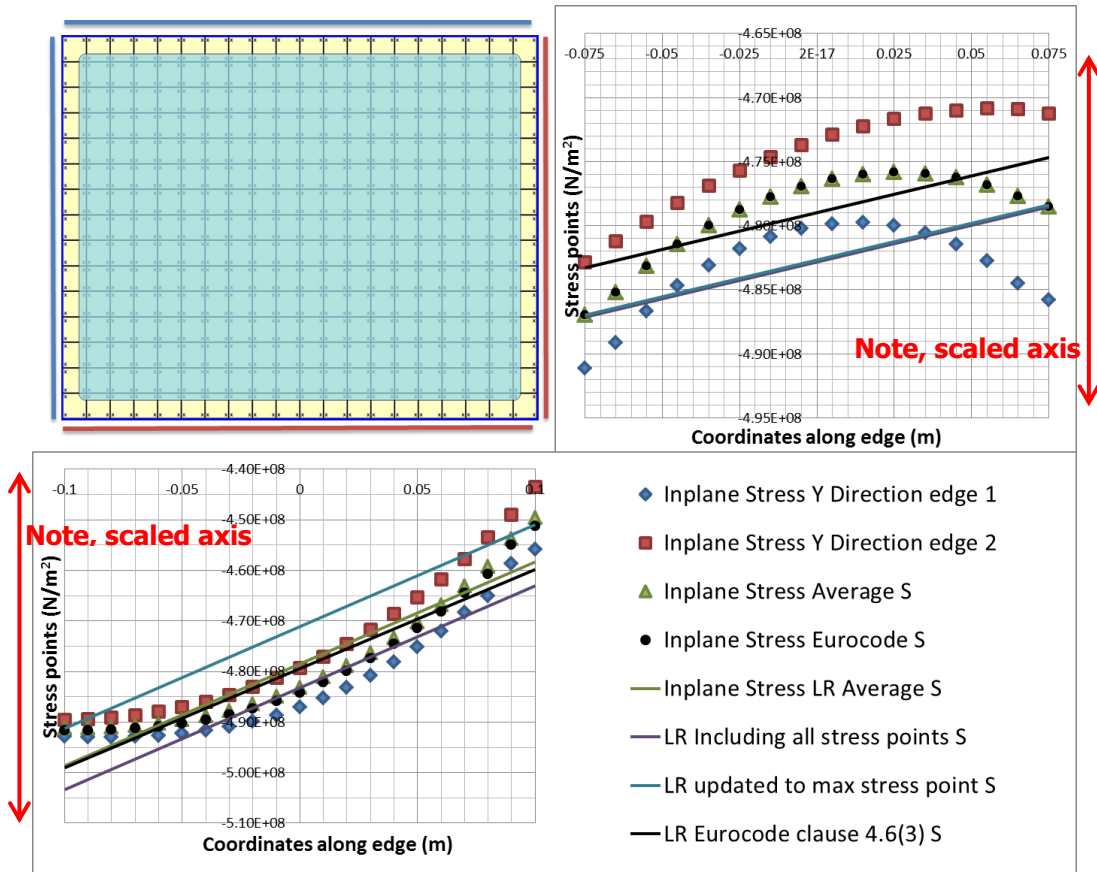
Fig 8.9 Focus on difference between real stress distribution results for a plate field with load case 1. For clarification the linearizations are drawn as well.
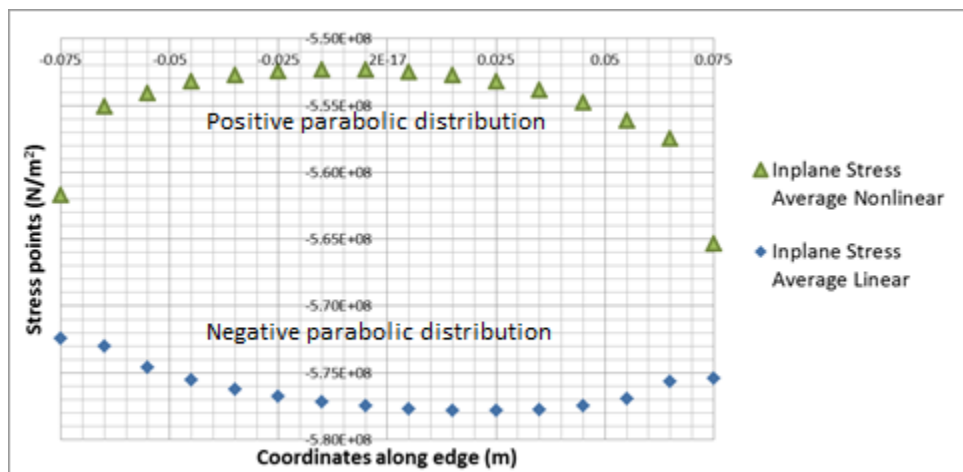
Fig 8.10 Difference between linear and nonlinear stress distribution over the plate field. Note that the linear results are calculated from a linear analysis over the complete model and the nonlinear results are a consequence of a nonlinear analysis over the complete model.

However, the parabolic shape of the stress distribution does influence the degree of resemblance between the linearization and the real results. With the simply supported boundary condition, the stresses in the middle of the plate have a larger influence on the linear eigenvalue analysis. A negative parabolic shape, with the largest stresses in the middle, has therefore a disadvantage. An average

linear regression may actually have a more conservative result than the opposite positive parabolic shape while the negative parabolic shape requires an adjustment such as method 2 or 3.

The shear stress distribution along the edges of the plate field need to be matched with an equal uniform shear stress altogether. Three different approaches have been proposed.

1. The average of all real shear stress results
2. The average of all absolute real shear stress results
3. The maximum of all absolute real shear stress results
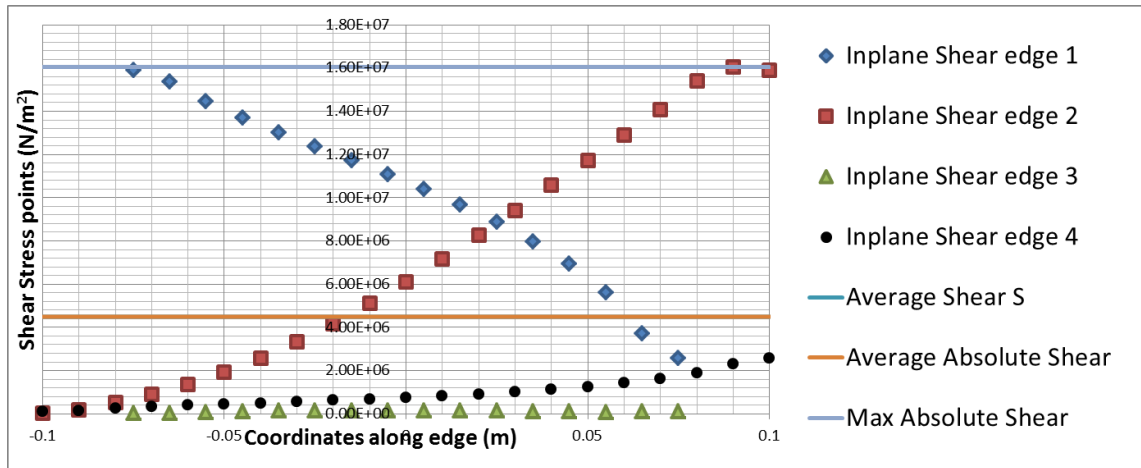
Fig 8.11 Shear stress results for a plate field with load case 1.

When plate fields have a free edge, the in-plane normal stresses should be zero. In reality at the corners of the plate can exist fairly high values. Therefore these edges cannot be processed with the same implementation method for you will get linearization as seen in figure 8.12. The stress σ_X or σ_Y should instead be taken as zero.
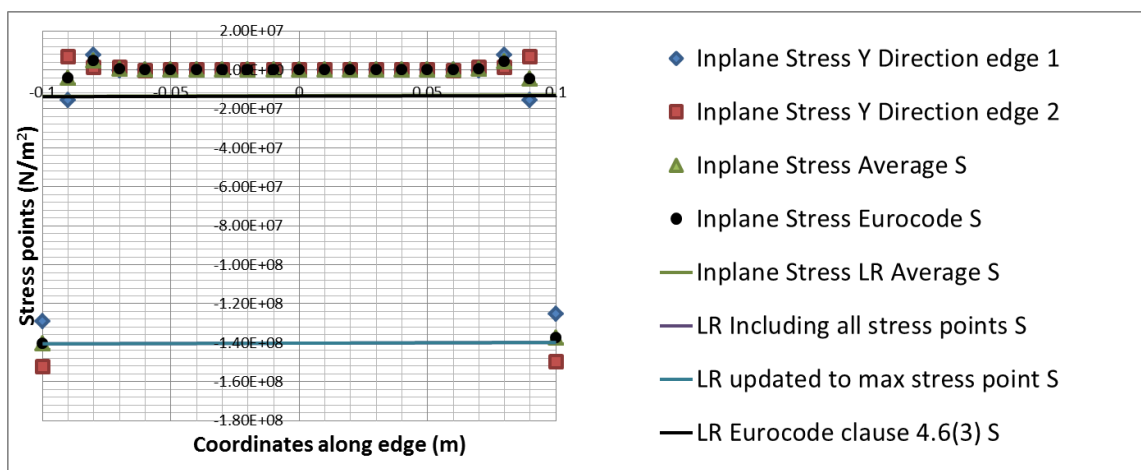
Fig 8.12 In-plane stress results on the long edge for a web with a free edge.

8.3   The stress gradient effect

Besides the out of plane bending moments and linearization problems there also exist another difference between the reality and the standards. Following figure 10, the in-plane stresses on opposite edges need to be symmetrical. Ottar Hillers mentions two options to follows. Take the maximum as specified in the DIN code or follow clause 4.6(3) in Eurocode 3, part 1.5. The DNV nor the ABS specifies details though. Theory does not really provide satisfying thoughts about it either. Considering the plate as a 2D element, the problem could be simplified to figure 8.13.
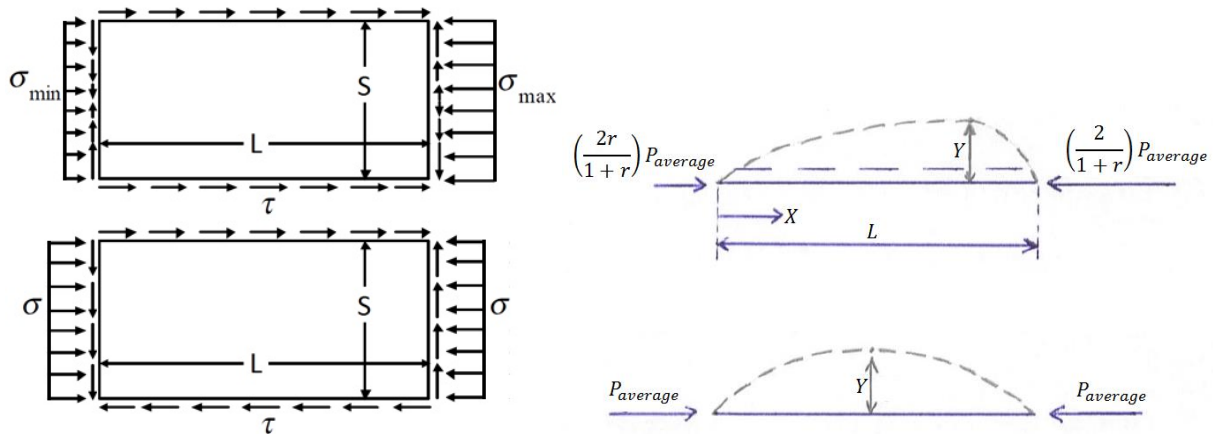
Fig 8.13 In-plane shear stress distributions (a) on the plate and (b) simplified as 2D problem.

For the version with average force and no shear force you get the following well known differential equation:

$$E \cdot I \cdot \frac{d^2y}{dx^2} = M = -P \cdot y$$

$$\frac{d^2y}{dx^2} + \left(\frac{P}{E \cdot I}\right)y = 0$$

{29}

Which has the general solution:

$$y(x) = C_1 \cdot \sin\left(\sqrt{\frac{P}{E \cdot I}}x\right) + C_2 \cdot \cos\left(\sqrt{\frac{P}{E \cdot I}}x\right)$$

{30}

Using the boundary condition gives the result:

$$\left.\begin{array}{l} y(0) = 0 \\ y(L) = 0 \end{array}\right\} C_1 \cdot \sin\left(\sqrt{\frac{P}{E \cdot I}}x\right) = 0$$

$$P = \frac{n^2 \cdot \pi^2 \cdot E \cdot I}{L^2}$$

{31}

This is the Euler column buckling critical load as described above. For the problem with non-uniform shear the following similar formula can be set up:

$$\frac{d^2y}{dx^2} + \left(\left(\frac{2-2r}{1+r}\right)\frac{P \cdot x}{E \cdot I \cdot L} + \left(\frac{2r}{1+r}\right)\frac{P}{E \cdot I}\right)y = 0$$

{32}

with $-1.0 < r < 1.0$ This second order differential equation has non constant coefficients and gives, together with the same boundary conditions as before, a much more tedious solution:

$$y(x) = C_1 \cdot \text{Ai}\left(\frac{\sqrt[3]{2}\,\sqrt[3]{\left(\frac{P\,(r-1)}{EIL\,(r+1)}\right)}\,(EI(r-1)x - EILr)}{EI(r-1)}\right)$$

$$+C_2 \cdot \text{Bi}\left(\frac{\sqrt[3]{2}\,\sqrt[3]{\left(\frac{P\,(r-1)}{EIL\,(r+1)}\right)}\,(EI(r-1)x - EILr)}{EI(r-1)}\right)$$

{33}

This formula contains the difficult Airy function and is therefore not analytically solvable.

$$Ai(x) = \frac{1}{\pi}\int_0^\infty \cos\left(\frac{t^3}{3} + xt\right) dt$$

$$Bi(x) = \frac{1}{\pi}\int_0^\infty \left(e^{\left(-\frac{t^3}{3}+xt\right)} + \sin\left(\frac{t^3}{3} + xt\right)\right) dt$$

{34}

C. Yu and B.W. Schafer approached this problem of the stress gradient effect with the Rayleigh-Ritz method to determine the buckling stress of plates. In this method, an assumed deflection function satisfying the boundary conditions is used in the expression for the total potential energy Π. The total potential energy is the summation of internal strain energy U of the plate during bending, and the work done by the external forces T. Classical solutions from thin plate theory from Timoshenko and Gere result in:

$$U = \frac{E}{2(1-v^2)}\int_{-t/2}^{t/2} z^2 \int_0^s \int_0^L \left[\left(\frac{\partial^2 w}{\partial x^2}\right)^2 + \left(\frac{\partial^2 w}{\partial y^2}\right)^2 + 2v\frac{\partial^2 w}{\partial x^2}\frac{\partial^2 w}{\partial y^2} + 2(1-v)\left(\frac{\partial^2 w}{\partial x \partial y}\right)^2\right] dxdydz$$

$$T = -\frac{t}{2}\int_0^s \int_0^L \left[\sigma_x\left(\frac{\partial w}{\partial x}\right)^2 + \sigma_y\left(\frac{\partial w}{\partial y}\right)^2 + 2\tau_{xy}\frac{\partial w}{\partial x}\frac{\partial w}{\partial y}\right] dxdy$$

{35}

With the deflection function:

$$w = \sum_{m=1}^{M}\sum_{n=1}^{N} w_{mn} \sin\frac{m\pi x}{L}\sin\frac{n\pi x}{s}$$

{36}

The following expression for σ_x, corresponding to a linear variation of compressive stress between σ_{min} and σ_{max}, is written [33]:

$$\sigma_x = -\sigma_{av}\left[\left(\frac{1-r}{1+r}\right)\frac{2x}{L} + \frac{2r}{1+r}\right]$$

$$\sigma_y = 0$$

$$\tau_{xy} = -\frac{\sigma_{av}}{\alpha}\left(\frac{1-r}{1+r}\right)\left(\frac{2y}{s} - 1\right)$$

{37}

Where σ_{av} is the average compressive stress in the x direction at the plate center, r is the ratio $\sigma_{min}/\sigma_{max}$ and α is the plate aspect ratio L/s. With this theory they solved the stress gradient for plate field with several different boundary conditions. For equation 6 they provided a closed-form expression for the traditional plate buckling coefficient k:

$$k = k_\infty + \frac{\beta_1 r + \beta_2}{\beta_3 r + \beta_4 + \alpha^{\beta_5}}$$
{38}

β_1 through β_5 are empirical coefficients dependent on the plate boundary conditions along the unloaded longitudinal edges as summarized in table 8.1. The results are also seen in figure 8.14.

	k_∞	β_1	β_2	β_3	β_4	β_5
ss-ss	4.000	-1.70	1.70	0.20	-0.20	0.75
fix-fix	6.970	-2.20	2.20	0.20	-0.20	0.65
ss-free	0.425	-0.80	1.00	0.00	-0.60	0.95
fix-free	1.277	-0.60	0.60	0.00	-0.65	0.60

Table 8.1 Coefficients for plate buckling under longitudinal stress gradients [34]

Note: applicable for $1 \leq \alpha \leq 30$ and $-1 \leq r \leq 1$, ss = simply supported

Regrettably they only research stress gradients in the longitudinal direction of the plate. However for the formula of the internal strain energy is made the assumption that normal stresses produce no shear stresses and vice versa (appendix L). It is possible to obtain strain energy of a plate element due to shear independent from the normal forces. And this assumption disagrees with the problem statement which seems to make the results incorrect. So for now, due to the unsolved issue only the Eurocode clause is used in combination with the linear regression methods as possible solution.
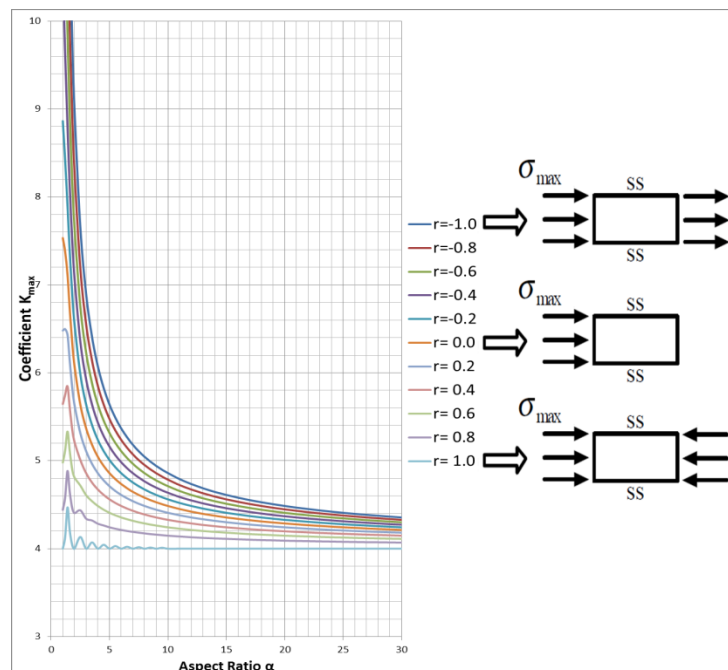

Fig 8.14 Relation between coefficient k_{max} and the aspect ratio by C. Yu and B.W. Schafer. [35]

8.4 Approach for verification of implementation method

The implementation method to define the five input design stresses for the standards is outlined now. Whether the actual method is applicable has to be checked first. O. Hillers did some initial checks. He compared the linearization with theoretical calculations with uniform applied loads and with the present check in SDC Verifier. However some real stress results will be checked now.

You could analyze a situation, use the implementation method and fill in the standard to get a result for the buckling probability. This result should be compared to the reality. But what is the reality? Doing real size tests is unfeasible so you would end up with the power method (nonlinear FEM analyses) However this would require detailed specifications about real size structures to implement the load cases, boundary conditions, imperfections, material properties and residual stresses. Or it would require an immense amount of tests to vary all those parameters described in this report. Hence you would get two analyses, one for the method and a second for comparing:

1. Linear static analysis -> Corner stress results -> Implementation method -> Standard -> Result =? Real Buckling factor =?
2. Linear static analysis -> Freebody load + Constraints + Imperfections + Properties + Residual stress -> Nonlinear analysis

You can make the problem at hand as complicated as you want with non-linear analyses and detailed parameters when modeling. Instead of opting for the power method the testing is done faster, simpler and with less uncertainties. Due to simplification in the standards, even with the correct input you will not get the exact same answer as reality. Instead of comparing end results, only the difference between real stress results and linearized stress results is checked. Only in-plane real stresses are compared with in-plane linearized stresses. The proposal is illustrated in figure 8.16. When linear regression is sufficiently matching with real stresses that would imply the method is validated. The same input design stress is interpreted as usable for both the ABS and DNV. Since all checks and calculations will be linear analyses, the actual values for the loads cases become irrelevant. When multiplied, the buckling factor will change with the same multiplication. The same holds for the boundary conditions since both checks are done with the exact same analysis.

There are seven checks that can be made, shown in figure 8.15 and simply stated as:

1. Linear static analysis -> Translation including rotations -> Eigenvalue Buckling analysis
2. Linear static analysis -> Translation excluding rotations -> Eigenvalue Buckling analysis
3. Linear static analysis -> Freebody load (including in-plane moments) -> Eigenvalue Buckling analysis
4. Linear static analysis -> Freebody load (excluding in-plane moments) -> Eigenvalue Buckling analysis
5. Linear static analysis -> Corner stress results -> In-plane forces -> Eigenvalue Buckling analysis
6. Linear static analysis -> Corner stress results -> Linear Regression -> In-plane forces -> Eigenvalue Buckling analysis
7. Linear static analysis -> Freebody load -> Linear Regression -> Eigenvalue Buckling analysis
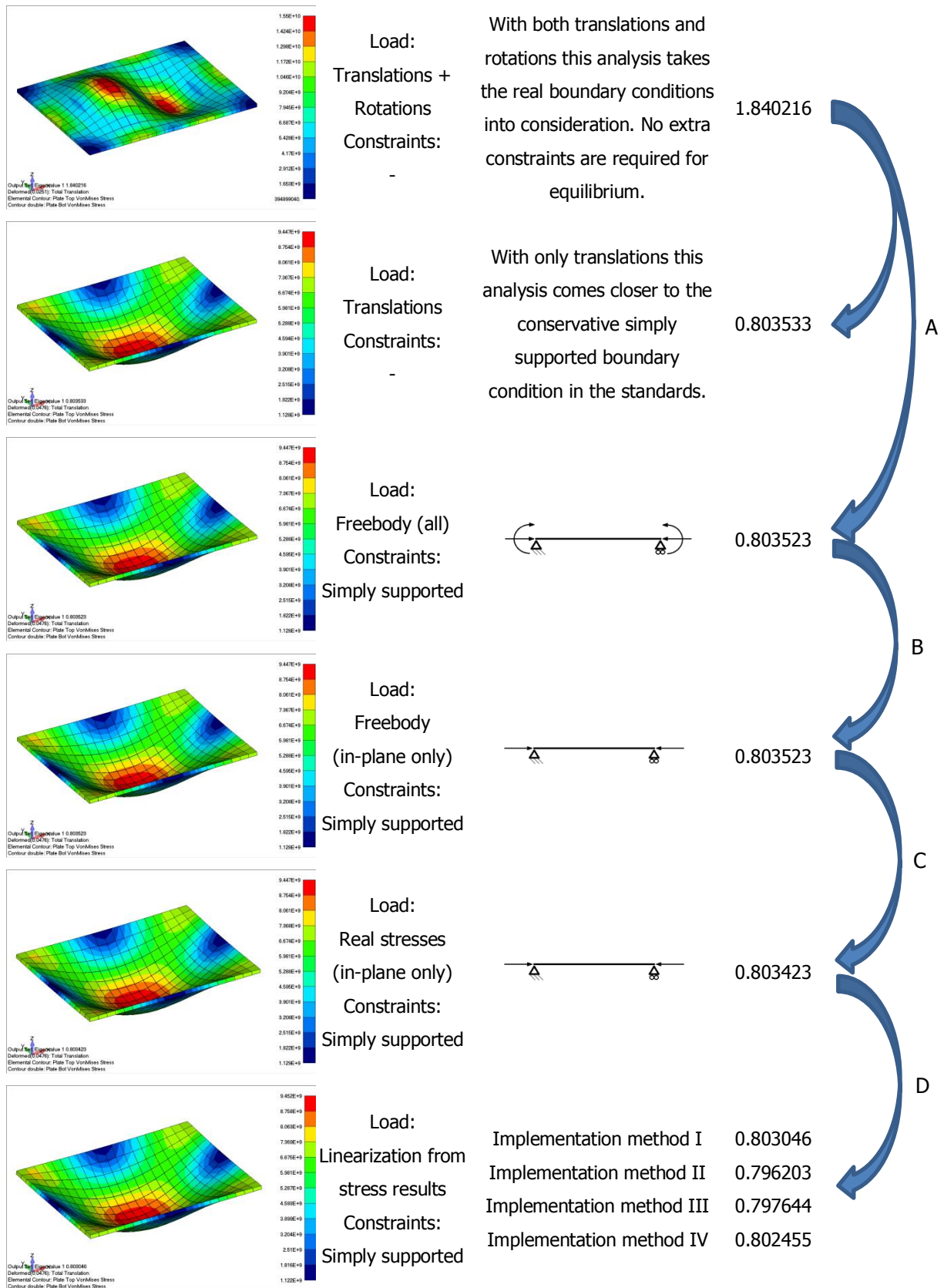
Fig 8.15 The first six linear eigenvalue analyses of an individual unstiffened plate field. For all 6 approaches it analyses the same plate field from the model as described above. On the right: (A) check of "Simply Supported" (B) check of "In-plane stresses only" (C) check of "conversion stresses to forces" and (D) check of "Linearization". For the last case: 4 different buckling factors due to the first 4 implementation methods with average shear: (I) Average Linear Regression (II) Updated to max stress point (III) Including all stress points (IV) Eurocode clause.
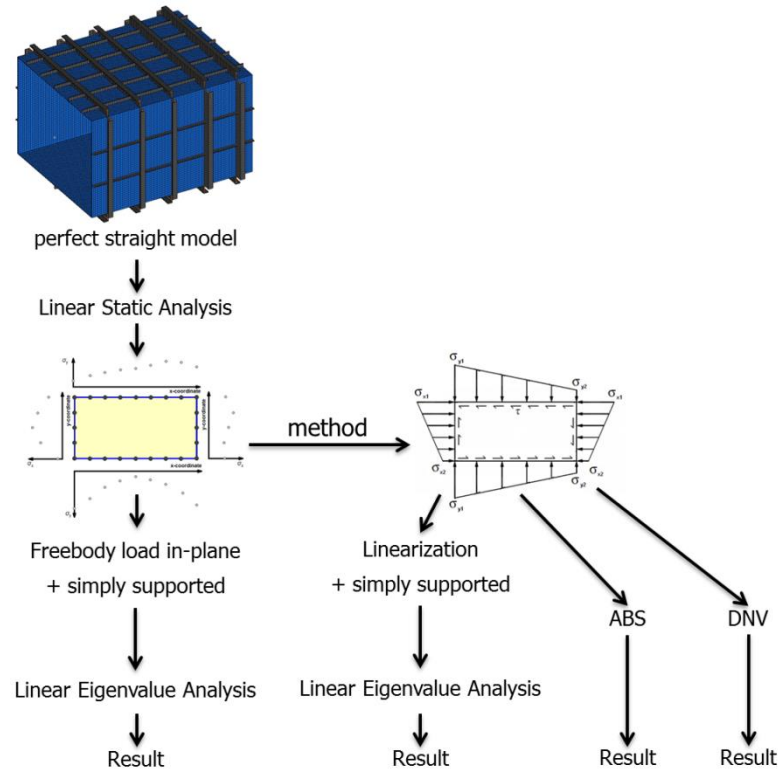
Fig 8.16 Approach overview.

With checks (1), (2) and (3) the boundary conditions can be observed. Simply supported lead to conservative values as expected but a quick check does also show a sufficient good match to validate the use of freebody forces. Therefore is opted for simply supported edges without holding them straight, see figures 5.12a and 8.15. Checks (3) and (4) together match so well for the FEM models used here that the assumption of in-plane loads only can be made without hesitation. This statement is conservative as well thus will most likely hold for other models too.

Now with check (5) there is some extra explanation in order. The freebody load produces for every individual section a set of forces that has equilibrium in all six directions. However the linear regression method is based on corner stress results from plate elements. A conversion from these stresses is made back to forces to be able to make an analysis in FEMAP. This conversion does not 100% match the freebody forces. This conversion can also be made with both the real stress results and with the linearized stress results. Buckling results match well between checks (4) and (5). Hence, while not being 100% equal the conversion is considered approved. Two valuable benefits result from this method. One, the implementation is easy enough to carry out a number of checks. And two, in this way a pure check between real stresses and linearized stresses, (5) and (6), remains. In the ideal situation we would like buckling factors which all match fairly well and have $k(1) \geq k(2) \geq k(3) \geq k(4) \geq k(5) \geq k(6)$.

Note that with the conversion from real corner stress results back to in-plane forces it would also be possible to check whether linearization of forces will give equal results compared to linearization of stresses (7). This is not further studied.

Fig 8.17 Boundary conditions used for individual unstiffened plate fields.

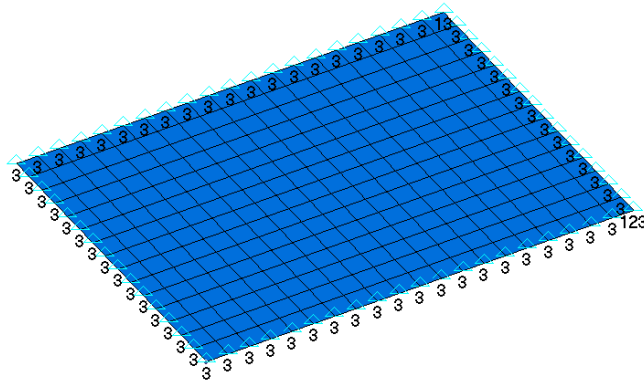The aim is to individually research in-plane normal stresses and shear stresses for two are defined by different methods. Comparing σ_X, σ_Y and τ separately is complicated since you need both σ_X and τ or both σ_Y and τ to get equilibrium in x or y direction. Shear only is not possible at all. At least not in the present situation. Figures 8.19 and 8.20 clearly show unbalanced shear forces. If $\sum F_x \neq 0$ or $\sum F_y \neq 0$ or $\sum M \neq 0$ then the constraint may have a serious influence on the results. The FEM program may provide eigenmodes and eigenvalues but they should be considered useless. Only the complete freebody load as in figure 8.18 has equilibrium.

However there is still the check that needs to be done on the individual σ_X, σ_Y and τ stresses. The shear stress results show three distinct patterns. One with fairly even and uniform shear over the plate field. One with an increasing amount of shear to one of the 4 corners of the plate field. And the last resembling figure 8.13. The proposed solution is seen in figure 8.21. All corner stress results are transformed back to in-plane forces and then subdivided into three separate combinations. σ_X is formed by the normal in-plane results and calculated shear forces τ_B. τ_B consists of uniform distributed forces along the long edges such that the difference due to the stress gradient is compensated. The in-plane normal results also produce a small moment which is compensated with a difference between τ_{B1} and τ_{B2}. What is done for σ_X is also done for σ_Y. These two separate combinations are hence in equilibrium and can be compared to the implementation methods which are already in equilibrium (checks 2 and 3 in figure 8.21).

The shear result τ_A is subsequently subtracted by τ_B and τ_C to get the remaining shear result τ_D. This is the actual remaining distribution that can be compared to a uniform applied shear stress (check 4 in figure 8.21). This τ_D does not necessarily have to look anything like the original result τ_A. Note that taking τ_B and τ_C as uniform distributed shear forces is a simplification and may not have to resemble the real distribution along the edge. However the total force should be is theoretically correct.

The conversion from stresses back to forces also produces some inaccuracies which cancel equilibrium. Therefore, the remaining shear forces are not completely in equilibrium either. However, these are minor errors and hence disregarded.
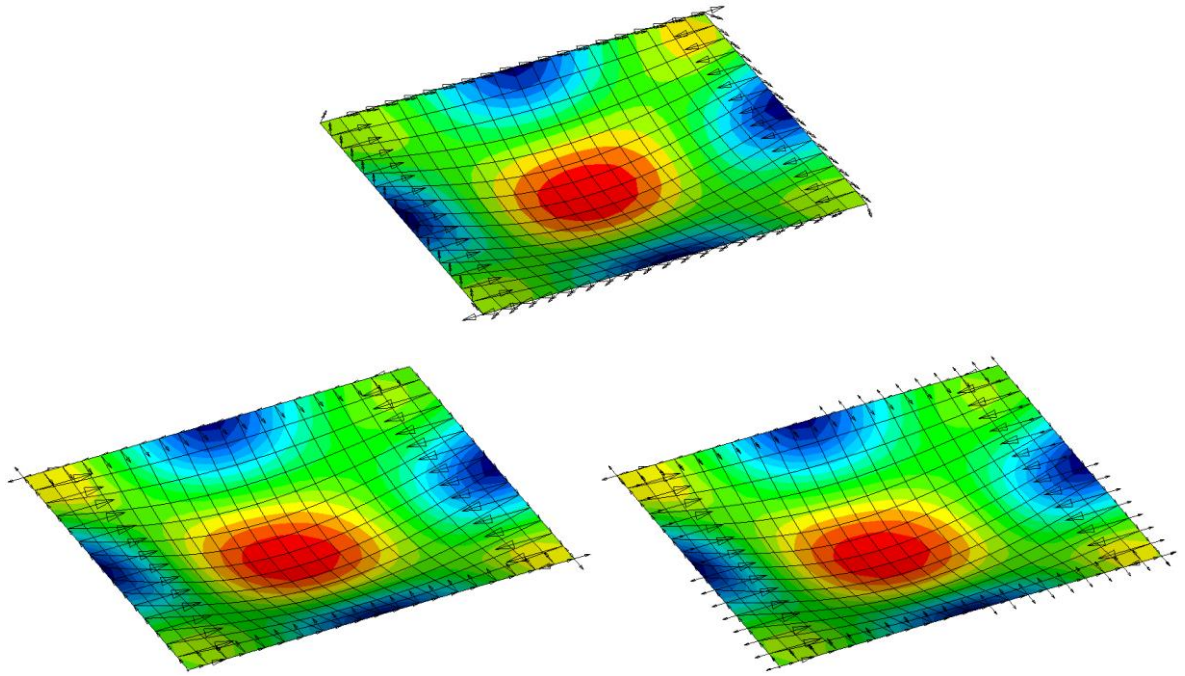
Fig 8.18 Load case 2 with (a) real freebody forces, (b) real in-plane forces and (c) linearized in-plane forces.
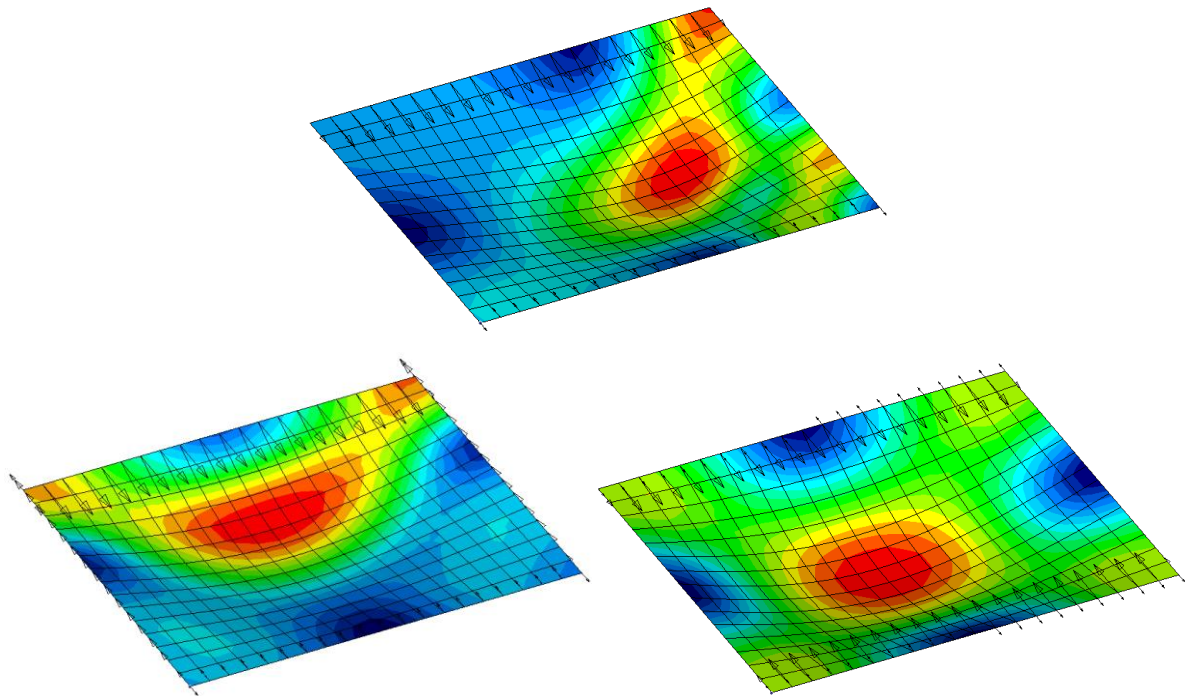
Fig 8.19 Load case 5 with (a) unbalanced real normal in-plane forces only, (b) unbalanced real in-plane forces in y direction on all edges and (c) balanced linearized in-plane forces.
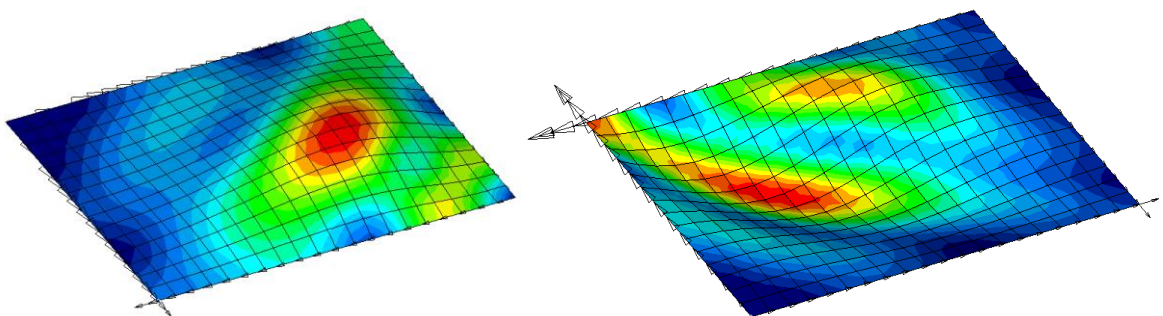
Fig 8.20 Load case 1 real shear forces and Load case 7 real shear forces.
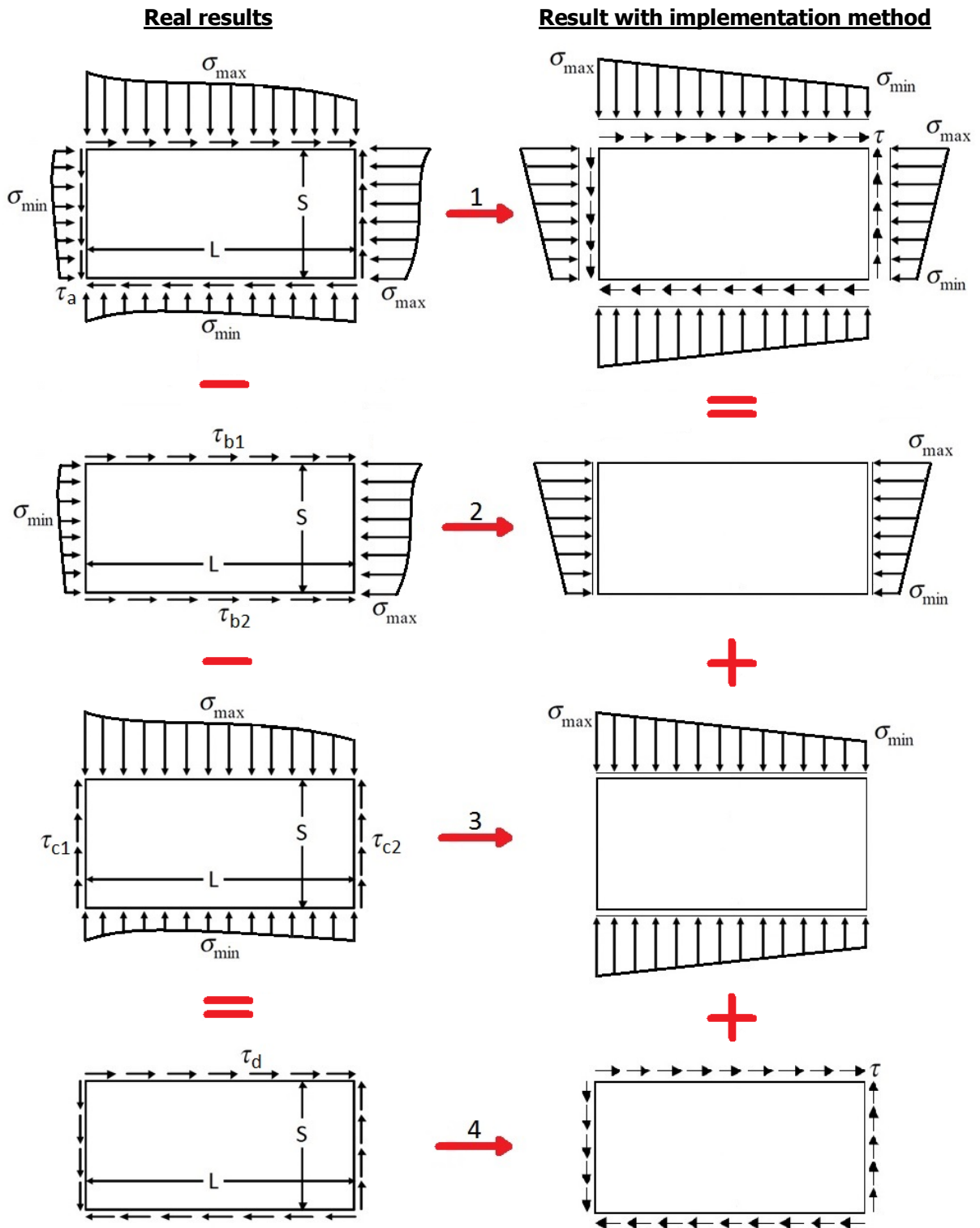
Fig 8.21 Comparison checks between (a) the real stress results and (b) stresses determined by the implementation methods.

Due to the fact that the standards combine the subdivided buckling strengths as well for stress distributions in x-direction, y-direction and shear (eq 22-24), it makes perfect sense to divide the real stress results in these three arrangements to see whether the implementation methods are correct.

8.5 Experiments

Hence, above in figure 8.21, there are 4 comparisons between analyses made. To begin with comparison 1, the buckling factors are all summarized in figure 8.22. A better explanation of what is each result in the graph represents is given in figure 8.25 and 8.27 to 8.29. A borderline is drawn to easily distinguish conservative and non-conservative results due to the specific model / load cases / implementation methods. All these results are from all seven load cases on all eight fine meshed models described in chapter 6. Comparisons 2 and 3 are together summarized in figures 8.30 and 8.31. And Comparison 4 is summarized in figures 8.33 and 8.34.

Part of the main differences is found in positive and negative parabolic stress distribution results as illustrated in figure 8.23 and 8.24. The first gives conservative results and the second gives non-conservative results as expected and discussed before. A second part of the main differences is a consequence of the stress gradient effect. This effect has been discussed extensive as well but figure 8.26 illustrates that this distribution of stress may actually be present in real structures and hence also produces non-conservative results with the implementation methods.

The actual stress results and linearization results are shown in appendix B for only model 2. Appendix E summarizes all buckling factor results in tables. The overall results match fairly well with the implementation methods, however that cannot be said from individual checks Fx, Fy and shear. Conclusions may be made for the individual implementation methods:

- Implementation method 1 (Average linear regression) surprisingly seem to produce the, although slightly non-conservative, best overall matching results with the smallest deviations apart from a few exceptions. Deviations are only one to two percentages. Individual Fx or Fy results may however have substantial non-conservative calculated buckling strengths.
- Implementation method 2 (Average linear regression + Including all stress results) delivers almost only very conservative results. Even with this method the stress gradient effect is not resolved for the severe cases.
- Implementation method 3 (Average linear regression + Updated to σ_{max}) produce fluctuating unstable results although more often conservative than non-conservative.
- Implementation method 4 (Average linear regression + Eurocode clause) has similar overall matching results with small deviations like method 1 however conversely slightly conservative and thus having a preference in comparison. Individual Fx and Fy results are still not sufficient though.

The shear stress implementation method results show relative meaningless values. With τ_D there exists a fundamental different real shear stress distribution compared to simply taking the average, absolute average or absolute max shear stress. Therefore a better proposal would be to take the average or maximum shear from τ_D instead from the non-subdivided real initial stress results. This proposal is not further studied for the moment.
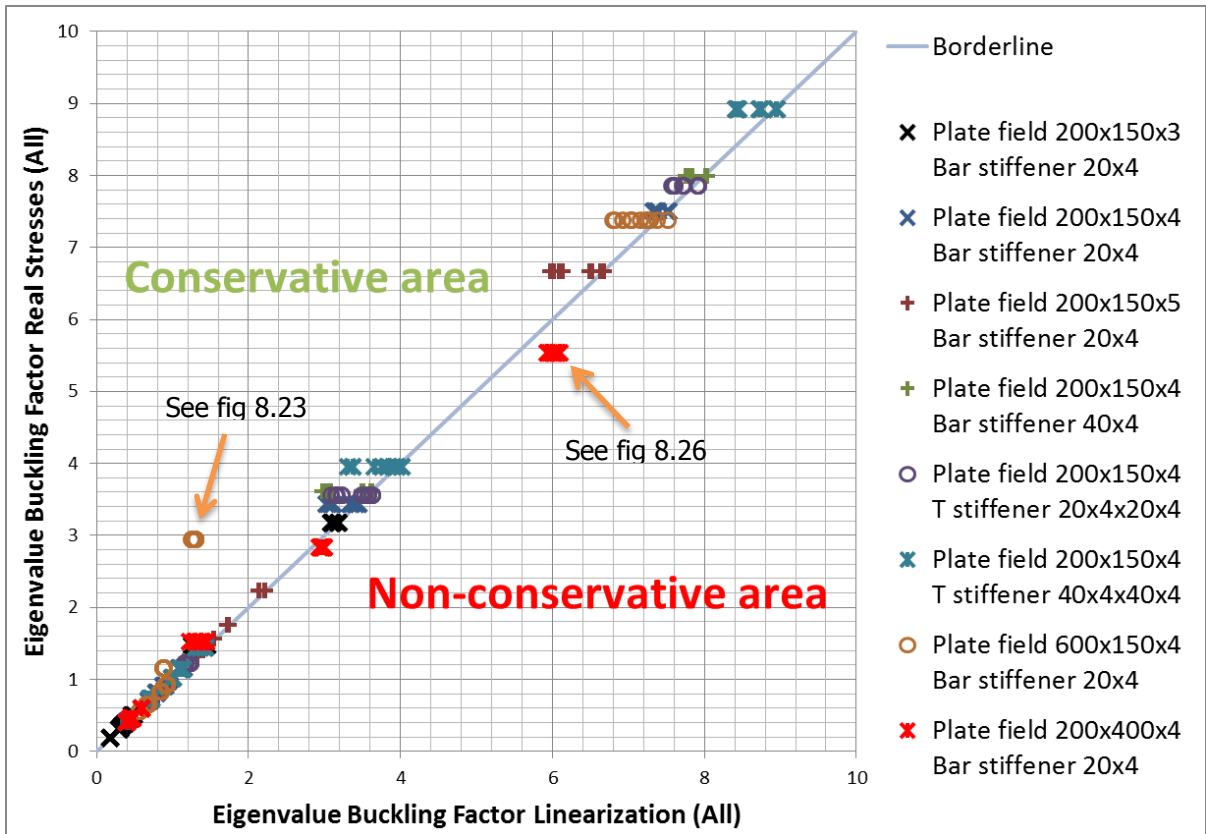
Fig 8.22 All buckling factors from the eight different models for all twelve different implementation methods.
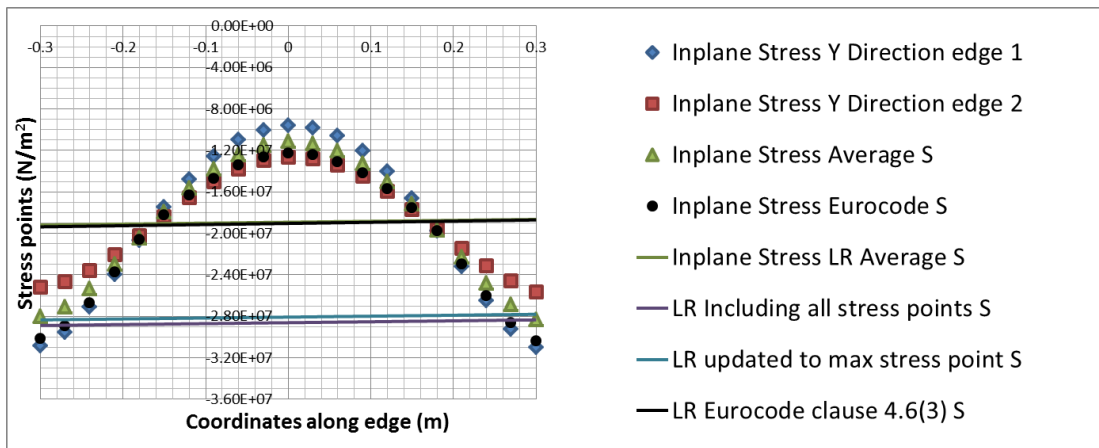
Fig 8.23 Stress results of model 7 with load case 1 on the long edge.
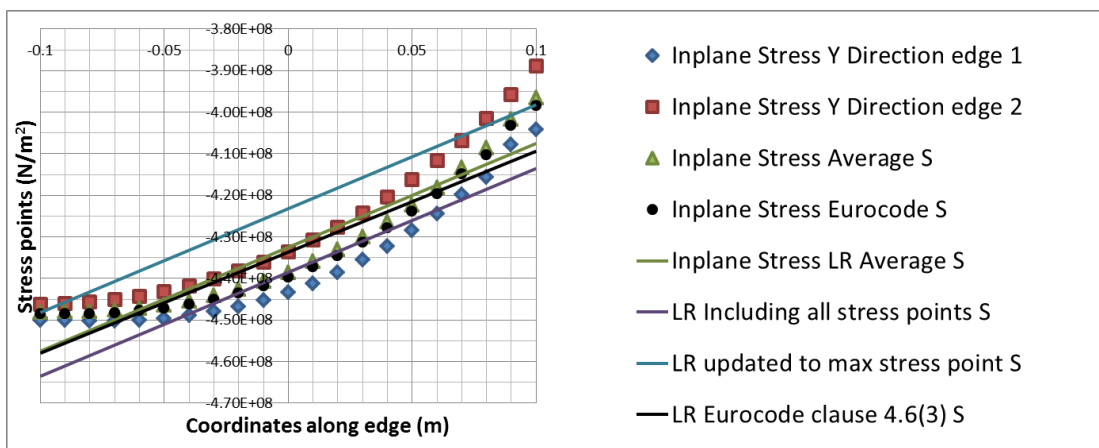
Fig 8.24 Stress results of model 2 with load case 6 on the long edge.
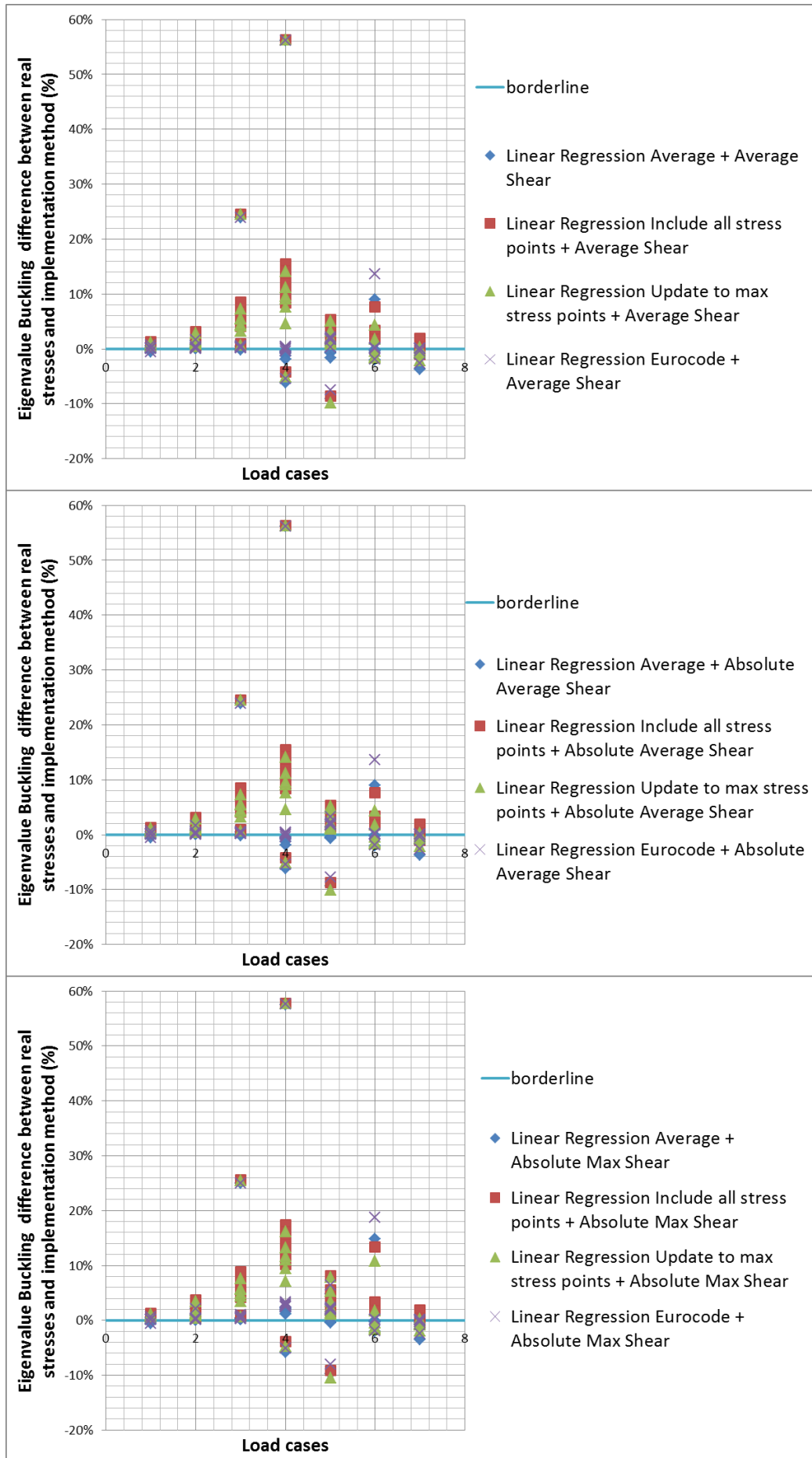
Fig 8.25 Results from figure 8.22 subdivided into the different implementation methods for the 7 load cases. The difference between real situation and implementation method is shown in percentages.
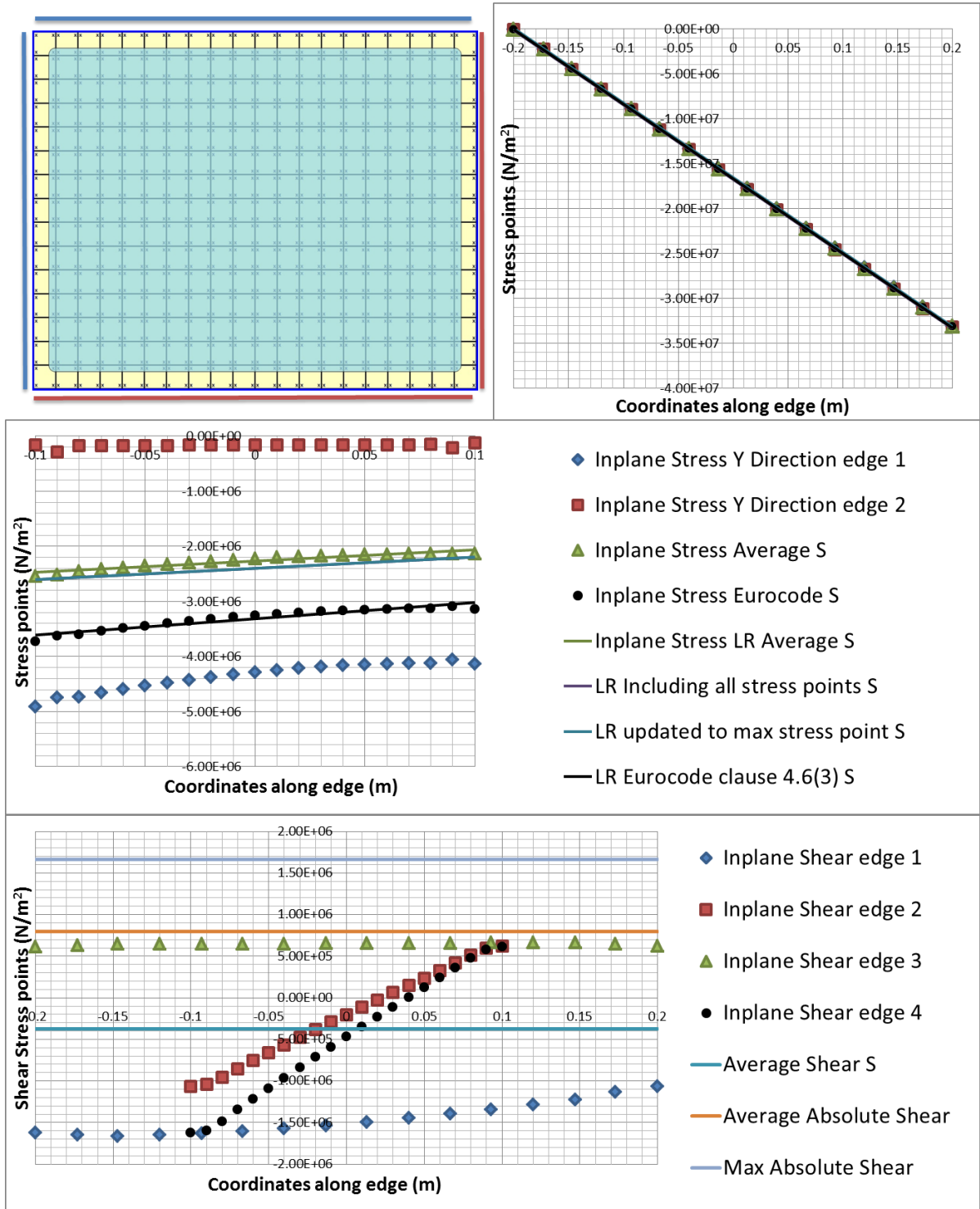
Fig 8.26 Normal stress and shear stress results of model 8 load case 5.
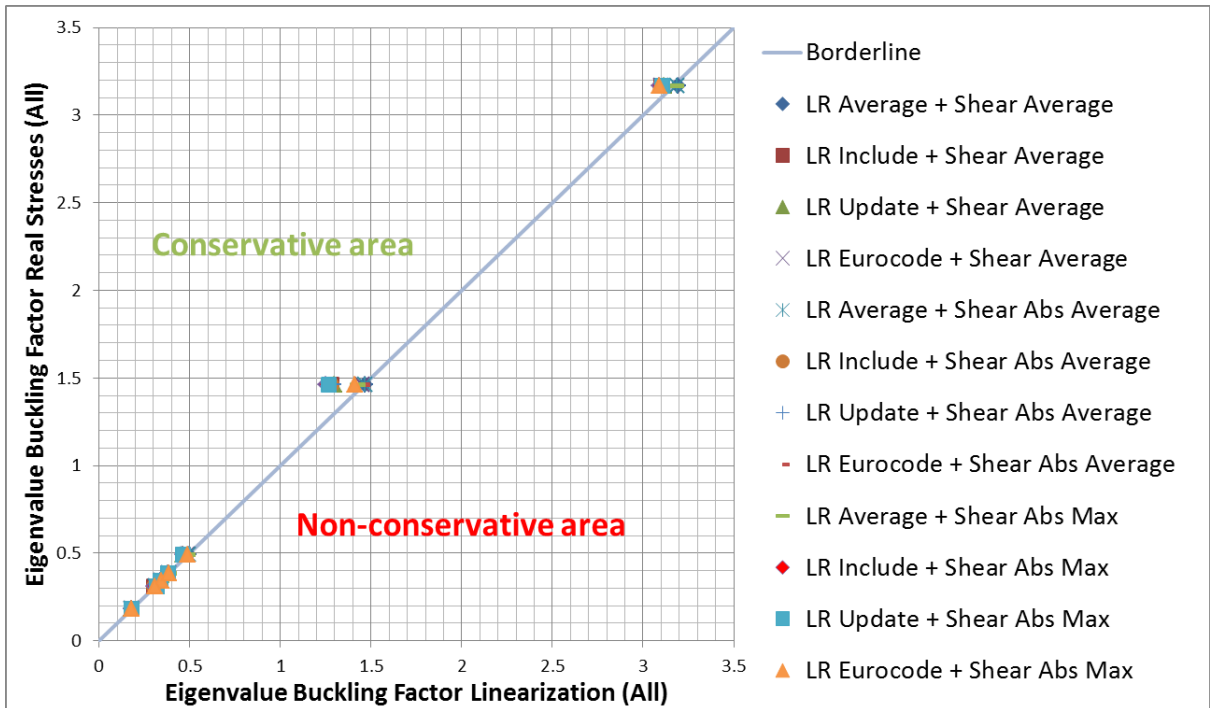
Fig 8.27 All buckling factors from only model 1 plotted along a minimum border line.
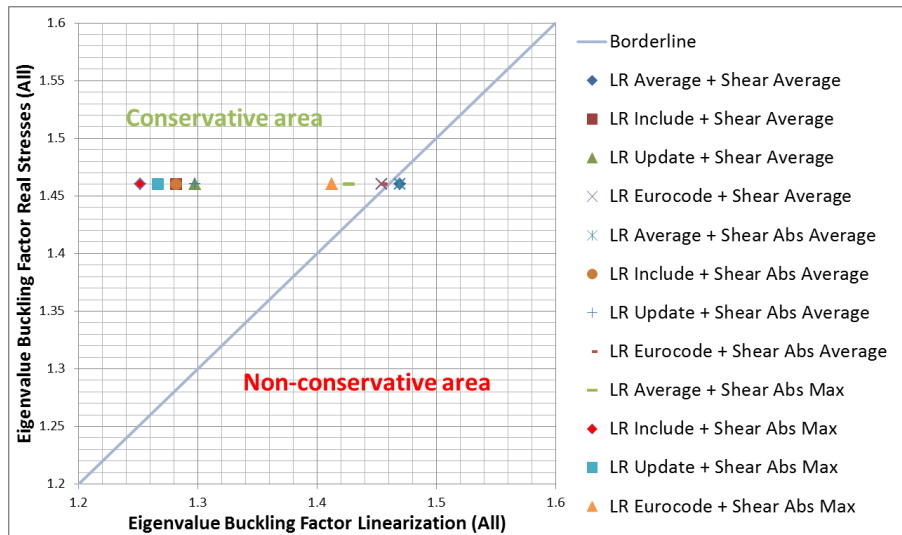
Fig 8.28 Zoomed in version of figure 8.22. All buckling factors from load case 4.
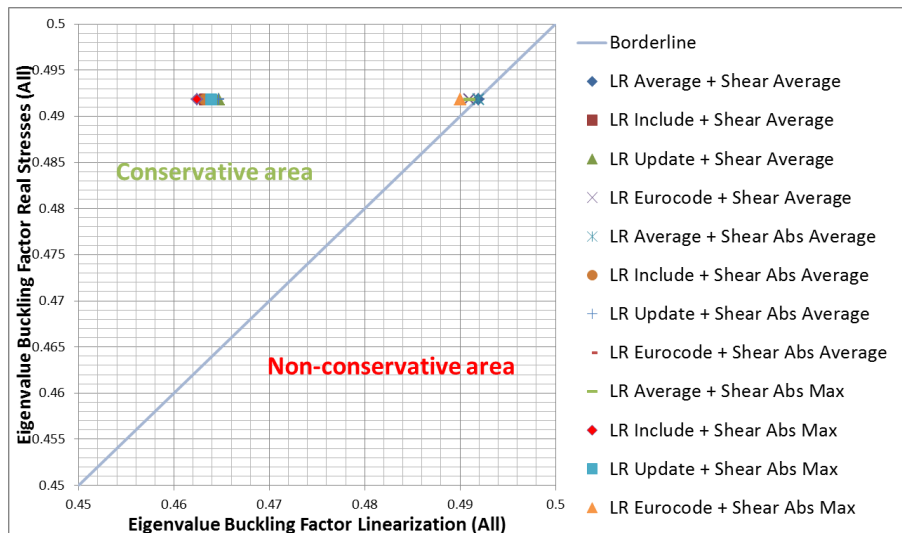
Fig 8.29 Zoomed in version of figure 8.22. All buckling factors from load case 3.
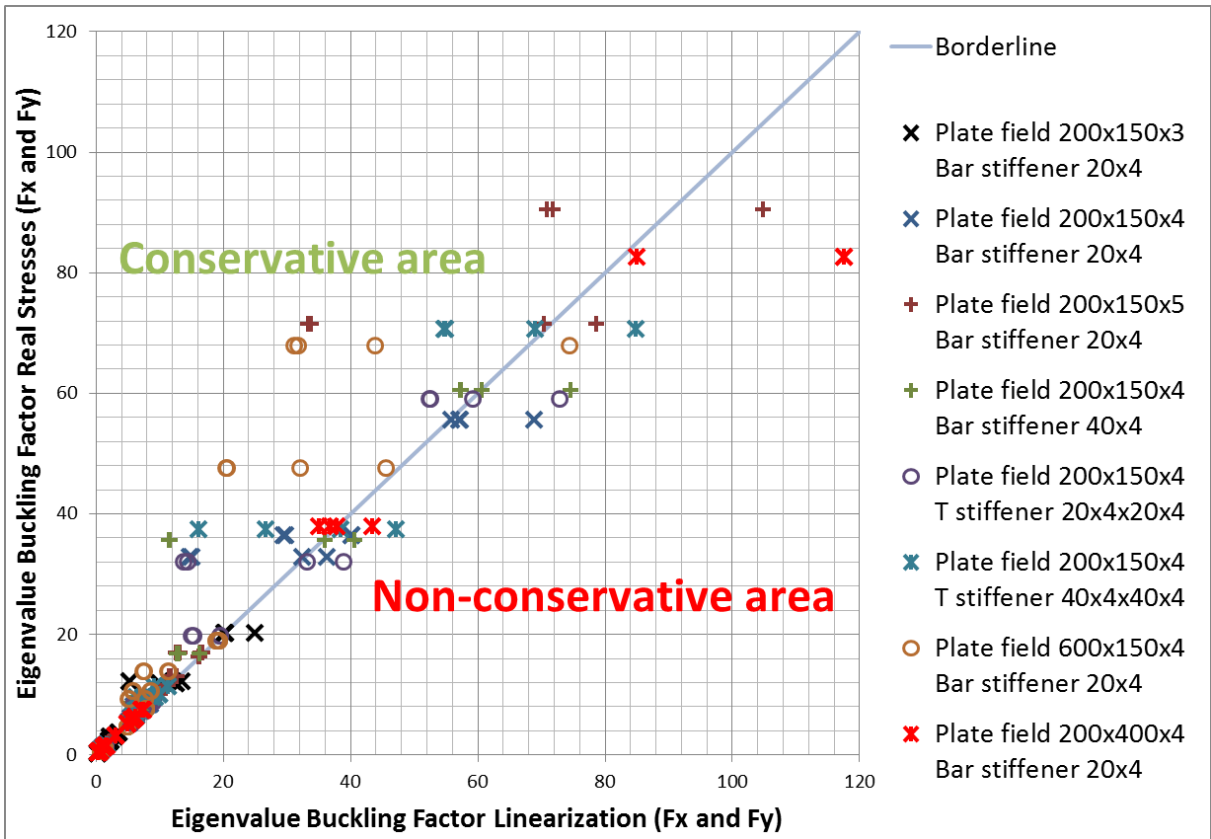
Fig 8.30 Comparison of Fx and Fy results.
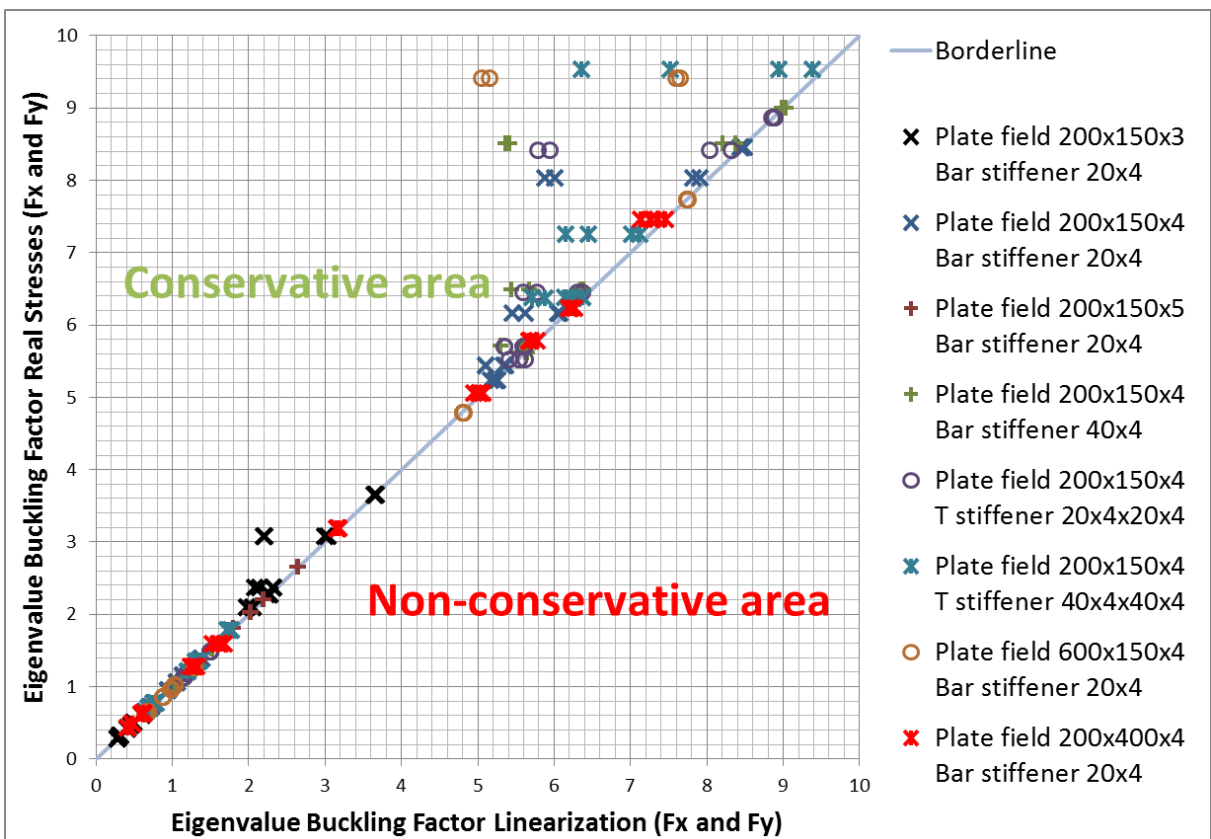
Fig 8.31 Comparison of Fx and Fy results. Zoomed in version of figure 8.24.
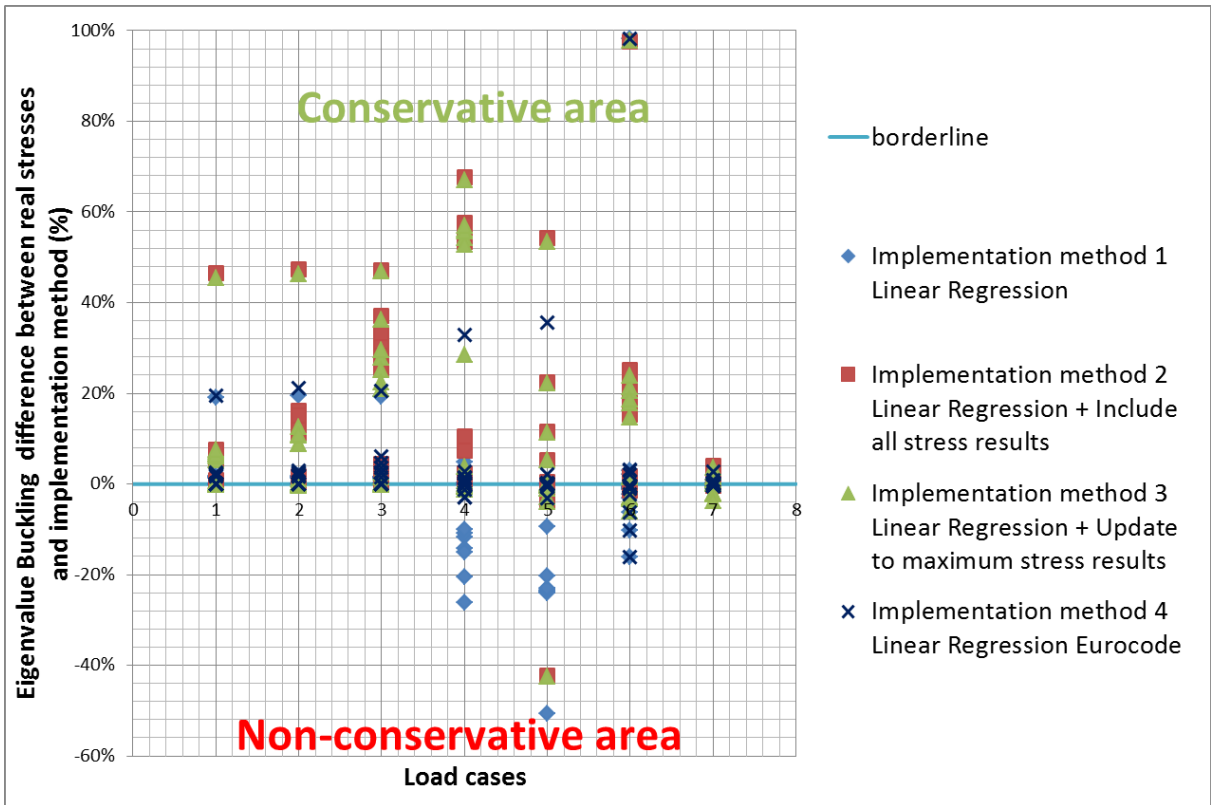
Fig 8.32 Results from figure 8.30 subdivided into the different implementation methods for the 7 load cases. The difference between real situation and implementation method is shown in percentages.
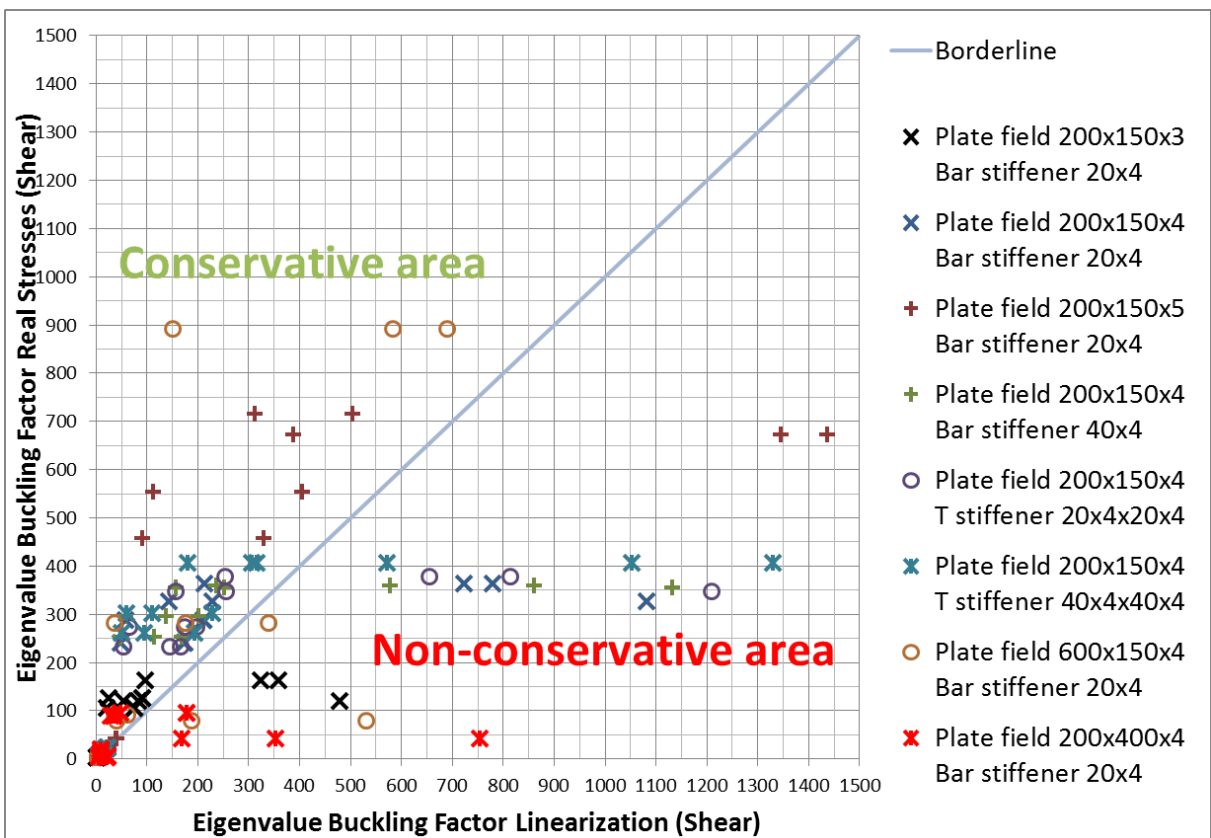
Fig 8.33 Comparison of shear results
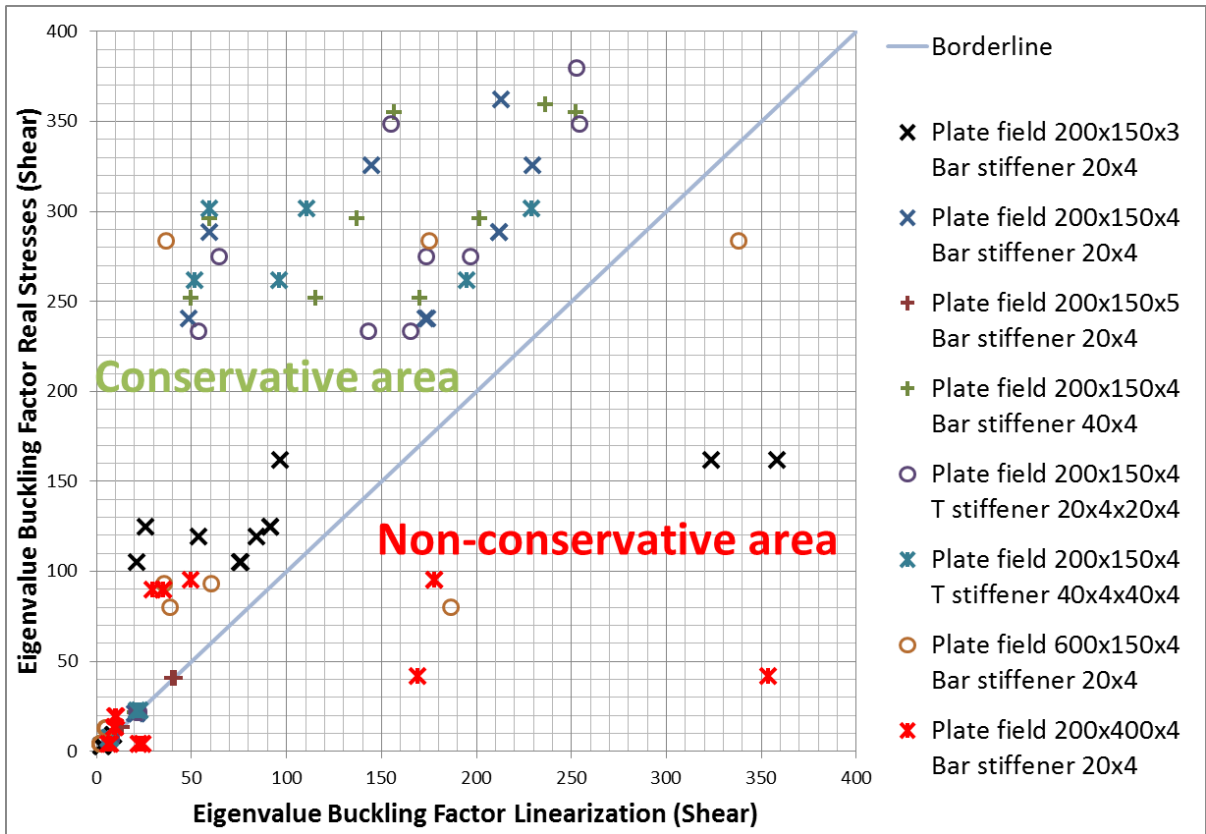
Fig 8.34 Comparison of shear results. Zoomed in version of figure 8.26.
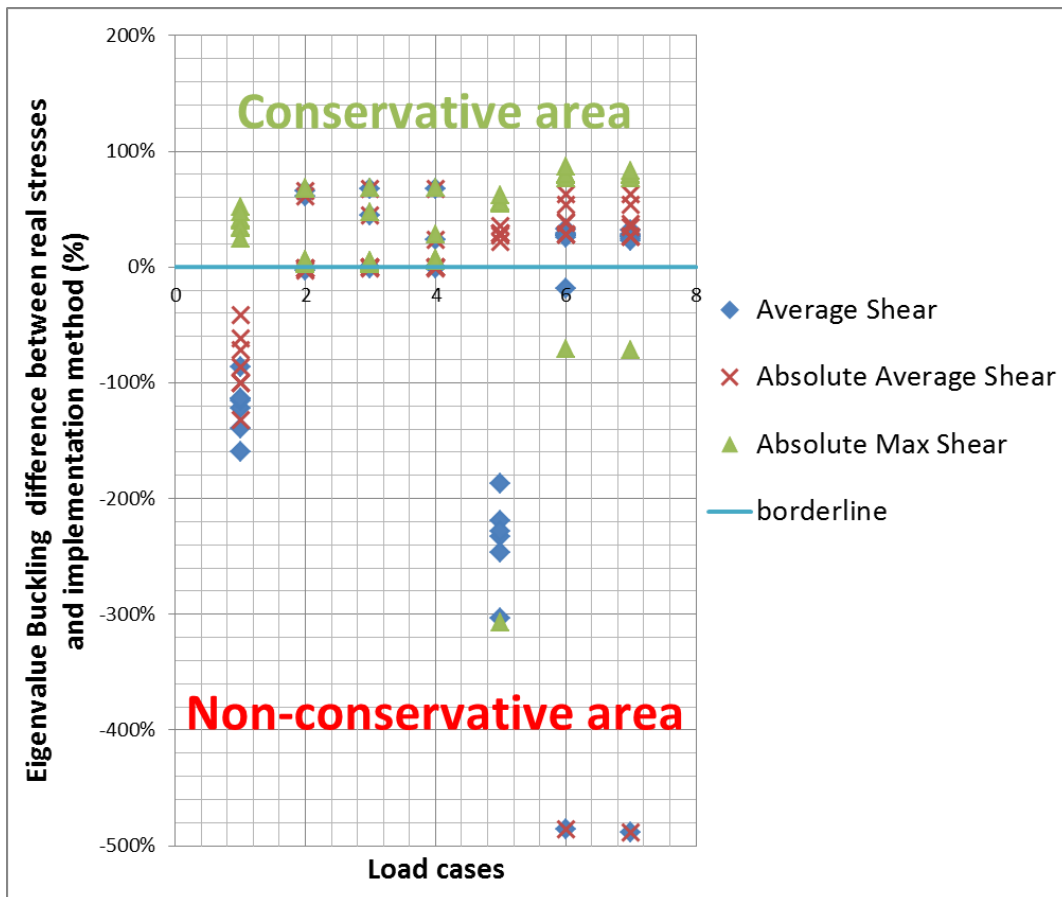
Fig 8.35 Results from figure 8.33 subdivided into the different implementation methods for the 7 load cases. The difference between real situation and implementation method is shown in percentages.

Furthermore there are made comparisons for all specific models and load cases with only implementation method 1 between three different mesh sizes. Appendix C shows the results for σ_{Xmax}, σ_{Xmin}, σ_{Ymax}, σ_{Ymin} and τ in graphs for only model 2 and appendix D contains these results from model 2 only as well summarized in a table. Here some expected and unexpected results as well.

The fine mesh sized models have higher stress results for load cases 1 to 5 (fig 8.33). Load cases 6 and 7, both with fairly large transverse stresses, have lower stress results for the fine meshed models (fig 8.34). The results vary mostly less than 1% for the severe loaded edges where the middle and fine mesh models have fairly similar results. The weakly loaded edges may have difference up to more than a factor 2 between the single element mesh and the other meshes.
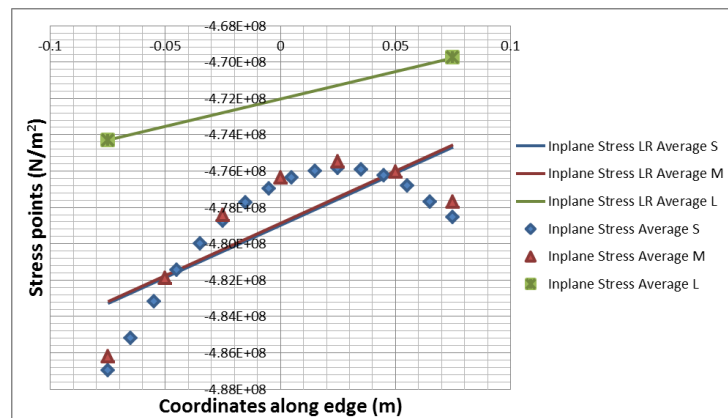
Fig 8.36 Load case 1 stress results on the short edge for the three different mesh sizes.
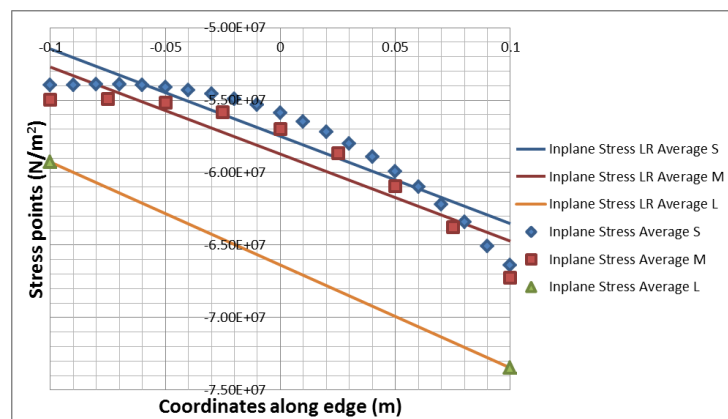
Fig 8.37 Load case 7 stress results on the long edge for the three different mesh sizes.

Shear stress results compared to the coarse meshed models vary heavily with the fine meshed models. No clear conclusions can be made from these results. This is not surprisingly since the implementation method has been rejected above. The comparison should be made again if the new proposal is implemented.

8.6   Recommendations

The implementation methods with linear regression have in overall results an approval. However, several situations show that it is still not completely accurate. The longer the edges of the plate, the more the influence will get from parabolic stress distributions along those edges. The standards do not accept any other input design stress than the linear distributions but a combination of these distributions with the principal of patch loads may provide better matching results. The standards would need an update for that. More research will be required for this.
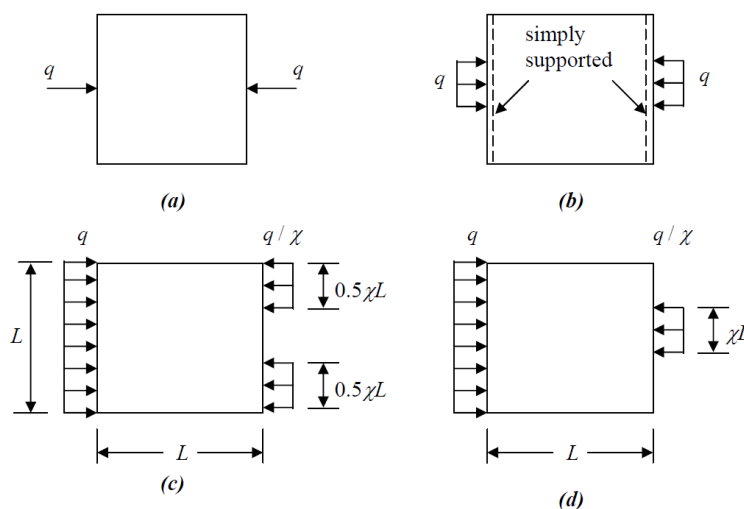
Fig 8.38 Buckling of plates under (a) point loads; (b) partially distributed loads; (c) patch loads near corners; (d) patch loads at edge center.

Another proposal to try is to adjust implementation method 3. Now it is a simple shifted linear regression. A better endeavour may be to define the σ_{max} first and then fit the curve such that it goes through that point and with a minimum of the sum of the squares of the deviations of the rest of the actual data.

The stress gradient effect calls for a more accurate implementation method as well. Maybe a combination of method 2 and 4 should be tried although that would result in mostly conservative results. Another idea would be to multiply the calculated stress results with the k factor from C. Yu and B.W. Schafer. A third and preferred approach as concluded from the results up to now would be to take method 1 and afterwards not going for an average of the two opposite edges but taking something in between the average and the maximum. Maybe 70% as the Eurocode shows that 60% provides small deviations but not always conservative. The problem is that when one edge stress distribution is more or less the opposite of the other edge stress distribution such that it becomes undefinable which of the two the maximum is. This is left for further study.

The implementation methods for the shear are rejected. Due to this conclusion the new proposal is to base the uniform input design shear stress on τ_D instead of τ_A to deliver more accurate and reliable values. This is left for further study as well.

9. Analysis of stiffeners local buckling limit

Stiffener local buckling is by far the unimportant factor in comparison with the plate and beam-column buckling limits. In practice a plated structure is designed with sufficient stiff stiffeners. A stiffness check is then disregarded if the dimensions pass some allowable limit for a surely sufficient stiffness. If not then the check is required by the ABS and DNV hence the plate buckling strength of the web and flanges should be calculated. Since the beam models do not have webs and flanges as plate fields modeled with plate elements, a new implementation method is required.

9.1 Stress results

Webs and flanges of stiffeners or girders are checked as individual plate fields equal to the previous chapter. In case the stiffeners are modeled with plate elements it becomes the exact same problem. The implementation method described in the previous chapter can be used here as well. Only the recognition of the webs and flanges will be required extra but since SDC can already do that there is no issue. However, beam elements cannot give any results for local buckling in finite element packages, see figure 9.1. Therefore there is need for a conversion method to get the five input design stresses σ_{Xmax}, σ_{Xmin}, σ_{Ymax}, σ_{Ymin} and τ.
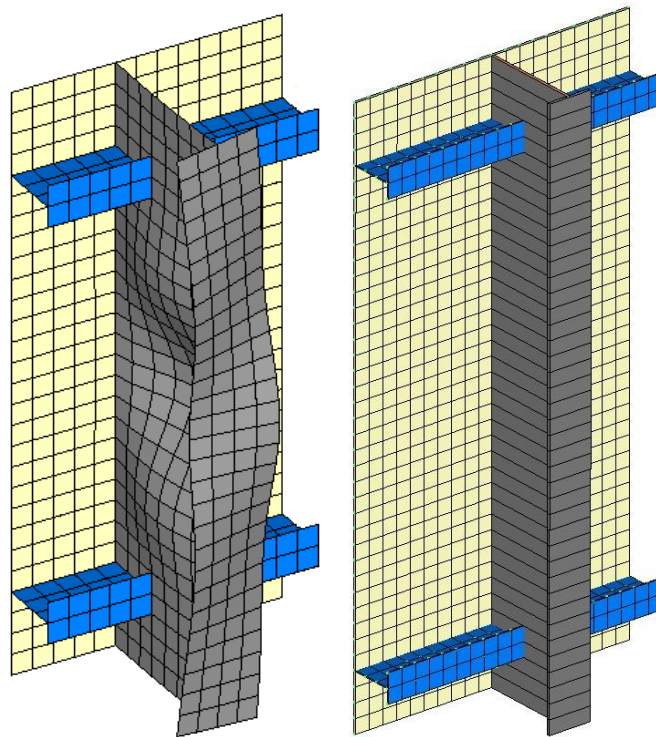
Fig 9.1 (a) Part of the plate model which shows local buckling in a girder. Induced by stresses in the axial directions and bending moments by the adjoining plates and stiffeners. (b) Part of the beam model without loads but unable to show the local buckling deformations anyway.

Note that if you are doing the checks with the plate model that the webs and flanges have one free edge in rather frequent situations and the boundary conditions have to be adjusted for these plate field checks.

When modeling stiffeners and girders with the use of beam elements the static analysis in FEMAP provides several different results for each element. Such as the three forces, the three bending moments and four corner stress results. The four stress recovery (corner) points are defined as in figure 9.2. The other six outputs are defined in figure 9.3.
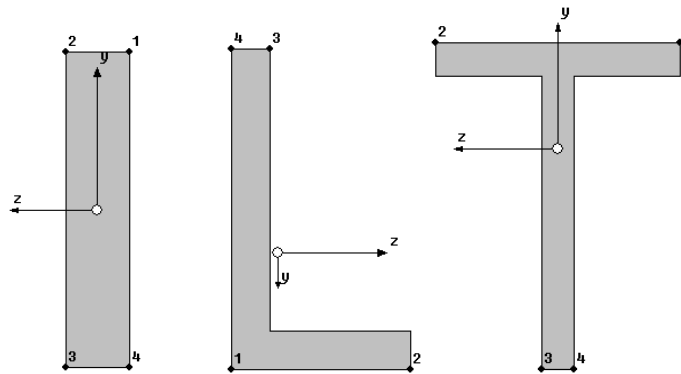
Fig 9.2 Corner stress definition points for the (a) flat bar stiffener, (b) L shaped stiffener and (c) T shaped stiffener.
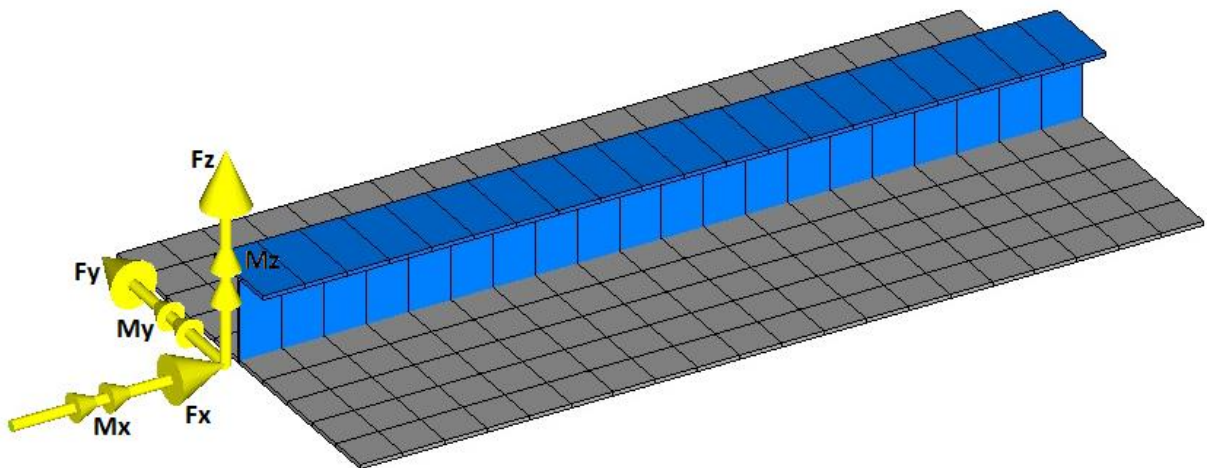
Fig 9.3 Section which is considered as the idealized beam-column in standards for flexural beam buckling for the specific stiffener.

F_x = uniform force

F_y = horizontal shear force

F_z = vertical shear force

M_x = torsional moment

M_y = vertical bending moment

M_z = horizontal bending moment

9.2   Proposal for implementation method

Flanges cannot absorb any transverse in-plane stresses since one side has no supporting structure. That indicates that $\sigma_{Ymax} = \sigma_{Ymin} = 0$ and reduces the amount of design stresses. The remaining stresses are illustrated in figure 9.4. The in-plane stresses can be calculated from the corner results. The maximum pressure from points 1 and 2 will give the σ_{Xmax}, for the flange. The T stiffener profile has two flanges but if the one with unfavourable load conditions is ok, then the other will not be a problem. The other point will provide σ_{Xmin} in case of a L profile. The average of points 1 and 2 will provide σ_{Xmin} in case of a T profile. The web has the same procedure. The average of points 3 and 4 at the bottom. The average of point 1 and 2 in case of a bar or T stiffener or just point 1 in case of an L stiffener at the top. Things are simplified with this method. Note that you will not have the in-plane stresses but some close by corner stress results. In theory they are conservative though, so this should be a safe approximation.
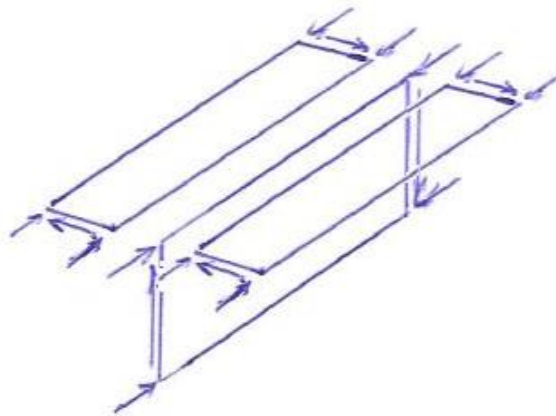
Fig 9.4 Stresses in web and flanges

There is no way of defining shear results in the axial direction in beam elements so the shear stress has to be determined on the ends. The proposal is to calculate the shear stress in the web by taking the vertical shear force and dividing this by the web area. And calculating the shear stress in the flanges by taking the horizontal shear force and dividing this by the flange areas. This is a large simplification though. The real shear stresses are complicated as seen before due to the shear lag, shear loads, bending moments, torsion and even warping (fig 9.5). However these separate shear stresses cannot be received from the results from beam elements.
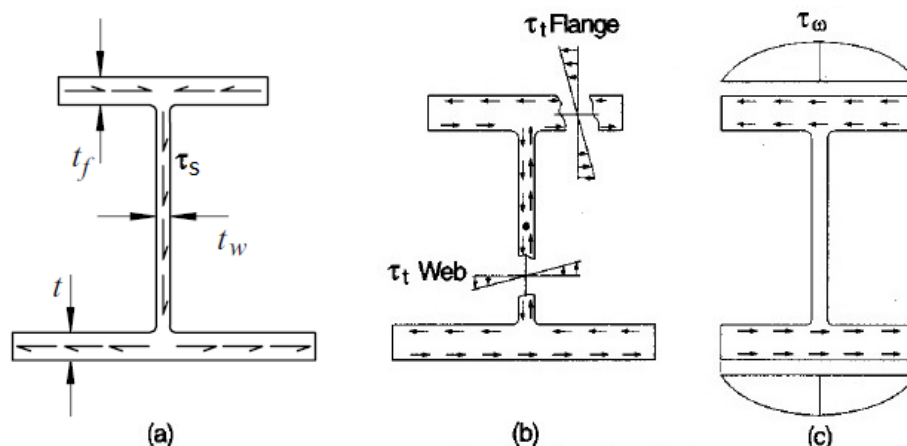
Fig 9.5 shear stress: due to (a) shear forces in the vertical direction, (b) pure torsion and (c) warping.

9.3 Approach for verification of implementation method

The basic idea is to simply take the plate model and the unstiffened plate buckling implementation method and compare that with the beam model and the stiffener local buckling implementation method. Results from the plate model sufficiently equal the results from the beam model as seen in chapter 6 therefore this comparison is understand to be allowable. Hence a comparison between the webs and flanges from the plate model and the beam elements from the beam model is assumed to provide realistic results.

9.4 Experiments

In principal there should be five design stress values for the stiffener webs and flanges: σ_{Xmax}, σ_{Xmin}, σ_{Ymax}, σ_{Ymin}, τ. However the stiffeners web investigated here has a free edge and hence σ_{Ymax} and σ_{Ymin} are zero and will not need an analysis. Summarized results of the other three can be seen in appendix F to H.

For now the shear stress results are not considered since there is just concluded that the implementation method for plate elements is incorrect. The results for σ_{Xmax} are surprisingly similar compared between the beam element implementation and the plate element implementation. However they are 3% less conservative while the plate element implementation with average linear regression is already the non-conservative method 1. Now the maximum stress results of all cross section areas along the stiffener is taken as well hence this is a little disappointing. Unfortunately only model 2 is analyzed for all load cases, in other words, for now there are no comparable variations in dimensions nor test results including actual flanges. Hence only one specific web is checked.

The question is whether deviations between results are due the implementation method for beam elements or due the implementation method for plate elements. The lack of checked results from the individual stiffener web with the plate element implementation method and the lack of the other cases has the consequence that no safe conclusion can be made for now. The results however look promising although a bit non-conservative compared to the plate model.

10. Analysis of Stiffener flexural buckling limit

The loads conditions at hand should subsequently be used to define the maximum compressive stress at the extreme fiber and compare that with the critical buckling strength of the structure. This critical stress is then considered to initiate buckling. Theoretically this critical stress can be determined in a bit simplified way by realizing that it is caused mainly by the axial load and the bending moment around the y axis. Namely the results F_x and M_y in figure 9.3. The standards make use of this simplification although just as with the plate buckling you have to specify loads that are simpler to describe but not that easy to match with stress results from your FEM analysis.
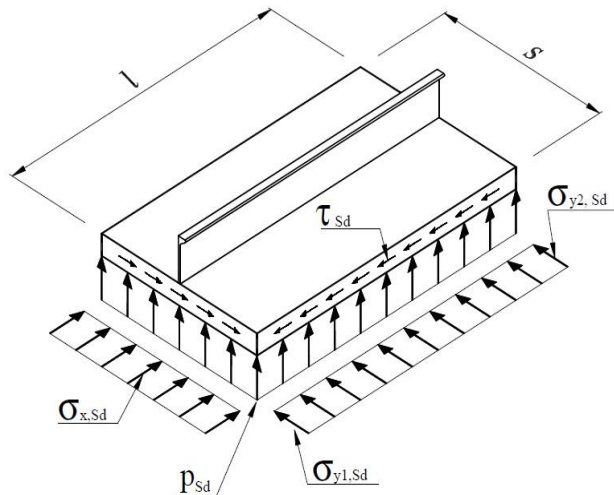
Fig 10.1 Beam-column input design stresses.

The DNV code is a bit more extensive concerning input parameters of the loads. Remember figure 10.1, as seen before in chapter 4. This figure is deliberately repeated to emphasize the importance of the input design loads on the beam-column. And remember figure 5.2 for axial stresses in the column. For both standards the shear stress and the stress distribution in y direction are needed almost only to define the effective plate width, one of the correction factors. At the same time the DNV also incorporates the shear stress in the main formula. The uniform stress in x direction and the lateral pressure remain the most important input design stresses though. The main formulas resemble equation 4 and can be described by:

$$(ABS) \rightarrow \underbrace{\frac{\sigma_a}{\eta \cdot f(\sigma_0, \sigma_E)}\left(\frac{A}{A_e}\right)}_{\text{Uniform axial load}} + \underbrace{\frac{\sigma_b}{\eta \cdot f(\sigma_0)}\left(\frac{1}{\left(1 - \frac{\sigma_x}{\eta \sigma_E}\right)}\right)}_{\text{Bending moment}} \leq 1 \qquad \{39\}$$

$$(DNV) \rightarrow \underbrace{\frac{\sigma_a}{\eta \cdot f(\sigma_0, \sigma_E, \sigma_T)}\left(\frac{A}{A_e}\right)}_{\text{Uniform axial load}} + \underbrace{\frac{\sigma_b}{\eta \cdot f(\sigma_0, \sigma_T)}\left(\frac{1}{\left(1 - \frac{\sigma_x \cdot A}{\sigma_E \cdot A_e}\right)}\right)}_{\text{Bending moment}} + \underbrace{\left(\frac{\tau_c}{f(\sigma_0)}\right)^2}_{\text{Shear stress}} \leq 1 \qquad \{40\}$$

σ_a = uniform stress in x direction

σ_b = the maximum stress only resulting from the bending moment

σ_0 = yield strength of material

σ_E = Euler buckling strength

σ_T = Torsional buckling strength

τ_c = Shear stress over the associated plating in the column

η = Safety factor defined in the standards

The input design stresses are divided by allowable, critical stresses defined by the Euler buckling strength and correction factors. In the DNV formula the design stress is divided by the Perry-Robertson correction and in the ABS formula the design stress is divided by the Johnson-Ostenfeld correction. The real stress divided by the corrected allowable stress forms an dimensionless values that must be lower than 1 to be sure that the results will remain below the critical stresses.

Now you can see the clear distinction between the uniform axial load, the bending moment and the shear stress. Both the ABS and DNV codes use the nominal calculated compressive stress and a bending stress around the y axis using full width of associated plating. As discussed are the standards not good in showing what is really going on so therefore first an overview of the input design stresses. The input design stresses and corrections factors are discussed in the following sections to make the formulas more comprehensible. For all details see the ABS and the DNV standards.

10.1   Axial load

O. Hillers did a suggestion on defining the axial load simply by choosing the largest stress from the linearized plate results. Instead it would be better to work with the actual stress results from the model including results which exist in the stiffener.
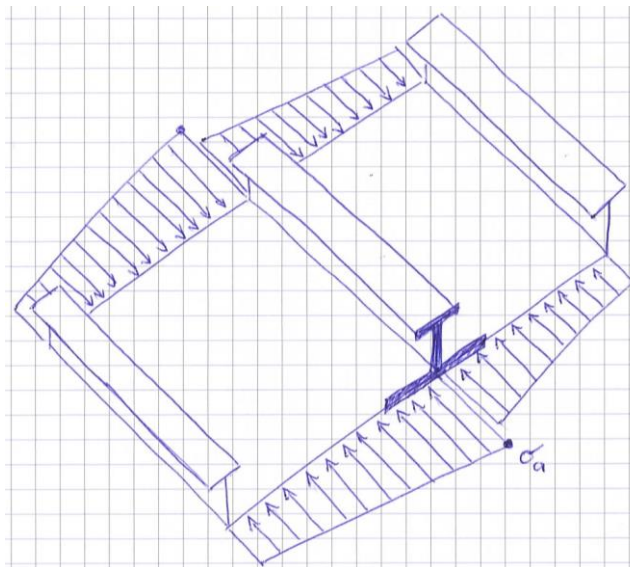
Fig 10.2 Axial load concept from Ottar Hillers.

The axial load for the ABS and DNV codes is nothing more than figure 5.2a. That means you can take the average stress over the entire column as shown in figure 10.3 below. The model gives a reasonably easy interpretation of calculating the stress results by just taking the average result over the area.
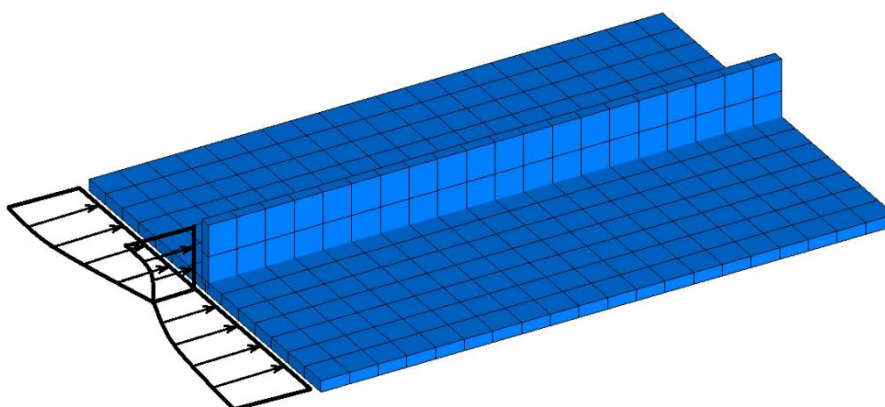
Fig 10.3 An exaggerated impression of the in-plane stresses in the described column for load cases 1.

On a side note, notice that the stresses become smaller at the connection between plate fields and stiffener. These are results from the linear static analysis but it should be clear that it is almost the opposite from the stress results you should have with the unstiffened plate ultimate strength shown in figure 3.11. It is the same behaviour as mentioned before in the check of the plate fields. Of course with the perfect straight model and linear static analysis it is only logical that the stresses do not match those post buckling stresses. But we are looking for the ultimate strength limit so that does

again indicate the difficult comparison which is aimed to make with reality. The smaller stress at the connection between plate fields and stiffener here in the figure probably is due to the bending moment in the stiffener which is subtracted from the uniform pressure.

Furthermore a note on the axial stress results from FEMAP. Considering the normal stress in y direction as defined in figure 10.1, you should expect this stress in the transverse direction to influence the results for the axial direction due to the poison ratio. The stress distribution in the plate due to stresses in y direction is therefore already included within σ_x. And knowing that it does have an influence, the transverse stress is therefore not necessary in the formula. Unlike the IACS Common Structural Rules for bulk carriers describes, as mentioned in chapter 8 and equation 27.

The DNV is set apart from the ABS due to the fact that it also distinguishes tension and compression limits. Both may not exceed the yield stress. The column is checked in four different points (fig 10.4). The sign change is due to the convention of positive compression stress. Calculation of the final flexural buckling acquires eight different formulas for each point and positive and negative axial loads.
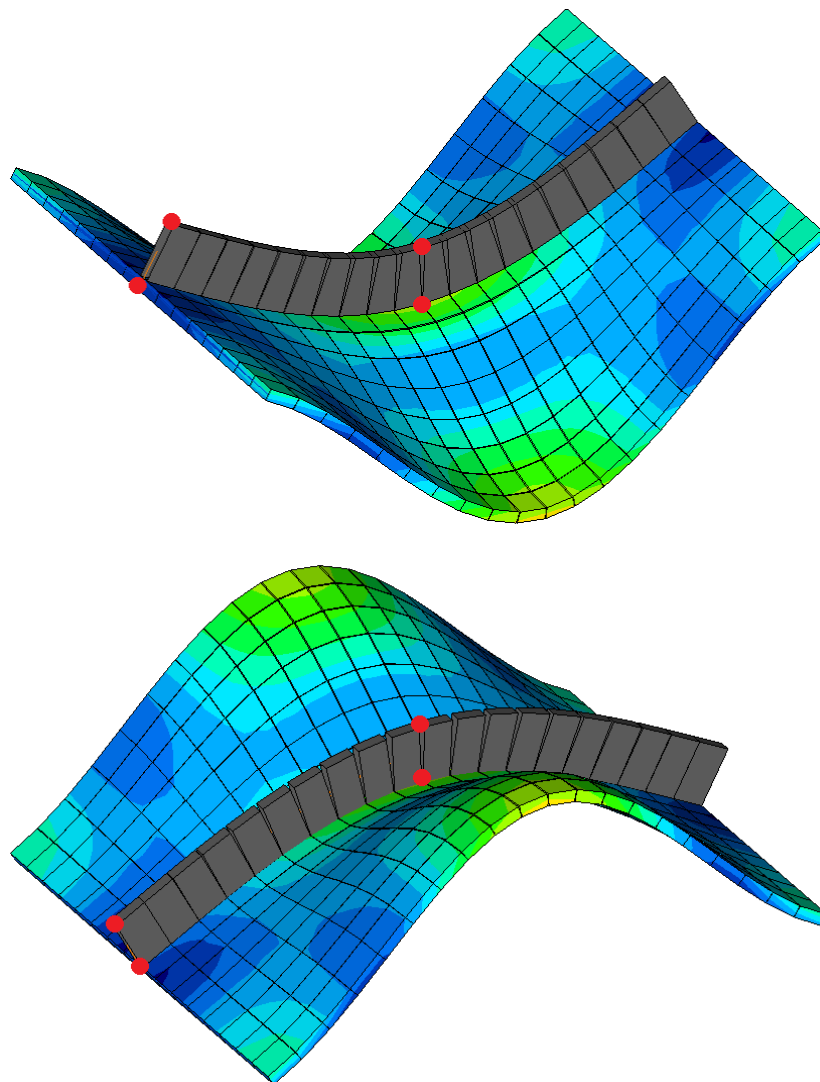
Fig 10.4 Four stress points which the DNV code distinguishes and sees as the spots with the maximum compressive stress at the extreme fiber.

10.2   Bending moments

Next to σ_a there is the maximum stress only resulting from the bending moment σ_b as discussed with equations 39 and 40. Unlike the uniform axial stress, this stress can consist of different sources as seen in figure 5.2: due to eccentric axial forces, lateral pressure, boundary restraints at the ends, or even lateral pressure in the transverse direction, warping and stress distributions in the adjacent plate fields. You will see the latter three returning primarily as part of the torsional buckling modes of the column. However the use of all these parameters is somewhat limited in the standards due to simplification. The standards define three possible maximum bending moments.

$$M_{max} = \frac{q_{Sd} \cdot l^2}{12} \ or \ M_{max} = \frac{q_{Sd} \cdot l^2}{24} \ or \ M_{max} = \frac{q_{Sd} \cdot l^2}{8} \tag{41}$$

The ABS literally speaks of the "the bending stress due to the maximum bending moment induced by the lateral loads" and gives one formula. The DNV speaks of the "absolute value of the actual largest support moment" and the "absolute value of the actual largest field moment" and gives three possibilities for the calculation of the bending moment. They are actually defined by the forget-me-not's, illustrated in figures 10.5 and 10.6 below. They differ in the boundary constraints at the ends, continuous (fixed at the ends) and Sniped (simply supported at the ends). Firstly this is not very realistic since the boundary condition of the stiffener-plate combination is neither simply supported nor fixed but something in between. And secondly it is in reality difficult to accurately specify the load q_{Sd} (w in the figures below). Again these are thus pure bending moments around the y axis, M_y. Unlike the DNV, the ABS does not make a distinction between different boundary conditions and uses only the maximum moment of the fixed beam. Both standards use the following relation to get the stress:

$$\sigma_b = \frac{M_{max}}{W_{min}} = \frac{M_{max} \cdot z}{I_e} \tag{42}$$

in which W_{min} is the effective section modulus which depends on the distance z between the neutral line and the outer fiber of the beam-column.

The standards thus rely on the lateral pressure q_{Sd} for the input load. Again, in the DNV code it gets a bit more complicated than in the ABS, for they make q_{Sd} a function of not only the lateral pressure P_{Sd} but also the in-plane stress distribution in transverse direction σ_y.

$$q_{sd} = \left(P_{Sd} + \left((0.6 + 0.4\varphi)C_0\sigma_{ySd}\right)\right)s \tag{43}$$

The details can be looked up in the DNV. The addition of this stress distribution in the transverse direction is understandable since the in-plane stresses certainly have influence on the lateral pressure and vice versa as illustrated in fig 3.27.
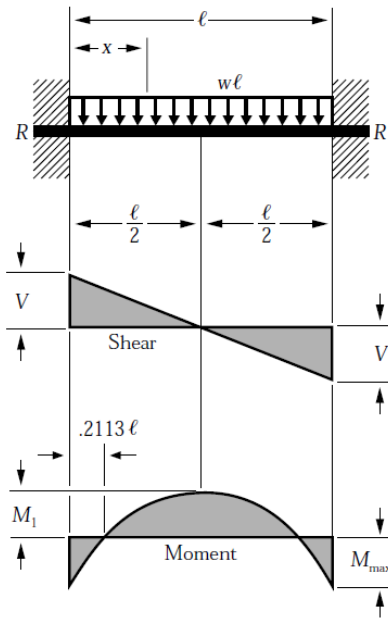
$$R = V \quad \ldots \ldots \ldots \ldots \ldots \ldots = \frac{w\ell}{2}$$

$$V_x \quad \ldots \ldots \ldots \ldots \ldots \ldots = w\left(\frac{\ell}{2} - x\right)$$

$$M_{max} \text{ (at ends)} \quad \ldots \ldots \ldots = \frac{w\ell^2}{12}$$

$$M_1 \text{ (at center)} \quad \ldots \ldots \ldots = \frac{w\ell^2}{24}$$

$$M_x \ldots \ldots \ldots \ldots \ldots \ldots = \frac{w}{12}(6\ell x - \ell^2 - 6x^2)$$

$$\Delta_{max} \text{ (at center)} \ldots \ldots \ldots = \frac{w\ell^4}{384EI}$$

$$\Delta_x \ldots \ldots \ldots \ldots \ldots \ldots = \frac{wx^2}{24EI}(\ell - x)^2$$

Fig 10.5 Fixed beam – Uniformly distributed load. [36]
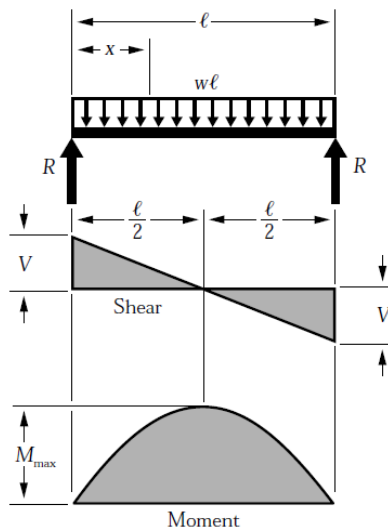
$$R = V \quad \ldots \ldots \ldots \ldots \ldots = \frac{w\ell}{2}$$

$$V_x \quad \ldots \ldots \ldots \ldots \ldots = w\left(\frac{\ell}{2} - x\right)$$

$$M_{max} \text{ (at center)} \quad \ldots \ldots \ldots = \frac{w\ell^2}{8}$$

$$M_x \ldots \ldots \ldots \ldots \ldots \ldots = \frac{wx}{2}(\ell - x)$$

$$\Delta_{max} \text{ (at center)} \quad \ldots \ldots \ldots = \frac{5w\ell^4}{384 \, EI}$$

$$\Delta_x \quad \ldots \ldots \ldots \ldots \ldots = \frac{wx}{24 \, EI}(\ell^3 - 2\ell x^2 + x^3)$$

Fig 10.6 Simply supported beam - Uniformly distributed load.

(a) *Plate induced.*   (b) *Stiffener induced.*   (c) *Tripping failure of stiffner.*
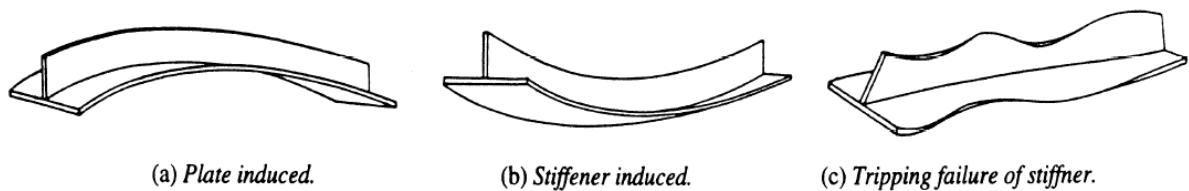
Fig 10.7 Failure modes for the beam-column hence positive or negative lateral pressures are important to distinguish. [37]

10.3 Shear stress

Notice the additional part in only the DNV formula (eq 39) with shear stresses τ_c. The Euler column buckling does not speak of shear stresses but just as with the Von Misses does shear have an influence on the structural behavior so this addition seem natural. The definition of the uniform input τ_{Sd} does not result in serious stresses in the stiffeners but do have their effect on the associated plate. It is however odd that this is completely disregarded in the ABS code.

When the overall shear stress in the associated plates is uniform, they have the same sign. The stress gradient effect however produces opposite signs for the 2 associated plates and an actual stress result in the longitudinal direction within the area of the weld. A similar kind of longitudinal stress is produced due to the shear lag.
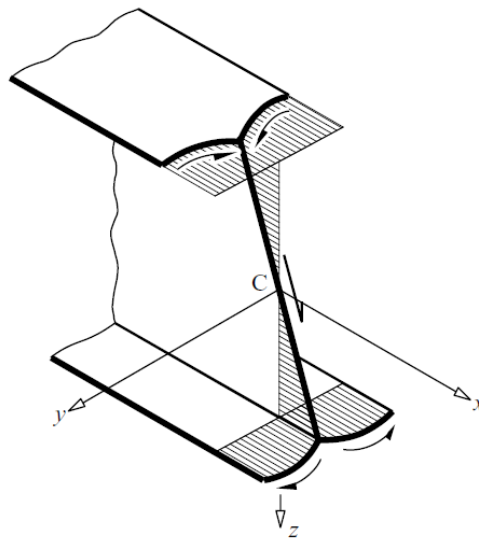
Fig 10.8 Illustration of the shear lag which also influence the axial in-plane stresses.

The DNV code is a bit more complicated for defining the axial stress as discussed in chapter 10.1. The stiffeners act as support and are meant to prevent out of plane deformations. Hence, the strength against axial stresses and bending is understandable influenced. However the shear stress plays part as well. Again remember the shear stress defined in figure 10.1. The effect of that on the associated plates is clear. The question is whether the shear has effect on the stiffener as well. The DNV incorporates this in the input design force F_x in the calculation. The compressive force F_x therein is a function of σ_x but also of the shear stress τ_c in a special combination.

$$F_x = \sigma_x\left(A_p + A_s\right) + \tau_{tf} * A_s \qquad \{44\}$$

If the stresses in the web are allowed to be beyond the elastic plate buckling limit then

$$\tau_{tf} = \tau_c - \tau_{crg} = \tau_c - k_g \frac{\pi^2 E}{12(1 - v^2)}\left(\frac{t}{l}\right)^2 \qquad \{45\}$$

This is one of those parts in the standard in which clearly is tried to make things as a blank form and omitting the explanation. For example, some of these parameters are exchanged with numbers as seen in formula 7.4 in the DNV. It is understandable that the actual shear stress can be much higher than the column-like critical buckling shear stress τ_{crg} because the stiffener provides extra strength in comparison with only the plate. But notice the use of $\left(\frac{t}{l}\right)^2$ instead of $\left(\frac{t}{s}\right)^2$. This makes that the second part (τ_{crg}) is the Euler column-like critical buckling stress instead of the plate-like critical buckling stress. To make this more accessible remember that the boundary condition for column buckling is defined with only the ends constraint.

Little research is necessary to see that the shear appears to have no or at least negligible effect on the axial stress in the stiffeners. This does raise a disbelieve in whether the addition of a pure uniform shear stress is correct or not. This is of course an empirically determined introduction of this input but not very logical unless the real shear stress distribution is as illustrated in figure 8.14 instead of uniform. This creates the effect that the shear stress does indeed influence the axial load on the stiffener. But no explanation is given about what τ_c should be taken as input for the standard. Whether they should be the average or maximum etc. is unknown.

Since the definition concerns the maximum compressive stress at the extreme fiber anyway and it is a conservative approach, the maximum of σ_a of all cross-sections along the column as calculated above is taken without considering the shear stress results in the FEM analysis.

10.4 Correction factors

The effective width:

A more detailed definition of the empirical and partly theoretical correction factors is in order. The associated plating contains half the plate width on both sides of the stiffener. The loads on this part of the model are compared to some specified critical stress in the stiffener defined using simple beam theory. To correct the simplified formula the effective plate width s_e combination is used, mainly defined by plate slenderness as described in chapter 3.4. This s_e is further corrected with influence of the transverse stress and the shear stress. Together this translates to a factor A/A_e in the formula. A smaller effective plate width results in a decrease of the allowable stresses. This effective width may have a fairly large impact on allowable stress. Therefore the also σ_y and τ_C may need an accurate approximation.

$$A = A_{stiffener} + s \cdot t$$

$$A_e = A_{stiffener} + s_e \cdot t$$

{46}
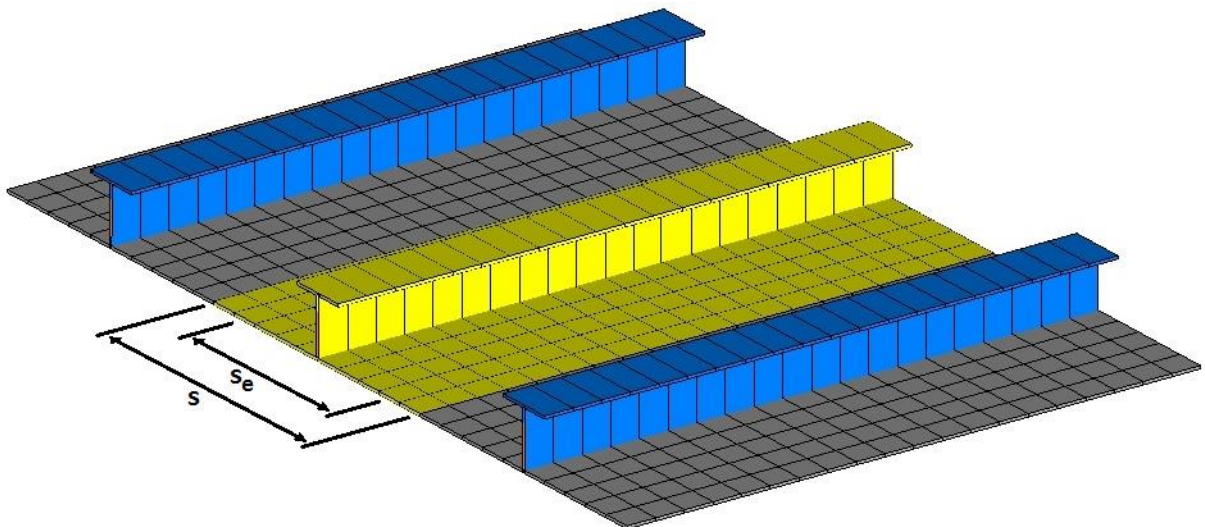
Fig 10.9 Illustration of the considered part of the construction for the flexural buckling and tripping checks
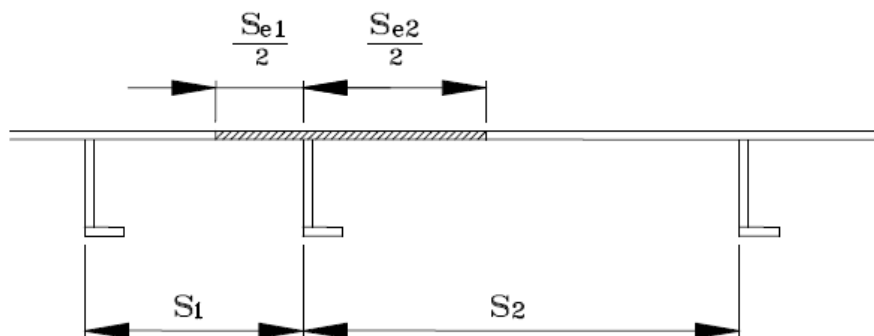
Fig 10.10 The effective width illustrated for varying stiffener spacing in the DNV standard.

The correction on the Euler's critical stress:

The strength curves seen above in figure 10.11 form the base of the methods used for other correction factors in the formula. Different correction methods on the Euler buckling have been developed. Notice formulas in equations 39 and 40 by which the input loads are divided: $f(\sigma_0, \sigma_E)$, $f(\sigma_0)$, $f(\sigma_0, \sigma_E, \sigma_T)$ and $f(\sigma_0, \sigma_T)$. These combinations of the yield, Euler and torsional strength are described by the Perry-Robertson correction employed by the DNV and the Johnson-Ostenfeld correction employed by the ABS. Both originate from empirical research and theoretical formulations.
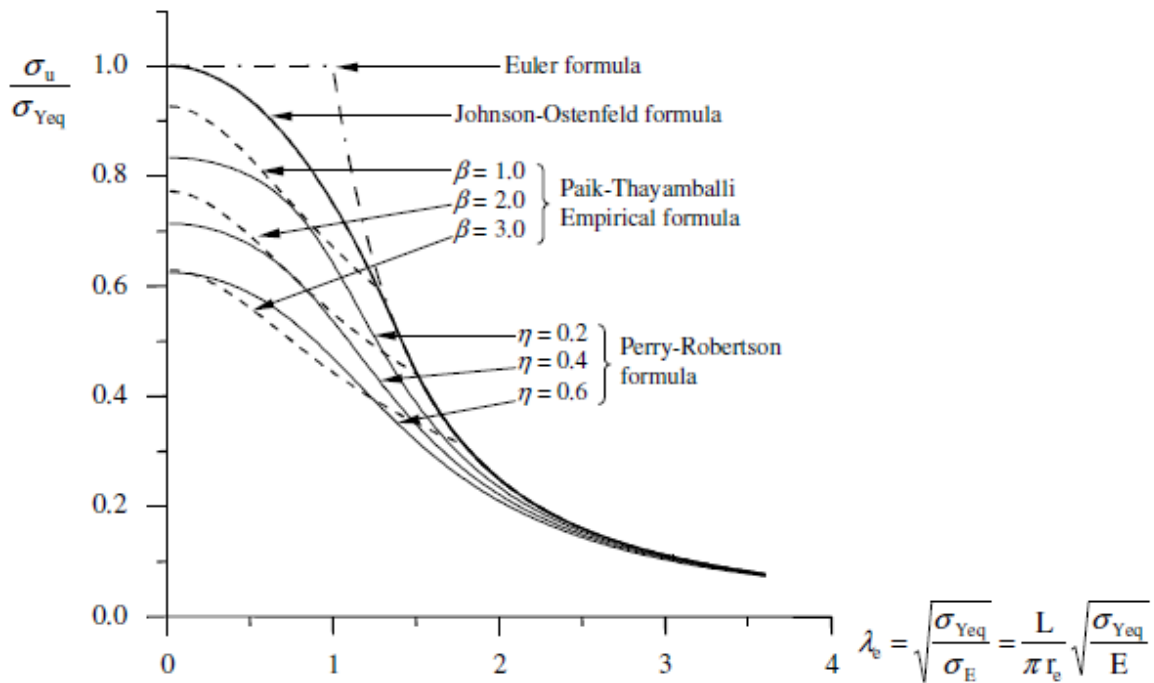
Fig 10.11 Comparison of empirical methods to predict aluminum column strength.

The Perry-Robertson formulation is a formula for the ultimate load and assumes that the plate-beam combination will collapse when the maximum compressive stress at the extreme fiber reaches the yield strength of material. Without further explanation it gives the following formula:

$$\sigma_P = \frac{1}{2}(\sigma_0 + (\eta + 1)\sigma_E) - \sqrt{\left(\frac{1}{2}\sigma_0 + \frac{1}{2}(\eta + 1)\sigma_E\right)^2 - \sigma_0 \sigma_E} \qquad \{47\}$$

η is herein a factor including the effect of imperfection in the column. The DNV standard implements this exact same method to define the critical stresses for both flexural and torsional buckling strengths. Exact definitions can be found in the standard but it results in the following formula for the characteristic strength and the torsional strength in which you can see the resemblance:

$$\frac{\sigma_k}{\sigma_r} = \frac{1 + \mu + \lambda^2 - \sqrt{(1 + \mu + \lambda^2)^2 - 4\lambda^2}}{2\lambda^2} \qquad \{48\}$$

$$\frac{\sigma_T}{\sigma_0} = \frac{1 + \mu + {\lambda_T}^2 - \sqrt{\left(1 + \mu + {\lambda_T}^2\right)^2 - 4{\lambda_T}^2}}{2{\lambda_T}^2} \tag{49}$$

The Johnson-Ostenfeld takes into account the effect of plasticity into the elastic buckling strength. The resulting "elastic-plastic" buckling strength is often termed the "critical" buckling strength.

$$\sigma_{cr} = \begin{cases} \sigma_E \ for \ \sigma_E \leq \eta\sigma_0 \\ \sigma_0 \left(1 - \dfrac{\sigma_0}{4\sigma_E}\right) \ for \ \sigma_E > \eta\sigma_0 \end{cases} \tag{50}$$

The correction in the ABS is surprisingly good in accordance with this relation.

$$\sigma_{CA} = \begin{cases} \sigma_E \ for \ \sigma_E \leq P_r\sigma_0 \\ \sigma_0 \left(1 - P_r(1 - P_r) \dfrac{\sigma_0}{\sigma_E}\right) \ for \ \sigma_E > P_r\sigma_0 \end{cases} \tag{51}$$

Pr is stated as the proportional linear elastic limit of structure, which may be taken as 0,6 for steel and simplifies the formula to:

$$\sigma_{CA} = \begin{cases} \sigma_E \ for \ \sigma_E \leq P_r\sigma_0 \\ \sigma_0 \left(1 - 0,24 \dfrac{\sigma_0}{\sigma_E}\right) \ for \ \sigma_E > P_r\sigma_0 \end{cases} \tag{52}$$

The magnification factor:

Yet another correction is brought into both the ABS and DNV codes. For a column the deflection will tend to infinity, as P is increased to P_{cr} as shown by curve-A in fig 10.12 below. Provided the material remains elastic, it is possible to show that the applied force P, enhances the initial deflection at every point along the length of the column by a magnification factor, given

$$\frac{1}{1 - \left(\frac{P}{P_{cr}}\right)}$$

{53}

The derivation is made in appendix N. This factor is only multiplied with stress due to the bending moment since this only concerns the initial imperfection and hence the eccentric loading conditions.
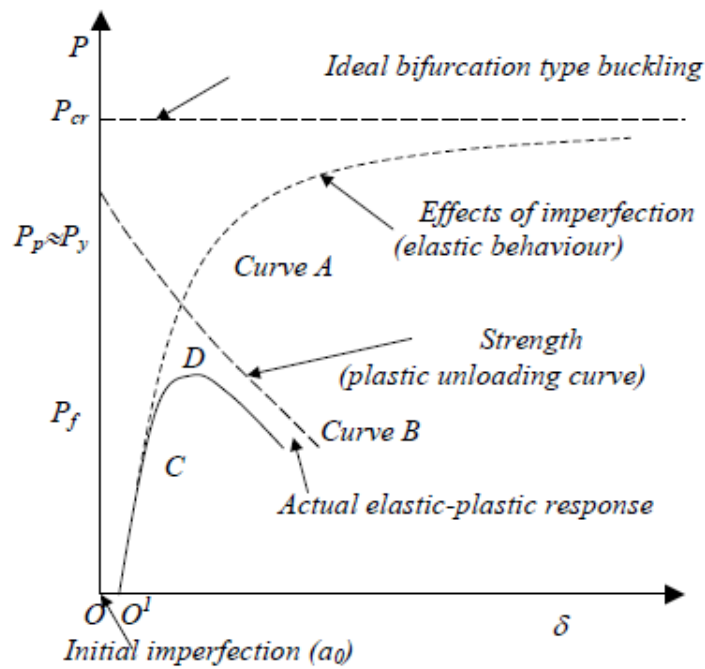
Fig 10.12 Theoretical and actual load deflection response with initial imperfection.

10.5   Proposal for implementation method

The input design stresses as discussed above may be simple but the aim was to search a new implementation method for the beam model. Figure 4.9c already stressed out the preference of using only beam element results. Instead of assembling and sorting out the necessary stress results from the plate elements within the associated plate fields. Taking all plate elements into account would require an enormous extra implementation and calculation time since every cross section along every stiffener will need to be sorted out. The new approach has an effect on both the axial stress and the bending stress.

The idea is to extrapolate the corner stress results from the beam elements, points 1 and 2 in figure 10.13 below (points 3 and 4 in figure 9.2), to the rest of the adjacent plate fields. Then the average over the extrapolated stress and the F_x in the beam elements is taken. Hereby is thus opted for the cross section in figure 4.9c instead of 4.9b while still taking the associated plates into account.
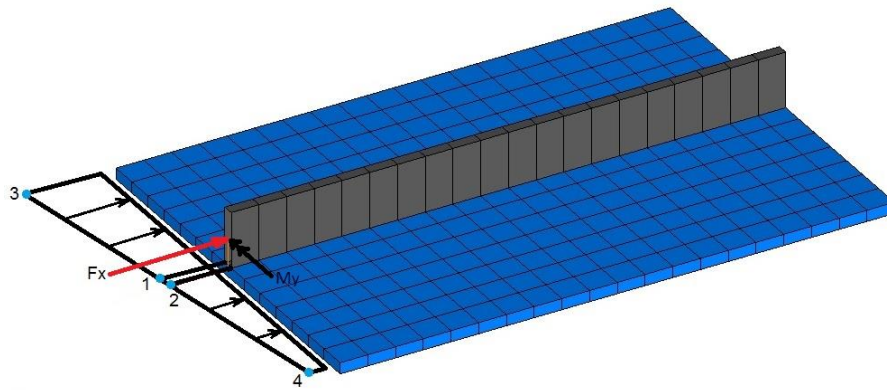
Fig 10.13 Illustration of the method to define the uniform axial load.

To generalize this principle not simply the average stress is taken but the total force is divided by the total area for if the adjacent plate fields do not have the same width (fig 10.10).

$$\sigma_a = \left(\sigma_{average\ plate1} \cdot A_{plate1} + \sigma_{average\ plate2} \cdot A_{plate2} + F_x\right)/A \qquad \{54\}$$

$$\sigma_a = \left(\frac{(\sigma_1 + \sigma_3)}{2}\frac{s_{plate1} * t}{2} + \frac{(\sigma_2 + \sigma_4)}{2}\frac{s_{plate2} * t}{2} + F_x\right)/A \qquad \{55\}$$

It is difficult, if not impossible, to relate the stress results in the beam elements to the lateral pressure on the entire column. However, the DNV states it is equal to the "absolute value of the actual largest support moment for the stiffeners with unequal spans and/or unequal lateral pressure in adjacent spans". It therefore proposes a workaround beyond the forget-me-not's although without specifying how to calculate it.

Instead of calculating with q_{Sd}, it is faster to define M_y immediately which would also discard the troubles with boundary conditions. The result from above give 3 axial forces divided by the area whereupon these same forces can be used together with the bending moment in the beam element to define the total M_y around the centroid. The stress results due to out of plane bending moments in the plates are neglected though. The concept is illustrated in fig 10.14. The check can be done on all cross-sections over the length and taking F_{xmax} and M_{ymax} as specified by the standards. The maximum values might come across as conservative but the check does actually search for the maximum compressive stress at the extreme fiber. The benefit for analyzing all individual cross-sectional areas is that second order effects are taken into account. Especially when the model has a finer mesh size.

$$M_y = F_{x\,plate1} \cdot z_p + F_{x\,plate2} \cdot z_p + F_{x\,stiffener} \cdot z_s + M_{stiffener} \qquad \{56\}$$
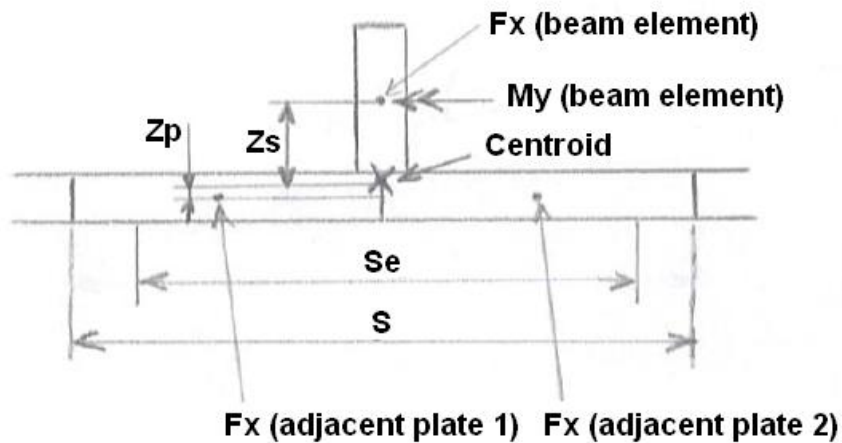
Fig 10.14 The parameters to define the combined bending moment M_y.

There is another option as well to select the maximum bending stress. Femap gives results of the maximum combined stress in the beam elements. This has to be subtracted with the uniform axial stress to define the amount of stress due to bending moments. The result however also includes the part of bending moment M_z and neglects the fact that the maximum stress could be in the plate instead of the stiffener. And although you can make equation 42 and the rest redundant altogether it would probably result in a conservative value and unverifiable.

For now the shear stress is simply taken as the average of the two adjacent plate fields due to the absence of other possible methods. That means the shear stress calculated with the use of the unstiffened plate fields worked out in chapter 8. Note that this should be the correct shear stress as the implementation method was rejected in the conclusions.

From the original 4 input parameters σ_x, τ, σ_z and σ_y the first three are defined now, so far neglecting σ_y. This last input design stress is however necessary for the definition of the effective plate width. The approach is equal to that of the shear stress for now, due to an absence of other possible methods. Hence, σ_y is taken as the average transverse stress from both associated plate fields.

10.6 Approach for verification of implementation method

With the help of the methods described above the design loads can be defined from the linear static analysis but they still have to be verified. Comparable to the approach used for the unstiffened plate fields, the input design stresses F_X, M_Y, τ_C and σ_Y should be verified individually and a separate checks are required to evaluate each of the implementation methods. The extrapolation of the stress results will need to be verified before other checks are meaningful. And furthermore, the bending moment M_y is not really of importance since no lateral pressure is applied in the load cases. The bending moments are therefore small and deviations between real M_y's and those calculated with the implementation method are out of proportions.
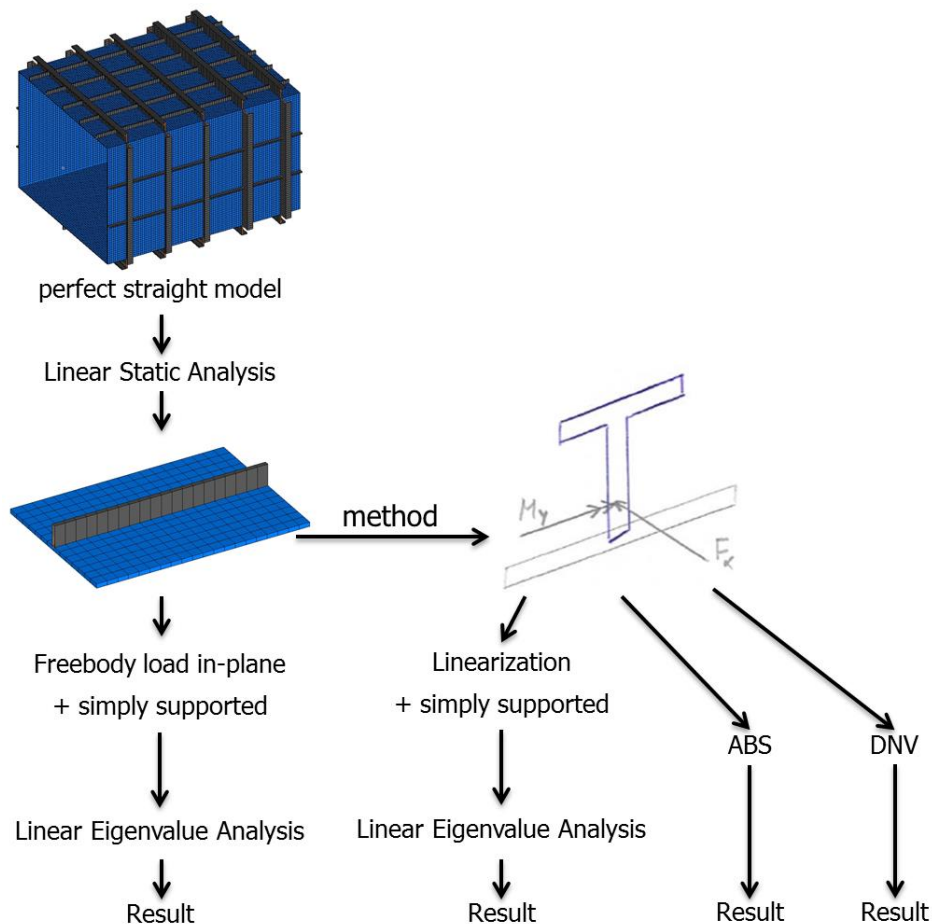
Fig 10.15 The approach to verify the proposed method for beam-columns.

However checking the column with the real applied loads and comparing it to the proposed method with the help of a linear eigenvalue buckling analysis is even more difficult you would think at first sight, remember figure 5.11. Implementation methods for the shear τ_C and transverse stresses σ_Y are not verified for the moment.

First the implementation method. Applying Fx an My are complicated because of the combination of plate elements and beam elements. Therefore a rigid body tie may be used again as defined in

chapter 6. The center of the tie is located at the neutral line of the stiffener plate combination with the total plate width. The constraints have to be adjusted accordingly as shown in figure 10.18.

The freebody load on the other hand is the real problem. Neither the freebody load or the prescribed translations and rotations have a satisfying result (fig 10.16). The transverse and shear stresses have obviously effect on the buckling but for now only the axial stress is taken into account. However, taking only one of the directions cancels the equilibrium of forces like the phenomenon seen before with plate fields. And again the stress gradient effect has its impact on the analysis. Hence some axial force should be divided along the length such that it produces equilibrium. However the position of this axial force / shear stress is not clear. It should be within the entire column section area. Only the prescribed translation on the column ends is an adequate, although conservative, substitution (fig 10.17).
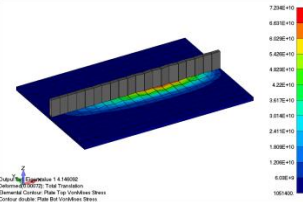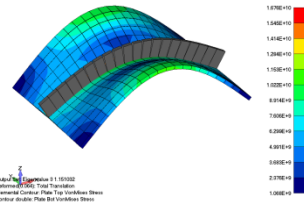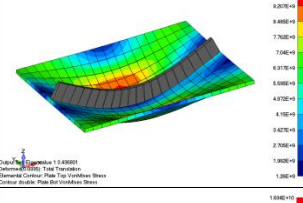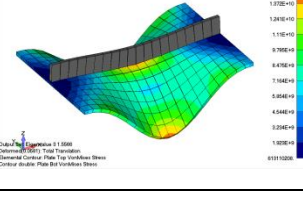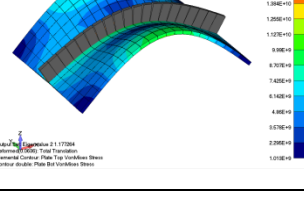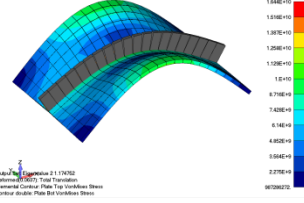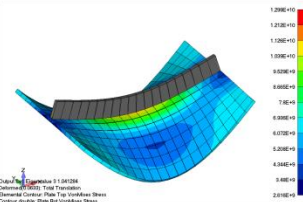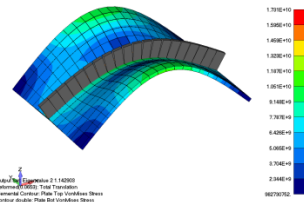
Eigenmode	Load case	Eigenvalue	Eigenmode	Load case	Eigenvalue
	Translations + Rotations on all edges	4.146092		Freebody forces and moments on all edges	1.151032
	Translations on all edges	3.436801			
	Translations + Rotations only on the ends of the column	1.5566		Freebody in-plane forces and My moments on ends only	1.177264
				Freebody Forces in longitudinal direction and My moments on all edges	1.174752
	Translations only on the ends of the column	1.041284		Freebody in-plane forces on ends only	1.142903

Fig 10.16 Eigenvalue analyses of the beam-column with different applied load cases. The left shows results with prescribed translations and the right shows results of freebody loads. All for only load case 1.
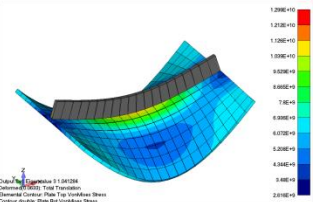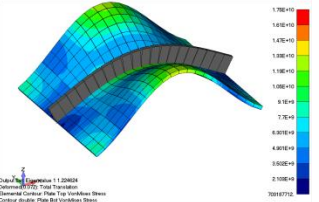
Eigenmode	Load case	Eigenvalue	Eigenmode	Load case	Eigenvalue
	Translations only on the ends of the column	1.041284		Implementation method with Fx	1.224624

Fig. 10.17 The remaining available check.

The analysis is further complicated with other buckling modes (fig 10.19 and 10.20). Most eigenmodes only cover the behaviour of the associated plates hence a number of modes should be analyzed in order to take the relevant column buckling mode.
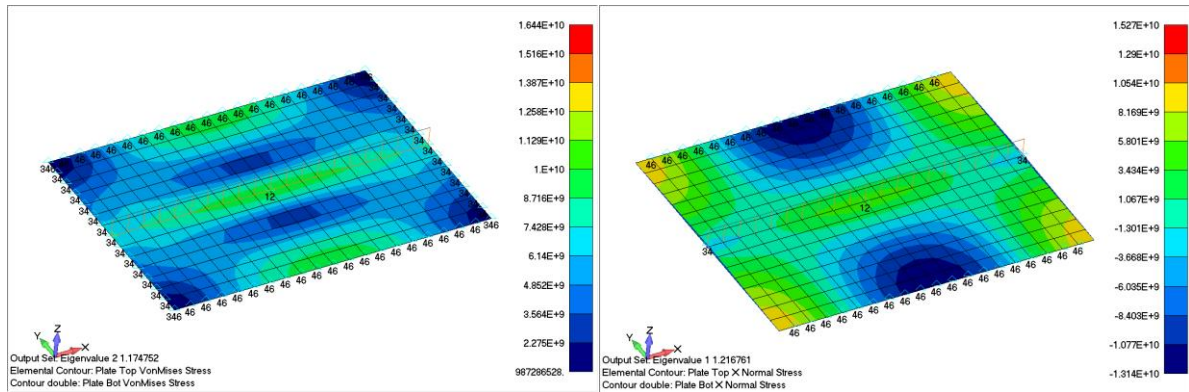
Fig 10.18 Definition of the column with boundary conditions for the freebody load and the design load calculated with the implementation method.
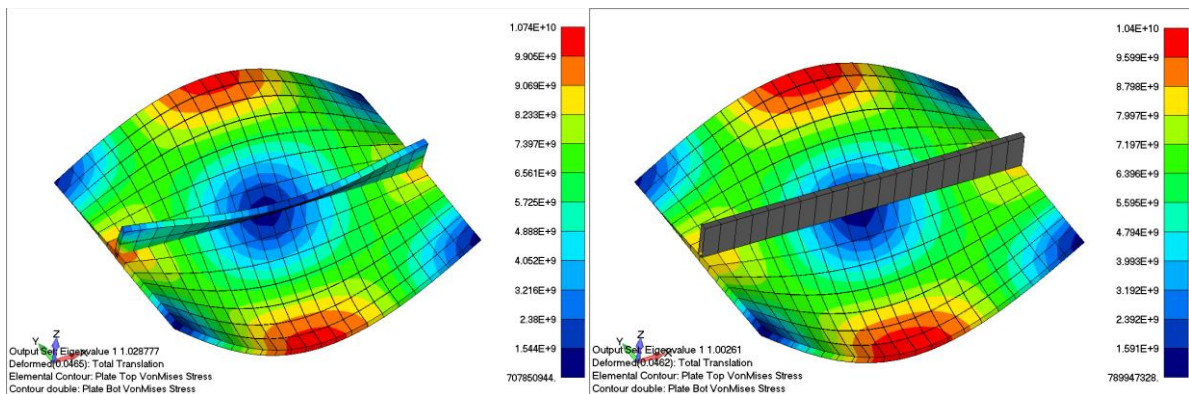
Fig 10.19 Load case 1: The first eigenvalue mode for the Freebody load.
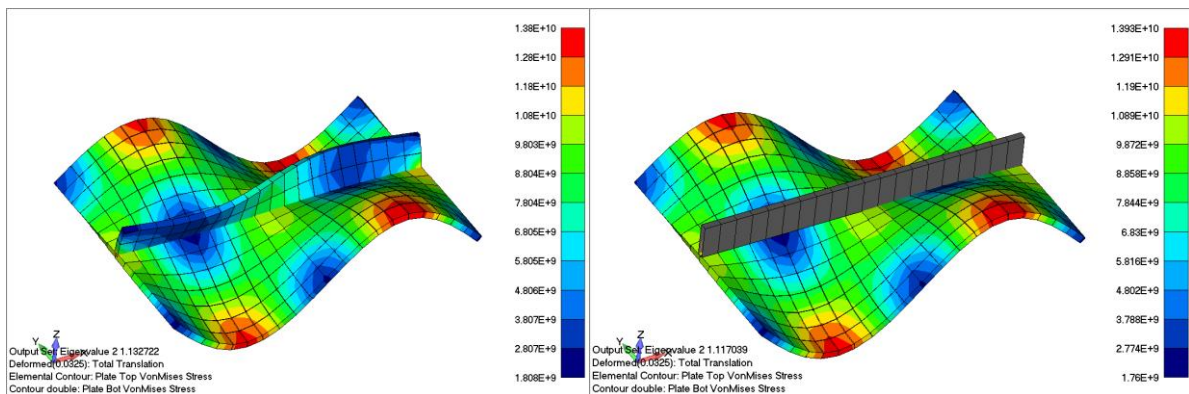
Fig 10.20 Load case 1: The second eigenvalue mode for the Freebody load.

10.7   Experiments

The load cases (or the specific stiffener in the model) are chosen a bit unfortunate. Especially load case 5 has a horizontal bending moment which is so significant that buckling results will not provide useful data for beam-column buckling. As this situation will likely indicate that the critical section is not in this stiffener it will not be a problem. Furthermore, load case 6 produces tension in the longitudinal stiffeners and is thus not usable either. Hence only load cases 1, 2, 3, 4 and 7 remain for proper analyses. Note that all models have equal plate widths for both associated plate fields for every stiffener that is checked. Unequal plate widths will require an extra check.

Overall it is difficult to conclude whether the deviations in eigenvalue results are because of the unequal ways of applying the load or because of the implementation method. Therefore, for now, only the stress values are compared. The results are summarized in appendix I.

The differences seem to be very similar at first sight when you look at the first few load cases on the basic models. However, as other checks are examined, the results are not that similar anymore, non-conservative and deviate up to almost 42% from what real stresses give. Even though the maximum stress is taken from all cross section areas along the beam-column. The implementation method is therefore considered not entirely correct. The basic model with different plate thicknesses and the longitudinal stretched model 7 have similar results for the first 4 load cases but these are mainly longitudinal loads. Load case 7 with the transverse load has surprisingly a considerable effect on the stress results in the beam elements. Furthermore the shape and dimensions of the stiffeners seem to have considerable influence on the results as well. Both in a negative way (fig 10.21). Obviously, the lower two stress recovery points in the beam elements do not equal the stress in the plate. With more detailed examination of the model this also applies to the plate model (fig 10.23 and 10.24). The reason is difficult to explain. The strain results do have a good transition in the place of attachment between the stiffener and the associated plates however stress results as given by the linear static analysis do not. Hence the implementation method with extrapolations is not sufficient and should not be allowed to define the present axial stress in the beam-column.
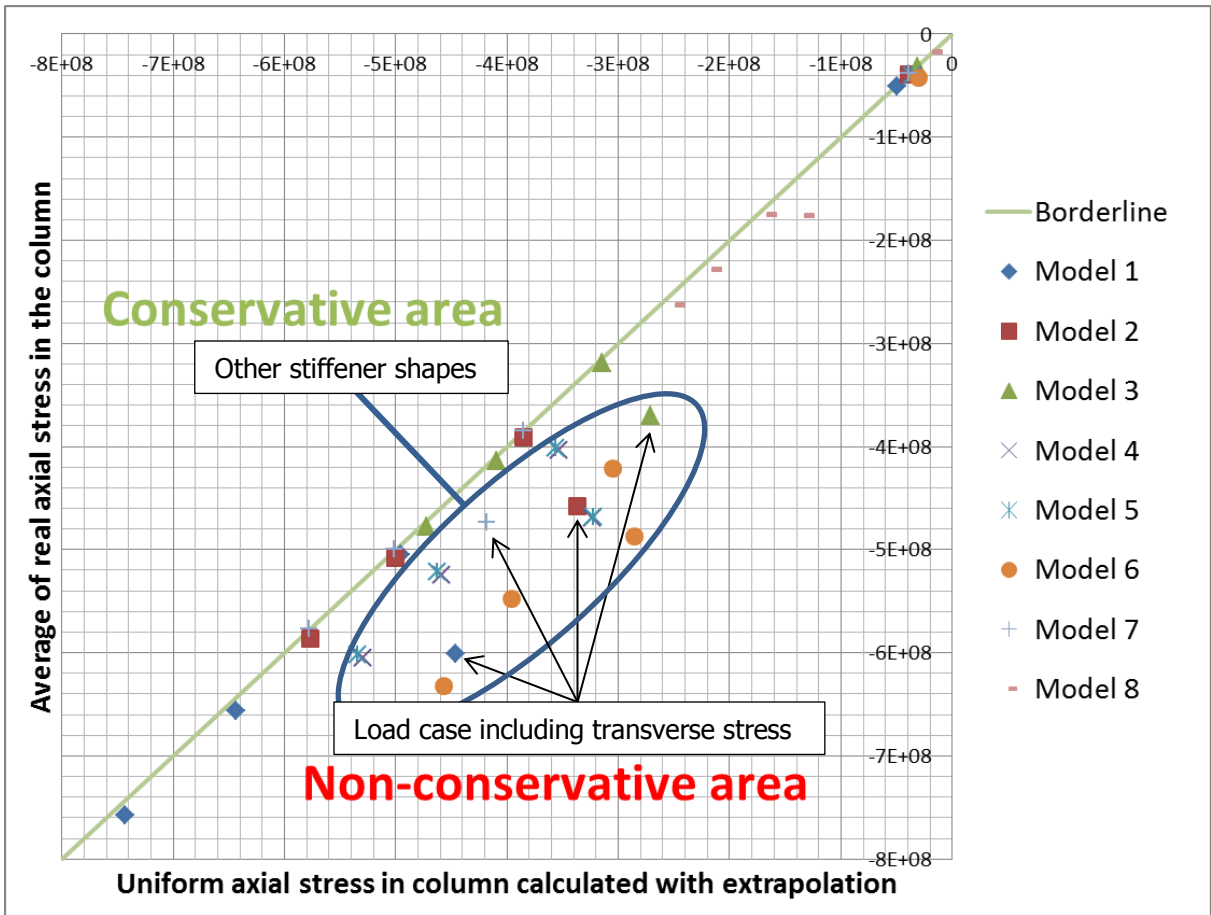
Fig 10.21 Comparison of real axial beam-column stresses and the implementation method.
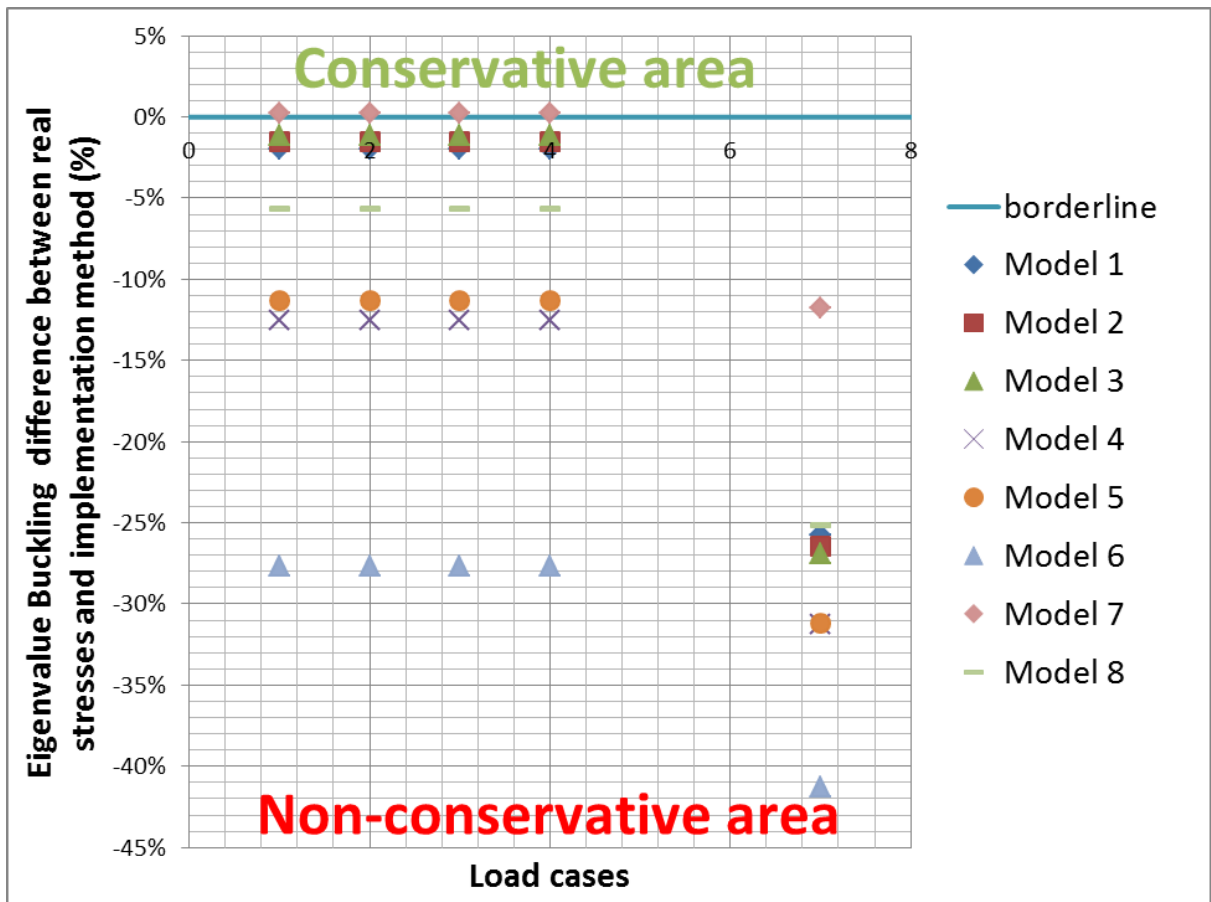
Fig 10.22 Focus on differences in figure 10.21 subdivided between the load cases.
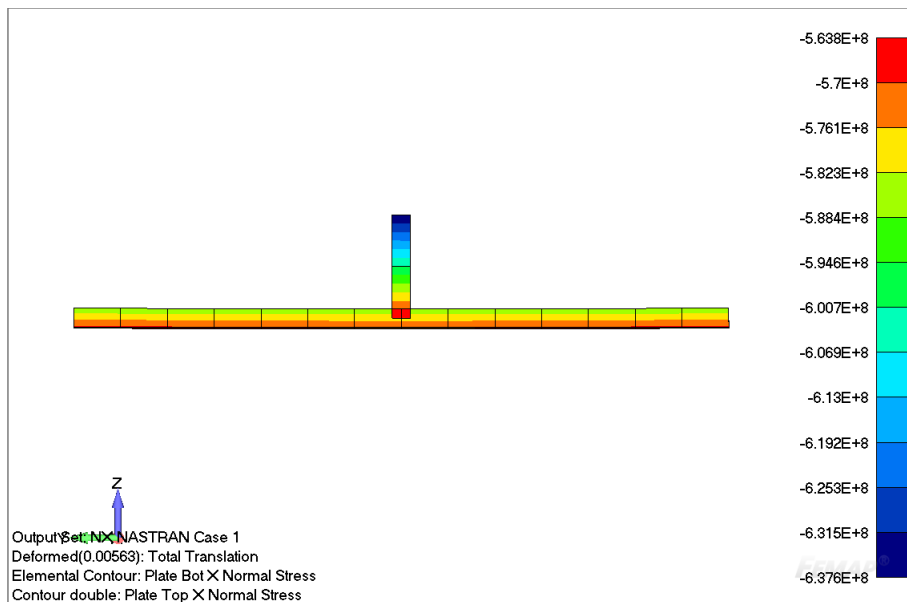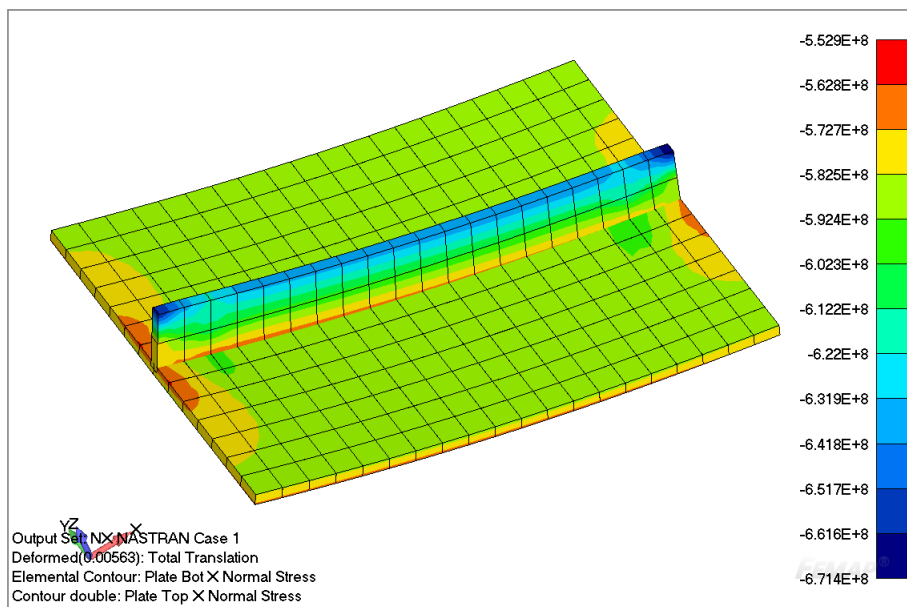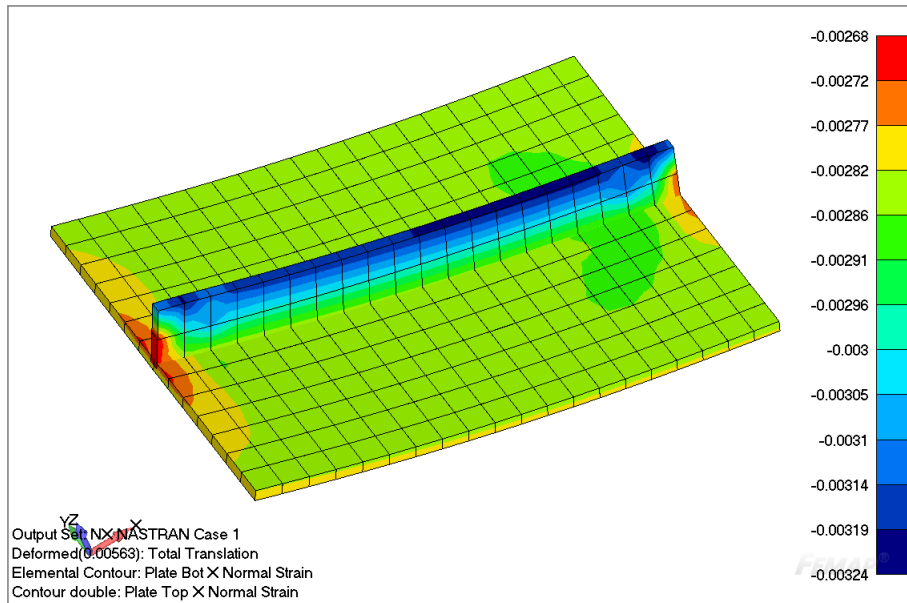
Fig 10.23 Axial strain and stress results in the stiffener and associated plates for load case 1. Stress results slightly diverge at the place of attachment.
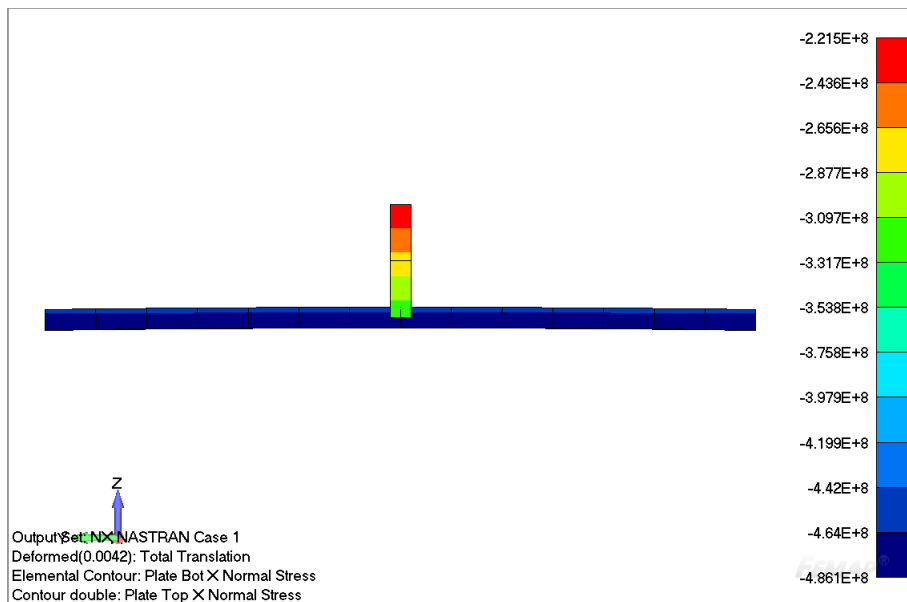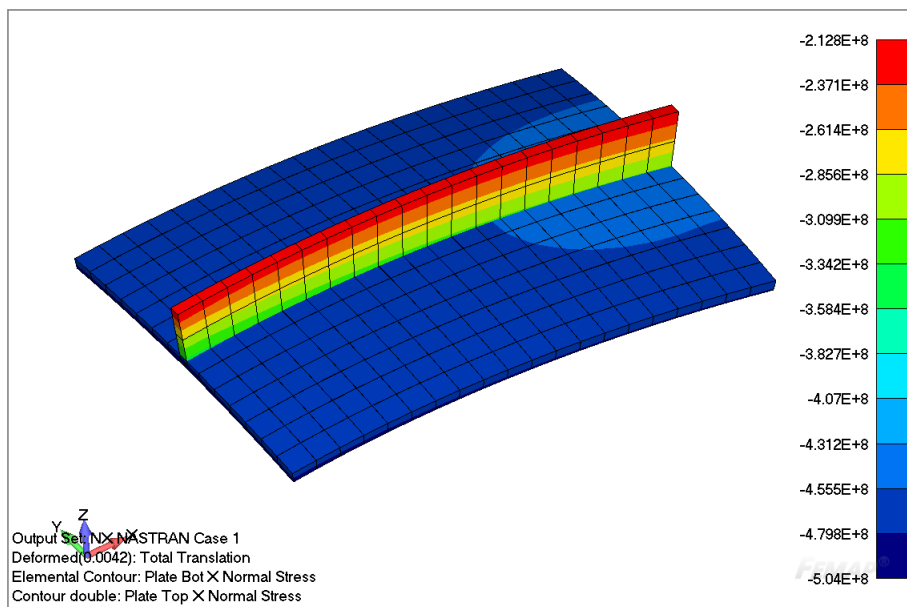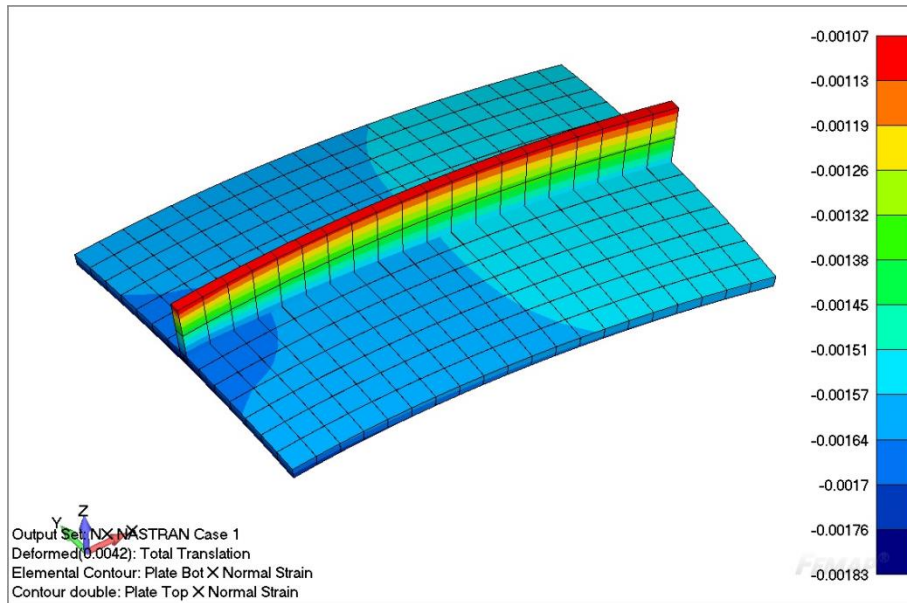
Fig 10.24 Axial strain and stress results in the stiffener and associated plates for load case 7. Stress results seriously diverge at the place of attachment.

11. Analysis of stiffener torsional buckling limit

The deflection shape is of stiffener torsional buckling or the so called tripping is a complex combination of different parameters. The torsional moment around the line of attachment and the shear forces due to the warping phenomenon are the main loads. The mode seem to be generally coupled with plate buckling.
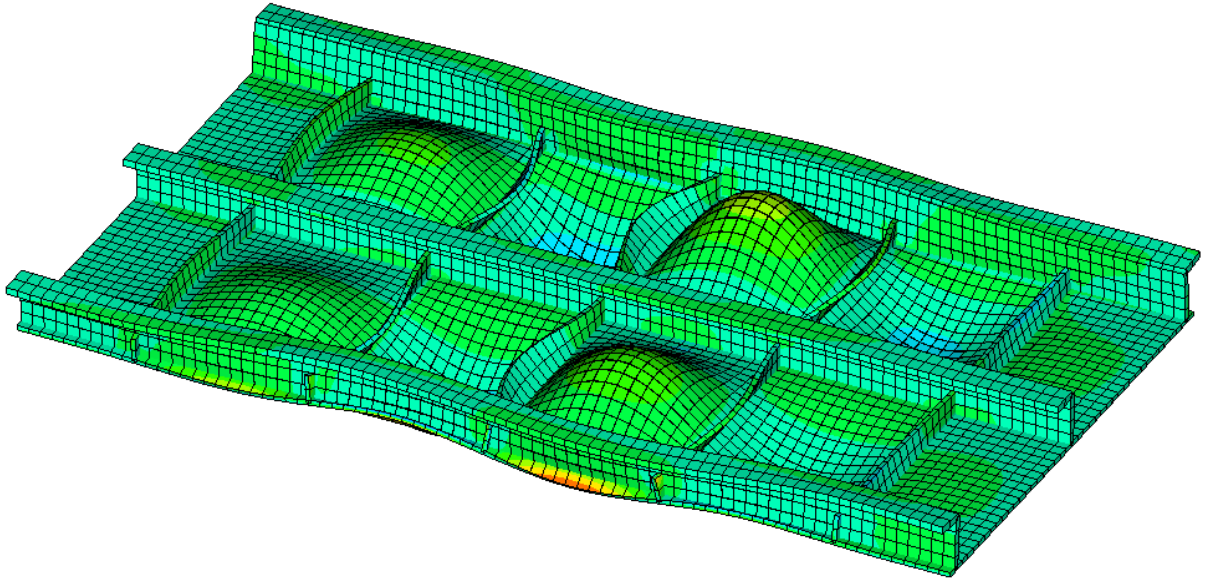
Fig 11.1 A combination of plate buckling and stiffener tripping.
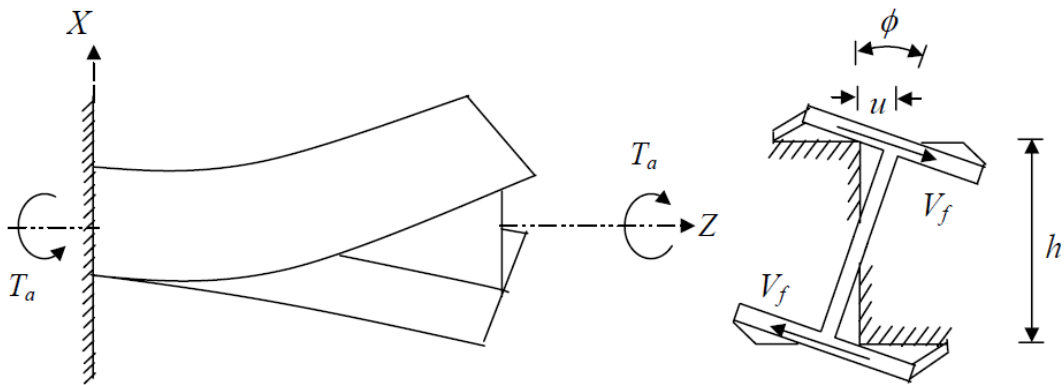
Fig 11.2 Non uniform torsion: twisting and warping.

11.1 Standards

Notice the torsional strength σ_T in the DNV formula (eq 40) only. Hence the DNV code does also include the stiffener tripping check within this same formula. The approach for calculating the strength is already described in chapter 3.5, a more extensive derivation is found in appendix O. The ABS utilizes a separate formula in which only the uniform pressure is compared to the allowable stress and bending moments are disregarded.

$$(ABS) \quad \rightarrow \quad \frac{\sigma_a}{\eta \sigma_{ET}} \leq 1 \qquad \{57\}$$

$$\sigma_{ET} = \frac{\frac{I_t}{2.6} + \left(\frac{n\pi}{L}\right)^2 \Gamma + \frac{t^3}{3s}\left(\frac{L}{n\pi}\right)^2}{I_p + \frac{E\frac{t^3}{3s}\left(\frac{L}{n\pi}\right)^2}{\frac{\pi^2 E\left(\frac{n}{\alpha} + \frac{\alpha}{n}\right)^2\left(\frac{t}{s}\right)^2}{12(1-v^2)}}}$$

{58}

This critical buckling stress for associated plating corresponds to the number of n half-waves that yield the smallest critical stress.

$$(DNV) \quad \rightarrow \quad \sigma_{ET} = torsion + warping = \left(\beta\frac{GI_t}{I_p}\right) + \left(h_s^2\frac{\pi^2 EI_z}{I_p l^2}\right)$$

{59}

Note that σ_{ET} from the DNV does not go into equation 57 but is used within equation 39.

I_t = torsional moment of inertia (St. Venant torsion) of stiffener only

I_z = moment of inertia of stiffener about axis through centroid of stiffener and parallel to web (Z1)

I_p = polar moment of inertia of stiffener about center of rotation ($I_y + I_z$)

Γ = warping constant
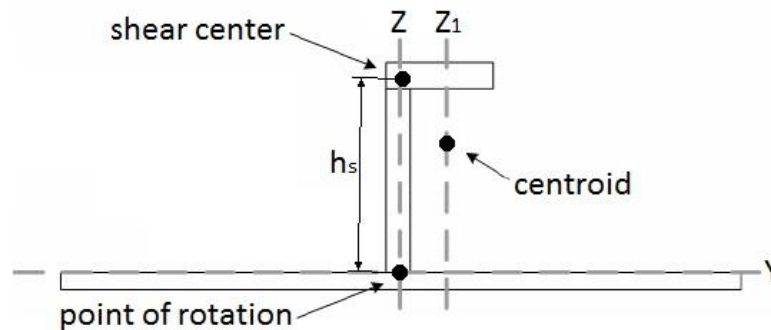
Fig 11.3 Cross section of a stiffener and its plate.

11.2 The implementation method

The implementation of the torsional stiffener buckling check is not further worked out for the moment. The standards however only need already available parameters or values which can be calculated with the known dimensions. The input design loads remain the used axial and bending stress and hence the checks could be evaluated.
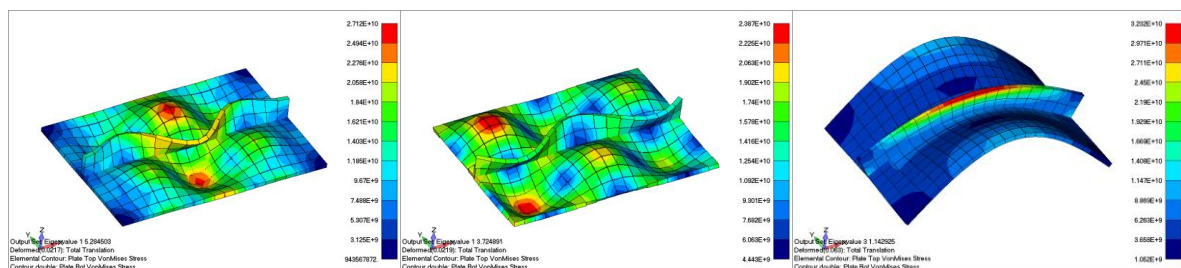
Fig 11.4 Several buckling modes of the beam-column in the plate model.

12. Conclusions

An extensive overview of the buckling phenomena is given. All buckling modes such as local plate buckling, local stiffener buckling and beam-column buckling have been discussed. Each have their influencing parameters as load cases, geometry, boundary conditions, imperfections, material properties and residual stresses. The following preferred assessment of the buckling resistance is a combination of linear static FEM analyses and standards. It simplifies the analysis so many of these parameters and details do not have to be defined since they are taken already into consideration within the standards. Plus the approach will make it possible to assess models with any kind of mesh size.

It simplifies the complicated buckling phenomenon such that the coupled relationships between buckling modes and influences such as shear lag and warping are taken into account with relative basic load cases. However the actual load case on each individual section still has to be defined sufficiently accurate in order to make use of the standards. The implementation method hence only requires to define input design stresses which are attempted to specify for plate fields, stiffener webs/flanges and beam-columns.

The approach for plate fields have been observed with a top down view. Real stress distributions are formed with corner stress results along the edges. Longitudinal and transverse in-plane stress results are transformed into a design stress by a linear regression of these distributions. Shear stress results are grouped together with an average or maximum. However as results showed more and more deviations from the real situations it was clear that implementation needed a more satisfying distinction between real stress results. A new subdivision into a longitudinal stress gradient, a transverse stress gradient and the remaining shear stress is proposed. This is logical from the viewpoint of the standards since they also assess plate fields on their buckling strength by a simplified combination of these σ_X, σ_Y and τ. Hence this new subdivision also recreates equilibrium for the individual portions again, something which is absent in the original stress distributions and needed for realistic checks. Verification concludes that linear regression is allowable as long as the stress gradient effect is taken into account. The shear stress however cannot be simply an average or maximum from the original shear stresses as seen in the results hence a new proposal is made to do that from the new subdivided shear stress. Extra research is recommended for this proposal.

To go more in-depth into the actual linearization it shows that adaptations on linear regression almost always have an undesired effect on the input design stress. Most of the investigated situations end up in far too conservative end results. Simple linear regression of in-plane stresses however generally only deviate several hundredth or tenth of percentages compared to the real load case. The stress gradient however has more influence than expected and is understand to be the actual problem area when defining the input design stresses. The Clause 4.6(3) in Eurocode 3, part 1.5 does indeed provide some prevention of this phenomenon however is not completely satisfying either. This is primarily because it states an adjustment for only the long edges instead of both the short and long

edges. And secondary because some situations do not come in the conservative region with 60%. The new proposal would be to take the normal linear regression and go for about 70 percent of the two opposite edges instead of the average or 60 percent from the Eurocode.

The assumption has been made that the model has stiffeners modeled with beam elements. Identifying load cases on the stiffener web and flanges separately is therefore problematic. An interpolation of the stress recovery points from the beam elements is made to define the correct input design stresses for the individual web and flange. The implementation method for stiffener webs and flanges is insufficiently tested and hence there is a lack of solid conclusion that can be made. However the single check shows slightly non-conservative but fairly similar and thus promising results.

While decomposing the approaches of the standards for the beam-columns it can be shown that there is a simplified separation of the loads and correction factors. Identified correction factors include the effective width concept which is used to justify implementation of Euler's column buckling. Furthermore, the ABS formula implements the Johnson-Ostenfeld correction in the allowable design stress while the DNV formula implements the Perry-Robertson correction. Lastly there is the magnification factor due to initial imperfections. Hence, the procedure of the standards provides a surprisingly good match with theoretical approaches. The loads consist of the axial uniform pressure, the bending moment and maybe a uniform shear stress distribution on the associated plate fields. The definition of the axial stress is based on an eccentric force and shear stresses. The definition of the bending moment is based on a lateral pressure, the for-get-me-not's and a choice of boundary conditions. All these parameters are problematic to define from your FEM model.

Instead it is much more straightforward within the new proposal, which takes the axial stress results and bending moments directly from the linear static analysis. Hence, a by-pass can be made such that the above mentioned parameters do not have to be defined. The following simplification / implementation method bases the axial uniform stress and the bending moment only on results of the stiffener beam elements. An extrapolation of the stress recovery points is used to estimate the results in the associated plate fields. This implementation method does however not meet the expectations. Considering only results from the beam elements shows to be insufficient to base the associated plate fields on. This is partly due to the poison ratio which results in non-conservative deviations up to 40%. Extrapolation of stress results might still be allowable but they should be based on plate elements within the associated plate fields. This is left for further study.

References

[1]   T. M. Larsen, „Plate buckling in Movable Scaffolding Systems," Oslo, 2011.

[2]   S. F. Stiemer en D. Fitch, „Design of Steel Plate and Box Girders," 2007.

[3]   American Bureau of Shipping, „ABS Guide for Buckling and Ultimate strength assessment for offshore structures," American Bureau of Shipping, New York, 2013.

[4]   Det Norske Veritas , „Recommended Practice DNV-RP-C201 Buckling strength of plated structures," DNV, 2010.

[5]   K. Ghavami en M. R. Khedmati, „Numerical and experimental investigations on the compression behaviour of stiffened plates," Elsevier Ltd., Rio de Janeiro, 2006.

[6]   „FutureShip GmbH," *Ship Structural Analysis Enhance structural reliability & operational functionality.*

[7]   Institute for steel development & growth, „Teaching material chapter 6," [Online]. Available: http://www.steel-insdag.org/TeachingMaterial/Chapter6.pdf.

[8]   R. C. Hibbeler, Mechanics of Materials, Singapore: Pearson Education South Asia Pte Ltd, 2008.

[9]   Ship structure committee, „SSC-331 Design guide for ship structural details," 1990.

[10]   E. V. Lewis, Principles of Naval Architecture, Jersey City: The Society of Naval Architects and Marine Engineers, 1988.

[11]   S. A. Patten, „Inelastic Analysis of Tripping Failure of Stiffened Steel Panels due to Stiffener Flange Transverse Initial Eccentricity," Faculty of Polytechnic Institute, Virginia, 2006.

[12]   Institute for steel development & growth, „Teaching material chapter 19," [Online]. Available: http://www.steel-insdag.org/TeachingMaterial/Chapter19.pdf.

[13]   Y. B. Kwona en E. Seo, „Prediction of the compressive strength of welded RHS columns undergoing buckling interaction," Department of Civil Engineering Yeungnam University, Gyongsan.

[14]   L. Gannon, Y. Liu, N. Pegg en M. Smith, „Effect of welding-induced risidual stress and distortion on ship hull girder ultimate strength".

[15]   A. Varma, „CE 405: Design of Steel Structures".

[16]   O. F. Hughes en J. K. Paik, Ship Structural Analysis and Design.

[17]   „Design of Plate Girders," [Online]. Available: http://hcgl.eng.ohio-state.edu/~ceg532/pdf_files/chap9.pdf.

[18]   S. Benson, J. Downes en R. S. Dow, „An automated finite element methodology for hull girder progressive collapse analysis," School of Marine Science and Technology, Newcastle, 2012.

[19]   Institute for steel development & growth, „Teaching material chapter 17," [Online]. Available: http://www.steel-insdag.org/TeachingMaterial/Chapter17.pdf.

[20]   P. H. Miller en J. W. Stettler, „EN358 Ship Structures Notes for an Undergraduate Course,"

Naval Architecture Program US Naval Academy, Annapolis, Maryland.

[21] O. Hillers, „Automatic buckling checks on stiffened panels based on finite element results," Faculty of Civil Engineering & Geosciences - department Structural Mechanics, Delft, 2011.

[22] W. D. Pilkey, Analysis and design of elastic beams, 2007.

[23] W. J. Raven, J. Blaauwendraad en J. N. J. A. Vambersky, „Elastic compressive-flexural-torsional buckling in structural members," Faculty of Civil Engineering and Geosciences, Delft.

[24] A. W. Leissa en J. H. Kang, „Exact solutions for vibration and buckling of an SS-C-SS-C rectangular plate loaded by linearly varying in-plane stresses," *International Journal of Mechanical Sciences 44,* pp. 1925-1945, 2002.

[25] T. Ren en G. S. Tong, „Elastic buckling of web plates in I-girders under patch and wheel loading," Hangzhou, 2005.

[26] K. E. Klöppel en J. Scheer, Beulwerte ausgesteifter rechteckplatten - Kurventafeln zum direkten Nachweis der Beulsicherheit für verschiedene Steifenanordnungen und Belastungen, Berlin: Wilhelm Ernst & Sohn, 1960.

[27] S. Benson, „Progressive Collapse Assessment of Lightweight Ship Structures," Faculty of Sciennce, Agriculture and Engineering, Newcastle UK, 2011.

[28] S. Benson, J. Downes en R. S. Dow, „An automated finite element methodology for hull girder progressive collapse analysis," 2012.

[29] J. K. Paik, „Elastic buckling of plates," Pusan National University Busan.

[30] N. S. Trahair, M. A. Bradford, D. A. Nethercot en L. Gardner, The Behaviour and Design of Steel Structures to EC3, London: Taylor&Francis, 2008.

[31] T. Yusuke, R. Sherif, O. Yasuhisa en M. Hidekazu, „Prediction of Welding Distortion and Panel Buckling of Car Carrier Decks using Database Generated by FEA," Transactions of JWRI, 2007.

[32] J. M. Gordo en C. G. Soares, „Tests on ultimate strength of hull box girders made of high tensile steel," Centre for Marine Technology and Engineering (CENTEC), Technical University of Lisbon, 2009.

[33] C. Libove, S. Ferdman en J. J. Rousch, „Elastic Buckling of a simply supported Plate under a Compressive stress that varies linearly in the direction of loading," NACA National advisory committee for aeronautics, Washington, 1891.

[34] Israel Institute of Technology, „Chapter 4 Plates," [Online]. Available: http://ae-www.technion.ac.il/admin/serve.php?id=27184. [Geopend Dec 2013].

[35] C. Yu en B. W. Schafer, „Stress Gradient Effect on the Buckling of Thin Plates," Johns Hopkins University, Baltimore.

[36] American Forest & Paper Association Inc., „Beam Formulas with Shear and Moment Diagrams," American Wood Council, Washington, 2007.

[37] J. Amdahl, „TMR4205 Buckling and Ultimate Strength of Marine Structures - Chapther 3: Buckling of Stiffened Plates," 2009.

[38]   Yawlou, „Implicit and explicit finite element method," iMechanica, [Online]. Available: http://imechanica.org/node/5396.

[39]   T. Wierzbicki, „2.081J/16.230J Plates and Shells".

[40]   Samuel Ginn College of Engineering, „Chapter 6," [Online]. Available: http://www.google.nl/url?sa=t&rct=j&q=&esrc=s&frm=1&source=web&cd=1&ved=0CC8QFjAA&url=http%3A%2F%2Fwww.eng.auburn.edu%2Fusers%2Fchyoo%2FCIVL7690%2FChapter%25206%2520less%2520HW%2520solution.doc&ei=fIWYUrSBOKX-ygPjr4Io&usg=AFQjCNGLZdxQOoSrYd7DHZ1lHIw7h2chOQ&bvm=bv.57155469,d.Yms&cad=rja. [Geopend 2013].

[41]   J. Ringsberg, „Ship structures advanced course 2011," [Online]. Available: http://129.16.218.54/SSAC/SSAC2011_Lecture11.pdf.

[42]   S. S. Committee, „SSC-433 Interactive buckling testing of stiffened steel plate panels," 2004.

[43]   Ship structure committee, „SSC-411 Evaluation of the effect of construction tolerances on vessel strength," SSC, 2000.

[44]   J. K. Paik, „Large deflection behavior and ultimate strength of plates," Pusan National University, Busan.

Appendix A: Scientific Research Paper

A scientific paper of the research.

Defining parameters for buckling checks of plated structures in finite element software packages

B. Aberkrom, ir. W. Van den Bos[1], ir. A.T. Naatje[2], prof. ir. J.C. Rijsenbrij[1]

[1] Delft University of Technology, Section of Transport Engineering & Logistics, Faculty of Mechanical, Maritime and Materials Engineering, the Netherlands
[2] Femto Engineering B.V., the Netherlands

Abstract Different standards specify allowable buckling stresses in plated structures. A method on how to use standards in combination with linear static analyses is aimed to form a simple buckling assessment of your FEM model. It more specifically concerns the definition of the input design stresses. This paper presents a study to the development and validation of this implementation method.

Introduction

Big models for planes, cranes, ships or other kind of offshore structures can consist of a large amount of plated structures. Therefore FEM analyses become necessary but the size of complete models complicates correct use of available buckling analyses. You most likely get an upper bound value which only says something over a specific part of the structure and gives no information about the rest of the model. Instead you would like an individual check of each section, which is not only a lot of engineering work but also brings more uncertainties in the calculation. What parameters do you take into account? Or even, what kind of analysis do you carry out?

The buckling phenomena

An extensive overview of the buckling phenomena reveal buckling modes such as local plate buckling, local stiffener buckling, stiffener tripping and beam-column buckling. Each have their influencing parameters as load cases, geometry, boundary conditions, imperfections, material properties and residual stresses. The following preferred assessment of the buckling resistance is a combination of linear static FEM analyses and standards. It simplifies things so many of these parameters do not have to be defined separately by the engineer. The implementation method hence only requires to define input design stresses.

A test setup at LISNAVE shipyard is presented in figure 1. The experimental study [1] which was conducted is also described and worked out in the work of S. Benson [2]. This same model is used in the present study and is analyzed due to its relatively simple geometry and easily applied boundary constraints and load cases.

Fig. 1 Test setup of the box girder including part of the supporting structure and the loading device.

Problems with present checks

Whether it is a linear or non-linear analysis, your model might not be suitable for a buckling analysis. Figure 2 shows the first eigenmode for the same model with different mesh sizes. While the linear static stress results are rather consistent, the eigenmodes and eigenvalues are not. The question whether the buckling analyses from finite element modeling software programs are correct or not, hence indicates the need for a different check. The standards are already specifically the method which the engineer would like to compare his or her model with, even though the analysis is being done in a FEM package. However even the linear static stress results

cannot be compared directly to standards. Their inputs are no stress results but simplified applied loads (fig 3).
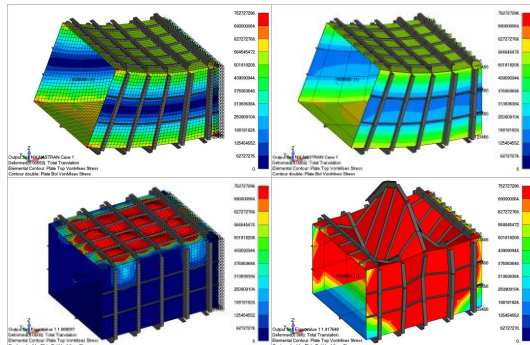

Fig. 2 Comparison of eigenvalue analyses on different mesh size models.

Considerable research has been done on theoretical buckling modes, deflection functions and reduction factors. However the method to extract results from the finite element analysis and using them for the check in the standard seems to be rather non-existent for general FEM programs such as Femap. Two specific standards [3][4] are considered for an in-depth evaluation.

- American Bureau of Shipping (ABS) Guide for buckling and ultimate strength assessment for offshore structures provides formulation to assess buckling criteria of plates and stiffened panels.
- Det Norske Veritas (DNV) Recommended practise DNV-RP-C201: Buckling strength of plated structures is a buckling code for stiffened and unstiffened panels of steel.

The interaction formulae given in these standards are conservative and simple, considering the complicated nature of buckling, which is not that obvious from a FEM perspective. Still the checks provided by the standards are some sort of blank form with large and complicated formulas which should be filled in to check if your design is ok. Whether average engineers also understand how the checks work is questionable. Nowadays everyone can model something in a finite element package but doing a correct analysis is something completely different. Even more, it is already surprisingly difficult to define these input design stresses. Several proposals for implementation methods are worked out for plate fields, stiffener webs/flanges and beam-columns.

Plate field buckling

Real stress distributions of a plate field are formed by the corner stress result from FEM plate elements along each edge. Linearizations of these stresses are used to form the distribution such as in the standards. A simple linear regression is not always conservative however. Therefore several adjustments on the linearization are attempted.

1. **Linear Regression Stress Average**: A simple linear regression from all corner stress points. The principle is explained in earlier work from Ottar Hillers [5].
2. **Linear Regression Stress Average + Including all stress results**: The proposed adaption by Hillers. It shifts the line to the point in which all stress points fall under the area such that an overestimate and very conservative load is taken for each edge.
3. **Linear Regression Stress Average + Updated to σmax**: A new proposal to adapt the linear regression such that σmax of the linear regression matches the σmax of all stress points along the edge. The standards specifically use the maximum compressive stress in the longitudinal or transvers direction which raises the question whether taking a higher value than the highest stress points is not an overestimate already.
4. **Linear Regression by the Eurocode clause**: Clause 4.6(3) in Eurocode 3, part 1.5 delivers an adaption to compensate the stress gradient phenomenon described in the next section.

The first three methods produce linear lines on all four edges and afterwards take the average of opposite edges because the in-plane stresses on opposite edges need to be symmetrical. Thus the idea is to first make two conservative linear distributions and then take a non-conservative average.

The shear stress distribution along the edges of the plate field need to be matched with an equal uniform shear stress altogether. Three different approaches have been proposed.

1. The average of all real shear stress results
2. The average of all absolute real shear stress results
3. The maximum of all absolute real shear stress results

Notice that all four of the linear regression methods produce equal results for the single element mesh size models. These models provide a linearized stress distribution by definition. Not surprisingly this fact is used in available buckling analyses. However in practice it is generally not possible or desired to only have one element per field.
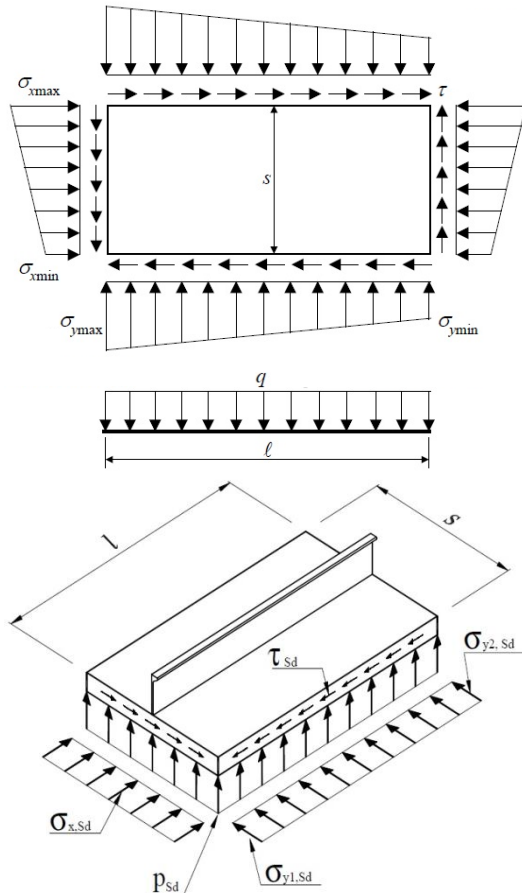
Fig. 3 Overview of the input design stresses for (a) plate buckling and (b) column buckling as defined by the standards.

The implementation methods for in-plane normal stresses and for shear stresses are individually researched. However comparing σ_X, σ_Y and τ separately is complicated since the stress gradient effect also requires a shear distribution along unloaded edges to get equilibrium in x or y direction. A uniform distribution of shear stresses is applied such that $\sum F_x = 0$, $\sum F_y = 0$ and $\sum M = 0$. The remaining shear stress may be fundamentally different in many situations. Instead of that only the complete freebodyload is in equilibrium, now each individual check becomes possible (fig 5).

Note that taking τ_B and τ_C as uniform distributed shear forces is a simplification and may not have to resemble the real distribution along the edge. However the total force should be theoretically correct.
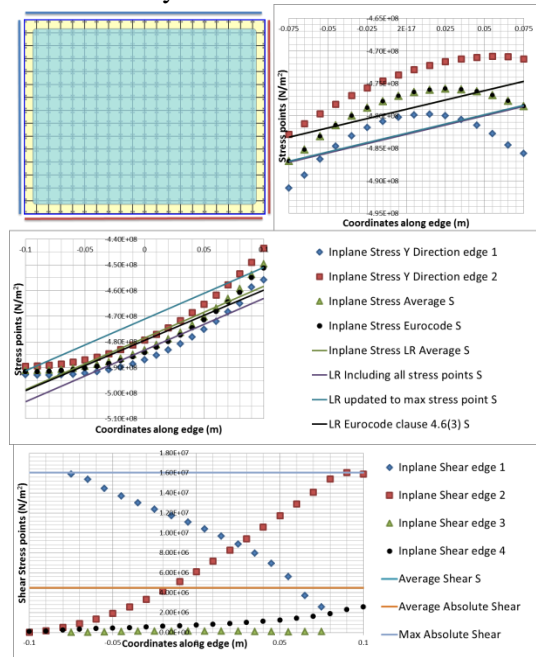
Fig. 4 Real in-plane and shear stress distributions and linearized implementation methods on a plate field for a random load cases.
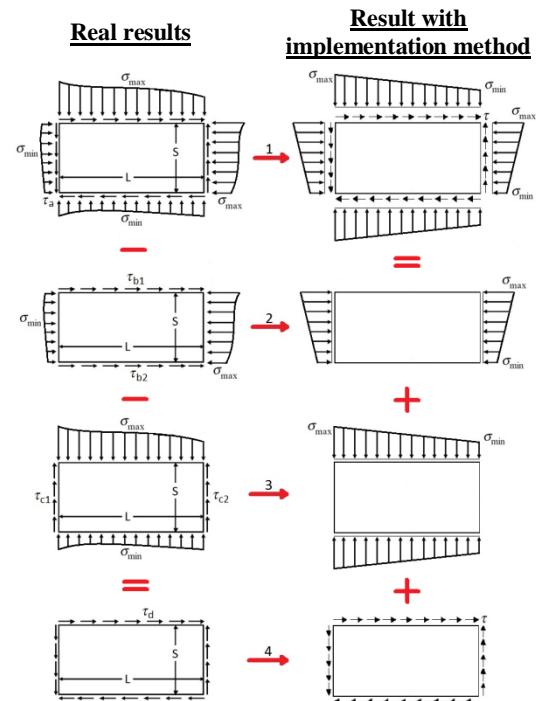
Fig. 5 Comparison checks between (a) the real stress results and (b) stresses determined by the implementation methods.

Due to the fact that the standards combine the subdivided buckling strengths for stress distributions in x-direction, y-direction and

shear as well, it makes perfect sense to divide the real stress results in these three arrangements to see whether the implementation methods are correct.

$$\left(\frac{\sigma_{xmax}}{\eta\sigma_{Cx}}\right)^2 + \left(\frac{\sigma_{ymax}}{\eta\sigma_{Cy}}\right)^2 + \left(\frac{\tau}{\eta\tau_C}\right)^2 \leq 1$$

The complete freebodyload, the two stress gradient loads and the shear load are compared to the implementation methods as showed in figures 6, 7 and 8. You can see that the overall implementation is surprisingly similar with the real stress distributions. If reviewed separately, you can see that method 1 has the least deviations, although slightly non-conservative. The other methods mostly produce far more conservative results than desired. The preferred approach as concluded from the results up to now would be to take method 4. However several situations still lead to non-conservative transformations due to the stress gradient effect. Therefore a combination of two opposite edges but slightly bigger than 60% is recommended for both the long and short edges. Overall the implementation method is considered as an allowable and good solution to transform actual stress distributions to input design stresses.

As a result of subdividing the real stresses into longitudinal stress gradient, transverse stress gradient and shear portions there can also be concluded that simply using the average of maximum shear stress is incorrect. Due to this conclusion the new proposal is to base the uniform input design shear stress on τ_D instead of τ_A to deliver more accurate and reliable values. This is left for further study.
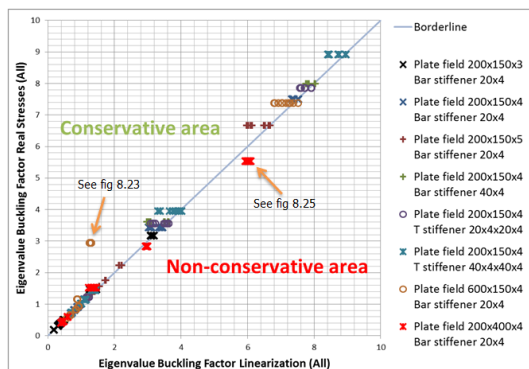
Fig. 6 Buckling factors from the eight different models for seven different load cases and twelve different implementation methods.
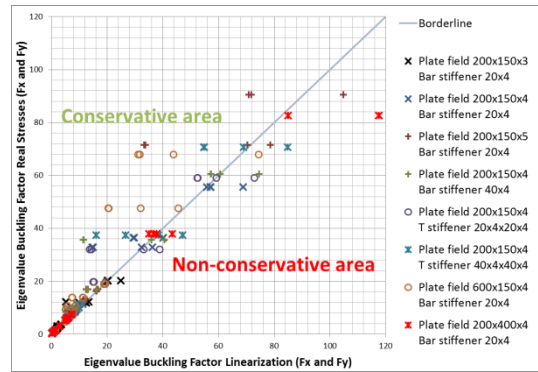
Fig. 7 Comparison of σ_X and σ_Y results.
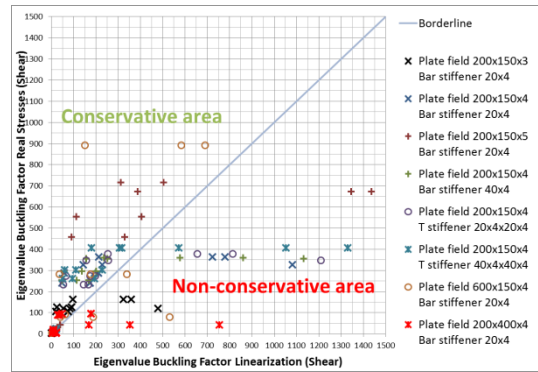
Fig. 8 Comparison of shear results.

Stiffener local buckling limit

Webs and flanges of stiffeners are checked as individual plate fields equal to the previous chapter in case the stiffeners are modeled with plate elements. However, beam elements cannot give any results for local buckling in finite element packages (fig 9). Therefore a conversion method to get the five input design stresses σ_{Xmax}, σ_{Xmin}, σ_{Ymax}, σ_{Ymin} and τ is formed.
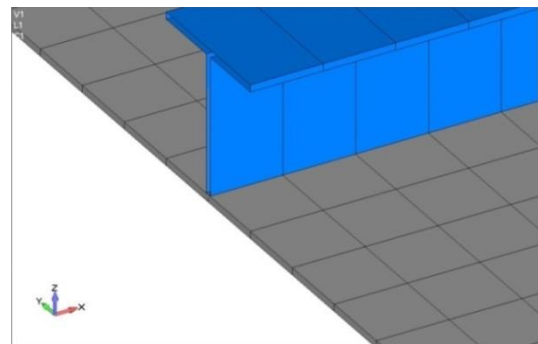
Fig. 9 Specified way of modelling plate fields and stiffeners.

Flanges cannot absorb any transverse in-plane stresses since one side has no supporting structure. That indicates that $\sigma_{Ymax} = \sigma_{Ymin} = 0$ and reduces the amount of design stresses. The remaining stresses are illustrated in figure 11.

The in-plane stresses can be calculated from combinations of the corner results (fig 10). Things are simplified with this method though. Note that some results will not be in-plane stresses but some close by corner stress results. In theory they are conservative though, so this should be a safe approximation.
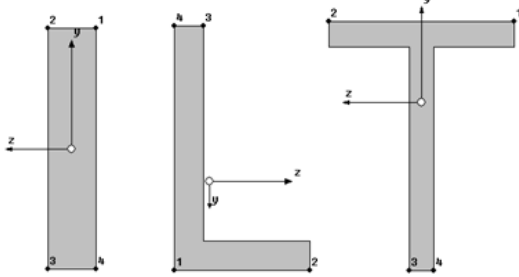
Fig. 10 Corner stress definition points for the (a) flat bar stiffener, (b) L shaped stiffener and (c) T shaped stiffener.
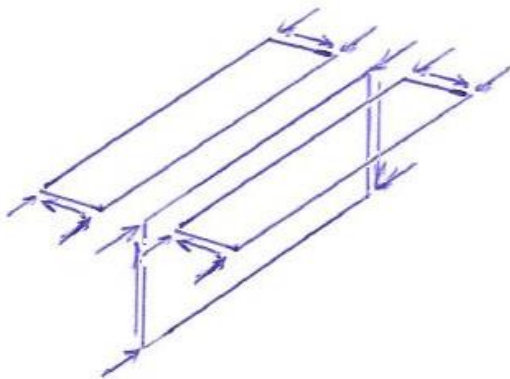
Fig. 11 Stresses in stiffener web and flanges

There is no way of defining shear results in the axial direction in beam elements. The proposal is to calculate the shear stress by taking the vertical or horizontal shear force and dividing this by the web area or the flange area. This is a large simplification as well. The real shear stresses are complicated due to the shear lag, shear loads, bending moments, torsion and even warping. However these separate shear stresses cannot be received from the results from beam elements.

The implementation method for stiffener webs and flanges is insufficiently tested and hence there is a lack of solid conclusion that can be made. However the single check shows slightly non-conservative but fairly similar and thus promising results.

Beam-column buckling

For the stiffener-plate combination the input design stresses are divided by allowable, critical stresses. These are defined by the Euler buckling strength and correction factors such as the Perry-Robertson correction, Johnson-Ostenfeld correction, the effective width method and the magnification factor.

ABS

$$\frac{\sigma_a}{f(\sigma_0, \sigma_E)}\left(\frac{A}{A_e}\right) + \frac{\sigma_b}{f(\sigma_0, \sigma_E)}\left(\frac{1}{\left(1 - \frac{\sigma_x}{\eta \sigma_E}\right)}\right) \leq 1$$

$\underbrace{\qquad}_{\text{Uniform axial load}}$ $\underbrace{\qquad}_{\text{Bending moment}}$

DNV

$$\frac{\sigma_a}{f(\sigma_0, \sigma_E, \sigma_T)}\left(\frac{A}{A_e}\right) + \frac{\sigma_b}{f(\sigma_0, \sigma_E, \sigma_T)}\left(\frac{1}{\left(1 - \frac{\sigma_x \cdot A}{\sigma_E \cdot A_e}\right)}\right) + \left(\frac{\tau_c}{f(\sigma_0)}\right)^2 \leq 1$$

$\underbrace{\qquad}_{\text{Uniform axial load}}$ $\underbrace{\qquad}_{\text{Bending moment}}$ $\underbrace{\qquad}_{\text{Shear stress}}$

σ_a = Uniform stress in x direction
σ_b = The maximum stress only resulting from the bending moment
σ_0 = Yield material strength
σ_E = Euler buckling strength
σ_T = Torsional buckling strength
τ_c = Shear stress over the associated plating in the column
η = Safety factor defined in the standards

You can see the clear distinction between the uniform axial load, the bending moment and the shear stress. Both the ABS and DNV codes use the nominal calculated compressive stress and a bending stress around the y axis using full width of associated plating. For all details see the ABS and the DNV standards.

The ABS literally speaks of the "the bending stress due to the maximum bending moment induced by the lateral loads" while the DNV also implements an eccentricity of the axial pressure. They both make use of the forget-me-not's to define the axial stress:

$$\sigma_b = \frac{M_{max}}{W_{min}} = \frac{M_{max} \cdot z}{I_e}$$

$$M_{max} = \frac{q_{Sd} \cdot l^2}{12} \ or \ M_{max} = \frac{q_{Sd} \cdot l^2}{24} \ or \ M_{max} = \frac{q_{Sd} \cdot l^2}{8}$$

It results in a distinction between boundary constraints, continuous (fixed at the ends) and Sniped (simply supported at the ends). Firstly this is not very realistic since the boundary condition of the stiffener-plate combination is neither simply supported nor fixed and secondly it is in reality difficult to accurately specify the lateral load.
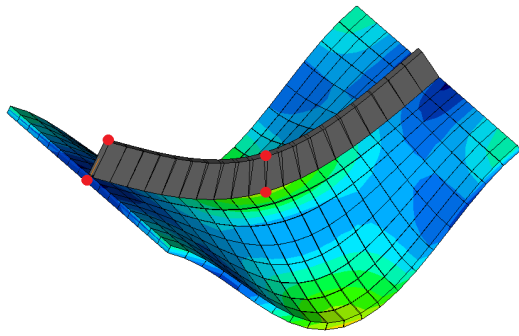
Fig. 12 The use of the forget-me-not's result in a check of present stresses in four theoretical points in the beam-column as where you could actually check your model along the entire length.

Instead the proposal is to use actual axial stress results from the model (fig 13) which has the consequence that also the difficulties above become redundant. Hereby a by-pass of defining several parameters in the standards can be made including the eccentricity of the axial load, the lateral load, the use of for-get-me-not's and the choice of boundary conditions. In the present study only the axial pressure is analyzed from the input design stresses F_X, M_Y, τ_C and σ_Y. The proposed implementation method contains an extrapolation of the lower two corner stress results in the beam elements (fig 14).

The simplification does however not meet the expectations. Considering only results from the beam elements is insufficient to base the associated plate fields on as the stress results in the stiffener do not match results in the associated plates at the place of attachment (fig 15).
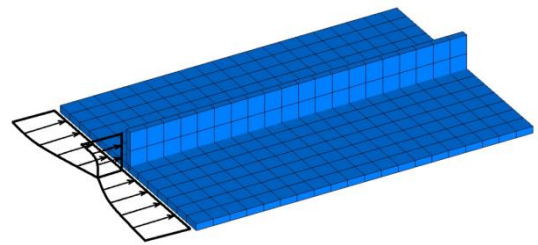
Fig. 13 An exaggerated impression of the in-plane stresses in a beam-column for a random load case.
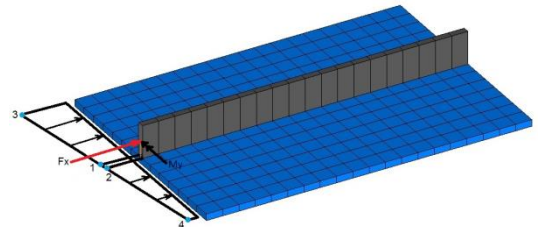
Fig. 14 The proposed implementation method to define the axial in-plane stresses in the associated plate fields.
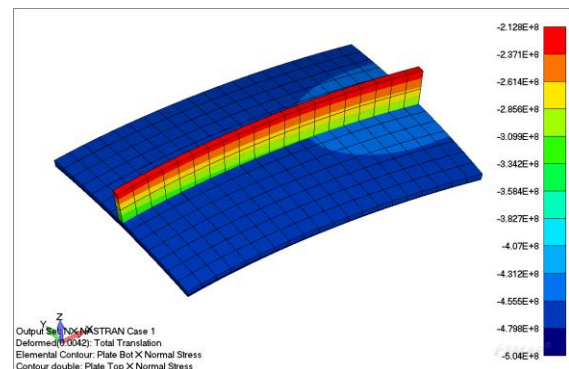
Fig. 15 The stress results in the stiffener are significantly different from results in the associated plates at the place of attachment.

References

[1] J. M. Gordo en C. G. Soares (2009), „Tests on ultimate strength of hull box girders made of high tensile steel," Centre for Marine Technology and Engineering (CENTEC), Technical University of Lisbon.

[2] S. Benson (2011), „Progressive Collapse Assessment of Lightweight Ship Structures," Faculty of Sciennce, Agriculture and Engineering, Newcastle UK.

[3] American Bureau of Shipping (2013), „ABS Guide for Buckling and Ultimate strength assessment for offshore structures," American Bureau of Shipping, New York.

[4] Det Norske Veritas (2010), „Recommended Practice DNV-RP-C201 Buckling strength of plated structures," DNV.

[5] O. Hillers (2011), „Automatic buckling checks on stiffened panels based on finite element results," Faculty of Civil Engineering & Geosciences - department Structural Mechanics, Delft.

Appendix B (Plate field Real In-plane Stress Results)

Each figure represents a single Load case. (top) Normal in-plane stress on short edge of plate field, (middle) normal in-plane stress on long edge of plate field and (bottom) in-plane shear stress on all edges of the plate field. (left) General scale and (right) zoomed in.

Fig B.1 Plate model, plate01, Load case 1, Nonlinear stress results
Fig B.2 Plate model, plate01, Load case 1, Linear stress results
Fig B.3 Beam model, plate01, Load case 1, Linear stress results
Fig B.4 Beam model, plate01, Load case 2, Linear stress results
Fig B.5 Beam model, plate01, Load case 3, Linear stress results
Fig B.6 Beam model, plate01, Load case 4, Linear stress results
Fig B.7 Beam model, plate01, Load case 5, Linear stress results
Fig B.8 Beam model, plate01, Load case 6, Linear stress results
Fig B.9 Beam model, plate01, Load case 7, Linear stress results
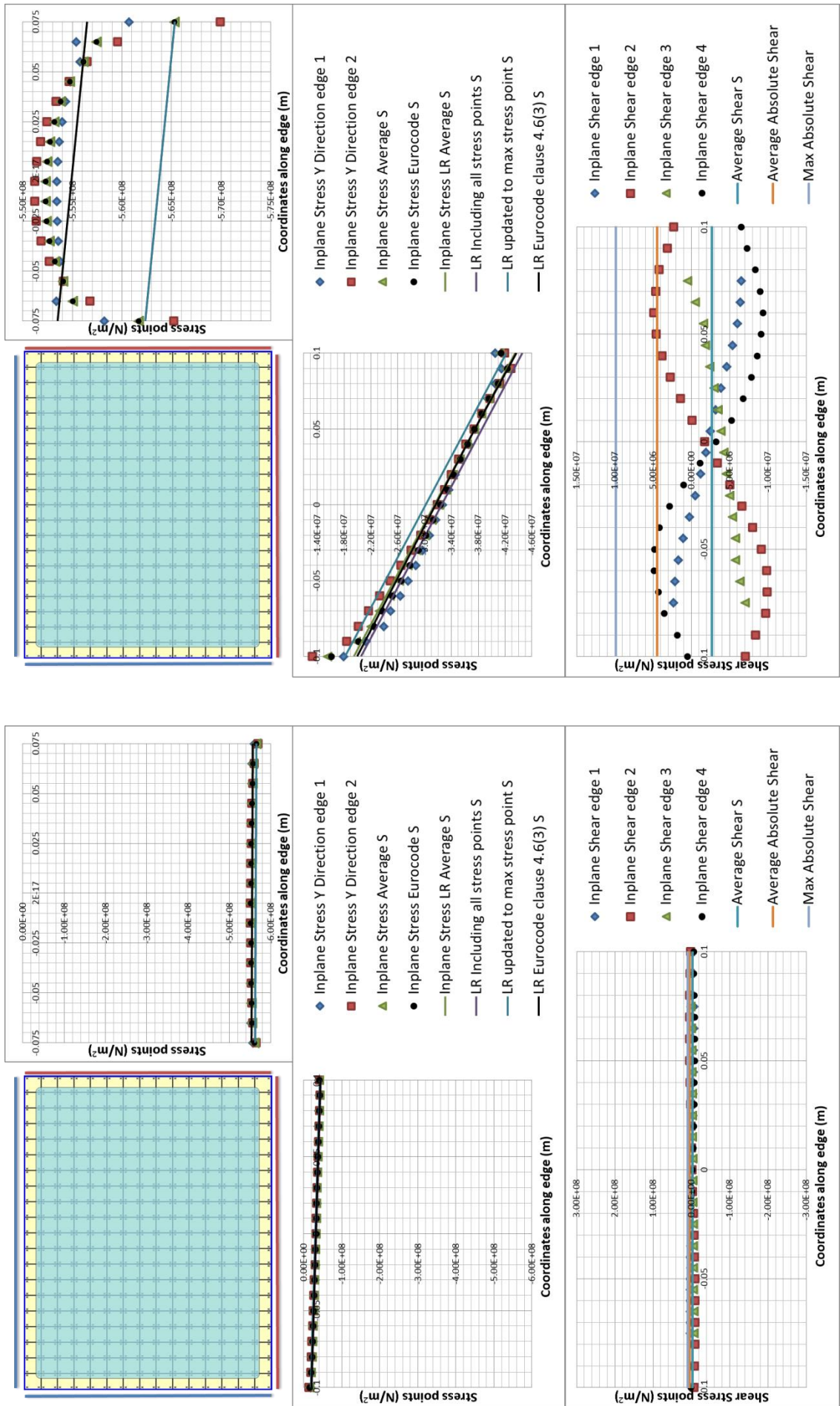
Fig B.1 Plate model, Load case 1, Nonlinear stress results
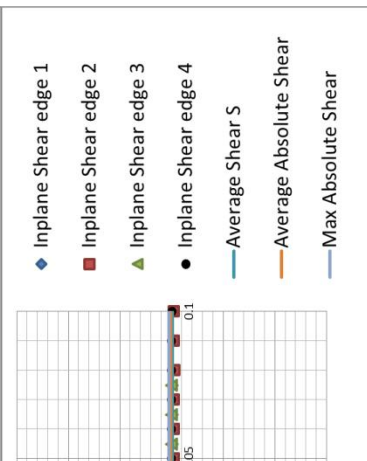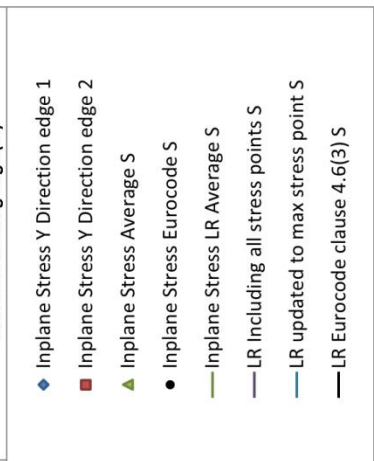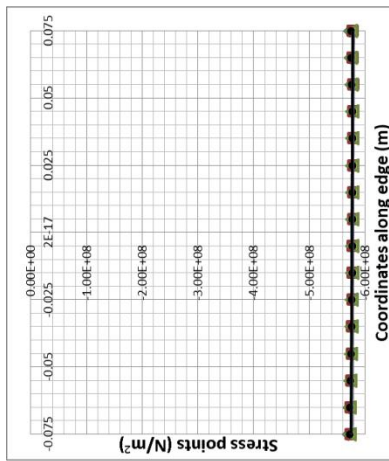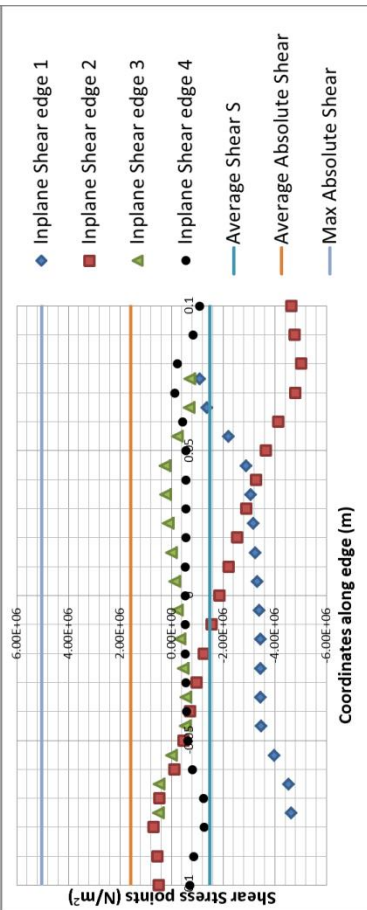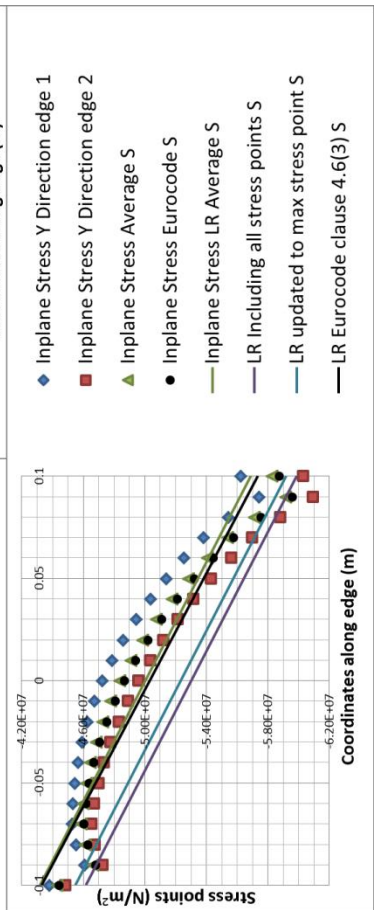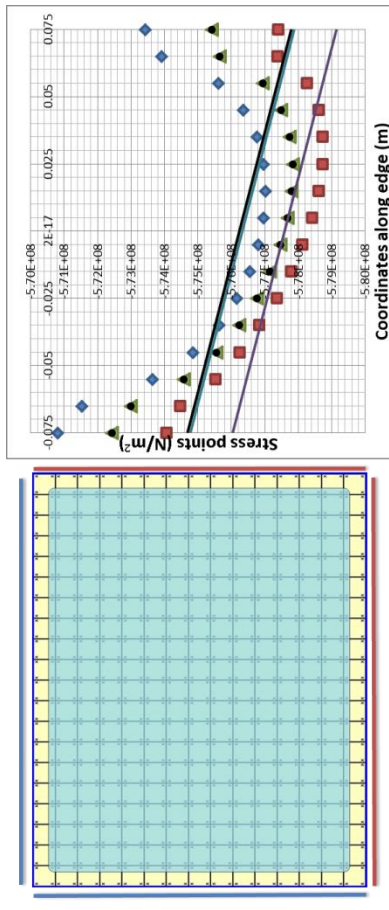
Fig B.2 Plate model, Load case 1, Linear stress results
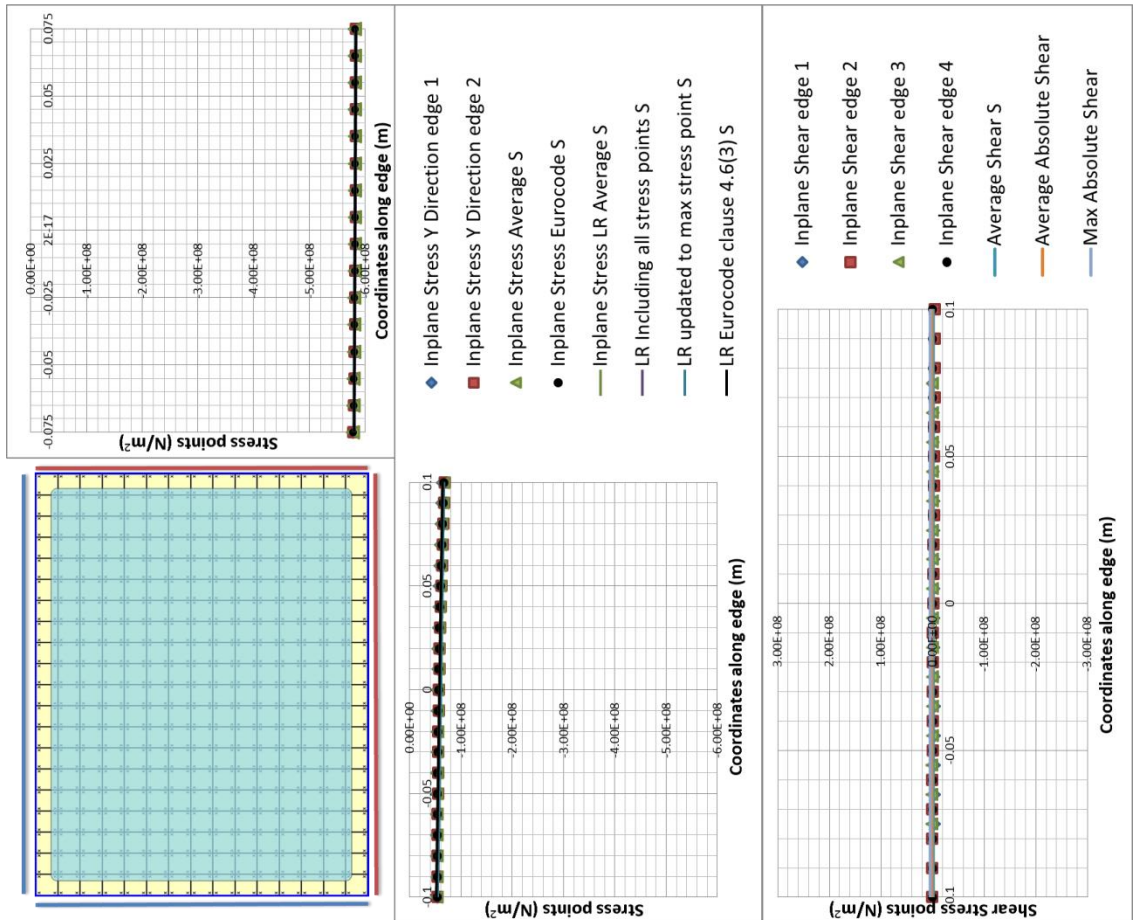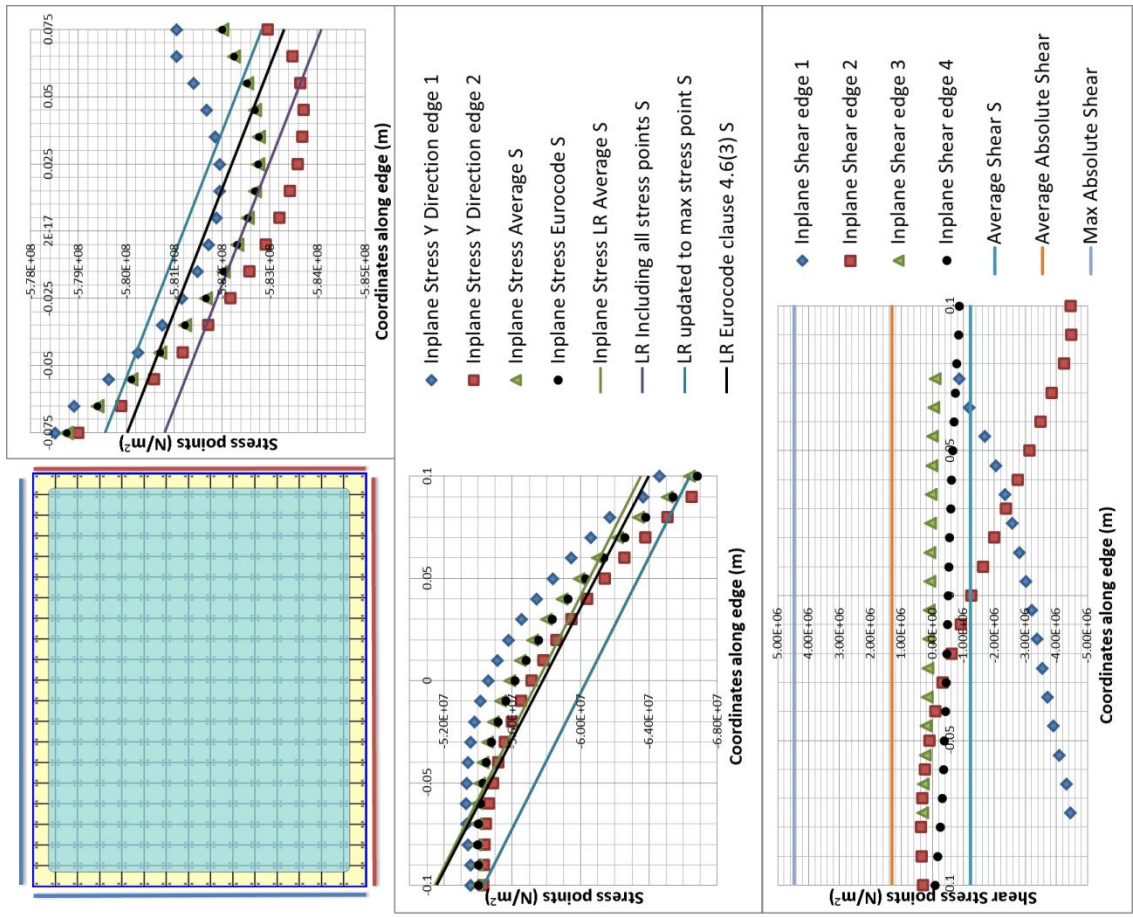
Fig B.3 Beam model, Load case 1, Linear stress results
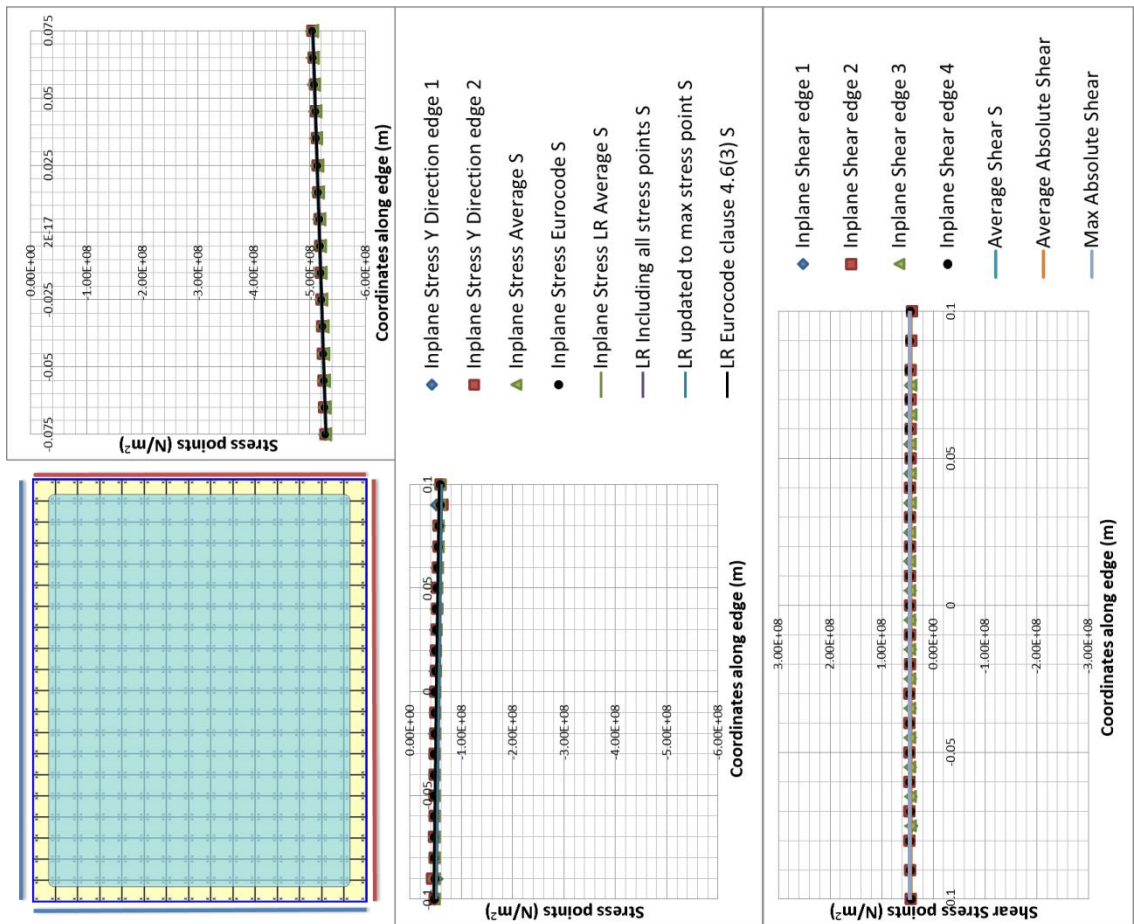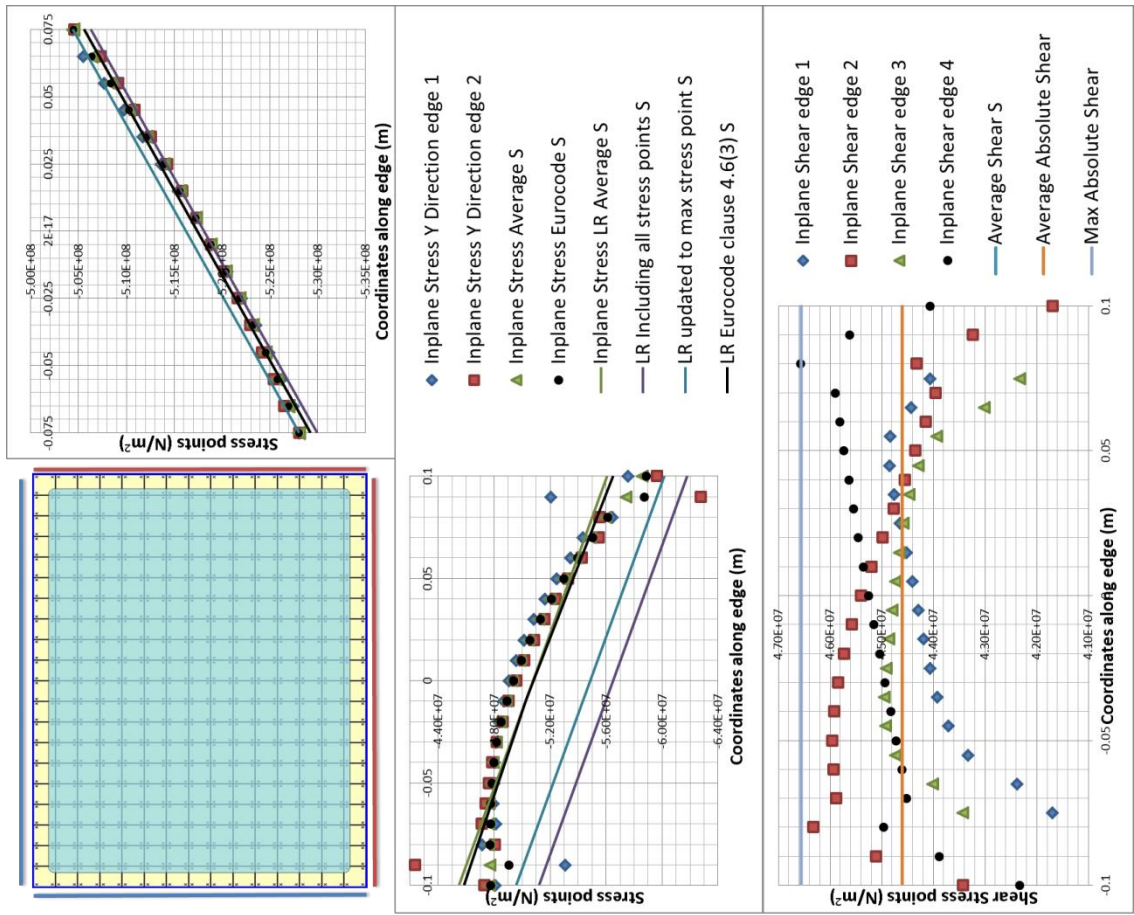
Fig B.4 Beam model, Load case 2, Linear stress results

Fig B.5 Beam model, Load case 3, Linear stress results

Fig B.6 Beam model, Load case 4, Linear stress results

Fig B.7 Beam model, Load case 5, Linear stress results
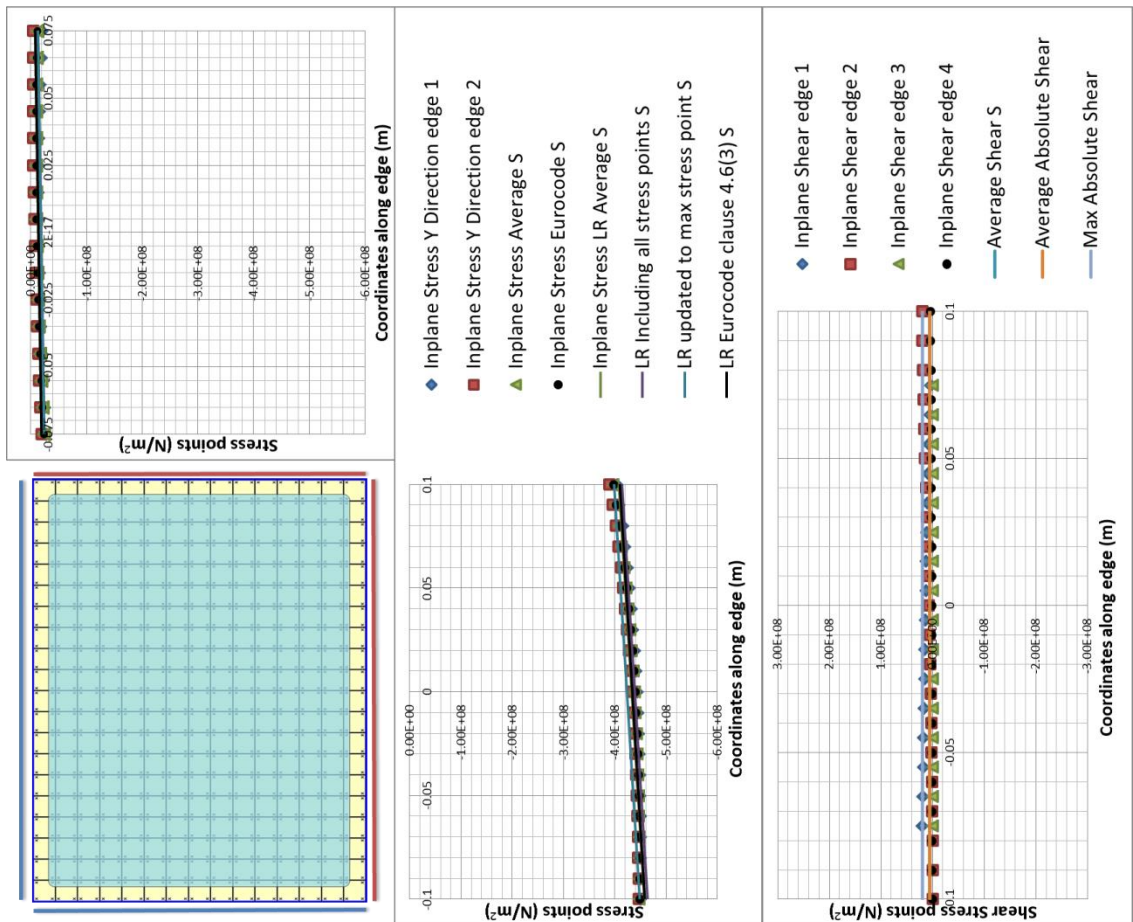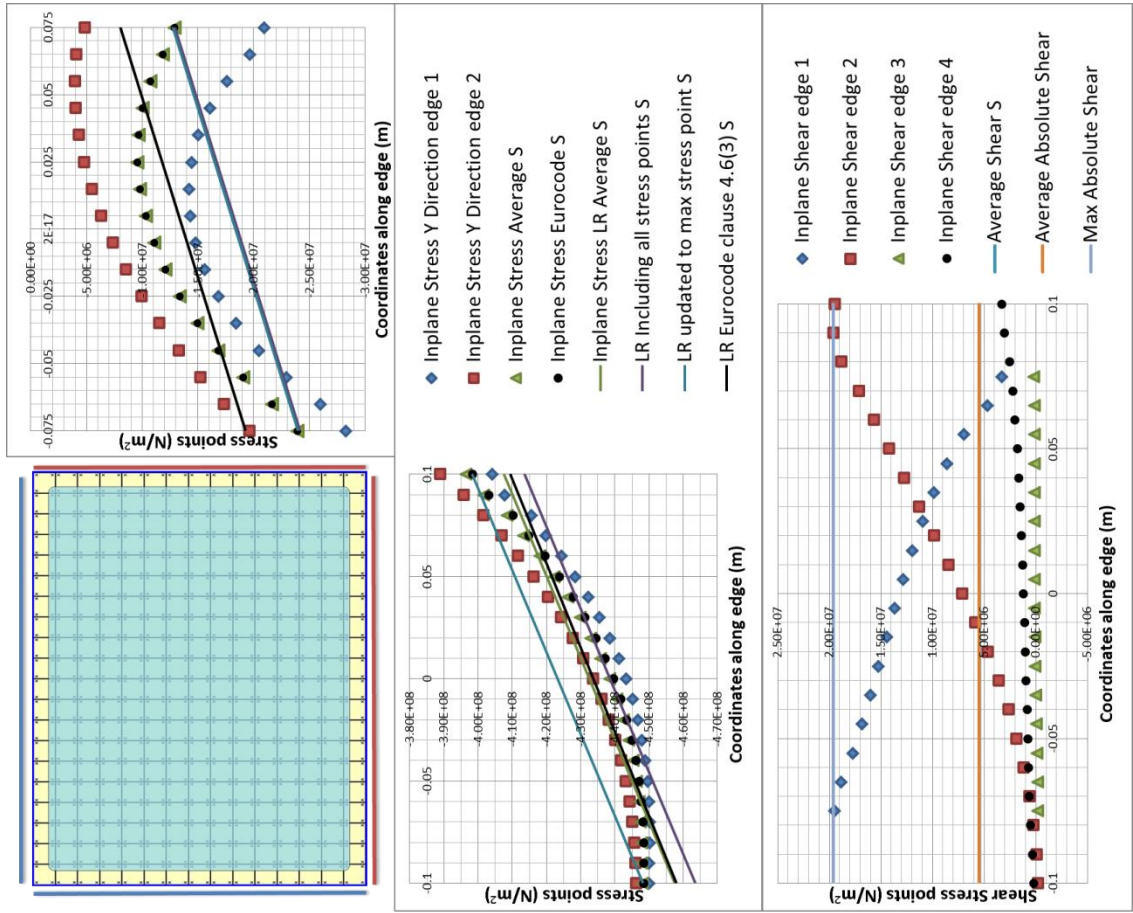
Fig B.8 Beam model, Load case 6, Linear stress results
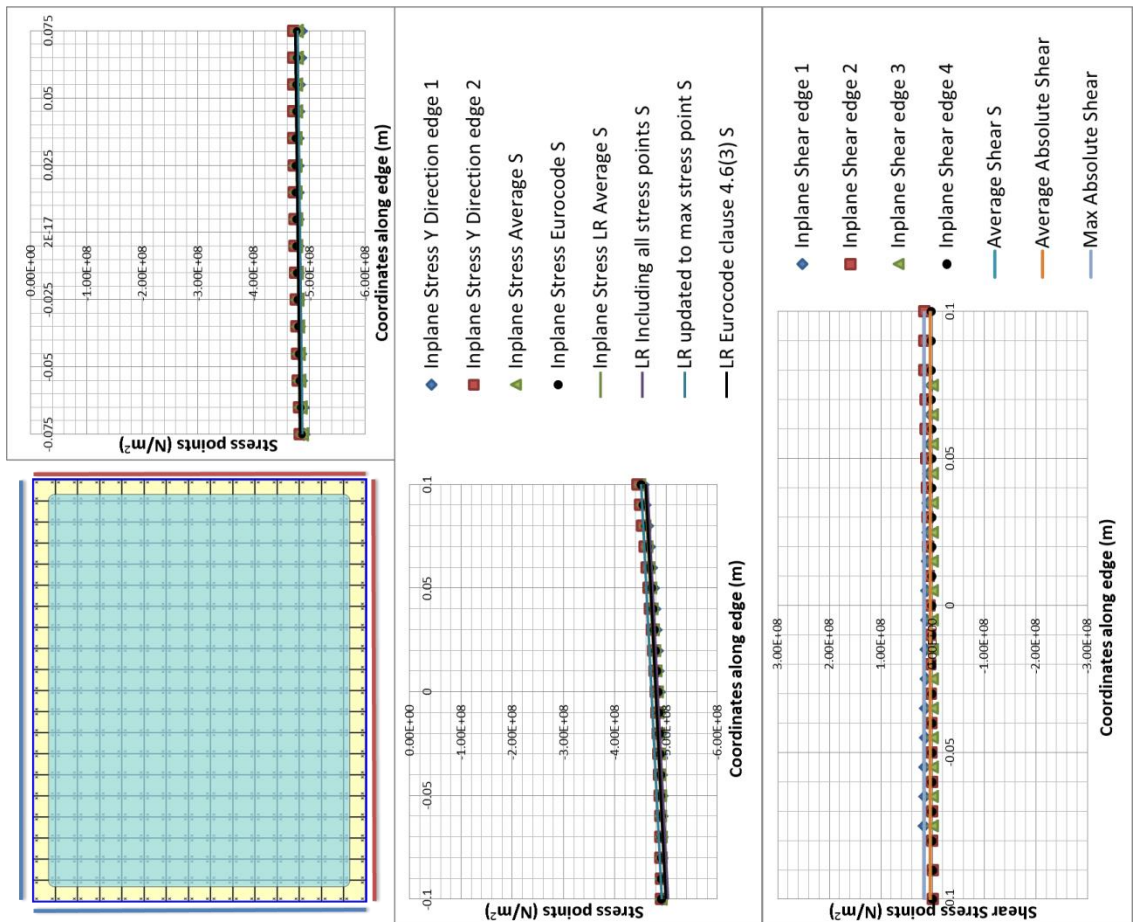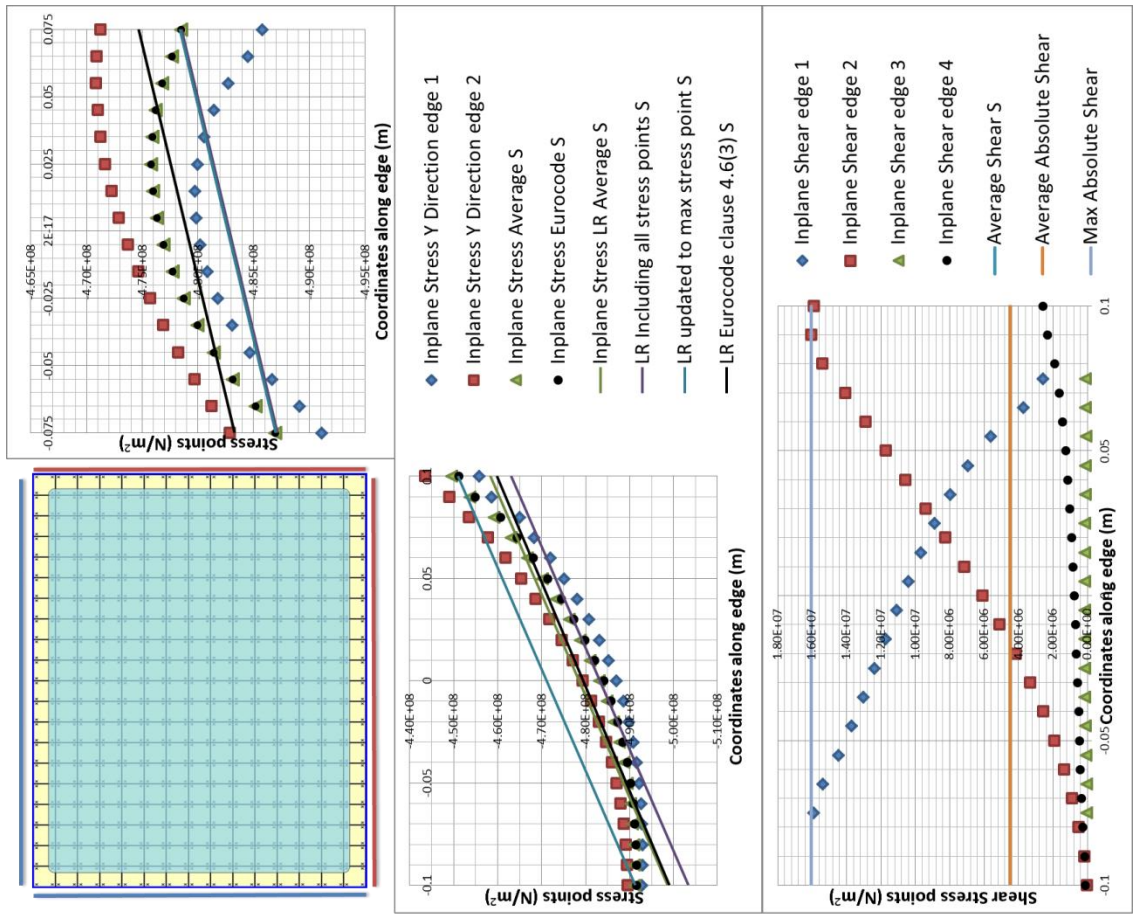
Fig B.9 Beam model, Load case 7, Linear stress results

Appendix C (Plate field comparison Mesh Sizes)

Fig C.1 Beam model, plate01, Load case 1, Linear results, mesh size comparison

Fig C.2 Beam model, plate01, Load case 2, Linear results, mesh size comparison

Fig C.3 Beam model, plate01, Load case 3, Linear results, mesh size comparison

Fig C.4 Beam model, plate01, Load case 4, Linear results, mesh size comparison

Fig C.5 Beam model, plate01, Load case 5, Linear results, mesh size comparison

Fig C.6 Beam model, plate01, Load case 6, Linear results, mesh size comparison

Fig C.7 Beam model, plate01, Load case 7, Linear results, mesh size comparison
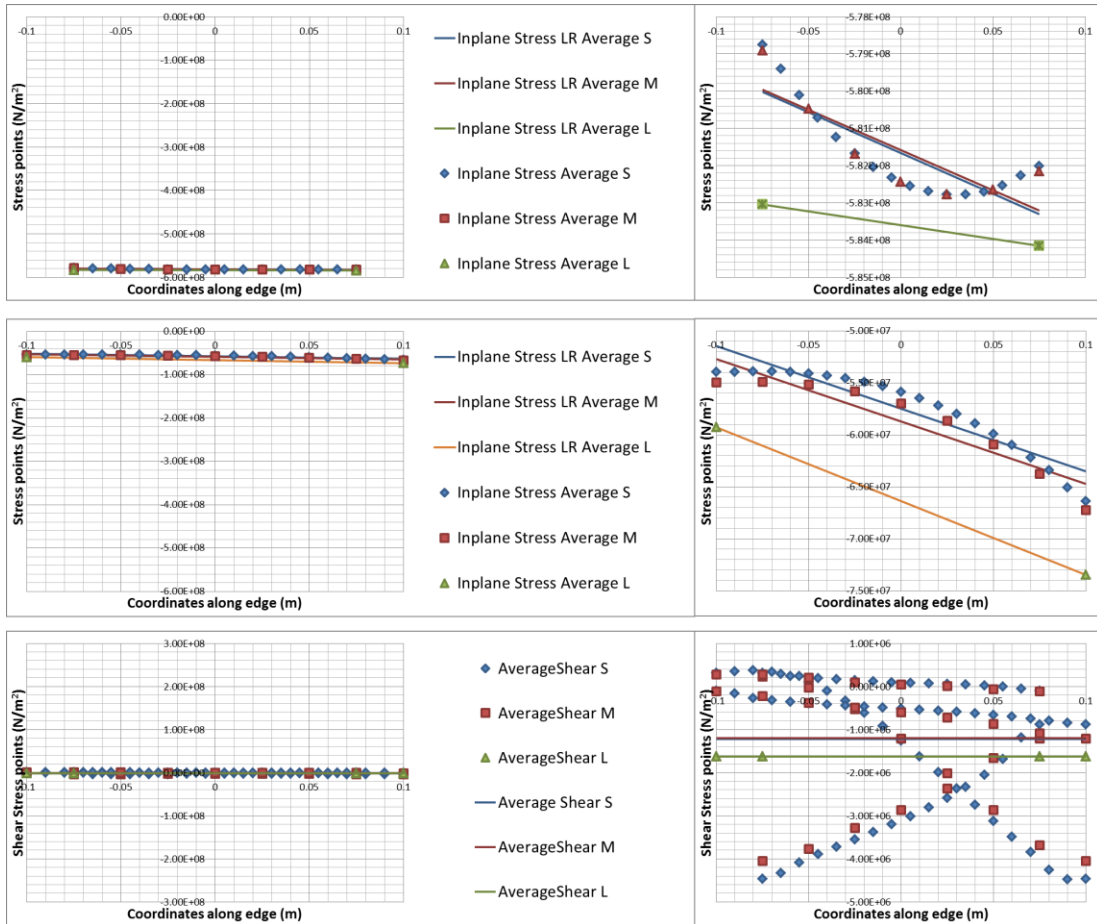
Fig C.1 Beam model, Load case 1, Linear results, mesh size comparison
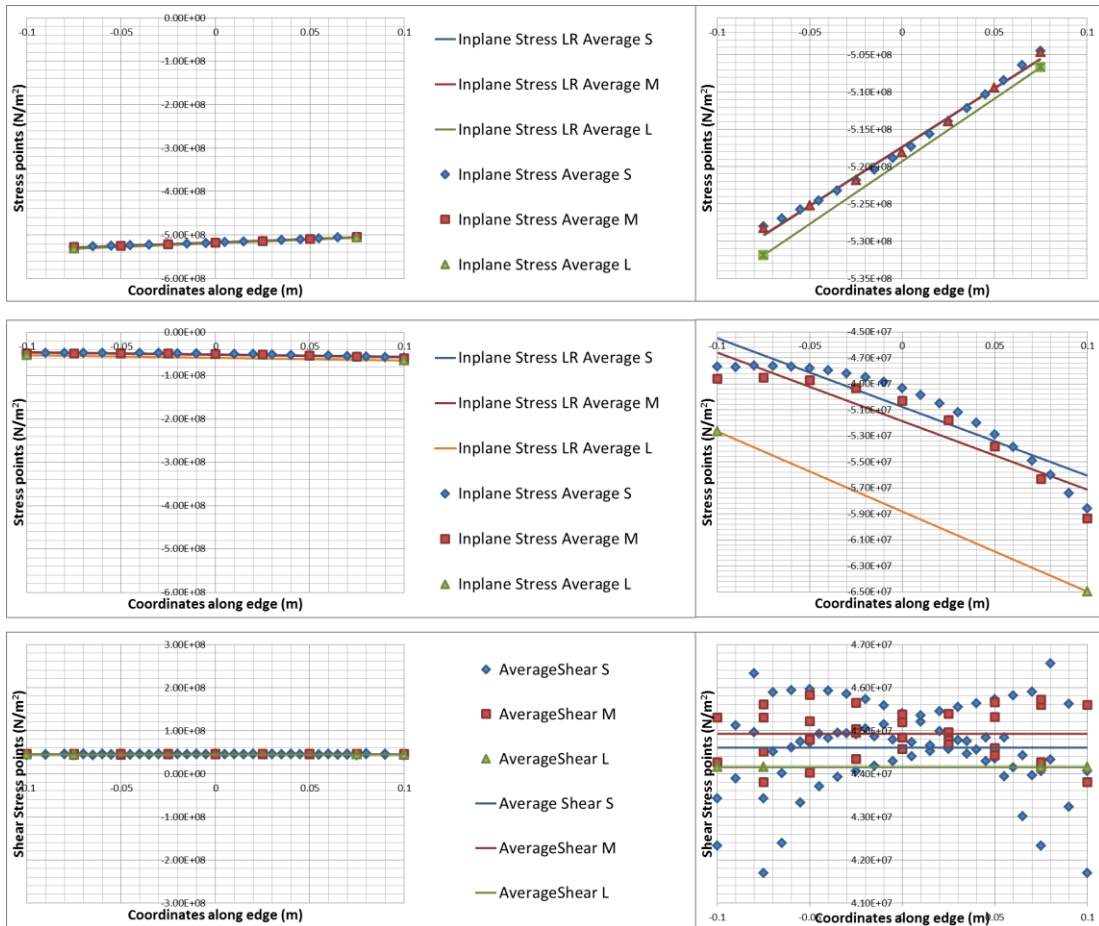
Fig C.2 Beam model, Load case 2, Linear results, mesh size comparison
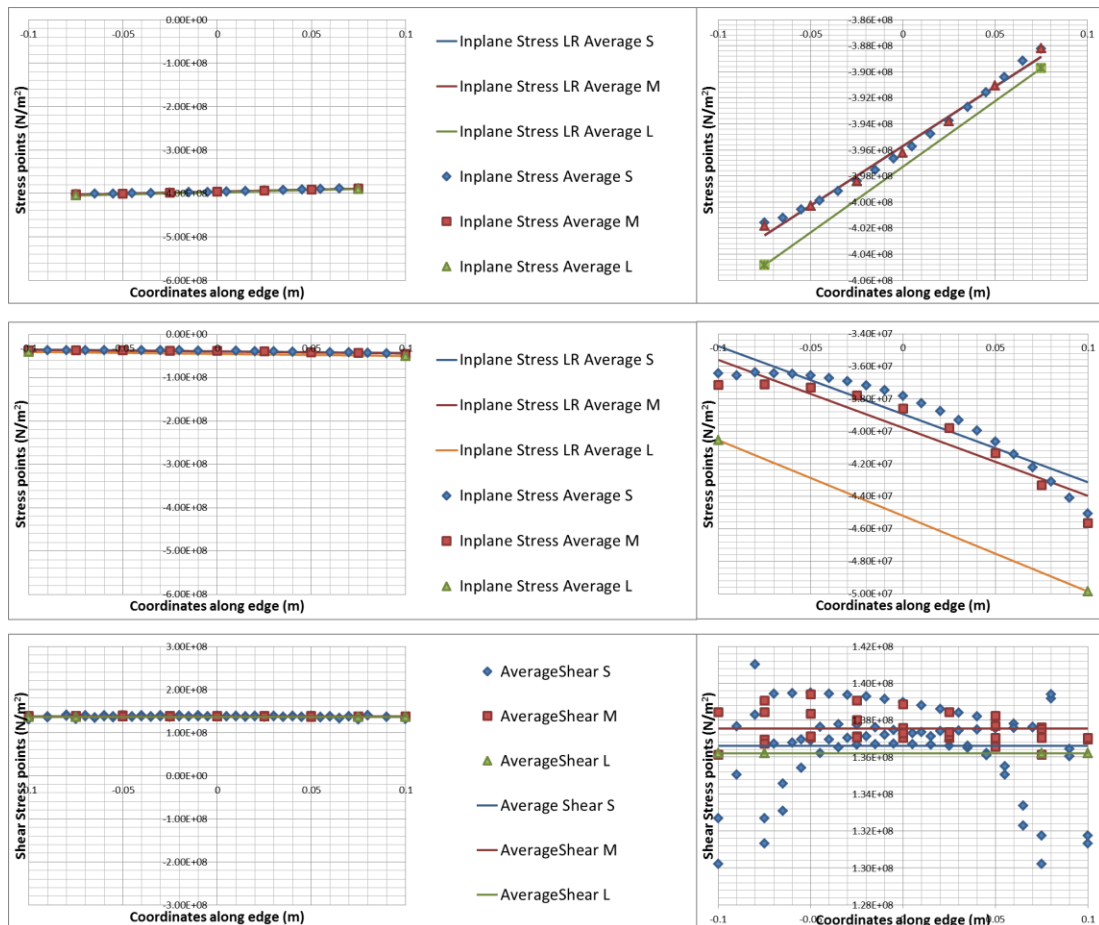
Fig C.3 Beam model, Load case 3, Linear results, mesh size comparison
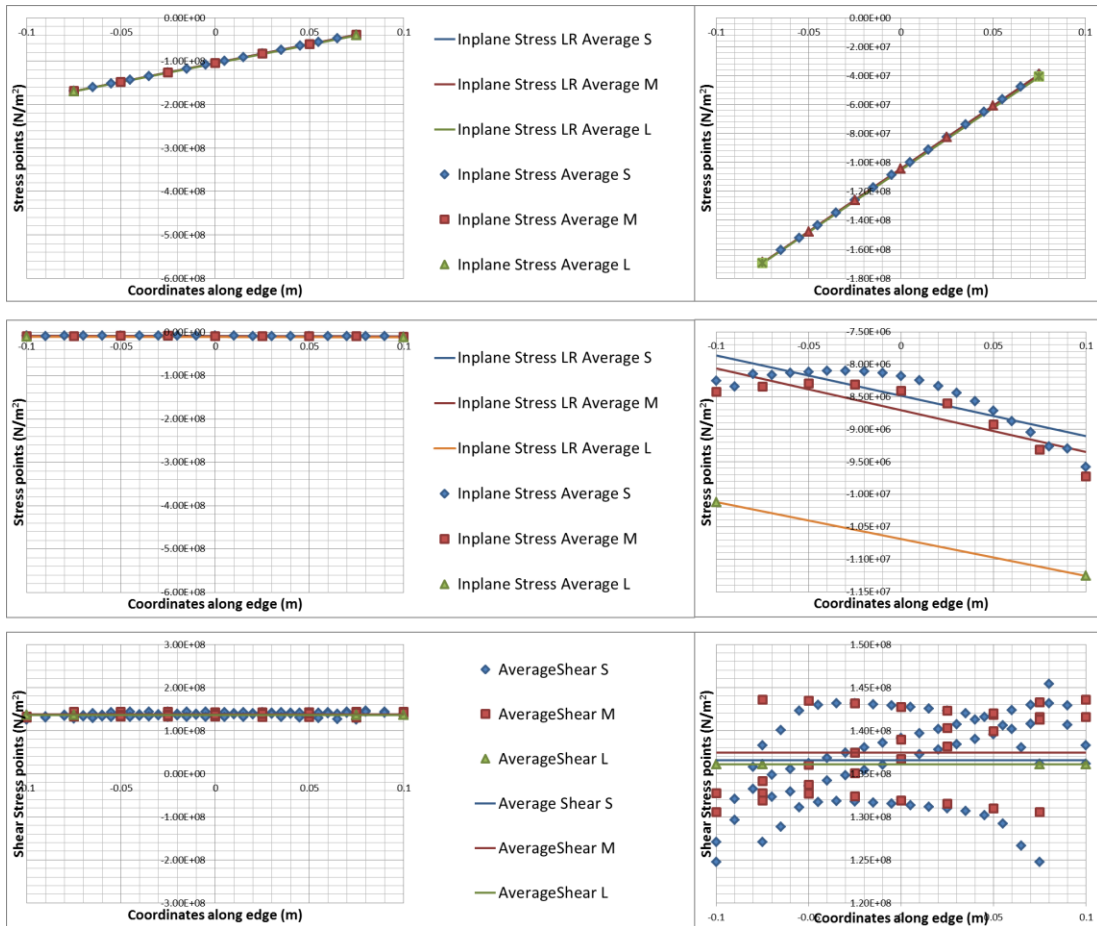
Fig C.4 Beam model, Load case 4, Linear results, mesh size comparison

Fig C.5 Beam model, Load case 5, Linear results, mesh size comparison

Fig C.6 Beam model, Load case 6, Linear results, mesh size comparison

Fig C.7 Beam model, Load case 7, Linear results, mesh size comparison

Appendix D (Plate field Design Stresses)

Illustration of results produced while analyzing the implementation methods for different mesh sizes.

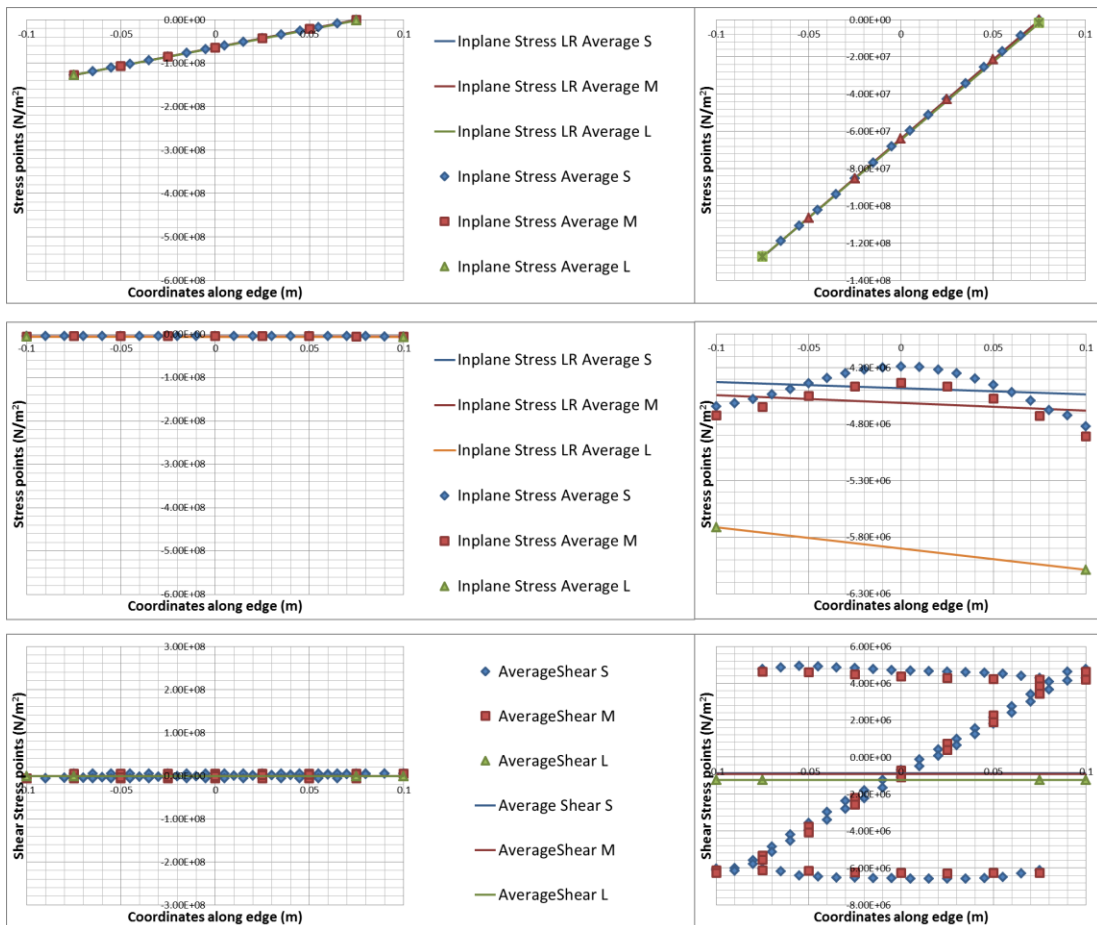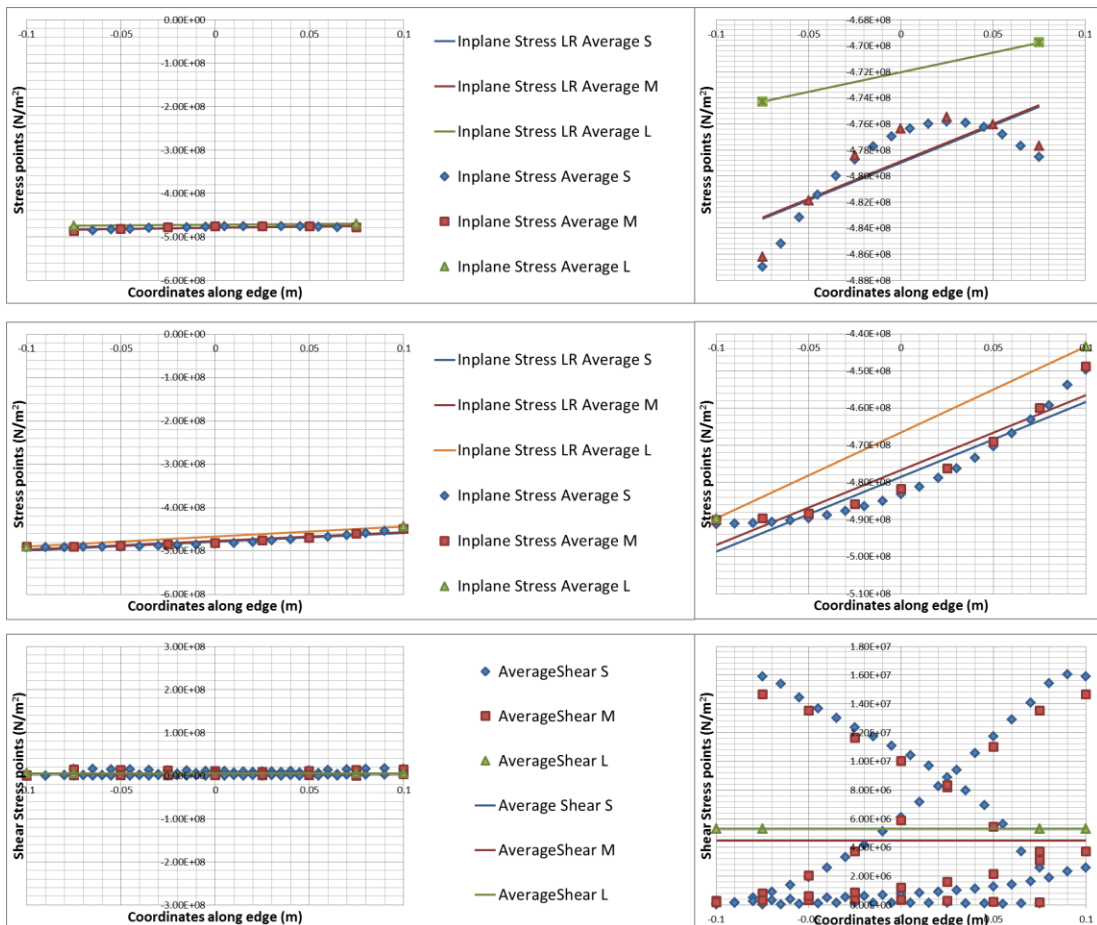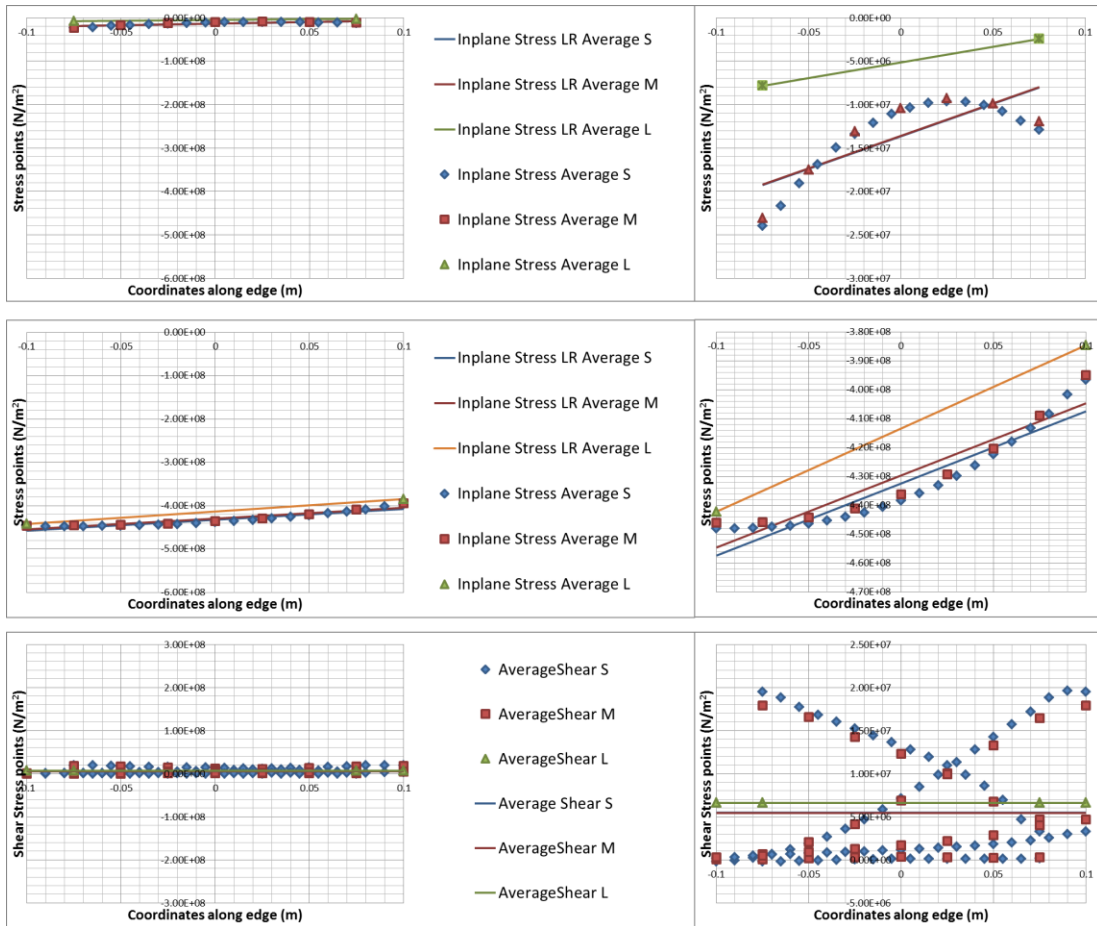| Plate field 200x150x4 Bar stiffener 20x4			σxmax	σxmin	σymax	σymin	difference with single element mesh			
Load case 1	Fine mesh size	LR average	5.8330E+08	5.8002E+08	6.3517E+07	5.1461E+07	-0.15%	-0.52%	-13.55%	-13.18%
0.15.0	Fine mesh size	LR average + update	5.8284E+08	5.7955E+08	6.6382E+07	5.4326E+07	-0.23%	-0.60%	-9.65%	-8.35%
	Fine mesh size	LR average + include	5.8408E+08	5.8080E+08	6.6382E+07	5.4326E+07	-0.01%	-0.38%	-9.65%	-8.35%
	Fine mesh size	LR Eurocode	5.8330E+08	5.8002E+08	6.3974E+07	5.1569E+07	-0.15%	-0.52%	-12.93%	-13.00%
	Coarse mesh size	LR average	5.8321E+08	5.7996E+08	6.4724E+07	5.2712E+07	-0.16%	-0.53%	-11.91%	-11.07%
	Coarse mesh size	LR average + update	5.8283E+08	5.7958E+08	6.7242E+07	5.5231E+07	-0.23%	-0.59%	-8.48%	-6.82%
	Coarse mesh size	LR average + include	5.8406E+08	5.8081E+08	6.7242E+07	5.5231E+07	-0.02%	-0.38%	-8.48%	-6.82%
	Coarse mesh size	LR Eurocode	5.8321E+08	5.7996E+08	6.5135E+07	5.2804E+07	-0.16%	-0.53%	-11.35%	-10.91%
	Single element mesh size	LR average	5.8415E+08	5.8304E+08	7.3475E+07	5.9273E+07				
Load case 2	Fine mesh size	LR average	5.2925E+08	5.0556E+08	5.6067E+07	4.5487E+07	-0.50%	-0.22%	-13.73%	-13.63%
2.13.2	Fine mesh size	LR average + update	5.2806E+08	5.0438E+08	6.0154E+07	4.9574E+07	-0.72%	-0.45%	-7.44%	-5.87%
	Fine mesh size	LR average + include	5.2995E+08	5.0626E+08	6.1788E+07	5.1208E+07	-0.37%	-0.08%	-4.92%	-2.77%
	Fine mesh size	LR Eurocode	5.2925E+08	5.0556E+08	5.6493E+07	4.5846E+07	-0.50%	-0.22%	-13.07%	-12.95%
	Coarse mesh size	LR average	5.2917E+08	5.0550E+08	5.7148E+07	4.6594E+07	-0.51%	-0.23%	-12.06%	-11.52%
	Coarse mesh size	LR average + update	5.2822E+08	5.0455E+08	5.9370E+07	4.8817E+07	-0.69%	-0.42%	-8.64%	-7.31%
	Coarse mesh size	LR average + include	5.2992E+08	5.0625E+08	5.9404E+07	4.8851E+07	-0.37%	-0.08%	-8.59%	-7.24%
	Coarse mesh size	LR Eurocode	5.2917E+08	5.0550E+08	5.7337E+07	4.6743E+07	-0.51%	-0.23%	-11.77%	-11.24%
	Single element mesh size	LR average	5.3191E+08	5.0666E+08	6.4986E+07	5.2664E+07				
Load case 3	Fine mesh size	LR average	4.0257E+08	3.8886E+08	4.3133E+07	3.4756E+07	-0.56%	-0.22%	-13.50%	-14.27%
6.10.1	Fine mesh size	LR average + update	4.0235E+08	3.8864E+08	5.5505E+07	4.7128E+07	-0.62%	-0.28%	11.32%	16.24%
	Fine mesh size	LR average + include	4.0321E+08	3.8951E+08	5.6622E+07	4.8245E+07	-0.40%	-0.05%	13.56%	19.00%
	Fine mesh size	LR Eurocode	4.0257E+08	3.8886E+08	4.4063E+07	3.5533E+07	-0.56%	-0.22%	-11.63%	-12.36%
	Coarse mesh size	LR average	4.0253E+08	3.8882E+08	4.3971E+07	3.5602E+07	-0.57%	-0.23%	-11.82%	-12.19%
	Coarse mesh size	LR average + update	4.0184E+08	3.8813E+08	4.5654E+07	3.7285E+07	-0.74%	-0.41%	-8.44%	-8.03%
	Coarse mesh size	LR average + include	4.0307E+08	3.8936E+08	4.6018E+07	3.7649E+07	-0.44%	-0.09%	-7.71%	-7.14%
	Coarse mesh size	LR Eurocode	4.0253E+08	3.8882E+08	4.4233E+07	3.5752E+07	-0.57%	-0.23%	-11.29%	-11.82%
	Single element mesh size	LR average	4.0484E+08	3.8972E+08	4.9863E+07	4.0543E+07				
Load case 4	Fine mesh size	LR average	1.6940E+08	3.9064E+07	9.1048E+06	7.8627E+06	-0.13%	-4.31%	-19.11%	-22.30%
6.1.10	Fine mesh size	LR average + update	1.6892E+08	3.8590E+07	2.1151E+07	1.9909E+07	-0.41%	-5.47%	87.91%	96.75%
	Fine mesh size	LR average + include	1.7057E+08	4.0235E+07	2.1442E+07	2.0200E+07	0.56%	-1.44%	90.49%	99.62%
	Fine mesh size	LR Eurocode	1.6940E+08	3.9064E+07	9.6216E+06	9.4112E+06	-0.13%	-4.31%	-14.52%	-7.00%
	Coarse mesh size	LR average	1.6927E+08	3.9153E+07	9.3481E+06	8.0630E+06	-0.20%	-4.09%	-16.95%	-20.32%
	Coarse mesh size	LR average + update	1.6896E+08	3.8844E+07	1.0270E+07	8.9850E+06	-0.38%	-4.85%	-8.76%	-11.21%
	Coarse mesh size	LR average + include	1.6946E+08	3.9342E+07	1.0623E+07	9.3380E+06	-0.09%	-3.63%	-5.62%	-7.72%
	Coarse mesh size	LR Eurocode	1.6927E+08	3.9153E+07	1.0215E+07	9.1224E+06	-0.20%	-4.09%	-9.25%	-9.85%
	Single element mesh size	LR average	1.6961E+08	4.0822E+07	1.1256E+07	1.0119E+07				
Load case 5	Fine mesh size	LR average	1.2760E+08	2.0287E+05	4.5353E+06	4.4260E+06	0.21%	-88.54%	-25.49%	-22.50%
0.0.10	Fine mesh size	LR average + update	1.2731E+08	8.0745E+04	5.4477E+06	5.3384E+06	-0.01%	-95.44%	-10.51%	-6.53%
	Fine mesh size	LR average + include	1.2772E+08	3.2214E+05	5.4499E+06	5.3407E+06	0.31%	-81.80%	-10.47%	-6.49%
	Fine mesh size	LR Eurocode	1.2760E+08	2.0287E+05	5.6040E+06	5.4449E+06	0.21%	-88.54%	-7.94%	-4.66%
	Coarse mesh size	LR average	1.2746E+08	2.8604E+05	4.6791E+06	4.5421E+06	0.11%	-83.84%	-23.13%	-20.47%
	Coarse mesh size	LR average + update	1.2719E+08	1.7745E+04	4.9757E+06	4.8386E+06	-0.11%	-99.00%	-18.26%	-15.28%
	Coarse mesh size	LR average + include	1.2763E+08	4.5501E+05	4.9833E+06	4.8462E+06	0.24%	-74.29%	-18.14%	-15.14%
	Coarse mesh size	LR Eurocode	1.2746E+08	2.8604E+05	5.6581E+06	5.4912E+06	0.11%	-83.84%	-7.05%	-3.85%
	Single element mesh size	LR average	1.2733E+08	1.7697E+06	6.0872E+06	5.7111E+06				
Load case 6	Fine mesh size	LR average	1.9265E+07	8.0314E+06	4.5746E+08	4.0749E+08	145.36%	228.22%	3.44%	5.95%
Fy	Fine mesh size	LR average + update	2.3968E+07	1.2735E+07	4.4817E+08	3.9820E+08	205.26%	420.43%	1.34%	3.53%
	Fine mesh size	LR average + include	2.4158E+07	1.2924E+07	4.6349E+08	4.1352E+08	207.68%	428.19%	4.80%	7.52%
	Fine mesh size	LR Eurocode	1.9265E+07	8.0314E+06	4.5795E+08	4.0935E+08	145.36%	228.22%	3.55%	6.43%
	Coarse mesh size	LR average	1.9212E+07	7.9862E+06	4.5467E+08	4.0471E+08	144.68%	226.38%	2.81%	5.23%
	Coarse mesh size	LR average + update	2.3086E+07	1.1860E+07	4.4616E+08	3.9620E+08	194.02%	384.68%	0.88%	3.01%
	Coarse mesh size	LR average + include	2.3183E+07	1.1957E+07	4.6124E+08	4.1128E+08	195.25%	388.65%	4.29%	6.93%
	Coarse mesh size	LR Eurocode	1.9212E+07	7.9862E+06	4.5509E+08	4.0640E+08	144.68%	226.38%	2.90%	5.66%
	Single element mesh size	LR average	7.8518E+06	2.4469E+06	4.4225E+08	3.8461E+08				
Load case 7	Fine mesh size	LR average	4.8328E+08	4.7468E+08	4.9863E+08	4.5831E+08	1.90%	1.04%	1.83%	3.36%
0.15.0 + Fy	Fine mesh size	LR average + update	4.8697E+08	4.7837E+08	4.9126E+08	4.5093E+08	2.67%	1.83%	0.32%	1.70%
	Fine mesh size	LR average + include	4.8713E+08	4.7853E+08	5.0336E+08	4.6303E+08	2.71%	1.86%	2.80%	4.43%
	Fine mesh size	LR Eurocode	4.8328E+08	4.7468E+08	4.9903E+08	4.5980E+08	1.90%	1.04%	1.91%	3.70%
	Coarse mesh size	LR average	4.8318E+08	4.7455E+08	4.9684E+08	4.5649E+08	1.88%	1.02%	1.47%	2.95%
	Coarse mesh size	LR average + update	4.8622E+08	4.7759E+08	4.9008E+08	4.4972E+08	2.52%	1.66%	0.08%	1.43%
	Coarse mesh size	LR average + include	4.8631E+08	4.7768E+08	5.0202E+08	4.6167E+08	2.53%	1.68%	2.52%	4.12%
	Coarse mesh size	LR Eurocode	4.8318E+08	4.7455E+08	4.9718E+08	4.5785E+08	1.88%	1.02%	1.54%	3.26%
	Single element mesh size	LR average	4.7429E+08	4.6977E+08	4.8967E+08	4.4339E+08				

Table D.1 In-plane Stress results of the plate field after applying the implementation method for the beam model in the three different mesh sizes of model 2.

	Plate field 200x150x4 Bar stiffener 20x4		τ	difference with single element mesh
Load case 1 0.15.0	Fine mesh size	τ average	1.221E+06	-25.05%
	Fine mesh size	τ absolute average	1.316E+06	-19.20%
	Fine mesh size	τ absolute max	4.474E+06	174.67%
	Coarse mesh size	τ average	1.199E+06	-26.37%
	Coarse mesh size	τ absolute average	1.270E+06	-22.02%
	Coarse mesh size	τ absolute max	4.058E+06	149.12%
	Single element mesh size	τ average	1.629E+06	
Load case 2 2.13.2	Fine mesh size	τ average	4.460E+07	1.03%
	Fine mesh size	τ absolute average	4.460E+07	1.03%
	Fine mesh size	τ absolute max	4.656E+07	5.46%
	Coarse mesh size	τ average	4.492E+07	1.76%
	Coarse mesh size	τ absolute average	4.492E+07	1.76%
	Coarse mesh size	τ absolute max	4.582E+07	3.79%
	Single element mesh size	τ average	4.415E+07	
Load case 3 6.10.1	Fine mesh size	τ average	1.366E+08	0.30%
	Fine mesh size	τ absolute average	1.366E+08	0.30%
	Fine mesh size	τ absolute max	1.410E+08	3.54%
	Coarse mesh size	τ average	1.375E+08	0.98%
	Coarse mesh size	τ absolute average	1.375E+08	0.98%
	Coarse mesh size	τ absolute max	1.394E+08	2.34%
	Single element mesh size	τ average	1.362E+08	
Load case 4 6.1.10	Fine mesh size	τ average	1.366E+08	0.35%
	Fine mesh size	τ absolute average	1.366E+08	0.35%
	Fine mesh size	τ absolute max	1.454E+08	6.84%
	Coarse mesh size	τ average	1.374E+08	1.00%
	Coarse mesh size	τ absolute average	1.374E+08	1.00%
	Coarse mesh size	τ absolute max	1.436E+08	5.49%
	Single element mesh size	τ average	1.361E+08	
Load case 5 0.0.10	Fine mesh size	τ average	8.796E+05	-28.72%
	Fine mesh size	τ absolute average	4.145E+06	235.89%
	Fine mesh size	τ absolute max	6.578E+06	432.98%
	Coarse mesh size	τ average	9.135E+05	-25.97%
	Coarse mesh size	τ absolute average	4.169E+06	237.84%
	Coarse mesh size	τ absolute max	6.289E+06	409.59%
	Single element mesh size	τ average	1.234E+06	
Load case 6 Fy	Fine mesh size	τ average	5.470E+06	-17.24%
	Fine mesh size	τ absolute average	5.495E+06	-16.86%
	Fine mesh size	τ absolute max	1.963E+07	196.98%
	Coarse mesh size	τ average	5.433E+06	-17.80%
	Coarse mesh size	τ absolute average	5.433E+06	-17.80%
	Coarse mesh size	τ absolute max	1.791E+07	170.96%
	Single element mesh size	τ average	6.609E+06	
Load case 7 0.15.0 + Fy	Fine mesh size	τ average	4.494E+06	-15.32%
	Fine mesh size	τ absolute average	4.494E+06	-15.32%
	Fine mesh size	τ absolute max	1.605E+07	202.46%
	Coarse mesh size	τ average	4.474E+06	-15.69%
	Coarse mesh size	τ absolute average	4.474E+06	-15.69%
	Coarse mesh size	τ absolute max	1.466E+07	176.32%
	Single element mesh size	τ average	5.306E+06	

Table D.2 Shear Stress results of the plate field after applying the implementation method for the beam model in the three different mesh sizes of model 2.

Appendix E (Plate field Tables Buckling Factors)

The buckling factors for all analyses on each model. These are the comparisons between the real stresses and the complete implementation methods (fig 8.21).

Plate field 200x150x3 Bar stiffener 20x4	Real load case	Femap buckling factor k≥1	Linearized load case	Femap buckling factor k≥1	Difference with real loads ≥0
	Load case 1	0.3439	Linear Regression Average + Average Shear	0.3437	0.047%
	Load case 2	0.3862		0.3860	0.045%
	Load case 3	0.4918		0.4920	-0.022%
	Load case 4	1.4604		1.4697	-0.641%
	Load case 5	3.1668		3.1920	-0.798%
	Load case 6	0.3113		0.3118	-0.154%
	Load case 7	0.1805		0.1807	-0.070%
	Load case 1	0.3439	Linear Regression Include all stress points + Average Shear	0.3409	0.874%
	Load case 2	0.3862		0.3782	2.078%
	Load case 3	0.4918		0.4633	5.814%
	Load case 4	1.4604		1.2817	12.238%
	Load case 5	3.1668		3.0993	2.132%
	Load case 6	0.3113		0.3054	1.879%
	Load case 7	0.1805		0.1790	0.868%
	Load case 1	0.3439	Linear Regression Update to max stress points + Average Shear	0.3414	0.710%
	Load case 2	0.3862		0.3815	1.217%
	Load case 3	0.4918		0.4647	5.513%
	Load case 4	1.4604		1.2977	11.142%
	Load case 5	3.1668		3.1165	1.587%
	Load case 6	0.3113		0.3165	-1.691%
	Load case 7	0.1805		0.1820	-0.786%
	Load case 1	0.3439	Linear Regression Eurocode + Average Shear	0.3435	0.116%
	Load case 2	0.3862		0.3857	0.114%
	Load case 3	0.4918		0.4910	0.180%
	Load case 4	1.4604		1.4544	0.409%
	Load case 5	3.1668		3.1008	2.085%
	Load case 6	0.3113		0.3109	0.112%
	Load case 7	0.1805		0.1804	0.056%
	Load case 1	0.3439	Linear Regression Average + Absolute Average Shear	0.3437	0.047%
	Load case 2	0.3862		0.3860	0.045%
	Load case 3	0.4918		0.4920	-0.022%
	Load case 4	1.4604		1.4697	-0.641%
	Load case 5	3.1668		3.1875	-0.654%
	Load case 6	0.3113		0.3118	-0.154%
	Load case 7	0.1805		0.1807	-0.070%
	Load case 1	0.3439	Linear Regression Include all stress points + Absolute Average Shear	0.3409	0.874%
	Load case 2	0.3862		0.3782	2.078%
	Load case 3	0.4918		0.4633	5.814%
	Load case 4	1.4604		1.2817	12.238%
	Load case 5	3.1668		3.0951	2.262%
	Load case 6	0.3113		0.3054	1.879%
	Load case 7	0.1805		0.1790	0.868%
	Load case 1	0.3439	Linear Regression Update to max stress points + Absolute Average Shear	0.3414	0.710%
	Load case 2	0.3862		0.3815	1.217%
	Load case 3	0.4918		0.4647	5.513%
	Load case 4	1.4604		1.2977	11.142%
	Load case 5	3.1668		3.1123	1.719%
	Load case 6	0.3113		0.3165	-1.691%
	Load case 7	0.1805		0.1820	-0.786%
	Load case 1	0.3439	Linear Regression Eurocode + Absolute Average Shear	0.3435	0.116%
	Load case 2	0.3862		0.3857	0.114%
	Load case 3	0.4918		0.4910	0.180%
	Load case 4	1.4604		1.4544	0.409%
	Load case 5	3.1668		3.0966	2.216%
	Load case 6	0.3113		0.3109	0.112%
	Load case 7	0.1805		0.1804	0.056%
	Load case 1	0.3439	Linear Regression Average + Absolute Max Shear	0.3437	0.048%
	Load case 2	0.3862		0.3859	0.063%
	Load case 3	0.4918		0.4910	0.173%
	Load case 4	1.4604		1.4267	2.309%
	Load case 5	3.1668		3.1808	-0.442%
	Load case 6	0.3113		0.3117	-0.135%
	Load case 7	0.1805		0.1807	-0.065%
	Load case 1	0.3439	Linear Regression Include all stress points + Absolute Max Shear	0.3409	0.875%
	Load case 2	0.3862		0.3781	2.096%
	Load case 3	0.4918		0.4624	5.978%
	Load case 4	1.4604		1.2516	14.297%
	Load case 5	3.1668		3.0891	2.454%
	Load case 6	0.3113		0.3054	1.897%
	Load case 7	0.1805		0.1790	0.872%
	Load case 1	0.3439	Linear Regression Update to max stress points + Absolute Max Shear	0.3414	0.711%
	Load case 2	0.3862		0.3814	1.235%
	Load case 3	0.4918		0.4639	5.678%
	Load case 4	1.4604		1.2666	13.270%
	Load case 5	3.1668		3.1062	1.914%
	Load case 6	0.3113		0.3165	-1.671%
	Load case 7	0.1805		0.1820	-0.781%
	Load case 1	0.3439	Linear Regression Eurocode + Absolute Max Shear	0.3435	0.117%
	Load case 2	0.3862		0.3857	0.132%
	Load case 3	0.4918		0.4900	0.374%
	Load case 4	1.4604		1.4125	3.281%
	Load case 5	3.1668		3.0905	2.408%
	Load case 6	0.3113		0.3109	0.132%
	Load case 7	0.1805		0.1804	0.061%

Table E.01 Model 1, Buckling factors for all stresses (fig 8.21 check 1).

Plate field 200x150x4 Bar stiffener 20x4	Real load case	Femap buckling factor k≥1	Linearized load case	Femap buckling factor k≥1	Difference with real loads ≥0
	Load case 1	0.8034	Linear Regression Average + Average Shear	0.8030	0.047%
	Load case 2	0.9026		0.9022	0.045%
	Load case 3	1.1497		1.1498	-0.012%
	Load case 4	3.4328		3.4506	-0.521%
	Load case 5	7.4902		7.5373	-0.629%
	Load case 6	0.6998		0.7008	-0.140%
	Load case 7	0.4125		0.4127	-0.063%
	Load case 1	0.8034	Linear Regression Include all stress points + Average Shear	0.7962	0.899%
	Load case 2	0.9026		0.8863	1.797%
	Load case 3	1.1497		1.0947	4.780%
	Load case 4	3.4328		3.0902	9.980%
	Load case 5	7.4902		7.3623	1.707%
	Load case 6	0.6998		0.6871	1.816%
	Load case 7	0.4125		0.4090	0.850%
	Load case 1	0.8034	Linear Regression Update to max stress points + Average Shear	0.7976	0.719%
	Load case 2	0.9026		0.8932	1.033%
	Load case 3	1.1497		1.1008	4.248%
	Load case 4	3.4328		3.1216	9.065%
	Load case 5	7.4902		7.4021	1.176%
	Load case 6	0.6998		0.7116	-1.677%
	Load case 7	0.4125		0.4157	-0.778%
	Load case 1	0.8034	Linear Regression Eurocode + Average Shear	0.8025	0.120%
	Load case 2	0.9026		0.9016	0.105%
	Load case 3	1.1497		1.1479	0.151%
	Load case 4	3.4328		3.4204	0.360%
	Load case 5	7.4902		7.3514	1.853%
	Load case 6	0.6998		0.6990	0.124%
	Load case 7	0.4125		0.4122	0.062%
	Load case 1	0.8034	Linear Regression Average + Absolute Average Shear	0.8030	0.047%
	Load case 2	0.9026		0.9022	0.045%
	Load case 3	1.1497		1.1498	-0.012%
	Load case 4	3.4328		3.4506	-0.521%
	Load case 5	7.4902		7.5292	-0.521%
	Load case 6	0.6998		0.7008	-0.140%
	Load case 7	0.4125		0.4127	-0.063%
	Load case 1	0.8034	Linear Regression Include all stress points + Absolute Average Shear	0.7962	0.899%
	Load case 2	0.9026		0.8863	1.797%
	Load case 3	1.1497		1.0947	4.780%
	Load case 4	3.4328		3.0902	9.980%
	Load case 5	7.4902		7.3549	1.807%
	Load case 6	0.6998		0.6871	1.816%
	Load case 7	0.4125		0.4090	0.850%
	Load case 1	0.8034	Linear Regression Update to max stress points + Absolute Average Shear	0.7976	0.719%
	Load case 2	0.9026		0.8932	1.033%
	Load case 3	1.1497		1.1008	4.248%
	Load case 4	3.4328		3.1216	9.065%
	Load case 5	7.4902		7.3945	1.277%
	Load case 6	0.6998		0.7116	-1.677%
	Load case 7	0.4125		0.4157	-0.778%
	Load case 1	0.8034	Linear Regression Eurocode + Absolute Average Shear	0.8025	0.120%
	Load case 2	0.9026		0.9016	0.105%
	Load case 3	1.1497		1.1479	0.151%
	Load case 4	3.4328		3.4204	0.360%
	Load case 5	7.4902		7.3440	1.952%
	Load case 6	0.6998		0.6990	0.124%
	Load case 7	0.4125		0.4122	0.062%
	Load case 1	0.8034	Linear Regression Average + Absolute Max Shear	0.8030	0.048%
	Load case 2	0.9026		0.9020	0.061%
	Load case 3	1.1497		1.1479	0.158%
	Load case 4	3.4328		3.3634	2.021%
	Load case 5	7.4902		7.5165	-0.350%
	Load case 6	0.6998		0.7007	-0.122%
	Load case 7	0.4125		0.4127	-0.059%
	Load case 1	0.8034	Linear Regression Include all stress points + Absolute Max Shear	0.7962	0.900%
	Load case 2	0.9026		0.8862	1.812%
	Load case 3	1.1497		1.0930	4.927%
	Load case 4	3.4328		3.0249	11.883%
	Load case 5	7.4902		7.3431	1.964%
	Load case 6	0.6998		0.6870	1.834%
	Load case 7	0.4125		0.4089	0.855%
	Load case 1	0.8034	Linear Regression Update to max stress points + Absolute Max Shear	0.7976	0.721%
	Load case 2	0.9026		0.8931	1.048%
	Load case 3	1.1497		1.0991	4.398%
	Load case 4	3.4328		3.0545	11.019%
	Load case 5	7.4902		7.3826	1.437%
	Load case 6	0.6998		0.7114	-1.657%
	Load case 7	0.4125		0.4156	-0.773%
	Load case 1	0.8034	Linear Regression Eurocode + Absolute Max Shear	0.8024	0.122%
	Load case 2	0.9026		0.9015	0.121%
	Load case 3	1.1497		1.1460	0.320%
	Load case 4	3.4328		3.3351	2.845%
	Load case 5	7.4902		7.3323	2.109%
	Load case 6	0.6998		0.6988	0.143%
	Load case 7	0.4125		0.4122	0.067%

Table E.02 Model 2, Buckling factors for all stresses (fig 8.21 check 1).

Plate field 200x150x5 Bar stiffener 20x4	Real load case	Femap buckling factor k≥1	Linearized load case	Femap buckling factor k≥1	Difference with real loads ≥0
	Load case 1	1.5542		1.5535	0.047%
	Load case 2	1.7463		1.7455	0.045%
	Load case 3	2.2243	Linear Regression	2.2244	-0.005%
	Load case 4	6.6567	Average + Average	6.6862	-0.443%
	Load case 5	14.6067	Shear	14.6809	-0.508%
	Load case 6	1.3169		1.3187	-0.130%
	Load case 7	0.7849		0.7854	-0.059%
	Load case 1	1.5542		1.5400	0.916%
	Load case 2	1.7463		1.7181	1.615%
	Load case 3	2.2243	Linear Regression	2.1327	4.115%
	Load case 4	6.6567	Include all stress	6.0961	8.423%
	Load case 5	14.6067	points + Average	14.3944	1.453%
	Load case 6	1.3169	Shear	1.2936	1.775%
	Load case 7	0.7849		0.7784	0.839%
	Load case 1	1.5542		1.5429	0.726%
	Load case 2	1.7463		1.7302	0.923%
	Load case 3	2.2243	Linear Regression	2.1507	3.305%
	Load case 4	6.6567	Update to max	6.1483	7.638%
	Load case 5	14.6067	stress points +	14.4707	0.931%
	Load case 6	1.3169	Average Shear	1.3390	-1.676%
	Load case 7	0.7849		0.7911	-0.778%
	Load case 1	1.5542		1.5523	0.124%
	Load case 2	1.7463		1.7445	0.101%
	Load case 3	2.2243	Linear Regression	2.2213	0.134%
	Load case 4	6.6567	Eurocode + Average	6.6357	0.317%
	Load case 5	14.6067	Shear	14.3620	1.675%
	Load case 6	1.3169		1.3152	0.135%
	Load case 7	0.7849		0.7844	0.068%
	Load case 1	1.5542		1.5535	0.047%
	Load case 2	1.7463		1.7455	0.045%
	Load case 3	2.2243	Linear Regression	2.2244	-0.005%
	Load case 4	6.6567	Average + Absolute	6.6862	-0.443%
	Load case 5	14.6067	Average Shear	14.6684	-0.423%
	Load case 6	1.3169		1.3187	-0.130%
	Load case 7	0.7849		0.7854	-0.059%
	Load case 1	1.5542		1.5400	0.916%
	Load case 2	1.7463		1.7181	1.615%
	Load case 3	2.2243	Linear Regression	2.1327	4.115%
	Load case 4	6.6567	Include all stress	6.0961	8.423%
	Load case 5	14.6067	points + Absolute	14.3828	1.533%
	Load case 6	1.3169	Average Shear	1.2936	1.775%
	Load case 7	0.7849		0.7784	0.839%
	Load case 1	1.5542		1.5429	0.726%
	Load case 2	1.7463	Linear Regression	1.7302	0.923%
	Load case 3	2.2243	Update to max	2.1507	3.305%
	Load case 4	6.6567	stress points +	6.1483	7.638%
	Load case 5	14.6067	Absolute Average	14.4590	1.011%
	Load case 6	1.3169	Shear	1.3390	-1.676%
	Load case 7	0.7849		0.7911	-0.778%
	Load case 1	1.5542		1.5523	0.124%
	Load case 2	1.7463		1.7445	0.101%
	Load case 3	2.2243	Linear Regression	2.2213	0.134%
	Load case 4	6.6567	Eurocode + Absolute	6.6357	0.317%
	Load case 5	14.6067	Average Shear	14.3505	1.754%
	Load case 6	1.3169		1.3152	0.135%
	Load case 7	0.7849		0.7844	0.068%
	Load case 1	1.5542		1.5535	0.048%
	Load case 2	1.7463		1.7453	0.059%
	Load case 3	2.2243	Linear Regression	2.2209	0.150%
	Load case 4	6.6567	Average + Absolute	6.5358	1.816%
	Load case 5	14.6067	Max Shear	14.6476	-0.280%
	Load case 6	1.3169		1.3184	-0.111%
	Load case 7	0.7849		0.7854	-0.054%
	Load case 1	1.5542		1.5400	0.917%
	Load case 2	1.7463		1.7179	1.628%
	Load case 3	2.2243	Linear Regression	2.1297	4.252%
	Load case 4	6.6567	Include all stress	5.9780	10.196%
	Load case 5	14.6067	points + Absolute	14.3634	1.666%
	Load case 6	1.3169	Max Shear	1.2933	1.792%
	Load case 7	0.7849		0.7783	0.843%
	Load case 1	1.5542		1.5429	0.728%
	Load case 2	1.7463		1.7300	0.937%
	Load case 3	2.2243	Linear Regression	2.1476	3.446%
	Load case 4	6.6567	Update to max	6.0276	9.452%
	Load case 5	14.6067	stress points +	14.4392	1.147%
	Load case 6	1.3169	Absolute Max Shear	1.3388	-1.656%
	Load case 7	0.7849		0.7910	-0.774%
	Load case 1	1.5542		1.5523	0.126%
	Load case 2	1.7463		1.7443	0.115%
	Load case 3	2.2243	Linear Regression	2.2178	0.289%
	Load case 4	6.6567	Eurocode + Absolute	6.4881	2.533%
	Load case 5	14.6067	Max Shear	14.3312	1.886%
	Load case 6	1.3169		1.3149	0.153%
	Load case 7	0.7849		0.7844	0.072%

Table E.03 Model 3, Buckling factors for all stresses (fig 8.21 check 1).

Plate field 200x150x4 Bar stiffener 40x4	Real load case	Femap buckling factor k≥1	Linearized load case	Femap buckling factor k≥1	Difference with real loads ≥0
	Load case 1	0.8775		0.8770	0.060%
	Load case 2	0.9851		0.9846	0.052%
	Load case 3	1.2505	Linear Regression Average + Average Shear	1.2512	-0.056%
	Load case 4	3.6057		3.6359	-0.839%
	Load case 5	7.9914		8.0412	-0.623%
	Load case 6	0.7103		0.7119	-0.225%
	Load case 7	0.4312		0.4316	-0.109%
	Load case 1	0.8775		0.8676	1.134%
	Load case 2	0.9851		0.9577	2.779%
	Load case 3	1.2505	Linear Regression Include all stress points + Average Shear	1.1532	7.780%
	Load case 4	3.6057		3.0472	15.489%
	Load case 5	7.9914		7.7771	2.682%
	Load case 6	0.7103		0.6908	2.748%
	Load case 7	0.4312		0.4251	1.410%
	Load case 1	0.8775		0.8690	0.969%
	Load case 2	0.9851		0.9684	1.697%
	Load case 3	1.2505	Linear Regression Update to max stress points + Average Shear	1.1591	7.307%
	Load case 4	3.6057		3.0943	14.181%
	Load case 5	7.9914		7.8174	2.177%
	Load case 6	0.7103		0.7191	-1.244%
	Load case 7	0.4312		0.4337	-0.597%
	Load case 1	0.8775		0.8761	0.160%
	Load case 2	0.9851		0.9836	0.151%
	Load case 3	1.2505	Linear Regression Eurocode + Average Shear	1.2473	0.254%
	Load case 4	3.6057		3.6034	0.063%
	Load case 5	7.9914		7.8464	1.814%
	Load case 6	0.7103		0.7090	0.181%
	Load case 7	0.4312		0.4307	0.099%
	Load case 1	0.8775		0.8770	0.060%
	Load case 2	0.9851		0.9846	0.052%
	Load case 3	1.2505	Linear Regression Average + Absolute Average Shear	1.2512	-0.056%
	Load case 4	3.6057		3.6359	-0.839%
	Load case 5	7.9914		8.0329	-0.520%
	Load case 6	0.7103		0.7119	-0.223%
	Load case 7	0.4312		0.4316	-0.108%
	Load case 1	0.8775		0.8676	1.134%
	Load case 2	0.9851		0.9577	2.779%
	Load case 3	1.2505	Linear Regression Include all stress points + Absolute Average Shear	1.1532	7.780%
	Load case 4	3.6057		3.0472	15.489%
	Load case 5	7.9914		7.7698	2.774%
	Load case 6	0.7103		0.6908	2.749%
	Load case 7	0.4312		0.4251	1.411%
	Load case 1	0.8775		0.8690	0.969%
	Load case 2	0.9851		0.9684	1.697%
	Load case 3	1.2505	Linear Regression Update to max stress points + Absolute Average Shear	1.1591	7.307%
	Load case 4	3.6057		3.0943	14.181%
	Load case 5	7.9914		7.8100	2.270%
	Load case 6	0.7103		0.7191	-1.242%
	Load case 7	0.4312		0.4337	-0.596%
	Load case 1	0.8775		0.8761	0.160%
	Load case 2	0.9851		0.9836	0.151%
	Load case 3	1.2505	Linear Regression Eurocode + Absolute Average Shear	1.2473	0.254%
	Load case 4	3.6057		3.6034	0.063%
	Load case 5	7.9914		7.8388	1.909%
	Load case 6	0.7103		0.7090	0.183%
	Load case 7	0.4312		0.4307	0.099%
	Load case 1	0.8775		0.8770	0.061%
	Load case 2	0.9851		0.9843	0.084%
	Load case 3	1.2505	Linear Regression Average + Absolute Max Shear	1.2471	0.272%
	Load case 4	3.6057		3.5234	2.280%
	Load case 5	7.9914		8.0194	-0.350%
	Load case 6	0.7103		0.7118	-0.207%
	Load case 7	0.4312		0.4316	-0.104%
	Load case 1	0.8775		0.8676	1.135%
	Load case 2	0.9851		0.9574	2.808%
	Load case 3	1.2505	Linear Regression Include all stress points + Absolute Max Shear	1.1499	8.038%
	Load case 4	3.6057		2.9763	17.455%
	Load case 5	7.9914		7.7577	2.925%
	Load case 6	0.7103		0.6907	2.764%
	Load case 7	0.4312		0.4251	1.415%
	Load case 1	0.8775		0.8690	0.970%
	Load case 2	0.9851		0.9681	1.727%
	Load case 3	1.2505	Linear Regression Update to max stress points + Absolute Max Shear	1.1558	7.569%
	Load case 4	3.6057		3.0205	16.228%
	Load case 5	7.9914		7.7978	2.423%
	Load case 6	0.7103		0.7190	-1.225%
	Load case 7	0.4312		0.4337	-0.592%
	Load case 1	0.8775		0.8761	0.161%
	Load case 2	0.9851		0.9833	0.183%
	Load case 3	1.2505	Linear Regression Eurocode + Absolute Max Shear	1.2432	0.579%
	Load case 4	3.6057		3.4935	3.111%
	Load case 5	7.9914		7.8264	2.065%
	Load case 6	0.7103		0.7089	0.199%
	Load case 7	0.4312		0.4307	0.103%

Table E.04 Model 4, Buckling factors for all stresses (fig 8.21 check 1).

Plate field 200x150x4 T stiffener 20x4x20x4 Real load case	Femap buckling factor k≥1	Linearized load case	Femap buckling factor k≥1	Difference with real loads ≥0
Load case 1	0.8605		0.8600	0.057%
Load case 2	0.9661		0.9656	0.052%
Load case 3	1.2277	Linear Regression	1.2288	-0.092%
Load case 4	3.5715	Average + Average	3.6185	-1.318%
Load case 5	7.8666	Shear	7.9182	-0.656%
Load case 6	0.6988		0.7001	-0.193%
Load case 7	0.4236		0.4240	-0.092%
Load case 1	0.8605		0.8518	1.008%
Load case 2	0.9661	Linear Regression	0.9442	2.268%
Load case 3	1.2277	Include all stress	1.1515	6.204%
Load case 4	3.5715	points + Average	3.1436	11.981%
Load case 5	7.8666	Shear	7.5787	3.660%
Load case 6	0.6988		0.6821	2.391%
Load case 7	0.4236		0.4185	1.198%
Load case 1	0.8605		0.8533	0.843%
Load case 2	0.9661	Linear Regression	0.9526	1.397%
Load case 3	1.2277	Update to max	1.1603	5.490%
Load case 4	3.5715	stress points +	3.2265	9.659%
Load case 5	7.8666	Average Shear	7.6093	3.270%
Load case 6	0.6988		0.7091	-1.482%
Load case 7	0.4236		0.4267	-0.722%
Load case 1	0.8605		0.8593	0.141%
Load case 2	0.9661		0.9642	0.202%
Load case 3	1.2277	Linear Regression	1.2226	0.417%
Load case 4	3.5715	Eurocode + Average	3.5735	-0.057%
Load case 5	7.8666	Shear	7.7250	1.800%
Load case 6	0.6988		0.6979	0.126%
Load case 7	0.4236		0.4233	0.067%
Load case 1	0.8605		0.8600	0.057%
Load case 2	0.9661		0.9656	0.052%
Load case 3	1.2277	Linear Regression	1.2288	-0.092%
Load case 4	3.5715	Average + Absolute	3.6185	-1.318%
Load case 5	7.8666	Average Shear	7.9104	-0.558%
Load case 6	0.6988		0.7001	-0.192%
Load case 7	0.4236		0.4240	-0.092%
Load case 1	0.8605		0.8518	1.008%
Load case 2	0.9661	Linear Regression	0.9442	2.268%
Load case 3	1.2277	Include all stress	1.1515	6.204%
Load case 4	3.5715	points + Absolute	3.1436	11.981%
Load case 5	7.8666	Average Shear	7.5720	3.744%
Load case 6	0.6988		0.6821	2.392%
Load case 7	0.4236		0.4185	1.198%
Load case 1	0.8605		0.8533	0.843%
Load case 2	0.9661	Linear Regression	0.9526	1.397%
Load case 3	1.2277	Update to max	1.1603	5.490%
Load case 4	3.5715	stress points +	3.2265	9.659%
Load case 5	7.8666	Absolute Average	7.6026	3.356%
Load case 6	0.6988	Shear	7.091	-1.481%
Load case 7	0.4236		0.4267	-0.722%
Load case 1	0.8605		0.8593	0.142%
Load case 2	0.9661		0.9642	0.202%
Load case 3	1.2277	Linear Regression	1.2226	0.417%
Load case 4	3.5715	Eurocode + Absolute	3.5735	-0.057%
Load case 5	7.8666	Average Shear	7.7178	1.891%
Load case 6	0.6988		0.6979	0.127%
Load case 7	0.4236		0.4233	0.068%
Load case 1	0.8605		0.8600	0.058%
Load case 2	0.9661		0.9654	0.077%
Load case 3	1.2277	Linear Regression	1.2254	0.185%
Load case 4	3.5715	Average + Absolute	3.5195	1.454%
Load case 5	7.8666	Max Shear	7.8969	-0.386%
Load case 6	0.6988		0.7000	-0.178%
Load case 7	0.4236		0.4240	-0.089%
Load case 1	0.8605		0.8518	1.009%
Load case 2	0.9661	Linear Regression	0.9440	2.292%
Load case 3	1.2277	Include all stress	1.1487	6.433%
Load case 4	3.5715	points + Absolute	3.0751	13.899%
Load case 5	7.8666	Max Shear	7.5604	3.892%
Load case 6	0.6988		0.6820	2.405%
Load case 7	0.4236		0.4185	1.202%
Load case 1	0.8605		0.8533	0.844%
Load case 2	0.9661	Linear Regression	0.9524	1.421%
Load case 3	1.2277	Update to max	1.1574	5.724%
Load case 4	3.5715	stress points +	3.1532	11.712%
Load case 5	7.8666	Absolute Max Shear	7.5908	3.506%
Load case 6	0.6988		0.7090	-1.466%
Load case 7	0.4236		0.4267	-0.718%
Load case 1	0.8605		0.8593	0.142%
Load case 2	0.9661		0.9639	0.227%
Load case 3	1.2277	Linear Regression	1.2192	0.690%
Load case 4	3.5715	Eurocode + Absolute	3.4777	2.626%
Load case 5	7.8666	Max Shear	7.7053	2.050%
Load case 6	0.6988		0.6978	0.141%
Load case 7	0.4236		0.4233	0.071%

Table E.05 Model 5, Buckling factors for all stresses (fig 8.21 check 1).

Plate field 200x150x4 T stiffener 40x4x40x4	Real load case	Femap buckling factor k≥1	Linearized load case	Femap buckling factor k≥1	Difference with real loads ≥0
	Load case 1	1.0155		1.0146	0.085%
	Load case 2	1.1389		1.1381	0.078%
	Load case 3	1.4389	Linear Regression	1.4410	-0.141%
	Load case 4	3.9454	Average + Average	4.0199	-1.886%
	Load case 5	8.9086	Shear	8.9649	-0.632%
	Load case 6	0.7236		0.7262	-0.361%
	Load case 7	0.4609		0.4618	-0.192%
	Load case 1	1.0155		1.0025	1.278%
	Load case 2	1.1389	Linear Regression	1.1063	2.868%
	Load case 3	1.4389	Include all stress	1.3169	8.477%
	Load case 4	3.9454	points + Average	3.3829	14.259%
	Load case 5	8.9086	Shear	8.4361	5.305%
	Load case 6	0.7236		0.6994	3.344%
	Load case 7	0.4609		0.4523	1.870%
	Load case 1	1.0155		1.0039	1.141%
	Load case 2	1.1389	Linear Regression	1.1180	1.836%
	Load case 3	1.4389	Update to max	1.3748	4.460%
	Load case 4	3.9454	stress points +	3.7624	4.640%
	Load case 5	8.9086	Average Shear	8.4540	5.104%
	Load case 6	0.7236		0.7266	-0.413%
	Load case 7	0.4609		0.4617	-0.165%
	Load case 1	1.0155		1.0134	0.206%
	Load case 2	1.1389		1.1356	0.293%
	Load case 3	1.4389	Linear Regression	1.4305	0.588%
	Load case 4	3.9454	Eurocode + Average	3.9602	-0.375%
	Load case 5	8.9086	Shear	8.7535	1.741%
	Load case 6	0.7236		0.7225	0.152%
	Load case 7	0.4609		0.4605	0.091%
	Load case 1	1.0155		1.0146	0.086%
	Load case 2	1.1389		1.1381	0.078%
	Load case 3	1.4389	Linear Regression	1.4410	-0.141%
	Load case 4	3.9454	Average + Absolute	4.0199	-1.886%
	Load case 5	8.9086	Average Shear	8.9577	-0.550%
	Load case 6	0.7236		0.7262	-0.357%
	Load case 7	0.4609		0.4618	-0.190%
	Load case 1	1.0155		1.0025	1.278%
	Load case 2	1.1389	Linear Regression	1.1063	2.868%
	Load case 3	1.4389	Include all stress	1.3169	8.477%
	Load case 4	3.9454	points + Absolute	3.3829	14.259%
	Load case 5	8.9086	Average Shear	8.4302	5.370%
	Load case 6	0.7236		0.6994	3.348%
	Load case 7	0.4609		0.4523	1.871%
	Load case 1	1.0155		1.0039	1.142%
	Load case 2	1.1389	Linear Regression	1.1180	1.836%
	Load case 3	1.4389	Update to max	1.3748	4.460%
	Load case 4	3.9454	stress points +	3.7624	4.640%
	Load case 5	8.9086	Absolute Average	8.4481	5.170%
	Load case 6	0.7236	Shear	0.7266	-0.409%
	Load case 7	0.4609		0.4617	-0.164%
	Load case 1	1.0155		1.0134	0.206%
	Load case 2	1.1389		1.1356	0.293%
	Load case 3	1.4389	Linear Regression	1.4305	0.588%
	Load case 4	3.9454	Eurocode + Absolute	3.9602	-0.375%
	Load case 5	8.9086	Average Shear	8.7467	1.817%
	Load case 6	0.7236		0.7225	0.157%
	Load case 7	0.4609		0.4605	0.092%
	Load case 1	1.0155		1.0146	0.086%
	Load case 2	1.1389		1.1375	0.126%
	Load case 3	1.4389	Linear Regression	1.4338	0.355%
	Load case 4	3.9454	Average + Absolute	3.9016	1.110%
	Load case 5	8.9086	Max Shear	8.9422	-0.377%
	Load case 6	0.7236		0.7261	-0.344%
	Load case 7	0.4609		0.4618	-0.186%
	Load case 1	1.0155		1.0025	1.279%
	Load case 2	1.1389	Linear Regression	1.1058	2.912%
	Load case 3	1.4389	Include all stress	1.3115	8.858%
	Load case 4	3.9454	points + Absolute	3.3071	16.179%
	Load case 5	8.9086	Max Shear	8.4177	5.511%
	Load case 6	0.7236		0.6993	3.360%
	Load case 7	0.4609		0.4523	1.875%
	Load case 1	1.0155		1.0039	1.142%
	Load case 2	1.1389	Linear Regression	1.1175	1.881%
	Load case 3	1.4389	Update to max	1.3685	4.892%
	Load case 4	3.9454	stress points +	3.6624	7.173%
	Load case 5	8.9086	Absolute Max Shear	8.4355	5.311%
	Load case 6	0.7236		0.7265	-0.395%
	Load case 7	0.4609		0.4617	-0.160%
	Load case 1	1.0155		1.0134	0.207%
	Load case 2	1.1389		1.1351	0.340%
	Load case 3	1.4389	Linear Regression	1.4235	1.074%
	Load case 4	3.9454	Eurocode + Absolute	3.8464	2.509%
	Load case 5	8.9086	Max Shear	8.7325	1.977%
	Load case 6	0.7236		0.7224	0.170%
	Load case 7	0.4609		0.4605	0.096%

Table E.06 Model 6, Buckling factors for all stresses (fig 8.21 check 1).

Plate field 600x150x4 Bar stiffener 20x4	Real load case	Femap buckling factor k≥1	Linearized load case	Femap buckling factor k≥1	Difference with real loads ≥0
	Load case 1	0.8381	Linear Regression Average + Average Shear	0.8430	-0.585%
	Load case 2	0.9382		0.9238	1.539%
	Load case 3	1.1642		0.8861	23.892%
	Load case 4	2.9512		1.2951	56.117%
	Load case 5	7.3912		7.5133	-1.653%
	Load case 6	0.6626		0.6759	-2.013%
	Load case 7	0.5594		0.5617	-0.416%
	Load case 1	0.8381	Linear Regression Include all stress points + Average Shear	0.8292	1.053%
	Load case 2	0.9382		0.9089	3.129%
	Load case 3	1.1642		0.8787	24.529%
	Load case 4	2.9512		1.2885	56.341%
	Load case 5	7.3912		7.2243	2.257%
	Load case 6	0.6626		0.6508	1.776%
	Load case 7	0.5594		0.5573	0.361%
	Load case 1	0.8381	Linear Regression Update to max stress points + Average Shear	0.8308	0.866%
	Load case 2	0.9382		0.9109	2.911%
	Load case 3	1.1642		0.8794	24.464%
	Load case 4	2.9512		1.2891	56.321%
	Load case 5	7.3912		7.2466	1.955%
	Load case 6	0.6626		0.6512	1.719%
	Load case 7	0.5594		0.5576	0.306%
	Load case 1	0.8381	Linear Regression Eurocode + Average Shear	0.8428	-0.565%
	Load case 2	0.9382		0.9233	1.597%
	Load case 3	1.1642		0.8860	23.895%
	Load case 4	2.9512		1.2932	56.180%
	Load case 5	7.3912		7.3667	0.331%
	Load case 6	0.6626		0.6754	-1.934%
	Load case 7	0.5594		0.5615	-0.389%
	Load case 1	0.8381	Linear Regression Average + Absolute Average Shear	0.8430	-0.584%
	Load case 2	0.9382		0.9238	1.539%
	Load case 3	1.1642		0.8861	23.892%
	Load case 4	2.9512		1.2951	56.117%
	Load case 5	7.3912		7.2827	1.468%
	Load case 6	0.6626		0.6759	-2.013%
	Load case 7	0.5594		0.5617	-0.416%
	Load case 1	0.8381	Linear Regression Include all stress points + Absolute Average Shear	0.8292	1.054%
	Load case 2	0.9382		0.9089	3.129%
	Load case 3	1.1642		0.8787	24.529%
	Load case 4	2.9512		1.2885	56.341%
	Load case 5	7.3912		7.0163	5.072%
	Load case 6	0.6626		0.6508	1.776%
	Load case 7	0.5594		0.5573	0.361%
	Load case 1	0.8381	Linear Regression Update to max stress points + Absolute Average Shear	0.8308	0.867%
	Load case 2	0.9382		0.9109	2.911%
	Load case 3	1.1642		0.8794	24.464%
	Load case 4	2.9512		1.2891	56.321%
	Load case 5	7.3912		7.0368	4.795%
	Load case 6	0.6626		0.6512	1.719%
	Load case 7	0.5594		0.5576	0.306%
	Load case 1	0.8381	Linear Regression Eurocode + Absolute Average Shear	0.8428	-0.564%
	Load case 2	0.9382		0.9233	1.597%
	Load case 3	1.1642		0.8860	23.895%
	Load case 4	2.9512		1.2932	56.180%
	Load case 5	7.3912		7.1490	3.276%
	Load case 6	0.6626		0.6754	-1.934%
	Load case 7	0.5594		0.5615	-0.389%
	Load case 1	0.8381	Linear Regression Average + Absolute Max Shear	0.8427	-0.558%
	Load case 2	0.9382		0.9187	2.079%
	Load case 3	1.1642		0.8737	24.953%
	Load case 4	2.9512		1.2529	57.548%
	Load case 5	7.3912		7.0331	4.844%
	Load case 6	0.6626		0.6759	-2.012%
	Load case 7	0.5594		0.5617	-0.416%
	Load case 1	0.8381	Linear Regression Include all stress points + Absolute Max Shear	0.8290	1.079%
	Load case 2	0.9382		0.9040	3.645%
	Load case 3	1.1642		0.8666	25.566%
	Load case 4	2.9512		1.2467	57.757%
	Load case 5	7.3912		6.7949	8.067%
	Load case 6	0.6626		0.6508	1.777%
	Load case 7	0.5594		0.5573	0.361%
	Load case 1	0.8381	Linear Regression Update to max stress points + Absolute Max Shear	0.8306	0.893%
	Load case 2	0.9382		0.9061	3.430%
	Load case 3	1.1642		0.8673	25.503%
	Load case 4	2.9512		1.2472	57.738%
	Load case 5	7.3912		6.8135	7.816%
	Load case 6	0.6626		0.6512	1.720%
	Load case 7	0.5594		0.5576	0.306%
	Load case 1	0.8381	Linear Regression Eurocode + Absolute Max Shear	0.8426	-0.538%
	Load case 2	0.9382		0.9182	2.136%
	Load case 3	1.1642		0.8737	24.956%
	Load case 4	2.9512		1.2511	57.607%
	Load case 5	7.3912		6.9152	6.440%
	Load case 6	0.6626		0.6754	-1.933%
	Load case 7	0.5594		0.5615	-0.389%

Table E.07 Model 7, Buckling factors for all stresses (fig 8.21 check 1).

Plate field 200x400x4 Bar stiffener 20x4	Real load case	Femap buckling factor k≥1	Linearized load case	Femap buckling factor k≥1	Difference with real loads ≥0
	Load case 1	0.4040		0.4019	0.515%
	Load case 2	0.4586		0.4569	0.371%
	Load case 3	0.5977	Linear Regression Average + Average Shear	0.5954	0.396%
	Load case 4	2.8277		3.0032	-6.207%
	Load case 5	5.5256		6.0317	-9.158%
	Load case 6	1.5192		1.3833	8.943%
	Load case 7	0.4578		0.4750	-3.757%
	Load case 1	0.4040		0.4013	0.661%
	Load case 2	0.4586		0.4560	0.586%
	Load case 3	0.5977	Linear Regression Include all stress points + Average Shear	0.5926	0.863%
	Load case 4	2.8277		2.9469	-4.215%
	Load case 5	5.5256		5.9987	-8.561%
	Load case 6	1.5192		1.4037	7.602%
	Load case 7	0.4578		0.4625	-1.018%
	Load case 1	0.4040		0.4015	0.604%
	Load case 2	0.4586		0.4565	0.460%
	Load case 3	0.5977	Linear Regression Update to max stress points + Average Shear	0.5936	0.690%
	Load case 4	2.8277		2.9705	-5.051%
	Load case 5	5.5256		6.0709	-9.869%
	Load case 6	1.5192		1.4526	4.379%
	Load case 7	0.4578		0.4677	-2.164%
	Load case 1	0.4040		0.4014	0.633%
	Load case 2	0.4586		0.4565	0.459%
	Load case 3	0.5977	Linear Regression Eurocode + Average Shear	0.5949	0.469%
	Load case 4	2.8277		2.9800	-5.388%
	Load case 5	5.5256		5.9423	-7.541%
	Load case 6	1.5192		1.3117	13.653%
	Load case 7	0.4578		0.4699	-2.649%
	Load case 1	0.4040		0.4019	0.515%
	Load case 2	0.4586		0.4569	0.371%
	Load case 3	0.5977	Linear Regression Average + Absolute Average Shear	0.5954	0.396%
	Load case 4	2.8277		3.0032	-6.207%
	Load case 5	5.5256		6.0422	-9.349%
	Load case 6	1.5192		1.3833	8.943%
	Load case 7	0.4578		0.4750	-3.757%
	Load case 1	0.4040		0.4013	0.661%
	Load case 2	0.4586		0.4560	0.586%
	Load case 3	0.5977	Linear Regression Include all stress points + Absolute Average Shear	0.5926	0.863%
	Load case 4	2.8277		2.9469	-4.215%
	Load case 5	5.5256		6.0091	-8.749%
	Load case 6	1.5192		1.4037	7.602%
	Load case 7	0.4578		0.4625	-1.018%
	Load case 1	0.4040		0.4015	0.604%
	Load case 2	0.4586		0.4565	0.460%
	Load case 3	0.5977	Linear Regression Update to max stress points + Absolute Average Shear	0.5936	0.690%
	Load case 4	2.8277		2.9705	-5.051%
	Load case 5	5.5256		6.0816	-10.062%
	Load case 6	1.5192		1.4526	4.379%
	Load case 7	0.4578		0.4677	-2.164%
	Load case 1	0.4040		0.4014	0.633%
	Load case 2	0.4586		0.4565	0.459%
	Load case 3	0.5977	Linear Regression Eurocode + Absolute Average Shear	0.5949	0.469%
	Load case 4	2.8277		2.9800	-5.388%
	Load case 5	5.5256		5.9527	-7.728%
	Load case 6	1.5192		1.3117	13.653%
	Load case 7	0.4578		0.4699	-2.649%
	Load case 1	0.4040		0.4019	0.516%
	Load case 2	0.4586		0.4569	0.375%
	Load case 3	0.5977	Linear Regression Average + Absolute Max Shear	0.5953	0.414%
	Load case 4	2.8277		2.9933	-5.856%
	Load case 5	5.5256		6.0624	-9.714%
	Load case 6	1.5192		1.2940	14.823%
	Load case 7	0.4578		0.4739	-3.504%
	Load case 1	0.4040		0.4013	0.662%
	Load case 2	0.4586		0.4559	0.589%
	Load case 3	0.5977	Linear Regression Include all stress points + Absolute Max Shear	0.5925	0.880%
	Load case 4	2.8277		2.9375	-3.884%
	Load case 5	5.5256		6.0290	-9.110%
	Load case 6	1.5192		1.3153	13.417%
	Load case 7	0.4578		0.4614	-0.784%
	Load case 1	0.4040		0.4015	0.605%
	Load case 2	0.4586		0.4565	0.464%
	Load case 3	0.5977	Linear Regression Update to max stress points + Absolute Max Shear	0.5935	0.707%
	Load case 4	2.8277		2.9609	-4.711%
	Load case 5	5.5256		6.1021	-10.432%
	Load case 6	1.5192		1.3550	10.809%
	Load case 7	0.4578		0.4666	-1.924%
	Load case 1	0.4040		0.4014	0.634%
	Load case 2	0.4586		0.4565	0.462%
	Load case 3	0.5977	Linear Regression Eurocode + Absolute Max Shear	0.5948	0.486%
	Load case 4	2.8277		2.9703	-5.045%
	Load case 5	5.5256		5.9725	-8.087%
	Load case 6	1.5192		1.2352	18.692%
	Load case 7	0.4578		0.4688	-2.400%

Table E.08 Model 8, Buckling factors for all stresses (fig 8.21 check 1).

Plate field 200x150x3 Bar stiffener 20x4	Real load case	Femap buckling factor k≥1	Linearized load case	Femap buckling factor k≥1	Difference with real loads ≥0
	Load case 1 Fx	0.41232		0.41243	-0.03%
	Load case 1 Fy	2.08766		2.06227	1.22%
	Load case 2 Fx	0.46341		0.46353	-0.03%
	Load case 2 Fy	2.36188		2.33260	1.24%
	Load case 3 Fx	0.60594		0.60611	-0.03%
	Load case 3 Fy	3.08009	Implementation method 1 Linear Regression Average	3.04310	1.20%
	Load case 4 Fx	2.26817		2.27189	-0.16%
	Load case 4 Fy	12.14262		13.56506	-11.71%
	Load case 5 Fx	3.65368		3.65547	-0.05%
	Load case 5 Fy	20.20318		24.96077	-23.55%
	Load case 6 Fx	11.84316		12.59581	-6.36%
	Load case 6 Fy	0.31734		0.31966	-0.73%
	Load case 7 Fx	0.49564		0.49530	0.07%
	Load case 7 Fy	0.28296		0.28442	-0.51%
	Load case 1 Fx	0.41232		0.41187	0.11%
	Load case 1 Fy	2.08766		1.97690	5.31%
	Load case 2 Fx	0.46341		0.46289	0.11%
	Load case 2 Fy	2.36188		2.08509	11.72%
	Load case 3 Fx	0.60594		0.60465	0.21%
	Load case 3 Fy	3.08009	Implementation method 2 Linear Regression + Include all stress results	2.20377	28.45%
	Load case 4 Fx	2.26817		2.23926	1.27%
	Load case 4 Fy	12.14262		5.24527	56.80%
	Load case 5 Fx	3.65368		3.64875	0.13%
	Load case 5 Fy	20.20318		20.40476	-1.00%
	Load case 6 Fx	11.84316		10.02511	15.35%
	Load case 6 Fy	0.31734		0.31502	0.73%
	Load case 7 Fx	0.49564		0.49139	0.86%
	Load case 7 Fy	0.28296		0.28151	0.51%
	Load case 1 Fx	0.41232		0.41269	-0.09%
	Load case 1 Fy	2.08766		1.97690	5.31%
	Load case 2 Fx	0.46341		0.46459	-0.25%
	Load case 2 Fy	2.36188		2.15326	8.83%
	Load case 3 Fx	0.60594		0.60604	-0.02%
	Load case 3 Fy	3.08009	Implementation method 3 Linear Regression + Update to maximum stress result	2.21954	27.94%
	Load case 4 Fx	2.26817		2.28310	-0.66%
	Load case 4 Fy	12.14262		5.32552	56.14%
	Load case 5 Fx	3.65368		3.67238	-0.51%
	Load case 5 Fy	20.20318		20.41273	-1.04%
	Load case 6 Fx	11.84316		10.10618	14.67%
	Load case 6 Fy	0.31734		0.32677	-2.97%
	Load case 7 Fx	0.49564		0.49153	0.83%
	Load case 7 Fy	0.28296		0.28892	-2.10%
	Load case 1 Fx	0.41232		0.41243	-0.03%
	Load case 1 Fy	2.08766		2.05379	1.62%
	Load case 2 Fx	0.46341		0.46353	-0.03%
	Load case 2 Fy	2.36188		2.32288	1.65%
	Load case 3 Fx	0.60594		0.60611	-0.03%
	Load case 3 Fy	3.08009	Implementation method 4 Linear Regression Eurocode	3.00455	2.45%
	Load case 4 Fx	2.26817		2.27189	-0.16%
	Load case 4 Fy	12.14262		12.05924	0.69%
	Load case 5 Fx	3.65368		3.65547	-0.05%
	Load case 5 Fy	20.20318		20.25855	-0.27%
	Load case 6 Fx	11.84316		12.59581	-6.36%
	Load case 6 Fy	0.31734		0.31879	-0.46%
	Load case 7 Fx	0.49564		0.49530	0.07%
	Load case 7 Fy	0.28296		0.28385	-0.31%

Table E.09 Model 1, Buckling factors for in-plane stresses (fig 8.21 check 2 and 3).

Plate field 200x150x4 Bar stiffener 20x4	Real load case	Femap buckling factor k≥1	Linearized load case	Femap buckling factor k≥1	Difference with real loads ≥0
	Load case 1 Fx	0.94415		0.94441	-0.03%
	Load case 1 Fy	5.43887		5.36411	1.37%
	Load case 2 Fx	1.06141		1.06169	-0.03%
	Load case 2 Fy	6.15921		6.07324	1.40%
	Load case 3 Fx	1.38778		1.38818	-0.03%
	Load case 3 Fy	8.02820	Implementation method 1 Linear Regression Average	7.91822	1.37%
	Load case 4 Fx	5.22610		5.23543	-0.18%
	Load case 4 Fy	32.80517		36.35704	-10.83%
	Load case 5 Fx	8.45029		8.45488	-0.05%
	Load case 5 Fy	55.59818		68.85168	-23.84%
	Load case 6 Fx	36.36674		40.13250	-10.35%
	Load case 6 Fy	0.70833		0.71326	-0.69%
	Load case 7 Fx	1.14764		1.14687	0.07%
	Load case 7 Fy	0.64157		0.64474	-0.49%
	Load case 1 Fx	0.94415		0.94314	0.11%
	Load case 1 Fy	5.43887		5.10970	6.05%
	Load case 2 Fx	1.06141		1.06025	0.11%
	Load case 2 Fy	6.15921		5.45870	11.37%
	Load case 3 Fx	1.38778		1.38592	0.13%
	Load case 3 Fy	8.02820	Implementation method 2 Linear Regression + Include all stress results	5.88237	26.73%
	Load case 4 Fx	5.22610		5.17802	0.92%
	Load case 4 Fy	32.80517		14.81686	54.83%
	Load case 5 Fx	8.45029		8.43964	0.13%
	Load case 5 Fy	55.59818		57.18136	-2.85%
	Load case 6 Fx	36.36674		29.58074	18.66%
	Load case 6 Fy	0.70833		0.70346	0.69%
	Load case 7 Fx	1.14764		1.13772	0.86%
	Load case 7 Fy	0.64157		0.63843	0.49%
	Load case 1 Fx	0.94415		0.94517	-0.11%
	Load case 1 Fy	5.43887		5.10970	6.05%
	Load case 2 Fx	1.06141		1.06413	-0.26%
	Load case 2 Fy	6.15921		5.62113	8.74%
	Load case 3 Fx	1.38778		1.38896	-0.09%
	Load case 3 Fy	8.02820	Implementation method 3 Linear Regression + Update to maximum stress result	6.01029	25.14%
	Load case 4 Fx	5.22610		5.25901	-0.63%
	Load case 4 Fy	32.80517		15.02650	54.19%
	Load case 5 Fx	8.45029		8.49133	-0.49%
	Load case 5 Fy	55.59818		57.20522	-2.89%
	Load case 6 Fx	36.36674		29.88603	17.82%
	Load case 6 Fy	0.70833		0.72892	-2.91%
	Load case 7 Fx	1.14764		1.13810	0.83%
	Load case 7 Fy	0.64157		0.65483	-2.07%
	Load case 1 Fx	0.94415		0.94441	-0.03%
	Load case 1 Fy	5.43887		5.33779	1.86%
	Load case 2 Fx	1.06141		1.06169	-0.03%
	Load case 2 Fy	6.15921		6.04871	1.79%
	Load case 3 Fx	1.38778		1.38818	-0.03%
	Load case 3 Fy	8.02820	Implementation method 4 Linear Regression Eurocode	7.82822	2.49%
	Load case 4 Fx	5.22610		5.23543	-0.18%
	Load case 4 Fy	32.80517		32.41817	1.18%
	Load case 5 Fx	8.45029		8.45488	-0.05%
	Load case 5 Fy	55.59818		55.84333	-0.44%
	Load case 6 Fx	36.36674		40.13250	-10.35%
	Load case 6 Fy	0.70833		0.71134	-0.42%
	Load case 7 Fx	1.14764		1.14687	0.07%
	Load case 7 Fy	0.64157		0.64347	-0.30%

Table E.10 Model 2, Buckling factors for in-plane stresses (fig 8.21 check 2 and 3).

Plate field 200x150x5 Bar stiffener 20x4	Real load case	Femap buckling factor k≥1	Linearized load case	Femap buckling factor k≥1	Difference with real loads ≥0
	Load case 1 Fx	1.80005		1.80054	-0.03%
	Load case 1 Fy	11.49564		11.32029	1.53%
	Load case 2 Fx	2.02394		2.02447	-0.03%
	Load case 2 Fy	13.02895		12.82747	1.55%
	Load case 3 Fx	2.64619		2.64691	-0.03%
	Load case 3 Fy	16.97559	Implementation method 1 Linear Regression Average	16.71612	1.53%
	Load case 4 Fx	10.00316		10.02217	-0.19%
	Load case 4 Fy	71.51640		78.74088	-10.10%
	Load case 5 Fx	16.21441		16.22394	-0.06%
	Load case 5 Fy	123.39450		153.02080	-24.01%
	Load case 6 Fx	90.41194		104.89980	-16.02%
	Load case 6 Fy	1.32640		1.33537	-0.68%
	Load case 7 Fx	2.20506		2.20367	0.06%
	Load case 7 Fy	1.21446		1.22034	-0.48%
	Load case 1 Fx	1.80005		1.79822	0.10%
	Load case 1 Fy	11.49564		10.72214	6.73%
	Load case 2 Fx	2.02394		2.02184	0.10%
	Load case 2 Fy	13.02895		11.56464	11.24%
	Load case 3 Fx	2.64619		2.64314	0.12%
	Load case 3 Fy	16.97559	Implementation method 2 Linear Regression + Include all stress results	12.64313	25.52%
	Load case 4 Fx	10.00316		9.93428	0.69%
	Load case 4 Fy	71.51640		33.36162	53.35%
	Load case 5 Fx	16.21441		16.19511	0.12%
	Load case 5 Fy	123.39450		128.34130	-4.01%
	Load case 6 Fx	90.41194		70.90047	21.58%
	Load case 6 Fy	1.32640		1.31757	0.67%
	Load case 7 Fx	2.20506		2.18625	0.85%
	Load case 7 Fy	1.21446		1.20867	0.48%
	Load case 1 Fx	1.80005		1.80223	-0.12%
	Load case 1 Fy	11.49564		10.72214	6.73%
	Load case 2 Fx	2.02394		2.02900	-0.25%
	Load case 2 Fy	13.02895		11.88375	8.79%
	Load case 3 Fx	2.64619		2.64948	-0.12%
	Load case 3 Fy	16.97559	Implementation method 3 Linear Regression + Update to maximum stress result	13.16207	22.46%
	Load case 4 Fx	10.00316		10.06382	-0.61%
	Load case 4 Fy	71.51640		33.80580	52.73%
	Load case 5 Fx	16.21441		16.29071	-0.47%
	Load case 5 Fy	123.39450		128.39630	-4.05%
	Load case 6 Fx	90.41194		71.87093	20.51%
	Load case 6 Fy	1.32640		1.36439	-2.86%
	Load case 7 Fx	2.20506		2.18704	0.82%
	Load case 7 Fy	1.21446		1.23930	-2.05%
	Load case 1 Fx	1.80005		1.80054	-0.03%
	Load case 1 Fy	11.49564		11.25625	2.08%
	Load case 2 Fx	2.02394		2.02447	-0.03%
	Load case 2 Fy	13.02895		12.77454	1.95%
	Load case 3 Fx	2.64619		2.64691	-0.03%
	Load case 3 Fy	16.97559	Implementation method 4 Linear Regression Eurocode	16.53871	2.57%
	Load case 4 Fx	10.00316		10.02217	-0.19%
	Load case 4 Fy	71.51640		70.40881	1.55%
	Load case 5 Fx	16.21441		16.22394	-0.06%
	Load case 5 Fy	123.39450		124.06220	-0.54%
	Load case 6 Fx	90.41194		104.89980	-16.02%
	Load case 6 Fy	1.32640		1.33179	-0.41%
	Load case 7 Fx	2.20506		2.20367	0.06%
	Load case 7 Fy	1.21446		1.21794	-0.29%

Table E.11 Model 3, Buckling factors for in-plane stresses (fig 8.21 check 2 and 3).

Plate field 200x150x4 Bar stiffener 40x4	Real load case	Femap buckling factor k≥1	Linearized load case	Femap buckling factor k≥1	Difference with real loads ≥0
	Load case 1 Fx	1.03863		1.03902	-0.04%
	Load case 1 Fy	5.71443		5.62297	1.60%
	Load case 2 Fx	1.16640		1.16682	-0.04%
	Load case 2 Fy	6.48991		6.38559	1.61%
	Load case 3 Fx	1.52449		1.52510	-0.04%
	Load case 3 Fy	8.50899	Implementation method 1 Linear Regression Average	8.38308	1.48%
	Load case 4 Fx	5.61433		5.62528	-0.20%
	Load case 4 Fy	35.55308		40.59811	-14.19%
	Load case 5 Fx	8.99715		9.00170	-0.05%
	Load case 5 Fy	60.53509		74.71123	-23.42%
	Load case 6 Fx	16.67995		16.32083	2.15%
	Load case 6 Fy	0.73707		0.74437	-0.99%
	Load case 7 Fx	1.20528		1.20305	0.18%
	Load case 7 Fy	0.66822		0.67314	-0.74%
	Load case 1 Fx	1.03863		1.03705	0.15%
	Load case 1 Fy	5.71443		5.30784	7.12%
	Load case 2 Fx	1.16640		1.16469	0.15%
	Load case 2 Fy	6.48991		5.44743	16.06%
	Load case 3 Fx	1.52449		1.51892	0.37%
	Load case 3 Fy	8.50899	Implementation method 2 Linear Regression + Include all stress results	5.36316	36.97%
	Load case 4 Fx	5.61433		5.51610	1.75%
	Load case 4 Fy	35.55308		11.47160	67.73%
	Load case 5 Fx	8.99715		8.98554	0.13%
	Load case 5 Fy	60.53509		57.33218	5.29%
	Load case 6 Fx	16.67995		12.76367	23.48%
	Load case 6 Fy	0.73707		0.73032	0.92%
	Load case 7 Fx	1.20528		1.18250	1.89%
	Load case 7 Fy	0.66822		0.66365	0.68%
	Load case 1 Fx	1.03863		1.03911	-0.05%
	Load case 1 Fy	5.71443		5.30784	7.12%
	Load case 2 Fx	1.16640		1.17027	-0.33%
	Load case 2 Fy	6.48991		5.67698	12.53%
	Load case 3 Fx	1.52449		1.52501	-0.03%
	Load case 3 Fy	8.50899	Implementation method 3 Linear Regression + Update to maximum stress result	5.41866	36.32%
	Load case 4 Fx	5.61433		5.64638	-0.57%
	Load case 4 Fy	35.55308		11.70889	67.07%
	Load case 5 Fx	8.99715		9.03834	-0.46%
	Load case 5 Fy	60.53509		57.37216	5.22%
	Load case 6 Fx	16.67995		13.11387	21.38%
	Load case 6 Fy	0.73707		0.76087	-3.23%
	Load case 7 Fx	1.20528		1.18495	1.69%
	Load case 7 Fy	0.66822		0.68416	-2.39%
	Load case 1 Fx	1.03863		1.03902	-0.04%
	Load case 1 Fy	5.71443		5.58723	2.23%
	Load case 2 Fx	1.16640		1.16682	-0.04%
	Load case 2 Fy	6.48991		6.34475	2.24%
	Load case 3 Fx	1.52449		1.52510	-0.04%
	Load case 3 Fy	8.50899	Implementation method 4 Linear Regression Eurocode	8.20704	3.55%
	Load case 4 Fx	5.61433		5.62528	-0.20%
	Load case 4 Fy	35.55308		36.03203	-1.35%
	Load case 5 Fx	8.99715		9.00170	-0.05%
	Load case 5 Fy	60.53509		60.61473	-0.13%
	Load case 6 Fx	16.67995		16.32083	2.15%
	Load case 6 Fy	0.73707		0.74122	-0.56%
	Load case 7 Fx	1.20528		1.20305	0.18%
	Load case 7 Fy	0.66822		0.67097	-0.41%

Table E.12 Model 4, Buckling factors for in-plane stresses (fig 8.21 check 2 and 3).

Plate field 200x150x4 T stiffener 20x4x20x4	Real load case	Femap buckling factor k≥1	Linearized load case	Femap buckling factor k≥1	Difference with real loads ≥0
	Load case 1 Fx	1.01513		1.01551	-0.04%
	Load case 1 Fy	5.70116		5.61647	1.49%
	Load case 2 Fx	1.14040		1.14081	-0.04%
	Load case 2 Fy	6.46092		6.36457	1.49%
	Load case 3 Fx	1.49090		1.49148	-0.04%
	Load case 3 Fy	8.41986	Implementation method 1 Linear Regression Average	8.31482	1.25%
	Load case 4 Fx	5.53354		5.53747	-0.07%
	Load case 4 Fy	32.16535		38.76153	-20.51%
	Load case 5 Fx	8.87022		8.87501	-0.05%
	Load case 5 Fy	59.19886		72.80770	-22.99%
	Load case 6 Fx	19.93868		19.36987	2.85%
	Load case 6 Fy	0.72047		0.72637	-0.82%
	Load case 7 Fx	1.19333		1.19135	0.17%
	Load case 7 Fy	0.65440		0.65832	-0.60%
	Load case 1 Fx	1.01513		1.01366	0.15%
	Load case 1 Fy	5.70116		5.33566	6.41%
	Load case 2 Fx	1.14040		1.13862	0.16%
	Load case 2 Fy	6.46092		5.58796	13.51%
	Load case 3 Fx	1.49090		1.48419	0.45%
	Load case 3 Fy	8.41986	Implementation method 2 Linear Regression + Include all stress results	5.77804	31.38%
	Load case 4 Fx	5.53354		5.40205	2.38%
	Load case 4 Fy	32.16535		13.66849	57.51%
	Load case 5 Fx	8.87022		8.84941	0.23%
	Load case 5 Fy	59.19886		52.32695	11.61%
	Load case 6 Fx	19.93868		14.92141	25.16%
	Load case 6 Fy	0.72047		0.71473	0.80%
	Load case 7 Fx	1.19333		1.17357	1.66%
	Load case 7 Fy	0.65440		0.65057	0.59%
	Load case 1 Fx	1.01513		1.01567	-0.05%
	Load case 1 Fy	5.70116		5.33566	6.41%
	Load case 2 Fx	1.14040		1.14356	-0.28%
	Load case 2 Fy	6.46092		5.76799	10.72%
	Load case 3 Fx	1.49090		1.48875	0.14%
	Load case 3 Fy	8.41986	Implementation method 3 Linear Regression + Update to maximum stress result	5.93815	29.47%
	Load case 4 Fx	5.53354		5.60660	-1.32%
	Load case 4 Fy	32.16535		14.26411	55.65%
	Load case 5 Fx	8.87022		8.88773	-0.20%
	Load case 5 Fy	59.19886		52.44481	11.41%
	Load case 6 Fx	19.93868		15.16292	23.95%
	Load case 6 Fy	0.72047		0.74391	-3.25%
	Load case 7 Fx	1.19333		1.17477	1.56%
	Load case 7 Fy	0.65440		0.67005	-2.39%
	Load case 1 Fx	1.01513		1.01551	-0.04%
	Load case 1 Fy	5.70116		5.58547	2.03%
	Load case 2 Fx	1.14040		1.14081	-0.04%
	Load case 2 Fy	6.46092		6.30209	2.46%
	Load case 3 Fx	1.49090		1.49148	-0.04%
	Load case 3 Fy	8.41986	Implementation method 4 Linear Regression Eurocode	8.02955	4.64%
	Load case 4 Fx	5.53354		5.53747	-0.07%
	Load case 4 Fy	32.16535		33.12802	-2.99%
	Load case 5 Fx	8.87022		8.87501	-0.05%
	Load case 5 Fy	59.19886		59.09967	0.17%
	Load case 6 Fx	19.93868		19.36987	2.85%
	Load case 6 Fy	0.72047		0.72397	-0.49%
	Load case 7 Fx	1.19333		1.19135	0.17%
	Load case 7 Fy	0.65440		0.65669	-0.35%

Table E.13 Model 5, Buckling factors for in-plane stresses (fig 8.21 check 2 and 3).

Plate field 200x150x4 T stiffener 40x4x40x4	Real load case	Femap buckling factor k≥1	Linearized load case	Femap buckling factor k≥1	Difference with real loads ≥0
	Load case 1 Fx	1.21044		1.21100	-0.05%
	Load case 1 Fy	6.36738		6.25673	1.74%
	Load case 2 Fx	1.35776		1.35837	-0.04%
	Load case 2 Fy	7.24521		7.12007	1.73%
	Load case 3 Fx	1.77558		1.77645	-0.05%
	Load case 3 Fy	9.52448	Implementation method 1 Linear Regression Average	9.39334	1.38%
	Load case 4 Fx	6.38085		6.37149	0.15%
	Load case 4 Fy	37.42377		47.24508	-26.24%
	Load case 5 Fx	10.00636		10.01260	-0.06%
	Load case 5 Fy	70.54436		84.93787	-20.40%
	Load case 6 Fx	11.30376		11.42946	-1.11%
	Load case 6 Fy	0.76613		0.77551	-1.22%
	Load case 7 Fx	1.33940		1.33672	0.20%
	Load case 7 Fy	0.69896		0.70559	-0.95%
	Load case 1 Fx	1.21044		1.20833	0.17%
	Load case 1 Fy	6.36738		5.88547	7.57%
	Load case 2 Fx	1.35776		1.35233	0.40%
	Load case 2 Fy	7.24521		6.15558	15.04%
	Load case 3 Fx	1.77558		1.72518	2.84%
	Load case 3 Fy	9.52448	Implementation method 2 Linear Regression + Include all stress results	6.36038	33.22%
	Load case 4 Fx	6.38085		5.71329	10.46%
	Load case 4 Fy	37.42377		16.12585	56.91%
	Load case 5 Fx	10.00636		9.95808	0.48%
	Load case 5 Fy	70.54436		54.72821	22.42%
	Load case 6 Fx	11.30376		9.15946	18.97%
	Load case 6 Fy	0.76613		0.75724	1.16%
	Load case 7 Fx	1.33940		1.30370	2.66%
	Load case 7 Fy	0.69896		0.69262	0.91%
	Load case 1 Fx	1.21044		1.21035	0.01%
	Load case 1 Fy	6.36738		5.88547	7.57%
	Load case 2 Fx	1.35776		1.35586	0.14%
	Load case 2 Fy	7.24521		6.45771	10.87%
	Load case 3 Fx	1.77558		1.75085	1.39%
	Load case 3 Fy	9.52448	Implementation method 3 Linear Regression + Update to maximum stress result	7.53053	20.93%
	Load case 4 Fx	6.38085		6.14476	3.70%
	Load case 4 Fy	37.42377		26.74924	28.52%
	Load case 5 Fx	10.00636		9.97770	0.29%
	Load case 5 Fy	70.54436		54.88886	22.19%
	Load case 6 Fx	11.30376		9.20577	18.56%
	Load case 6 Fy	0.76613		0.78887	-2.97%
	Load case 7 Fx	1.33940		1.30458	2.60%
	Load case 7 Fy	0.69896		0.71459	-2.24%
	Load case 1 Fx	1.21044		1.21100	-0.05%
	Load case 1 Fy	6.36738		6.21029	2.47%
	Load case 2 Fx	1.35776		1.35837	-0.04%
	Load case 2 Fy	7.24521		7.02515	3.04%
	Load case 3 Fx	1.77558		1.77645	-0.05%
	Load case 3 Fy	9.52448	Implementation method 4 Linear Regression Eurocode	8.95022	6.03%
	Load case 4 Fx	6.38085		6.37149	0.15%
	Load case 4 Fy	37.42377		38.50702	-2.89%
	Load case 5 Fx	10.00636		10.01260	-0.06%
	Load case 5 Fy	70.54436		69.01228	2.17%
	Load case 6 Fx	11.30376		11.42946	-1.11%
	Load case 6 Fy	0.76613		0.77127	-0.67%
	Load case 7 Fx	1.33940		1.33672	0.20%
	Load case 7 Fy	0.69896		0.70255	-0.51%

Table E.14 Model 6, Buckling factors for in-plane stresses (fig 8.21 check 2 and 3).

Plate field 600x150x4 Bar stiffener 20x4	Real load case	Femap buckling factor k≥1	Linearized load case	Femap buckling factor k≥1	Difference with real loads ≥0
	Load case 1 Fx	0.87017		0.87025	-0.01%
	Load case 1 Fy	9.42426		7.63596	18.98%
	Load case 2 Fx	0.97813		0.97824	-0.01%
	Load case 2 Fy	10.69000		8.61147	19.44%
	Load case 3 Fx	1.27844		1.27875	-0.02%
	Load case 3 Fy	13.99194	Implementation method 1 Linear Regression Average	11.30370	19.21%
	Load case 4 Fx	4.79636		4.80435	-0.17%
	Load case 4 Fy	47.72073		45.46400	4.73%
	Load case 5 Fx	7.73426		7.73467	-0.01%
	Load case 5 Fy	67.98957		74.39715	-9.42%
	Load case 6 Fx	19.07210		19.21582	-0.75%
	Load case 6 Fy	0.66585		0.68105	-2.28%
	Load case 7 Fx	1.02957		1.02954	0.00%
	Load case 7 Fy	0.63246		0.63569	-0.51%
	Load case 1 Fx	0.87017		0.86982	0.04%
	Load case 1 Fy	9.42426		5.04836	46.43%
	Load case 2 Fx	0.97813		0.97776	0.04%
	Load case 2 Fy	10.69000		5.62317	47.40%
	Load case 3 Fx	1.27844		1.27798	0.04%
	Load case 3 Fy	13.99194	Implementation method 2 Linear Regression + Include all stress results	7.40249	47.09%
	Load case 4 Fx	4.79636		4.79887	-0.05%
	Load case 4 Fy	47.72073		20.41928	57.21%
	Load case 5 Fx	7.73426		7.73103	0.04%
	Load case 5 Fy	67.98957		31.10751	54.25%
	Load case 6 Fx	19.07210		18.75996	1.64%
	Load case 6 Fy	0.66585		0.65569	1.53%
	Load case 7 Fx	1.02957		1.02901	0.05%
	Load case 7 Fy	0.63246		0.63017	0.36%
	Load case 1 Fx	0.87017		0.87073	-0.07%
	Load case 1 Fy	9.42426		5.14567	45.40%
	Load case 2 Fx	0.97813		0.97921	-0.11%
	Load case 2 Fy	10.69000		5.74003	46.30%
	Load case 3 Fx	1.27844		1.28010	-0.13%
	Load case 3 Fy	13.99194	Implementation method 3 Linear Regression + Update to maximum stress result	7.41658	46.99%
	Load case 4 Fx	4.79636		4.81293	-0.35%
	Load case 4 Fy	47.72073		20.52762	56.98%
	Load case 5 Fx	7.73426		7.74777	-0.17%
	Load case 5 Fy	67.98957		31.62178	53.49%
	Load case 6 Fx	19.07210		18.77119	1.58%
	Load case 6 Fy	0.66585		0.65606	1.47%
	Load case 7 Fx	1.02957		1.02915	0.04%
	Load case 7 Fy	0.63246		0.63055	0.30%
	Load case 1 Fx	0.87017		0.87025	-0.01%
	Load case 1 Fy	9.42426		7.58768	19.49%
	Load case 2 Fx	0.97813		0.97824	-0.01%
	Load case 2 Fy	10.69000		8.42965	21.14%
	Load case 3 Fx	1.27844		1.27875	-0.02%
	Load case 3 Fy	13.99194	Implementation method 4 Linear Regression Eurocode	11.12986	20.46%
	Load case 4 Fx	4.79636		4.80435	-0.17%
	Load case 4 Fy	47.72073		32.03455	32.87%
	Load case 5 Fx	7.73426		7.73467	-0.01%
	Load case 5 Fy	67.98957		43.75253	35.65%
	Load case 6 Fx	19.07210		19.21582	-0.75%
	Load case 6 Fy	0.66585		0.68052	-2.20%
	Load case 7 Fx	1.02957		1.02954	0.00%
	Load case 7 Fy	0.63246		0.63550	-0.48%

Table E.15 Model 7, Buckling factors for in-plane stresses (fig 8.21 check 2 and 3).

Plate field 200x400x4 Bar stiffener 20x4	Real load case	Femap buckling factor k≥1	Linearized load case	Femap buckling factor k≥1	Difference with real loads ≥0
	Load case 1 Fx	0.42339		0.42307	0.08%
	Load case 1 Fy	5.05956		5.07321	-0.27%
	Load case 2 Fx	0.48144		0.48103	0.08%
	Load case 2 Fy	5.77354		5.77906	-0.10%
	Load case 3 Fx	0.62885		0.62810	0.12%
	Load case 3 Fy	7.45887	Implementation method 1 Linear Regression Average	7.46198	-0.04%
	Load case 4 Fx	3.18738		3.18127	0.19%
	Load case 4 Fy	37.85135		43.52303	-14.98%
	Load case 5 Fx	6.21954		6.22377	-0.07%
	Load case 5 Fy	82.59242		124.49400	-50.73%
	Load case 6 Fx	192.57940		3.65721	98.10%
	Load case 6 Fy	1.58457		1.63309	-3.06%
	Load case 7 Fx	0.62402		0.61811	0.95%
	Load case 7 Fy	1.27666		1.29873	-1.73%
	Load case 1 Fx	0.42339		0.42266	0.17%
	Load case 1 Fy	5.05956		5.01808	0.82%
	Load case 2 Fx	0.48144		0.48037	0.22%
	Load case 2 Fy	5.77354		5.68234	1.58%
	Load case 3 Fx	0.62885		0.62651	0.37%
	Load case 3 Fy	7.45887	Implementation method 2 Linear Regression + Include all stress results	7.13518	4.34%
	Load case 4 Fx	3.18738		3.15153	1.13%
	Load case 4 Fy	37.85135		35.03580	7.44%
	Load case 5 Fx	6.21954		6.20073	0.30%
	Load case 5 Fy	82.59242		117.57950	-42.36%
	Load case 6 Fx	192.57940		4.52947	97.65%
	Load case 6 Fy	1.58457		1.60636	-1.37%
	Load case 7 Fx	0.62402		0.59914	3.99%
	Load case 7 Fy	1.27666		1.28324	-0.52%
	Load case 1 Fx	0.42339		0.42288	0.12%
	Load case 1 Fy	5.05956		5.02602	0.66%
	Load case 2 Fx	0.48144		0.48090	0.11%
	Load case 2 Fy	5.77354		5.70810	1.13%
	Load case 3 Fx	0.62885		0.62705	0.29%
	Load case 3 Fy	7.45887	Implementation method 3 Linear Regression + Update to maximum stress result	7.26413	2.61%
	Load case 4 Fx	3.18738		3.16551	0.69%
	Load case 4 Fy	37.85135		37.85544	-0.01%
	Load case 5 Fx	6.21954		6.27790	-0.94%
	Load case 5 Fy	82.59242		117.64080	-42.44%
	Load case 6 Fx	192.57940		4.35897	97.74%
	Load case 6 Fy	1.58457		1.68072	-6.07%
	Load case 7 Fx	0.62402		0.60216	3.50%
	Load case 7 Fy	1.27666		1.32592	-3.86%
	Load case 1 Fx	0.42339		0.42307	0.08%
	Load case 1 Fy	5.05956		4.95572	2.05%
	Load case 2 Fx	0.48144		0.48103	0.08%
	Load case 2 Fy	5.77354		5.67930	1.63%
	Load case 3 Fx	0.62885		0.62810	0.12%
	Load case 3 Fy	7.45887	Implementation method 4 Linear Regression Eurocode	7.35538	1.39%
	Load case 4 Fx	3.18738		3.18127	0.19%
	Load case 4 Fy	37.85135		36.78675	2.81%
	Load case 5 Fx	6.21954		6.22377	-0.07%
	Load case 5 Fy	82.59242		85.11327	-3.05%
	Load case 6 Fx	192.57940		3.65721	98.10%
	Load case 6 Fy	1.58457		1.53366	3.21%
	Load case 7 Fx	0.62402		0.61811	0.95%
	Load case 7 Fy	1.27666		1.24079	2.81%

Table E.16 Model 8, Buckling factors for in-plane stresses (fig 8.21 check 2 and 3).

Plate field 200x150x3 Bar stiffener 20x4	Real load case	Femap buckling factor k≥1	Linearized load case	Femap buckling factor k≥1	Difference with real loads ≥0
	Load case 1	161.5079		358.3403	-121.87%
	Load case 2	8.9908		9.1009	-1.22%
	Load case 3	2.9711		2.9755	-0.15%
	Load case 4	2.9794	Average Shear	2.9773	0.07%
	Load case 5	118.9145		479.8745	-303.55%
	Load case 6	105.1972		76.1197	27.64%
	Load case 7	124.5463		91.6996	26.37%
	Load case 1	161.5079		323.6876	-100.42%
	Load case 2	8.9908		9.1009	-1.22%
	Load case 3	2.9711		2.9755	-0.15%
	Load case 4	2.9794	Absolute Average Shear	2.9773	0.07%
	Load case 5	118.9145		84.4175	29.01%
	Load case 6	105.1972		75.5025	28.23%
	Load case 7	124.5463		91.6477	26.41%
	Load case 1	161.5079		96.5987	40.19%
	Load case 2	8.9908		8.6523	3.77%
	Load case 3	2.9711		2.8696	3.42%
	Load case 4	2.9794	Absolute Max Shear	2.7687	7.07%
	Load case 5	118.9145		54.0289	54.56%
	Load case 6	105.1972		21.2072	79.84%
	Load case 7	124.5463		25.7258	79.34%

Table E.17 Model 1, Buckling factors for shear stresses (fig 8.21 check 4).

Plate field 200x150x4 Bar stiffener 20x4	Real load case	Femap buckling factor k≥1	Linearized load case	Femap buckling factor k≥1	Difference with real loads ≥0
	Load case 1	362.1116		780.6334	-115.58%
	Load case 2	21.0957		21.3645	-1.27%
	Load case 3	6.9619		6.9756	-0.20%
	Load case 4	6.9847	Average Shear	6.9786	0.09%
	Load case 5	325.3145		1083.2150	-232.97%
	Load case 6	240.2345		174.2074	27.48%
	Load case 7	288.1987		212.0748	26.41%
	Load case 1	362.1116		724.1324	-99.97%
	Load case 2	21.0957		21.3645	-1.27%
	Load case 3	6.9619		6.9756	-0.20%
	Load case 4	6.9847	Absolute Average Shear	6.9786	0.09%
	Load case 5	325.3145		229.8916	29.33%
	Load case 6	240.2345		173.4228	27.81%
	Load case 7	288.1987		212.0748	26.41%
	Load case 1	362.1116		213.0111	41.18%
	Load case 2	21.0957		20.4671	2.98%
	Load case 3	6.9619		6.7572	2.94%
	Load case 4	6.9847	Absolute Max Shear	6.5549	6.15%
	Load case 5	325.3145		144.8815	55.46%
	Load case 6	240.2345		48.5485	79.79%
	Load case 7	288.1987		59.3744	79.40%

Table E.18 Model 2, Buckling factors for shear stresses (fig 8.21 check 4).

Plate field 200x150x5 Bar stiffener 20x4	Real load case	Femap buckling factor k≥1	Linearized load case	Femap buckling factor k≥1	Difference with real loads ≥0
	Load case 1	672.6210		1436.2030	-113.52%
	Load case 2	40.7710		41.3132	-1.33%
	Load case 3	13.4450		13.4759	-0.23%
	Load case 4	13.4929	Average Shear	13.4798	0.10%
	Load case 5	714.1860		2050.1800	-187.07%
	Load case 6	457.3314		330.9559	27.63%
	Load case 7	553.7399		405.7531	26.72%
	Load case 1	672.6210		1346.5880	-100.20%
	Load case 2	40.7710		41.3132	-1.33%
	Load case 3	13.4450		13.4759	-0.23%
	Load case 4	13.4929	Absolute Average Shear	13.4798	0.10%
	Load case 5	714.1860		504.9014	29.30%
	Load case 6	457.3314		329.2287	28.01%
	Load case 7	553.7399		405.7085	26.73%
	Load case 1	672.6210		388.5370	42.24%
	Load case 2	40.7710		39.7840	2.42%
	Load case 3	13.4450		13.0901	2.64%
	Load case 4	13.4929	Absolute Max Shear	12.7515	5.49%
	Load case 5	714.1860		313.4432	56.11%
	Load case 6	457.3314		91.6395	79.96%
	Load case 7	553.7399		112.9524	79.60%

Table E.19 Model 3, Buckling factors for shear stresses (fig 8.21 check 4).

Plate field 200x150x4 Bar stiffener 40x4	Real load case	Femap buckling factor k≥1	Linearized load case	Femap buckling factor k≥1	Difference with real loads ≥0
	Load case 1	359.1044		860.4590	-139.61%
	Load case 2	21.3953		21.6936	-1.39%
	Load case 3	7.0852		7.0933	-0.12%
	Load case 4	7.1134	Average Shear	7.0982	0.21%
	Load case 5	355.0072		1133.1250	-219.18%
	Load case 6	251.8614		170.0117	32.50%
	Load case 7	295.9977		201.9300	31.78%
	Load case 1	359.1044		578.8661	-61.20%
	Load case 2	21.3953		21.6936	-1.39%
	Load case 3	7.0852		7.0933	-0.12%
	Load case 4	7.1134	Absolute Average Shear	7.0982	0.21%
	Load case 5	355.0072		252.2054	28.96%
	Load case 6	251.8614		115.4052	54.18%
	Load case 7	295.9977		137.3040	53.61%
	Load case 1	359.1044		236.4367	34.16%
	Load case 2	21.3953		20.1409	5.86%
	Load case 3	7.0852		6.7291	5.03%
	Load case 4	7.1134	Absolute Max Shear	6.6024	7.18%
	Load case 5	355.0072		156.7688	55.84%
	Load case 6	251.8614		49.5075	80.34%
	Load case 7	295.9977		59.4698	79.91%

Table E.20 Model 4, Buckling factors for shear stresses (fig 8.21 check 4).

Plate field 200x150x4 T stiffener 20x4x20x4	Real load case	Femap buckling factor k≥1	Linearized load case	Femap buckling factor k≥1	Difference with real loads ≥0
	Load case 1	380.1507		813.6250	-114.03%
	Load case 2	21.7865		22.0854	-1.37%
	Load case 3	7.1953		7.2136	-0.25%
	Load case 4	7.2175	Average Shear	7.2140	0.05%
	Load case 5	348.6638		1208.1880	-246.52%
	Load case 6	233.5367		164.8859	29.40%
	Load case 7	275.0265		196.8007	28.44%
	Load case 1	380.1507		652.9348	-71.76%
	Load case 2	21.7865		22.0854	-1.37%
	Load case 3	7.1953		7.2136	-0.25%
	Load case 4	7.2175	Absolute Average Shear	7.2140	0.05%
	Load case 5	348.6638		254.1730	27.10%
	Load case 6	233.5367		143.0707	38.74%
	Load case 7	275.0265		173.1786	37.03%
	Load case 1	380.1507		252.5396	33.57%
	Load case 2	21.7865		20.6925	5.02%
	Load case 3	7.1953		6.8756	4.44%
	Load case 4	7.2175	Absolute Max Shear	6.7517	6.45%
	Load case 5	348.6638		154.8393	55.59%
	Load case 6	233.5367		53.4604	77.11%
	Load case 7	275.0265		64.3174	76.61%

Table E.21 Model 5, Buckling factors for shear stresses (fig 8.21 check 4).

Plate field 200x150x4 T stiffener 40x4x40x4	Real load case	Femap buckling factor k≥1	Linearized load case	Femap buckling factor k≥1	Difference with real loads ≥0
	Load case 1	404.9591		1052.9930	-160.02%
	Load case 2	22.4857		23.0823	-2.65%
	Load case 3	7.4607		7.5654	-1.40%
	Load case 4	7.4987	Average Shear	7.5715	-0.97%
	Load case 5	405.5971		1330.4830	-228.03%
	Load case 6	261.3397		195.1384	25.33%
	Load case 7	301.7133		229.1178	24.06%
	Load case 1	404.9591		571.5749	-41.14%
	Load case 2	22.4857		23.0823	-2.65%
	Load case 3	7.4607		7.5654	-1.40%
	Load case 4	7.4987	Absolute Average Shear	7.5715	-0.97%
	Load case 5	405.5971		316.8343	21.88%
	Load case 6	261.3397		96.0522	63.25%
	Load case 7	301.7133		110.9575	63.22%
	Load case 1	404.9591		306.4421	24.33%
	Load case 2	22.4857		21.0644	6.32%
	Load case 3	7.4607		7.0691	5.25%
	Load case 4	7.4987	Absolute Max Shear	7.0926	5.42%
	Load case 5	405.5971		181.6196	55.22%
	Load case 6	261.3397		51.7708	80.19%
	Load case 7	301.7133		59.5944	80.25%

Table E.22 Model 6, Buckling factors for shear stresses (fig 8.21 check 4).

Plate field 600x150x4 Bar stiffener 20x4	Real load case	Femap buckling factor k≥1	Linearized load case	Femap buckling factor k≥1	Difference with real loads ≥0
	Load case 1	80.3265		530.0159	-559.83%
	Load case 2	13.4816		4.6022	65.86%
	Load case 3	4.7160		1.5425	67.29%
	Load case 4	4.7636	Average Shear	1.5456	67.55%
	Load case 5	93.3343		6123.0790	-6460.38%
	Load case 6	283.9318		337.8250	-18.98%
	Load case 7	892.9224		689.4133	22.79%
	Load case 1	80.3265		186.1416	-131.73%
	Load case 2	13.4816		4.6022	65.86%
	Load case 3	4.7160		1.5425	67.29%
	Load case 4	4.7636	Absolute Average Shear	1.5456	67.55%
	Load case 5	93.3343		60.1505	35.55%
	Load case 6	283.9318		174.9780	38.37%
	Load case 7	892.9224		582.0562	34.81%
	Load case 1	80.3265		38.2976	52.32%
	Load case 2	13.4816		4.1891	68.93%
	Load case 3	4.7160		1.4989	68.22%
	Load case 4	4.7636	Absolute Max Shear	1.4852	68.82%
	Load case 5	93.3343		35.4326	62.04%
	Load case 6	283.9318		36.2920	87.22%
	Load case 7	892.9224		149.0325	83.31%

Table E.23 Model 7, Buckling factors for shear stresses (fig 8.21 check 4).

Plate field 200x400x4 Bar stiffener 20x4	Real load case	Femap buckling factor k≥1	Linearized load case	Femap buckling factor k≥1	Difference with real loads ≥0
	Load case 1	95.3750		178.0128	-86.65%
	Load case 2	89.6385		35.1664	60.77%
	Load case 3	19.0414		10.4704	45.01%
	Load case 4	13.1157	Average Shear	9.9931	23.81%
	Load case 5	41.5628		755.2192	-1717.06%
	Load case 6	3.7900		22.2114	-486.05%
	Load case 7	4.1902		24.6743	-488.85%
	Load case 1	95.3750		178.0128	-86.65%
	Load case 2	89.6385		35.1664	60.77%
	Load case 3	19.0414		10.4704	45.01%
	Load case 4	13.1157	Absolute Average Shear	9.9931	23.81%
	Load case 5	41.5628		353.8747	-751.42%
	Load case 6	3.7900		22.2028	-485.82%
	Load case 7	4.1902		24.6584	-488.47%
	Load case 1	95.3750		49.8111	47.77%
	Load case 2	89.6385		29.4343	67.16%
	Load case 3	19.0414		9.9456	47.77%
	Load case 4	13.1157	Absolute Max Shear	9.4616	27.86%
	Load case 5	41.5628		169.3804	-307.53%
	Load case 6	3.7900		6.4578	-70.39%
	Load case 7	4.1902		7.2036	-71.91%

Table E.24 Model 8, Buckling factors for shear stresses (fig 8.21 check 4).

Appendix F (Stiffener web Real In-plane Stress Results)

Fig F.1 Model 2, stiffener web, Load case 1, Linear stress results.

Fig F.2 Model 2, stiffener web, Load case 6, Linear stress results.

Fig F.3 Model 2, stiffener web, Load case 7, Linear stress results.
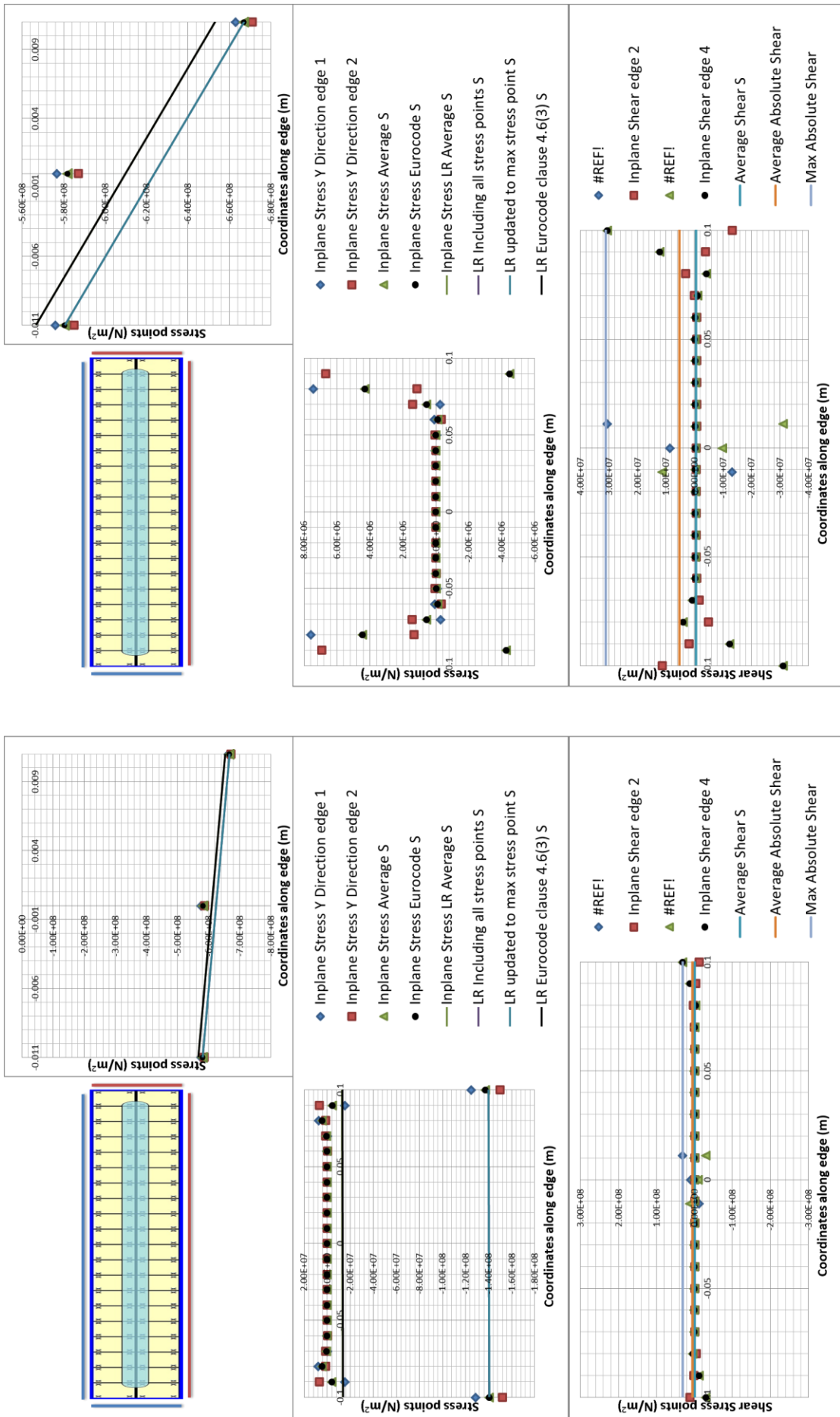
Fig F.1 Model 2, stiffener web, Load case 1, Linear stress results.
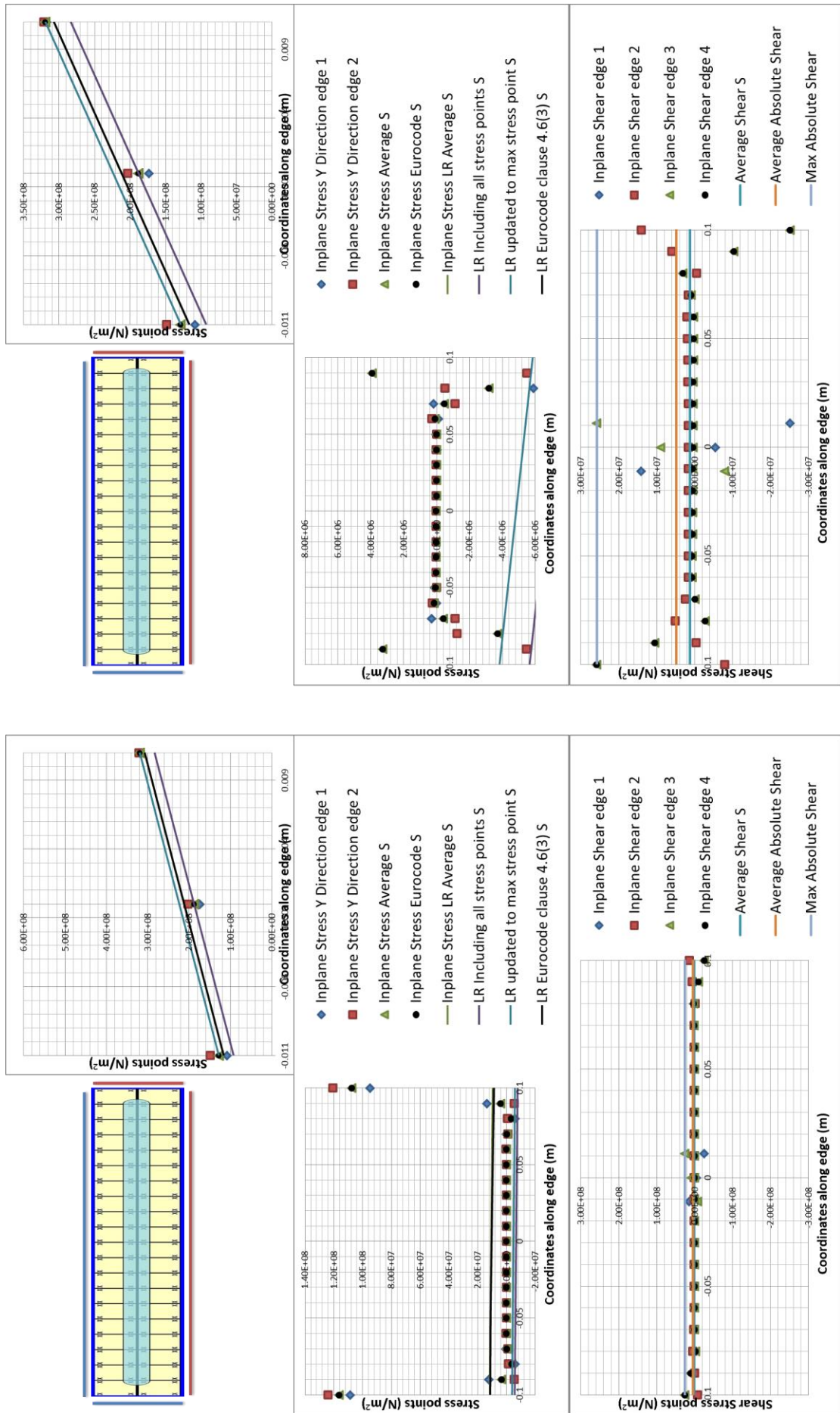
Fig F.2 Model 2, stiffener web, Load case 6, Linear stress results.
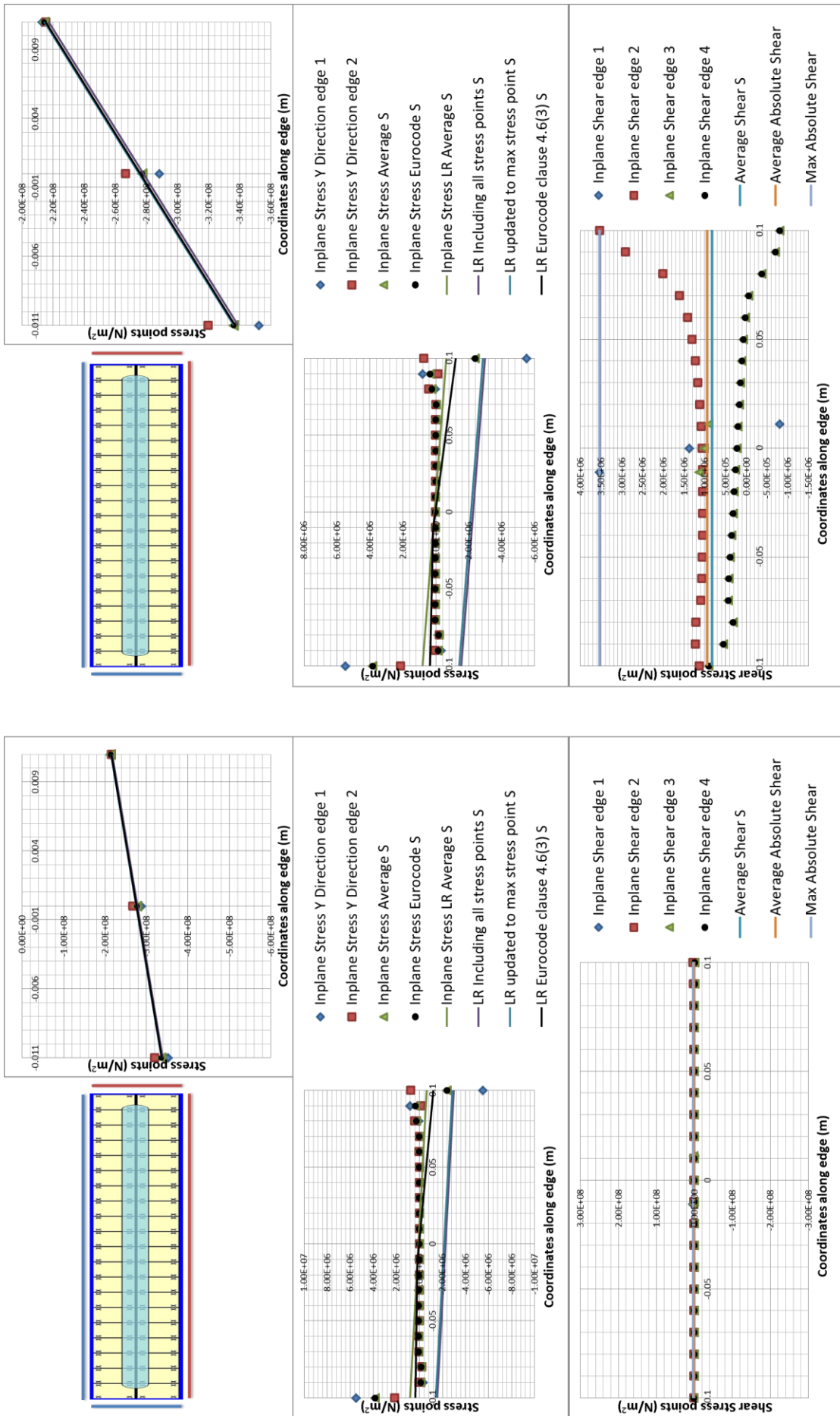
Fig F.3 Model 2, stiffener web, Load case 7, Linear stress results.

Appendix G (Stiffener web comparison Mesh Sizes)

Fig G.1 Plate model, stiffener web, Load case 1, Linear stress results, mesh size comparison.

Fig G.2 Plate model, stiffener web, Load case 6, Linear stress results, mesh size comparison.

Fig G.3 Plate model, stiffener web, Load case 7, Linear stress results, mesh size comparison.

Fig G.1 Plate model, stiffener web, Load case 1, Linear stress results, mesh size comparison.

Fig G.2 Plate model, stiffener web, Load case 6, Linear stress results, mesh size comparison.

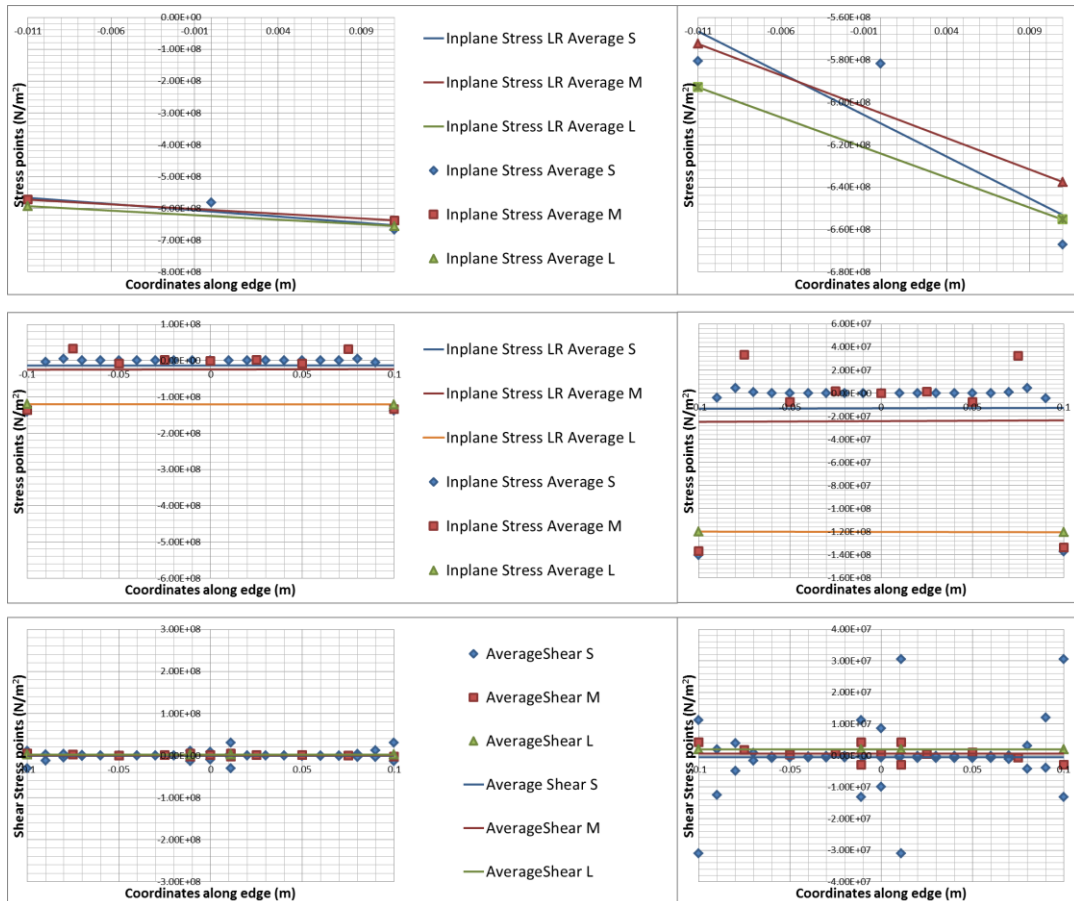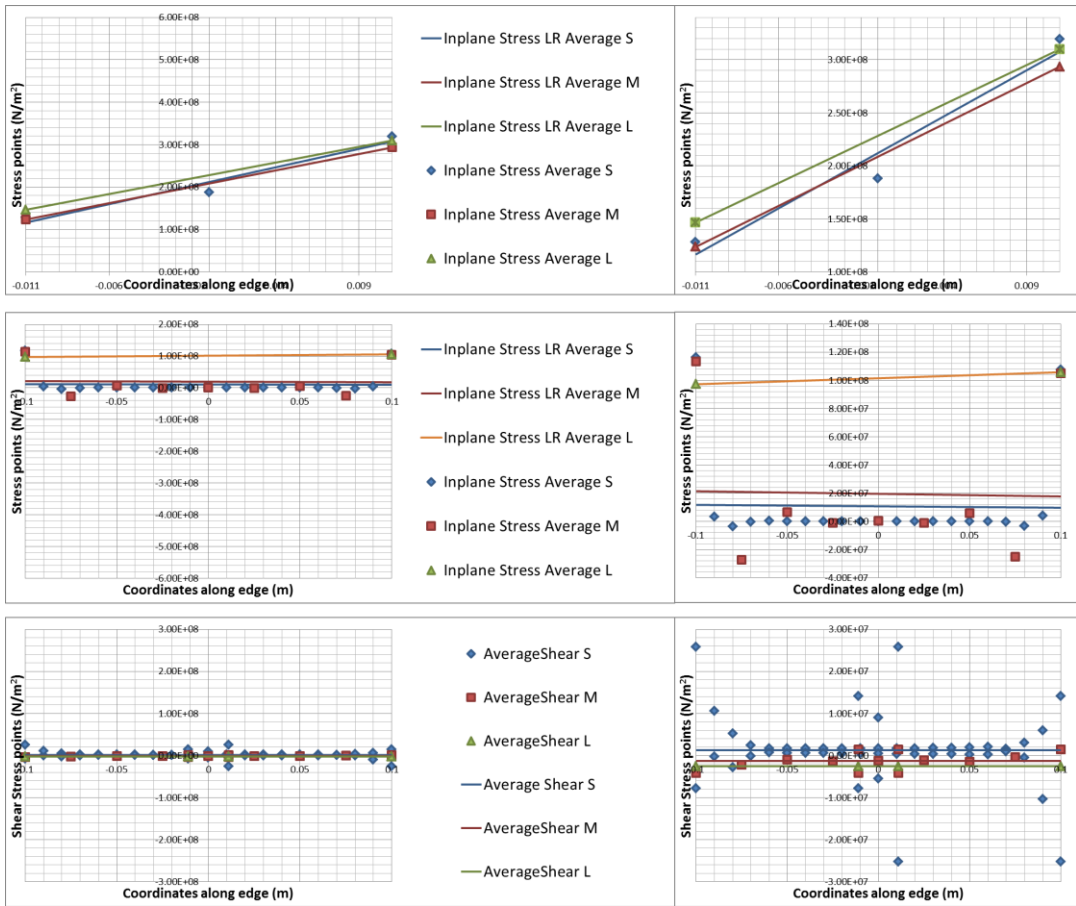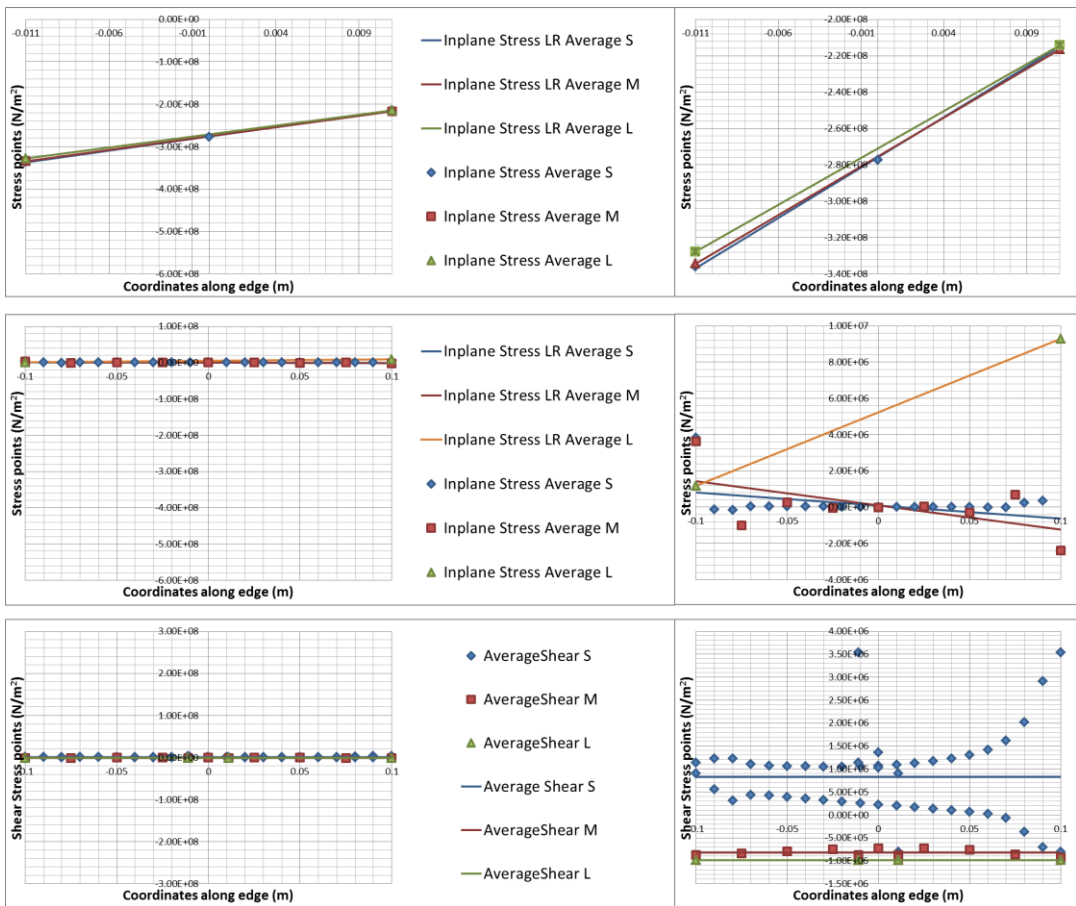Fig G.3 Plate model, stiffener web, Load case 7, Linear stress results, mesh size comparison.

Appendix H (Stiffener web implementation comparison)

Plate field 200x150x4 Bar stiffener 20x4		σxmax web	σxmin web	τ web	Difference Fine beam model and Single element beam model			Difference Fine beam model and Fine plate model		
Load case 1	SDC beam model fine	6.336E+08	5.739E+08	5.119E+05						
	SDC beam model coarse	6.326E+08	5.744E+08	5.313E+05	-0.42%	-4.55%	-54.23%			
	SDC beam model single element	6.363E+08	6.013E+08	1.118E+06				-2.99%	1.29%	-7.16%
	SDC plate model fine (average LR and average shear)	6.531E+08	5.666E+08	5.513E+05						
	SDC plate model single element (average LR and average shear)	6.553E+08	5.930E+08	1.935E+06						
Load case 2	SDC beam model fine	5.491E+08	4.974E+08	4.436E+05						
	SDC beam model coarse	5.483E+08	4.978E+08	4.605E+05	-0.42%	-4.55%	-54.23%			
	SDC beam model single element	5.515E+08	5.211E+08	9.693E+05				-2.98%	1.29%	-6.59%
	SDC plate model fine (average LR and average shear)	5.660E+08	4.911E+08	4.749E+05						
	SDC plate model single element (average LR and average shear)	5.679E+08	5.139E+08	1.677E+06						
Load case 3	SDC beam model fine	4.224E+08	3.826E+08	3.413E+05						
	SDC beam model coarse	4.217E+08	3.829E+08	3.542E+05	-0.42%	-4.55%	-54.23%			
	SDC beam model single element	4.242E+08	4.009E+08	7.456E+05				-2.99%	1.29%	-7.26%
	SDC plate model fine (average LR and average shear)	4.354E+08	3.778E+08	3.680E+05						
	SDC plate model single element (average LR and average shear)	4.369E+08	3.953E+08	1.290E+06						
Load case 4	SDC beam model fine	4.224E+07	3.826E+07	3.413E+04						
	SDC beam model coarse	4.217E+07	3.829E+07	3.543E+04	-0.42%	-4.55%	-54.23%			
	SDC beam model single element	4.242E+07	4.009E+07	7.456E+04				-1.92%	1.26%	64.26%
	SDC plate model fine (average LR and average shear)	4.307E+07	3.779E+07	2.077E+04						
	SDC plate model single element (average LR and average shear)	4.369E+07	3.953E+07	1.290E+05						
Load case 5	SDC beam model fine	0.000E+00	0.000E+00	6.050E-07						
	SDC beam model coarse	0.000E+00	0.000E+00	2.438E-07	-	-	-	-	-	-
	SDC beam model single element	0.000E+00	0.000E+00	1.084E-08						
	SDC plate model fine (average LR and average shear)	9.771E+03	5.339E+03	1.821E+04	Note, Tension stresses.			Note, Tension stresses.		
	SDC plate model single element (average LR and average shear)	0.000E+00	0.000E+00	0.000E+00						
Load case 6	SDC beam model fine	1.100E+08	2.437E+08	7.488E+05						
	SDC beam model coarse	1.098E+08	2.362E+08	7.937E+05	159.88%	179.51%	-73.17%			
	SDC beam model single element	4.233E+07	8.718E+07	2.791E+06				-5.55%	-20.77%	-41.08%
	SDC plate model fine (average LR and average shear)	1.165E+08	3.076E+08	1.271E+06	Note, Tension stresses.			Note, Tension stresses.		
	SDC plate model single element (average LR and average shear)	1.467E+08	3.100E+08	2.534E+06						
Load case 7	SDC beam model fine	3.427E+08	2.560E+08	3.427E+05						
	SDC beam model coarse	3.418E+08	2.601E+08	3.750E+05	-11.00%	-30.48%	-81.93%			
	SDC beam model single element	3.850E+08	3.682E+08	1.897E+06				1.73%	19.08%	-58.69%
	SDC plate model fine (average LR and average shear)	3.368E+08	2.149E+08	8.297E+05						
	SDC plate model single element (average LR and average shear)	3.277E+08	2.143E+08	9.865E+05						

Table H.1 Stiffener web stress results derived by the implementation method from beam elements and by the implementation method from plate elements.

Appendix I (Beam-column Tables)

200x150x3 Bar20x4		SDC fine model with the implementation method	SDC Coarse model implementation method	SDC Single element model implementation method	Fine model with plate results taken into account	Difference SDC Fine and SDC Single element	Difference SDC Coarse and SDC Single element	Difference SDC Fine and results from plate elements
Load case 1	σxmax	-7.428E+08	-7.428E+08	-7.592E+08	-7.576E+08	-2.16%	-2.15%	-1.96%
Load case 2	σxmax	-6.438E+08	-6.438E+08	-6.579E+08	-6.566E+08	-2.16%	-2.15%	-1.96%
Load case 3	σxmax	-4.952E+08	-4.952E+08	-5.061E+08	-5.051E+08	-2.16%	-2.15%	-1.96%
Load case 4	σxmax	-4.952E+07	-4.952E+07	-5.061E+07	-5.051E+07	-2.16%	-2.15%	-1.96%
Load case 7	σxmax	-4.459E+08	-4.446E+08	-4.807E+08	-6.010E+08	-7.24%	-7.52%	-25.79%

200x150x4 Bar20x4		SDC fine model with the implementation method	SDC Coarse model implementation method	SDC Single element model implementation method	Fine model with plate results taken into account	Difference SDC Fine and SDC Single element	Difference SDC Coarse and SDC Single element	Difference SDC Fine and results from plate elements
Load case 1	σxmax	-5.772E+08	-5.775E+08	-5.994E+08	-5.859E+08	-3.70%	-3.66%	-1.49%
Load case 2	σxmax	-5.003E+08	-5.005E+08	-5.195E+08	-5.078E+08	-3.70%	-3.66%	-1.49%
Load case 3	σxmax	-3.848E+08	-3.850E+08	-3.996E+08	-3.906E+08	-3.70%	-3.66%	-1.49%
Load case 4	σxmax	-3.848E+07	-3.850E+07	-3.996E+07	-3.906E+07	-3.70%	-3.66%	-1.49%
Load case 7	σxmax	-3.371E+08	-3.365E+08	-3.773E+08	-4.584E+08	-10.66%	-10.82%	-26.46%

200x150x5 Bar20x4		SDC fine model with the implementation method	SDC Coarse model implementation method	SDC Single element model implementation method	Fine model with plate results taken into account	Difference SDC Fine and SDC Single element	Difference SDC Coarse and SDC Single element	Difference SDC Fine and results from plate elements
Load case 1	σxmax	-4.726E+08	-4.730E+08	-4.959E+08	-4.779E+08	-4.69%	-4.60%	-1.11%
Load case 2	σxmax	-4.096E+08	-4.100E+08	-4.297E+08	-4.142E+08	-4.69%	-4.60%	-1.11%
Load case 3	σxmax	-3.151E+08	-3.154E+08	-3.306E+08	-3.186E+08	-4.69%	-4.60%	-1.11%
Load case 4	σxmax	-3.151E+07	-3.154E+07	-3.306E+07	-3.186E+07	-4.69%	-4.60%	-1.11%
Load case 7	σxmax	-2.708E+08	-2.703E+08	-3.099E+08	-3.703E+08	-12.63%	-12.78%	-26.89%

200x150x4 Bar40x4		SDC fine model with the implementation method	SDC Coarse model implementation method	SDC Single element model implementation method	Fine model with plate results taken into account	Difference SDC Fine and SDC Single element	Difference SDC Coarse and SDC Single element	Difference SDC Fine and results from plate elements
Load case 1	σxmax	-5.294E+08	-5.301E+08	-5.396E+08	-6.051E+08	-1.89%	-1.76%	-12.52%
Load case 2	σxmax	-4.588E+08	-4.594E+08	-4.676E+08	-5.244E+08	-1.89%	-1.76%	-12.52%
Load case 3	σxmax	-3.529E+08	-3.534E+08	-3.597E+08	-4.034E+08	-1.89%	-1.76%	-12.52%
Load case 4	σxmax	-3.529E+07	-3.534E+07	-3.597E+07	-4.034E+07	-1.89%	-1.76%	-12.52%
Load case 7	σxmax	-3.231E+08	-3.281E+08	-3.736E+08	-4.699E+08	-13.51%	-12.17%	-31.23%

200x150x4 T20x4x20x4		SDC fine model with the implementation method	SDC Coarse model implementation method	SDC Single element model implementation method	Fine model with plate results taken into account	Difference SDC Fine and SDC Single element	Difference SDC Coarse and SDC Single element	Difference SDC Fine and results from plate elements
Load case 1	σxmax	-5.339E+08	-5.351E+08	-5.545E+08	-6.021E+08	-3.70%	-3.48%	-11.32%
Load case 2	σxmax	-4.627E+08	-4.638E+08	-4.805E+08	-5.218E+08	-3.70%	-3.48%	-11.32%
Load case 3	σxmax	-3.559E+08	-3.568E+08	-3.696E+08	-4.014E+08	-3.70%	-3.48%	-11.32%
Load case 4	σxmax	-3.559E+07	-3.568E+07	-3.696E+07	-4.014E+07	-3.70%	-3.48%	-11.32%
Load case 7	σxmax	-3.220E+08	-3.266E+08	-3.776E+08	-4.681E+08	-14.71%	-13.50%	-31.21%

200x150x4 T40x4x40x4		SDC fine model with the implementation method	SDC Coarse model implementation method	SDC Single element model implementation method	Fine model with plate results taken into account	Difference SDC Fine and SDC Single element	Difference SDC Coarse and SDC Single element	Difference SDC Fine and results from plate elements
Load case 1	σxmax	-4.571E+08	-4.579E+08	-4.641E+08	-6.323E+08	-1.50%	-1.34%	-27.71%
Load case 2	σxmax	-3.962E+08	-3.968E+08	-4.022E+08	-5.480E+08	-1.50%	-1.34%	-27.71%
Load case 3	σxmax	-3.048E+08	-3.052E+08	-3.094E+08	-4.216E+08	-1.50%	-1.34%	-27.71%
Load case 4	σxmax	-3.048E+07	-3.052E+07	-3.094E+07	-4.216E+07	-1.50%	-1.34%	-27.71%
Load case 7	σxmax	-2.858E+08	-2.918E+08	-3.423E+08	-4.868E+08	-16.50%	-14.77%	-41.28%

600x150x4 Bar20x4		SDC fine model with the implementation method	SDC Coarse model implementation method	SDC Single element model implementation method	Fine model with plate results taken into account	Difference SDC Fine and SDC Single element	Difference SDC Coarse and SDC Single element	Difference SDC Fine and results from plate elements
Load case 1	σxmax	-5.782E+08	-5.792E+08	-6.075E+08	-5.767E+08	-4.82%	-4.65%	0.26%
Load case 2	σxmax	-5.011E+08	-5.020E+08	-5.265E+08	-4.998E+08	-4.82%	-4.65%	0.26%
Load case 3	σxmax	-3.855E+08	-3.861E+08	-4.050E+08	-3.845E+08	-4.82%	-4.65%	0.26%
Load case 4	σxmax	-3.855E+07	-3.861E+07	-4.050E+07	-3.845E+07	-4.82%	-4.65%	0.26%
Load case 7	σxmax	-4.181E+08	-4.192E+08	-4.188E+08	-4.739E+08	-0.15%	0.11%	-11.77%
200x400x4 Bar20x4		SDC fine model with the implementation method	SDC Coarse model implementation method	SDC Single element model implementation method	Fine model with plate results taken into account	Difference SDC Fine and SDC Single element	Difference SDC Coarse and SDC Single element	Difference SDC Fine and results from plate elements
Load case 1	σxmax	-2.480E+08	-2.478E+08	-2.459E+08	-2.628E+08	0.83%	0.75%	-5.64%
Load case 2	σxmax	-2.149E+08	-2.148E+08	-2.131E+08	-2.278E+08	0.83%	0.75%	-5.64%
Load case 3	σxmax	-1.653E+08	-1.652E+08	-1.640E+08	-1.752E+08	0.83%	0.75%	-5.64%
Load case 4	σxmax	-1.653E+07	-1.652E+07	-1.640E+07	-1.752E+07	0.83%	0.75%	-5.64%
Load case 7	σxmax	-1.316E+08	-1.379E+08	-1.771E+08	-1.757E+08	-25.72%	-22.12%	-25.13%

Table I.1 Input design stress results σ_X of the beam-column after applying the implementation method for the beam model in the three different mesh sizes and after calculation of the real design stresses.

Appendix J (Differences between FEM analyses)

So when subjected to buckling, nonlinear behavior takes place. This nonlinearity means coupling between membrane deformation and bending deformation. There are several types of nonlinearity: material, contact and geometric nonlinearity. The contact nonlinearity is completely out of the scope of this project. The Geometric nonlinear analysis is sort of out of the scope as well since large deformations are generally undesirable and when they take place then also collapse will more likely take place. The material nonlinearity however, has a highly noticeable influence on the results as can be seen in figure J.1.
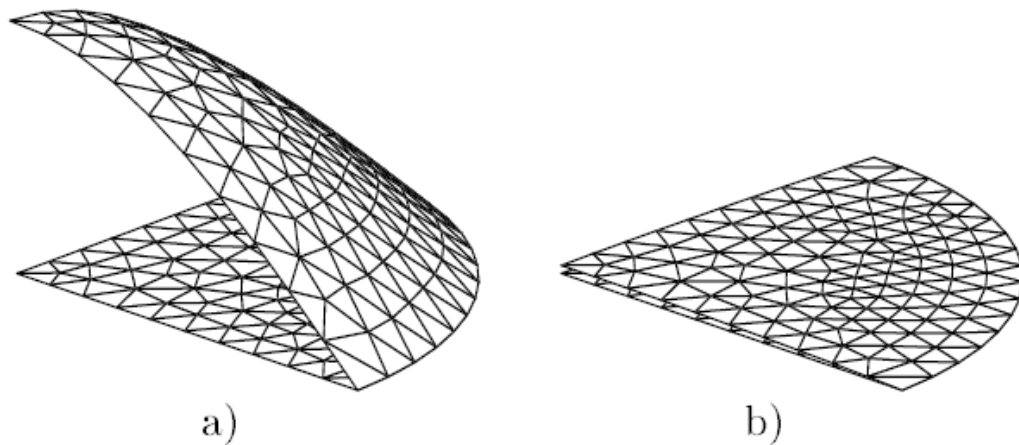

Fig J.1 A disk simply supported on the edge with a uniform lateral pressure. No geometric nonlinearity for both figures, so the magnitude of the loads stays the same. (a) A linear analysis and (b) a nonlinear analysis. The difference is a result of membrane stresses.

A static analysis, like a stress analysis in FEA, is done using Hooke's law, the simple linear equation $[K]\{x\}=\{F\}$. In such analysis time does not play any role. On the other hand a dynamic, transient or modal analysis is dependent on time and follows a more complex governing equation: $[M]\{x''\}+[C]\{x'\}+[K]\{x\}=\{F\}$.

Linear Eigenvalue buckling predicts the theoretical buckling strength while simultaneously you can ignore input details. The non-linear analyses however need as much detail as feasible before it gives a fairly accurate result of the buckling limit.

Eigenvalue buckling is generally used to estimate the critical buckling loads of stiff structures and is based on the linear relationships. However, even when the response of a structure is nonlinear before collapse, a general eigenvalue buckling analysis can provide useful estimates of collapse mode shapes. These buckling mode shapes are often the most useful outcome of the eigenvalue analysis, since they predict the likely failure mode of the structure. The base begins with Hooke's law.

In an eigenvalue buckling problem you look for the loads for which the model stiffness matrix becomes singular, so that the problem $[K]\{x\}=0$ has nontrivial solutions. $[K]$ is the tangent stiffness

matrix when the loads are applied, and the $\{x\}$ are nontrivial displacement solutions. The eigenvalue problem becomes: $([K_0]+\lambda_i[K_\Delta])\{x_i\}=0$ where $[K_0]$ is the stiffness matrix corresponding to the base state, which includes the effects of the preloads if any are present such as thermal loading. $[K_\Delta]$ is the differential initial stress and load stiffness matrix due to an incremental loading pattern. The magnitude of this loading is not important since it will be scaled by the load multipliers λ_i which are the eigenvalues. $\{x_i\}$ are the buckling mode shapes (eigenvectors) and i refers to the ith buckling mode. The buckling mode shapes are normalized vectors and thus do not represent actual magnitudes of deformation at critical load. The critical buckling loads results in preloads+$\lambda_i[K_\Delta]$. Normally, the lowest value of λ_i is of interest.

The non-linear analysis is an incremental procedure. A nonlinear analysis requires incremental load (or displacement) steps. At the end of each increment the structure geometry changes and possibly the material is nonlinear or the material has yielded. Each of these things, geometry change or material change, may then need to be considered for the next increment in the analysis. For details is referred to specific literature on the matter but a quick distinction regarding explicit and implicit analyses is in order.

An explicit FEM analysis updates the stiffness matrix based on geometry changes (if applicable) and material changes (if applicable) at the end of each increment. Then a new stiffness matrix is constructed and the next increment of load is applied to the system. In this type of analysis the hope is that if the increments are small enough the results will be accurate. One problem with this method is that you do need many small increments for good accuracy, hence it is not unconditionally stable. Furthermore it is time consuming and some problems cannot be solved by this type of analysis. Unless it is quite sophisticated it will not successfully do cyclic loading and will not handle problems of snap through or snap back.

An implicit FEM analysis is the same as explicit with the addition that after each increment the analysis does Newton-Raphson iterations to enforce equilibrium of the internal structure forces with the externally applied loads. This type of analysis remains stable, tends to be more accurate and can take somewhat bigger increment steps. Also, this type of analysis can handle problems better such as cyclic loading, snap through, and snap back so long as sophisticated control methods such as arc length control or generalized displacement control are used. One drawback of the method is that during the Newton-Raphson iterations one must update and reconstruct the stiffness matrix for each iteration. This can be computationally costly. As a result there are other techniques that try to avoid this cost by using Modified Newton-Raphson methods [38].

Appendix K (In-depth analysis of rotational constraints)

In a hard corner or any other combination of plates, the smaller plate will lose some strength due to the bigger plate that will buckle earlier. The bigger plate will however gain some strength from the smaller plate due to the rotational stiffness it provides until that plate will buckle as well. Thus, there is an interaction between the plates and a compromise must be established because the plates must buckle at the same time. If you would like to take the rotational restraint into account more realistically than just going for simply supported for both plate fields, than this would be a realistic assumption with some kind of axial force. Consider two adjacent plates of a section of the box girder as illustrated in figures K.1 and K.2. In general, there will be a restraining moment acting at the corner line between Plate 1 and Plate 2.
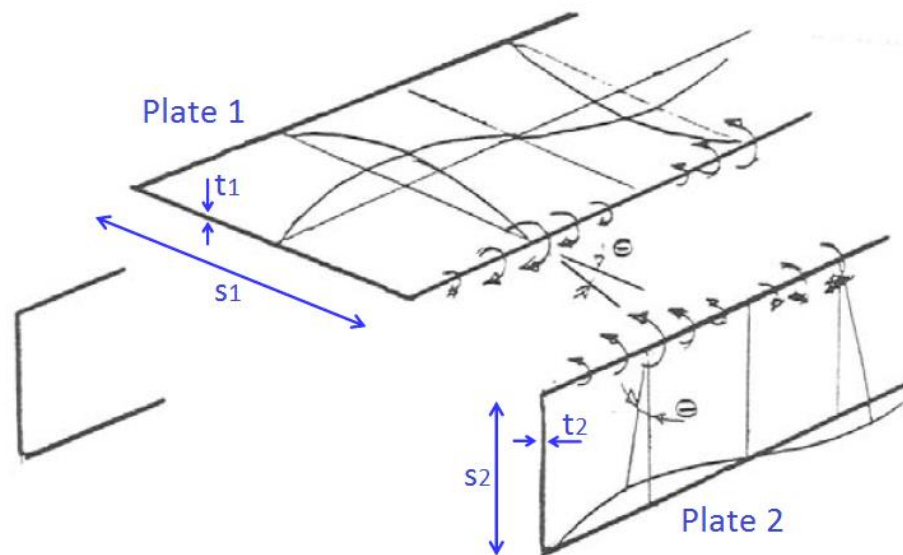

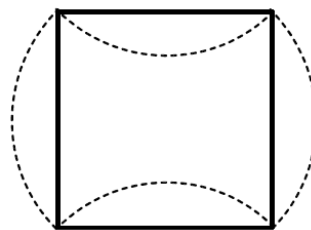Fig K.1 Rotational deformation and restraint relationship between parts of the structure.

Fig K.2 A buckling mode of a box girder.

The theoretical buckling stresses for those two plates are:

$$\sigma_{cr1} = k_1 \frac{\pi^2 E}{12(1 - v^2)} \left(\frac{t_1}{s_1}\right)^2$$

$$\sigma_{cr2} = k_2 \frac{\pi^2 E}{12(1 - v^2)} \left(\frac{t_2}{s_2}\right)^2$$

Before buckling, stresses in the entire cross-section are the same. So, at the point of buckling, one gets: $\sigma_{cr1} = \sigma_{cr2}$ from which the buckling coefficient k2 is relating to k1:

$$k_2 = k_1 \left(\frac{t_1 \, s_2}{t_2 \, s_1} \right)^2$$

The total buckling load on the angle element is:

$$P_{cr} = \sigma_{cr1} s_1 t_1 + \sigma_{cr2} s_2 t_2 = k_1 \frac{\pi^2 E}{12(1 - v^2)} \left(\frac{t_1}{s_1} \right)^2 A = \sigma_{cr1} A$$

where A the sectional area of two plate A = b1h1+b2h2. From this result can be concluded that only one buckling coefficient is needed to calculate the buckling load of the section consisting of two plates. The result assumes the critical stress in plate 1 is representative for the combination of the two plates. Therefore the assumption in the standards for checking individual plate fields instead of structures combined out of plate fields is considered as correct.

Determination of the buckling coefficient is still complicated because of the existence of the edge bending moment but since the conservative simply supported approach is maintained you will be on the safe side. The relation can be illustrated in an example of a box column with a rectangular cross section with the same thickness h. The buckling coefficient as a function of the ratio b2/b1 is plotted in figure K.3. In the limiting case of a square box (b1=b2=b), k1 =4 and the edge interactive moment between adjacent plates is zero.
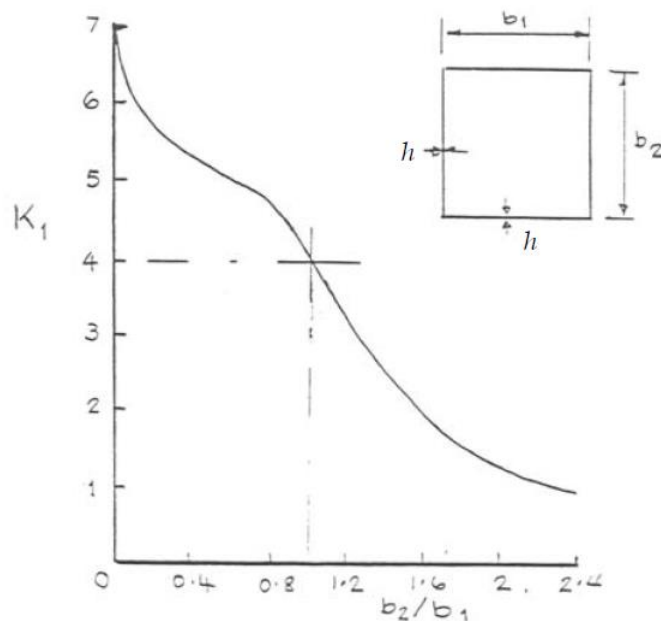

Fig K.3 Buckling coefficients for box girders following a theoretical assumption of buckling. [39]
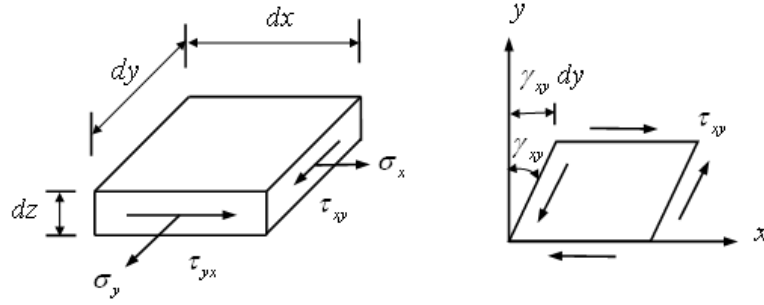
Appendix L (Strain Energy of Bending in Plates)

Fig L.1 O In-plane stress and shear strain [40]

For thin-walled plates where the thickness, t, is not greater than, say, one tenth of the plate side dimensions, the constitutive relationship becomes a plane stress problem; i.e., $\sigma_z = \gamma_{xz} = \gamma_{yz} = 0$. Consider the plate element shown in Figure O subjected first to σ_z only. Then, the force $P = \sigma_x dA = \sigma_x dz dy$ moves a distance equal to $\delta_x = \varepsilon_{xx} dx = \sigma_x dx/E$. Hence,

$$dU_1 = \frac{1}{2}\frac{1}{E}\sigma_x{}^2 dxdydz$$

then, the element is subjected to σ_y. The strain energy due to σ_y is

$$dU_2 = \frac{1}{2}\frac{1}{E}\sigma_y{}^2 dxdydz$$

However, this time, the force in the x direction rides a distance $= -v\frac{\sigma_y}{E}dx$. Hence,

$$dU_3 = -v\frac{1}{E}\sigma_y\sigma_x dxdydz$$

Assuming that normal stresses produce no shear stresses and vice versa, it is possible to obtain strain energy of a plate element due to shear independent from the normal forces. Due to a shear stress, there exists a force, $\tau_{xy}dxdy$ and a deformation $\gamma_{xy}dy$. Hence,

$$dU_4 = \frac{1}{2}\tau_{xy}dxdz(\gamma_{xy}dy) = \frac{1+v}{E}\tau_{xy}{}^2 dxdydz$$

The total strain energy is then

$$dU = \frac{1}{2E}\left[\sigma_x{}^2 + \sigma_y{}^2 - 2v\sigma_x\sigma_y + 2(1+v)\tau_{xy}{}^2\right]dxdydz$$

For the entire plate of length *a*, width *b*, and thickness t, the strain energy becomes

$$U = \int_{-t/2}^{t/2}\int_0^s\int_0^L \frac{1}{2E}\left[\sigma_x{}^2 + \sigma_y{}^2 - 2v\sigma_x\sigma_y + 2(1+v)\tau_{xy}{}^2\right]dxdydz$$

As a consequence of neglecting $\sigma_z, \gamma_{xz}, \gamma_{yz}$, the last equation is limited to thin plates only, but it is not limited to problems of neither small displacements nor membrane forces only. The equation can and will be used for other cases depending upon the proper expression of these stresses. If one considers only for bending and substituting the corresponding expressions for these stresses, one obtains;

$$U = \frac{E}{2(1-v^2)}\int_{-t/2}^{t/2}z^2\int_0^s\int_0^L\left[\left(\frac{\partial^2 w}{\partial x^2}\right)^2 + \left(\frac{\partial^2 w}{\partial y^2}\right)^2 + 2v\frac{\partial^2 w}{\partial x^2}\frac{\partial^2 w}{\partial y^2} + 2(1-v)\left(\frac{\partial^2 w}{\partial x\partial y}\right)^2\right]dxdydz$$

After carrying out the integral with respect to z, this equation becomes

$$U = \frac{D}{2}\int_0^s\int_0^L\left[\left(\frac{\partial^2 w}{\partial x^2}\right)^2 + \left(\frac{\partial^2 w}{\partial y^2}\right)^2 + 2v\frac{\partial^2 w}{\partial x^2}\frac{\partial^2 w}{\partial y^2} + 2(1-v)\left(\frac{\partial^2 w}{\partial x\partial y}\right)^2\right]dxdy$$

Appendix M (Use of beam elements in FEMAP)

Application of offsets and stress recovery points when using beam elements.
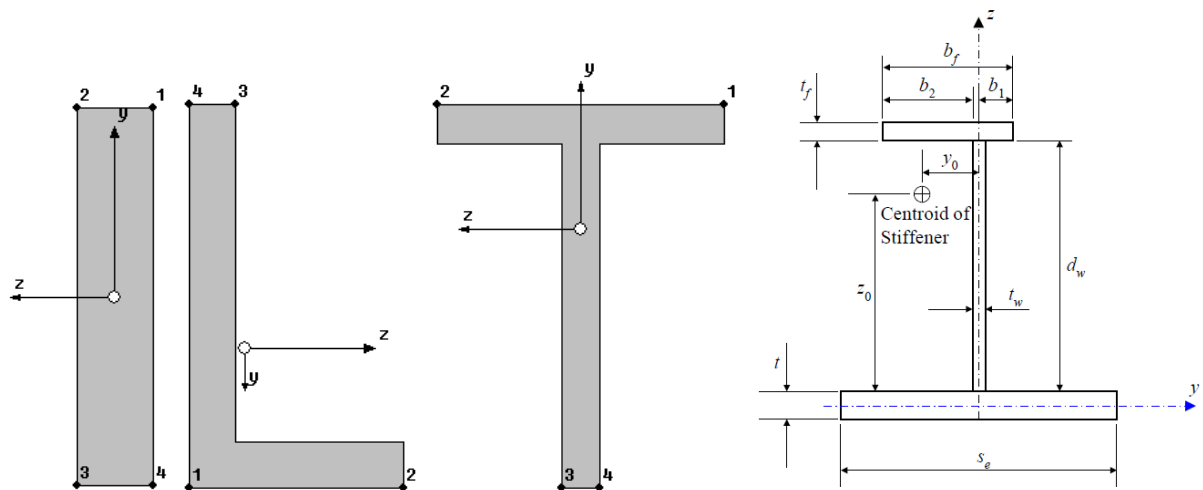

Fig M.1 Corner stress definition points for the (a) flat bar stiffener, (b) L shaped stiffener, (c) T shaped stiffener and (d) the stiffener dimensions as defined by the ABS.
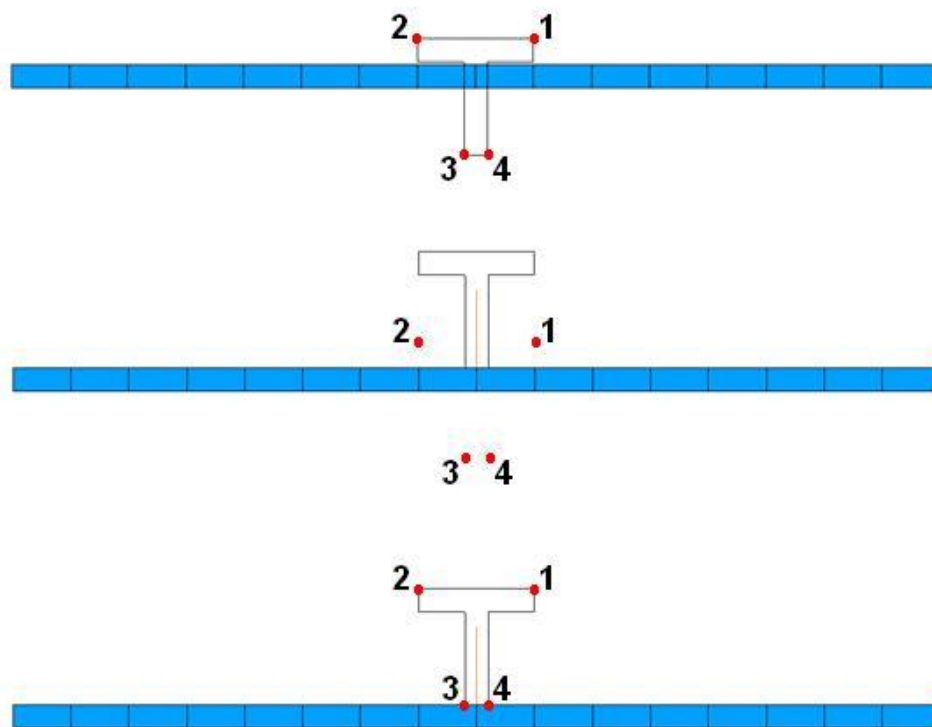

Fig M.2 (a) First place the stiffener without warping constant and offset, then (b) adjust the offset (positive Y neutral axis offset) and lastly (c) also adjust the Y placement of the stress recovery points such that they match the shape again.

In this example is used a T stiffener 20x4x20x4mm. That means that the neutral line distance z_0 is 13,5556mm. The plate thickness is also 4mm. Including half the plate thickness will produce a total offset of 15,5556mm. If you define the cross section area of the stiffener as described in figure N.1 and disable warping constant, z_0 will be filled in correctly for the y coordinate of two of the four stress recovery points (fig M.3). Afterwards adjust the y coordinate of the stress recovery points.

Points 1 and 2 -> Stiffener height + half the plate thickness (20mm + 2mm = 22mm)

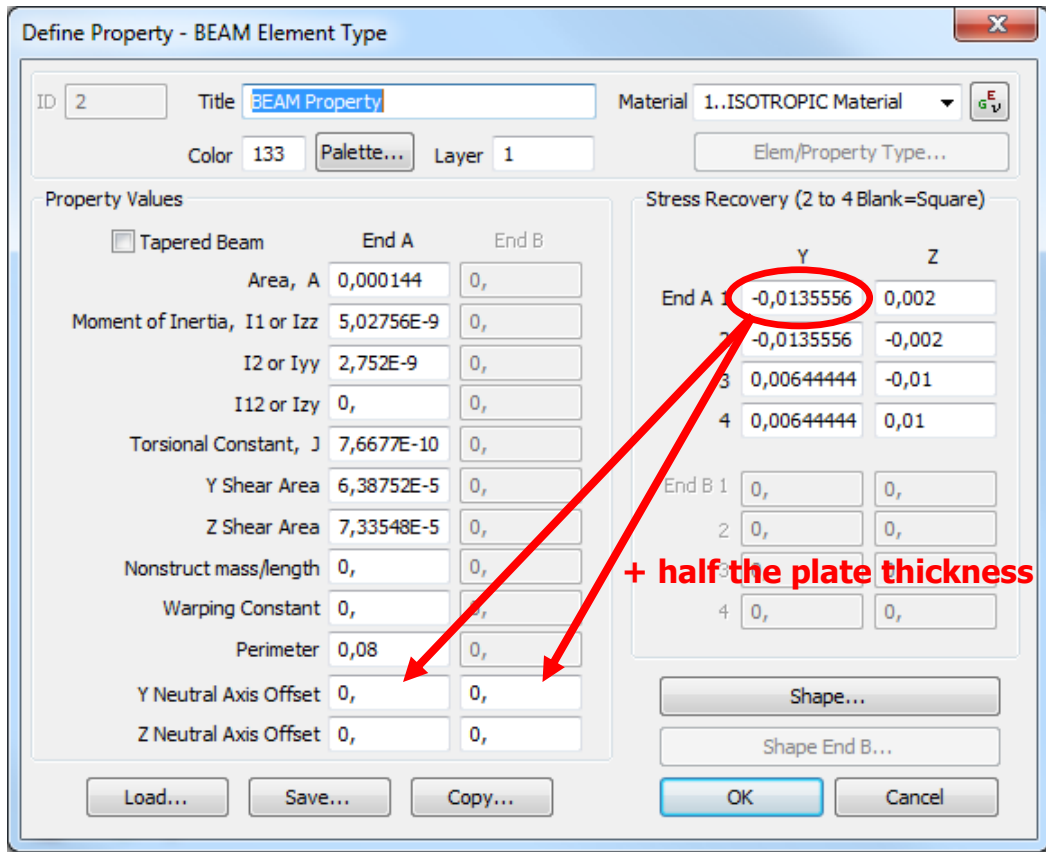Points 3 and 4 -> Half the plate thickness (2mm)

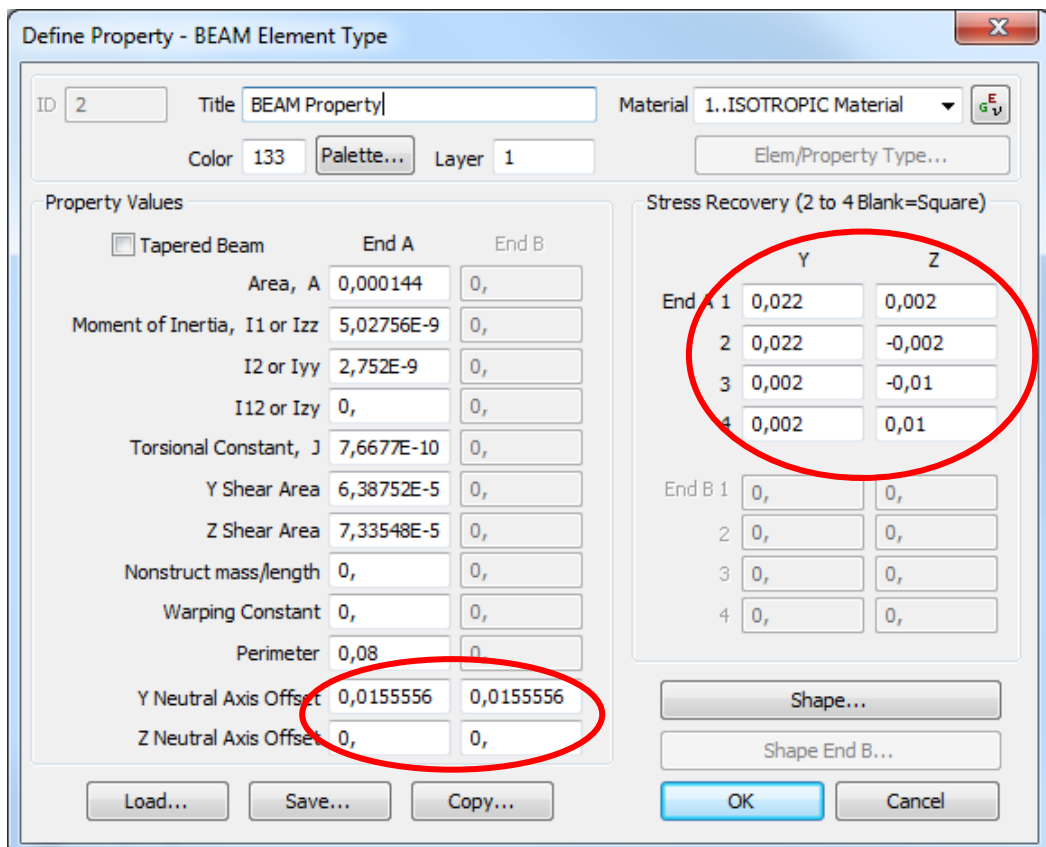Fig M.3 Initial properties after defining the cross section area.

Fig M.4 Adjusted properties after correcting the offset and stress recovery points.

Appendix N (Derivation of the magnification factor)

In practice, columns are seldom perfectly straight, nor is the loading perfectly axial. Imagine a pinned column with an initial deflection δ(x) and an additional deflection w(x) due to the axial load. For small deflections the governing equation is

$$\frac{d^2w}{dx^2} + \frac{F}{EI}(\delta + w) = 0$$

in which the combination of the total deflection and the axial force gives rise to a bending moment F(δ + w). This causes the deflection to increase further, and the deflection continues to grow. Thus there is no static equilibrium configuration and no sudden buckling. The solution depends on the initial imperfection. Let δ and w be represented by a Fourier series.

$$\delta = \sum_{n=1}^{\infty} \delta_n \sin\frac{n\pi x}{L}$$

$$w = \sum_{n=1}^{\infty} w_n \sin\frac{n\pi x}{L}$$

This must be true for any value of n as well as for the complete summation and therefore, since sin(nπx/L) cannot be zero, we must have

$$w_n = \frac{\delta_n}{\frac{n^2 P_E}{P} - 1} = 0$$

The dominant term is n=1. Hence for any configuration of the initial imperfection, the factor magnification factor which is induced by P is given by

$$\frac{1}{1 - \left(\frac{P}{P_{cr}}\right)}$$

Appendix O (Torsional strength formula derivation)

The DNV uses a formula for the torsional strength which is derived by the minimum potential energy method. [41]

U = potential energy of internal forces of the structure also called the elastic deformation energy.

W = potential energy of the external forces.

When torsion is restrained the torsional stiffness comes from both St Venant and Vlasov torsions. The load will force the beam to rotate and warp due to rotation φ. The deflection shape is assumed as

$$\left(\frac{du}{dx}\right) = \frac{h}{2}\left(\frac{d\varphi}{dx}\right)$$

$$\varphi = \varphi_0 \sin\left(\frac{\pi x}{l}\right)$$

Contributions from elastic bending and St Venant torsion:

$$U = \frac{1}{2}\int_0^l EI_w \left(\frac{d^2\varphi}{dx^2}\right)^2 dx + \frac{1}{2}\int_0^l GI_t \left(\frac{d\varphi}{dx}\right)^2 dx$$

Contribution from the applied load P:

$$W = -P\delta = -P\int_0^l \frac{1}{2}\left(\frac{du}{dx}\right)^2 dx = -P\frac{1}{2}h^2\varphi^2\, dx$$

Potential energy:

$$\prod = U + W = \frac{1}{2}EI_w \int_0^l (\ddot{\varphi})^2\, dx + \frac{1}{2}GI_t \int_0^l (\dot{\varphi})^2\, dx - P\frac{h^2}{2}\int_0^l (\dot{\varphi})^2\, dx$$

Minimum potential energy:

$$\frac{d\Pi}{d\varphi_0} = \frac{\pi^4}{2l^3}EI_w\varphi_0 + \frac{\pi^2}{2l}GI_t\varphi_0 - P\frac{h^2\pi^2}{8l} = 0$$

$$EI_w\frac{\pi^2}{l^2} + GI_t - P\frac{h^2}{4} = 0$$

$$\sigma_x = \frac{1}{I_p}\left(EI_w\frac{\pi^2}{l^2} + GI_t\right)$$

The polar moment of inertia comes in since the sectional properties should be determined with respect to the center of rotation, the connection between stiffener and plate.

$$\sigma_{ET} = torsion + warping = \left(\beta\frac{GI_t}{I_p}\right) + \left(h_s^2\frac{\pi^2 EI_z}{I_p l^2}\right)$$

Appendix P (Examples of test setups)
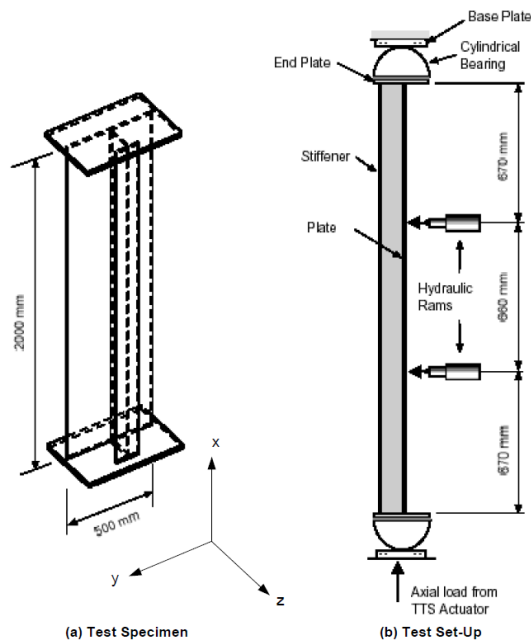
Two examples of real size test setups:

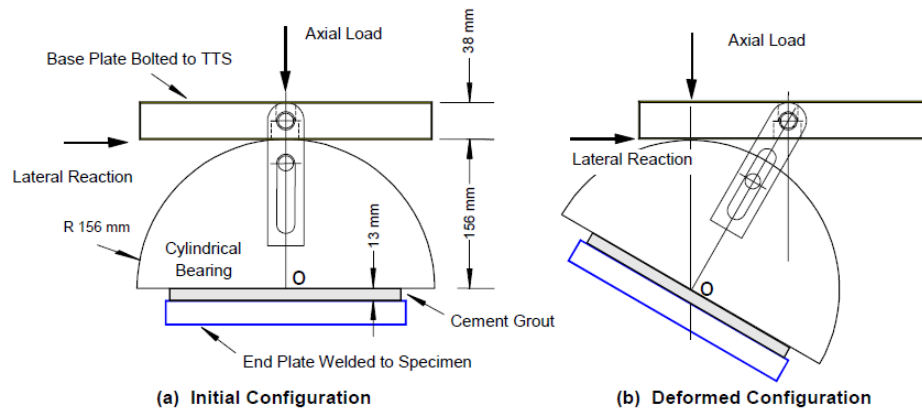Fig P.1 Schematic of Test Specimen and Set-Up [42].
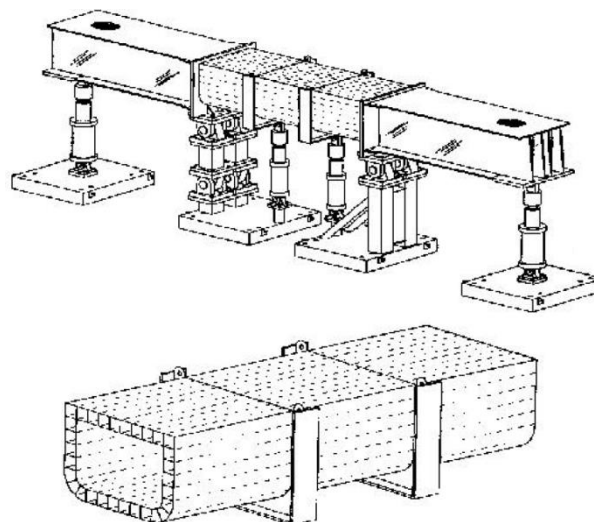

Fig P.2 End Support.

Fig P.3 Illustration of a six point bending facility and test specimen [43].